Understanding (p)ppGpp-mediated mechanisms of persistence and stress survival in *Bacillus subtilis*

By
Jessica Tse Barra

A dissertation submitted in partial fulfillment of
the requirements for the degree of

Doctor of Philosophy
(Microbiology)

at the
UNIVERSITY OF WISCONSIN-MADISON
2017

Date of final oral examination: 12/07/2017

The dissertation is approved by the following members of the Final Oral Committee:
Jue (Jade) D. Wang, Professor, Bacteriology
Richard Gourse, Professor, Bacteriology
Patricia Kiley, Professor, Biomolecular Chemistry
Michael Thomas, Professor, Bacteriology
Kalin Vestigian, Assistant Professor, Bacteriology

Table of Contents

Abstract

During amino acid starvation, the Gram-positive bacterium *Bacillus subtilis*, produces a molecule called (p)ppGpp, a nucleotide derived from GTP or GDP and ATP. This molecule is produced by almost all bacteria but its effects are best characterized in *E. coli* and *B. subtilis*. In *E. coli* and *B. subtilis*, (p)ppGpp shuts down cellular processes such as ribosomal RNA transcription, translation, and DNA replication. Cells without (p)ppGpp, called (p)ppGpp^0, cannot grow on minimal media and are auxotrophic for several amino acids. In this work, we showed that *B. subtilis* (p)ppGpp^0 cells were auxotrophic for valine, leucine, isoleucine (branched chain amino acids), methionine, threonine, and mildly for histidine, arginine, and tryptophan. The auxotrophy is due to hyperrepression of CodY and GTP-dependent processes. We also reveal a new role for (p)ppGpp: protection from and adaptation to amino acid downshift.

We examined the role of (p)ppGpp in mediating persistence, the ability of a subpopulation of bacteria to survive antibiotics for a prolonged period of time. We demonstrate that (p)ppGpp is one mechanism of persister formation and is necessary and sufficient to promote persistence. The most striking discovery is that (p)ppGpp antagonism of GTP is essential for persistence. We also show that there are diversified roles for the (p)ppGpp synthetases, allowing for production of varying levels of (p)ppGpp in individual cells as a bet-hedging strategy and through responsive mechanisms, all to ensure stress survival.

(p)ppGpp and GTP-dependent mechanisms protect cells against bacteriostatic antibiotics. We treated wild type and (p)ppGpp^0 cells with chloramphenicol and saw that (p)ppGpp^0 cells lose viability. Interestingly, RelA was the primary (p)ppGpp synthetase

that produced (p)ppGpp to protect cells against chloramphenicol. (p)ppGpp antagonism of GTP levels also correlates with chloramphenicol survival. Thus, (p)ppGpp inhibition of GTP is also critical for protection against bacteriostatic antibiotics. This response appears to only occur in the soil-dwelling *B. subtilis*, since the intestine-inhabiting *E. coli* does not produce (p)ppGpp in response to chloramphenicol, indicating that (p)ppGpp induction by bacteriostatic antibiotics may be niche-dependent.

In this work, we comprehensively examined the role of (p)ppGpp in mediating stress survival in persistence.

Acknowledgements

There's a lot of people that made my PhD and thesis possible. I'd like to thank my mentor, Dr. Jue (Jade) Wang for taking a chance on me when she first joined UW-Madison. I am grateful for her guidance, support, mentorship, and steering me in the right direction throughout the years. Her insistence on rigor has been indispensable for my development as a scientist.

I'd like to thank my thesis committee, Drs. Rick Gourse, Patricia Kiley, Michael Thomas, and Kalin Vetsigian for their continued support and encouragement. They have provided invaluable guidance and advice for my work. I am also very thankful for all of my collaborations and use of lab equipment: Stephen Vadia and Petra Levin, Andrew Berti and Warren Rose, Nikhil Jane and Robert Britton, Daniel Pensinger and JD Sauer, and John Barkei and John Mansfield. I am also thankful for my interactions with the Gourse, Cox, Keck, Burton, Amador-Noguez, Wassarman, and Sauer labs in our lab meetings and hallway conversations. The advice and stimulating discussions have been valuable for my work. I'd also like to thank our program coordinator, Cathy Davis Gray, for keeping us on track and making sure we have our ducks in a row. I'd like to thank the coordinators of Morgridge Entrepreneurial Bootcamp for giving me the wonderful opportunity to meet other scientists and teaching me about entrepreneurship and business.

I am grateful for my lab mates, past and present, for their guidance and help. Our conversations about science and Hogwarts houses have really made my lab experience enjoyable. Thanks to past lab members Alycia Bittner, Sabari Thirupathy, Kuanqing Liu, Yan Zhang, Jessica DeNapoli, Brigitta Wastuwidyaningtyas, and Allison Kriel for their

help and laying the foundation for my growth. Thanks to present lab members Danny Fung, Jeremy Schroeder, Louis Mak, Ponlkrit (Tame) Yeesin, Brent Anderson, Christina Johnson, Lucas Onder, and Jin Yang for continuously making sure that we remain rigorous in our work and that the science is sound. A special thanks to Tame for being here with me since first year and for our eating adventures, and Danny for providing me with great mentorship and stimulating discussions about persistence and life.

Throughout my time here, I have befriended lots of wonderful and intelligent people. I'm grateful for Dr. Vy Tran, who has been my roommate and best friend here since the beginning. I loved our adventures and I look forward to visiting you. Thanks to all my friends at MDTP for their continued support. A special thanks to Mengyi Cao, Grischa Chen, Anna Baker-McAlister, Thiago Santos, Daren Ginete, Zizi Pisithkul, Rachel Salemi (MH'16), Albert Chen, Grace Shrader, E-Beth Chan, and CJ Yang for all the scientific discussions and eating adventures. Thanks to all the Wellesley women and my friends from home for their visits, Evy, Ying, Esther, Hillary, Tina, and Laura, and the Wellesley community for their support.

I'd also like to thank my mom, Mama Tse (鄧素微), for being supportive in everything I do, whether it be art or Chinese class or encouraging me to do a biotechnology program in 10th grade, where I got to hold my first pipette. Thank you for instilling in me a sense of curiosity and a thirst for knowledge. I miss you every day.

Finally, words cannot express my gratitude for my husband, Matt Barra (and our dogs, Simon and Lucy) and his support. Thank you for everything. I'm excited for our new adventures! We did it.

List of Figures

List of Tables

Chapter 1: Introduction

This chapter is partially adapted from the book chapter “Fung, D.K., Anderson, B.W., Tse, J.L., and Wang, J.D. 2017. Nucleotide second messengers: (p)ppGpp and cyclic dinucleotides. p. 437-465. Peter Graumann (ed), Bacillus: Cellular and Molecular Biology, 3rd ed., Caister Academic Press, Norfolk, UK.”

J.T.B. wrote the entire chapter.

Introduction

The alarmone (p)ppGpp was first discovered in the Gram-negative bacterium *Escherichia coli* (Cashel and Gallant, 1969). Shortly after starving *E. coli* for amino acids, Cashel and Gallant observed intracellular accumulation of guanosine penta- and tetra-phosphate, collectively known as (p)ppGpp. The appearance of (p)ppGpp coincided with a stall in stable RNA synthesis. The synthesis of (p)ppGpp in response to amino acid starvation is known as the stringent response. Since then, decades of research have expanded upon the role of (p)ppGpp as a mediator of stress survival, virulence, and persistence (Fung et al., 2017; Liu et al., 2015a; Potrykus et al., 2011). Although our understanding of the roles of (p)ppGpp in the cell has deepened, the mechanisms by which (p)ppGpp enacts physiological changes in bacteria remain elusive. Part of the difficulty in completely defining the role of (p)ppGpp is that it exists in almost all bacteria and plant chloroplasts (Atkinson et al., 2011) but the binding targets and conditions that stimulate (p)ppGpp production vary from bacterium to bacterium (Boutte and Crosson, 2013; Liu et al., 2015a). In this chapter, I will delve into the existing knowledge surrounding the induction of (p)ppGpp production and its physiological effects, specifically in *E. coli*, *Bacillus subtilis*, and other relevant examples. In the second part of this chapter, I will highlight mechanisms of persistence, the focus of my work.

(p)ppGpp biosynthesis and metabolism

Structural insights into (p)ppGpp biosynthesis in Escherichia coli

(p)ppGpp can be synthesized by large, multidomain enzymes called RelA or SpoT, collectively known as RelA/SpoT homologs (RSH). Alternatively, it can be

synthesized by single domain small alarmone synthetases (SAS). RSHs often contain at least four domains: the N-terminal hydrolase and synthetase domains, and the C-terminal TGS (ThrRS, GTPase, and SpoT), and ACT (which comprises of the zinc-finger domain [ZFD] and the ribosomal recognition motif [RRM]) (Figure 1A) (Atkinson et al., 2011; Brown et al., 2016; Hauryliuk et al., 2015). It is important to note that not all RSHs have functional hydrolase domains, such as the *E. coli* RelA. During the canonical stringent response, upon amino acid starvation, RelA senses uncharged tRNAs in the A-site of the ribosome and synthesizes (p)ppGpp (Haseltine and Block, 1973; Liu et al., 2015a; Potrykus and Cashel, 2008) (Figure 1B). Recent work using cryo-electron microscopy further characterized this interaction in detail: Uncharged tRNAs adopt an A/T-like conformation, similar to aminoacylated-tRNAs brought to the A-site by EF-Tu (Agirrezabala et al., 2013; Arenz et al., 2016; Brown et al., 2016; Loveland et al., 2016). The RelA TGS domain contains highly conserved basic residues that form electrostatic interactions with the tRNA phosphate backbone, allowing RelA to sense the presence of a tRNA in the A-site (Brown et al., 2016) (Figure 1B). Additional residues in the TGS domain base-stack with the 3'-CCA on the acceptor stem loop, which positions the 3'-OH of the terminal adenosine (the site of aminoacylation) to interact with a β5-strand of the TGS domain. Presence of an amino acid at the 3'-CCA would sterically clash with the β5-strand, thus offering insight into the mechanism of recognition of uncharged tRNAs by RelA (Arenz et al., 2016; Brown et al., 2016; Loveland et al., 2016). The L11 ribosomal protein, critical for the stringent response, is also located near the tRNA and RelA interaction interface, and appears to interact with the tRNA, but not RelA (Loveland et al., 2016).

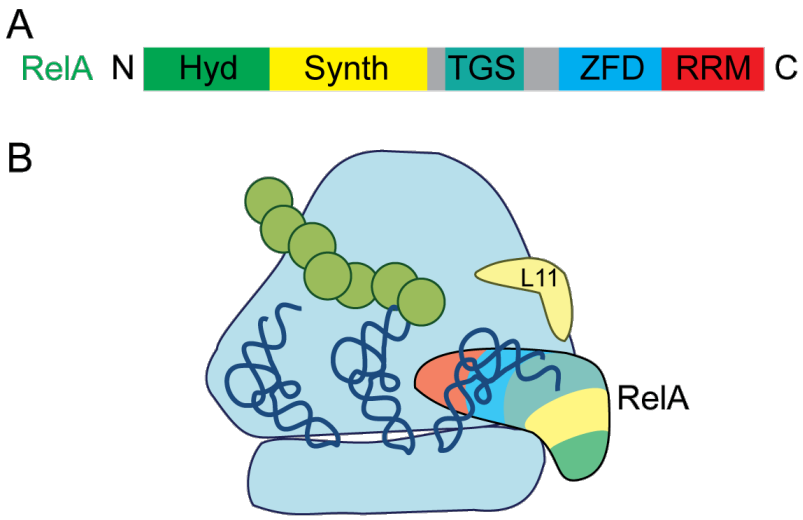

Figure 1. General RelA or RelA/SpoT homolog (RSH) structure and canonical response to amino acid starvation. A. RelA consists of the N-terminal hydrolase domain (Hyd), synthetase domain (Synth), TGS domain, zinc-finger domain (ZFD), and RNA recognition domain (RRM). Not all RSHs have a functional Hyd domains. B. During the stringent response, RelA binds to the ribosome and the TGS domain interacts with the 3'-OH of the terminal adenosine of the A-site tRNA. The L11 protein is located near the tRNA and RelA interaction interface. Adapted from (Brown et al., 2016; Fung et al., 2017)

L11, a ribosomal protein, is essential to activating the stringent response

Along with RelA, tRNA, and the ribosome, the ribosomal protein L11 (encoded by *rplK*) is also required for activation of the stringent response, as it was discovered that Δ*rplK* mutants were relaxed and cannot produce (p)ppGpp during nutrient downshift (Friesen et al., 1974). L11 is a 141 amino acid protein originally discovered as a critical factor for the stringent response when L11 mutants could not bind the ribosome-targeting antibiotic thiostrepton and could not produce (p)ppGpp (Porse and Garrett, 1999; Smith et al., 1978; Wimberly et al., 1999). L11 binds near the A-site, contacting helices in the 23S rRNA, and the Pro-22 in L11-NTD is critical for activating the stringent response (Jenvert and Schiavone, 2007; Yang and Ishiguro, 2001). The starvation signal is likely transmitted from the uncharged tRNA and bound RelA, through L11 (which only interacts with the tRNA) and the ribosome, coordinating (p)ppGpp synthesis (Loveland et al., 2016), likely while RelA is bound to the ribosome (Li et al., 2016). The interaction between L11, the ribosome, RelA, and tRNAs enables cells to sense nutritional status and respond by shutting down active cellular processes using (p)ppGpp.

Regulation of RelA activity

Cryo-EM work and genetics indicate that RelA-CTD is required for interaction with the ribosome in *E. coli* and regulation of RelA activity (Arenz et al., 2016; Brown et al., 2016; Gropp et al., 2001; Loveland et al., 2016) (Figure 1B). Overexpression of a truncated RelA-CTD in a *relA*$^{+}$ background inhibits (p)ppGpp production and cells cannot grow during histidine starvation, suggesting that the CTD inhibits *relA* synthetase activity (Gropp et al., 2001). A mutation in the RelA-CTD, Cys638Phe, produces high

levels of (p)ppGpp, indicating that the mutation relieves RelA inhibition (Gropp et al., 2001). Bacterial two-hybrid analysis showed that the RelA-CTD interacts with another RelA-CTD, and to a lesser extent RelA-NTD, suggesting that RelA activity is regulated by oligomerization (Gropp et al., 2001).

Further, *in vitro* work showed that ppGpp, the predominant species in *E. coli* because the enzyme GppA converts pppGpp to ppGpp (Hauryliuk et al., 2015; Mechold et al., 2013), activates *E. coli* RelA activity (Shyp et al., 2012). This positive feedback loop can amplify the signal from one ppGpp molecule and activate RelAs in the entire cell (likely 1 RelA molecules per 200 ribosomes) (Shyp et al., 2012; Wendrich et al., 2002).

(p)ppGpp degradation by RelA/SpoT homologs (RSH)

There is diversity in the bacterial systems that synthesize and degrade (p)ppGpp. *E. coli* contains two RelA-SpoT homologs (RSH). (p)ppGpp is synthesized by both RelA and SpoT, and is degraded by SpoT (Potrykus and Cashel, 2008), a homolog of bifunctional Rel proteins (Atkinson et al., 2011). Unlike RelA, which uses the ribosome to sense starvation, SpoT produces (p)ppGpp by sensing fatty acid starvation (Potrykus and Cashel, 2008). SpoT achieves this task by detecting the lipid-free form of acyl carrier protein using the SpoT-TGS domain, which interacts with the SpoT-NTD (Battesti and Bouveret, 2006). Mutations in the SpoT-TGS domain results in mutants that cannot produce (p)ppGpp during fatty acid starvation. The TGS domain plays a role in balancing the synthesis and hydrolysis activities of SpoT as well. A (p)ppGpp^0 strain cannot grow on minimal media plates unless it can overproduce (p)ppGpp from a plasmid, such as overexpression of SpoT-NTD (Battesti and Bouveret, 2006). However,

overexpression of SpoT-NTD and TGS fragment in a (p)ppGpp^0 strain cannot grow on minimal media plates, indicating (p)ppGpp is not produced. Thus, the presence of TGS favors (p)ppGpp hydrolysis function (Battesti and Bouveret, 2006).

(p)ppGpp induction in other Gram-negative bacteria: Caulobacter crescentus

The best characterized effects of (p)ppGpp is in *E. coli* during amino acid starvation, yet other bacteria have different requirements for activation of the stringent response depending on their environmental niche (Boutte and Crosson, 2013). One example of this is the freshwater oligotroph *Caulobacter crescentus*. *C. crescentus* live in freshwater and is well-adapted to this environment, as evidenced by its lifestyle – when it encounters favorable, nutrient-rich conditions, the bacterium develops a polar stalk that anchors it to its environment to obtain nutrients. However, when *C. crescentus* senses a drop in nutrients, it divides asymmetrically, giving rise to swarmer cells that search for more favorable environments (Boutte and Crosson, 2013). *C. crescentus* determines whether its environment is favorable using its sole RSH enzyme, SpoT. It was shown that SpoT interacts with ribosomes to produce (p)ppGpp in response to a variety of stresses. However, amino acid starvation was insufficient to induce (p)ppGpp production; either carbon or nitrogen starvation, coupled with amino acid starvation, is required for (p)ppGpp production (Boutte and Crosson, 2011). (p)ppGpp is a major determinant of the swarmer-to-stalk transition and ensures proper inhibition of replication initiation, stalk formation, and regulation of important cell cycle regulators (Boutte et al., 2012).

(p)ppGpp biosynthesis and metabolism in Bacillus subtilis

There are many parallels between the effects of (p)ppGpp in *E. coli* and *B. subtilis*, but the (p)ppGpp synthetases differ between the two model organisms. Unlike *E. coli*, *B. subtilis* contains a bifunctional RSH, RelA, and two SASs, YjbM and YwaC (Atkinson et al., 2011; Hogg et al., 2004; Nanamiya et al., 2008; Srivatsan et al., 2008) (Figure 2). Like, *E. coli*, *B. subtilis* RelA responds to amino acid starvation using the ribosome as a sensing platform to produce (p)ppGpp (Krásný and Gourse, 2004; Liu et al., 2015a). *B. subtilis* also requires the ribosomal protein L11 to activate the stringent response, likely through a mechanism similar to that of *E. coli* (Brown et al., 2016; Wendrich et al., 2002). Transcription of *relA* is under the control of σ^B, a sigma factor that is activated upon sensing phosphate and glucose starvation, as indicated by consensus sequence similarity to other σ^B-controlled promoters (Figure 3A) (Wendrich and Marahiel, 1997). RelA is also required for the activation of σ^B during phosphate and glucose starvation (Zhang and Haldenwang, 2003). Clearly, in addition to its role in the stringent response, RelA helps mediate stress survival in *B. subtilis*.

The small (p)ppGpp synthetases, YjbM and YwaC, were discovered years later by sequence homology to the synthetase domain of RelA (Nanamiya et al., 2008) and as suppressors of Δ*relA* (Srivatsan et al., 2010). YjbM (also called RelQ or SAS1) was shown to be transcribed during vegetative growth and required for basal production of (p)ppGpp (Figure 3B) (Nanamiya et al., 2008). Recently, kinetic and structural studies of YjbM showed that YjbM preferentially produces ppGpp and is allosterically activated by pppGpp (Steinchen et al., 2015) (Figure 2). The authors hypothesized that pppGpp produced by RelA in response to a stress could activate YjbM to produce ppGpp, increasing the (p)ppGpp pool and consuming GDP instead of GTP.

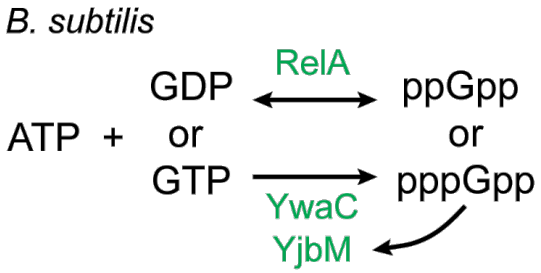

Figure 2. *Bacillus subtilis* synthesizes (p)ppGpp using the bifunctional RelA and the monofunctional YwaC and YjbM. pppGpp activates YjbM synthetase activity (Steinchen et al., 2015). Adapted from (Fung et al., 2017).

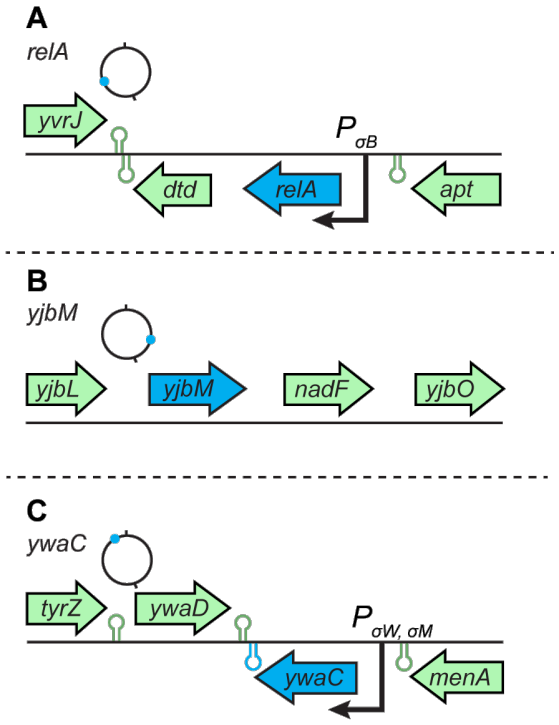

Figure 3. Operon structure of *B. subtilis* (p)ppGpp synthetases. A. *relA* regulatory regions have consensus sequences for σ^B binding (Wendrich et al., 1997). B. *yjbM* is expressed during early vegetative growth and is co-transcribed with *yjbL*, *nadF*, and *yjbO* (Nanamiya et al., 2008). C. *ywaC* is under the control of σ^W and σ^M, extracytoplasmic sigma factors that responds to cell wall and membrane damage (Cao et al., 2002). The chromosome map next to *relA*, *yjbM*, or *ywaC* denotes the gene's location on the chromosome (blue dot). All information is derived from the cited papers, BsubCyc, and SubtiList.

A recent study suggests that RelQ (YjbM or SAS1) from *Enterococcus faecalis* is allosterically regulated by single-stranded RNAs. Upon binding a single-stranded RNA, (p)ppGpp synthesis by RelQ is decreased. Further, binding of (p)ppGpp to RelQ also destabilizes pre-existing RelQ:RNA complexes. This regulation may offer insight into how RelQ may incorporate nutritional signals from other (p)ppGpp synthetases and alternate between a catalytically on and off state (Beljantseva et al., 2017).

YwaC (also called RelP or SAS2) is a (p)ppGpp synthetase that responds to cell wall stress and is part of the σ^W and σ^M regulon (Figure 3C). These extracytoplasmic sigma factors help to maintain cell membrane integrity by transcribing genes to alleviate or mitigate cell wall, membrane, or alkali damage (Cao et al., 2002; Helmann, 2016). Transcription from P_{ywaC} is robust and has been utilized as a reporter for screening for novel cell wall active compounds as well as studying wall teichoic acid biosynthesis (Czarny et al., 2014; D'Elia et al., 2009).

Physiological consequences of (p)ppGpp

(p)ppGpp has pleiotropic effects in the cells, all of which ultimately promote stress survival or adaptation to sudden changes in the environment. Thus far, (p)ppGpp has been shown to promote survival of amino acid starvation, activate transcription of virulence genes in pathogens, and encourage persister formation in bacteria of different phyla.

(p)ppGpp downregulates stable RNA transcription and replication and promotes survival of amino acid starvation

The consequences of (p)ppGpp production are diverse and have been shown to alter transcription, stable RNA synthesis, enzyme activity, virulence, and persistence.

Through crosslinking and genetic approaches, (p)ppGpp was shown to bind at two distinct sites in *E. coli* RNAP: Site 1 is located at the interface of the β' and ω subunit; Site 2, discovered later, requires both the transcription factor DksA and RNAP (Ross et al., 2013, 2016). Both sites are critical for adaptation to nutrient downshift, however, disruption of site 2 binding resulted in a more severe lag time after downshift than site 1 and disruption of both sites had over 30 hour lag time (Ross et al., 2016).

In addition to allowing cells to survive nutrient downshift, (p)ppGpp downregulates rRNA transcription. In *E. coli*, (p)ppGpp together with the DksA, bind to RNA polymerase (RNAP) and destabilizes promoter open complexes (Barker et al., 2001; Paul et al., 2004). The intrinsic properties of the promoters dictate whether the gene is upregulated or downregulated: ribosomal RNA promoters are intrinsically unstable and are destabilized further, resulting in downregulation. Conversely, amino acid biosynthesis genes have promoters that are intrinsically stable so further destabilization still results in transcription from these genes (Barker et al., 2001). Thus, in *E. coli*, (p)ppGpp directly binds to RNAP to massively modulate transcription and halt cell growth during amino acid starvation (Traxler et al., 2008). Mutants without Site 1 and/or Site 2 exhibit differences in ribosomal RNA regulation. As expected, strains with both (p)ppGpp binding sites intact are able to downregulate transcription from the *rrn* P1 promoter, whereas downregulation was attenuated in strains with mutated site 1 and site 2. A strain with neither site 1 or site 2 was similar to a Δ*dksA* or (p)ppGpp^0 strain (Ross et al., 2016).

Unlike *E. coli*, during amino acid starvation, *B. subtilis* alters ribosomal RNA levels by using (p)ppGpp to decrease GTP, the initiating nucleotide for ribosomal RNA

promoters (Krásný and Gourse, 2004). To reduce GTP levels, not only does (p)ppGpp consume GTP as a substrate, but more importantly, (p)ppGpp binds to and inhibits the GTP biosynthesis enzymes HprT, Gmk, and to a lesser extent, GuaB (Kriel et al., 2012). Inhibition of HprT is conserved across bacterial species. Inhibition of Gmk is conserved across multiple phyla of bacteria but is largely absent in Proteobacteria, (Gaca et al., 2015; Liu et al., 2015b; Nomura et al., 2014). Reduction of GTP is critical for survival of amino acid starvation (Bittner et al., 2014; Kriel et al., 2012, 2014). Further, (p)ppGpp is required for cells to maintain GTP homeostasis: increasing GTP levels in (p)ppGpp^0 cells by treatment with guanosine increases GTP through the salvage pathway, which correlates with GTP toxicity (Kriel et al., 2012). In general, (p)ppGpp allows for increased survival and adaptability to stresses.

In addition to downregulating stable RNA transcription, (p)ppGpp also inhibits replication elongation in *B. subtilis* by binding to and inhibiting the RNA polymerase domain of primase, encoded by *dnaG*, in a dose-dependent manner (DeNapoli et al., 2013; Rymer et al., 2012). Like decreasing rRNA transcription during amino acid starvation, inhibiting replication elongation may help to conserve energy and prevent depletion of dNTPs pools (Wang et al., 2007).

(p)ppGpp also regulates translation first by downregulating transcription of ribosomal RNAs and ribosomal proteins according to the cell's nutritional status (Liu et al., 2015a; Potrykus and Cashel, 2008). Second, translation GTPases involved in translation elongation and termination (EF-G, EF-Tu, and RF3) have been identified as (p)ppGpp targets, presenting another mechanism of decreasing translation (Kanjee et al., 2012; Nomura et al., 2012; Rojas et al., 1984). Multiple mechanisms to decrease

translation ensures conservation of nutrients and energy until the cells are in a more favorable environment.

Ribosome assembly GTPases (raGTPases) are also targets of (p)ppGpp (Corrigan et al., 2016; Kanjee et al., 2012). Using differential radial capillary action of ligand assay (DRaCALA) (Roelofs et al., 2011), Corrigan et al. identified several *S. aureus* raGTPases (RsgA, RbgA, Era, and HflX) that bound to radioactive (p)ppGpp. (p)ppGpp inhibited the GTP hydrolysis activity of these raGTPases (Corrigan et al., 2016). Since GTP hydrolysis is required for correct assembly of 70S ribosomes, it is possible that during starvation, (p)ppGpp inhibits raGTPases and prevents ribosome maturation in order to conserve energy (Corrigan et al., 2016). A similar, gatekeeper role has been proposed for the *E. coli* GTPase Obg (Feng et al., 2014). raGTPases also play a role in facilitating correct loading of ribosomal proteins into assembling subunits, since depletion of a raGTPase, *rbgA*, results in accumulation of 45S intermediates that are missing L16, L27, and L36 (Achila et al., 2012; Britton, 2009; Schaefer et al., 2006). The direct inhibition of GTPases by (p)ppGpp as well as GTPase's ability to sense fluctuations in GTP levels presents a robust mechanism for decreasing translation.

(p)ppGpp promotes virulence in pathogenic bacteria

(p)ppGpp has been shown to promote virulence in pathogenic bacteria, such as *Francisella tularensis, Pseudomonas aeruginosa*, *Enterococcus faecalis*, and *Staphylococcus aureus*. Recent work on the Gram-negative bioterrorism agent, *Francisella tularensis*, revealed the importance of ppGpp on regulation of virulence gene expression. A crystal structure showed that ppGpp binds to two regulators, MglA and SspA, forming a novel complex with increased affinity for PigR, a pathogenicity

regulator. MglA and Sspa forms a complex with RNAP and interacts with PigR, bringing RNAP to the promoter of the *Francisella* pathogenicity island (Cuthbert et al., 2017). Thus, ppGpp coordinates environmental cues with transcription of virulence genes in *F. tularensis* (Charity et al., 2009).

(p)ppGpp is also important for mediating stress survival for *P. aeruginosa*, a common, biofilm-forming pathogen found in the lungs of cystic fibrosis patients. In the absence of (p)ppGpp, cells are highly susceptible to the DNA gyrase inhibitor ofloxacin, increased autolysis in biofilm, and decreased virulence (Nguyen et al., 2011). Ofloxacin treatment of mice infected with Δ*relA* Δ*spoT* increased the survival of the mice when compared to infection with wild type strain, indicating that ofloxacin successfully cleared the infection. (p)ppGpp is thus an important regulator of biofilm formation and virulence in *P. aeruginosa*.

E. faecalis, a Gram-positive opportunistic pathogen normally present in the human gut microbiome, is one of the most common causes of hospital-acquired infections. It was revealed that (p)ppGpp production promotes resilience to many stresses, including high temperature, high pH, and vancomycin treatment (Abranches et al., 2009). Further, virulence was attenuated when Δ*relA* Δ*relQ* was used to infect *Caenorhabditis elegans*, highlighting the importance of (p)ppGpp on infectivity and promoting recalcitrant infections (Abranches et al., 2009).

CodY is a transcription factor in Gram-positive bacteria like *B. subtilis* and *S. aureus*. CodY is activated by high levels of GTP (Handke et al., 2008). In *B. subtilis*, (p)ppGpp production drastically decreases GTP levels, deactivating CodY, and removing inhibition of CodY-sensitive promoters, such as branched-chain amino acid

biosynthesis promoters (Kriel et al., 2014). *B. subtilis* and the Gram-positive pathogen *S. aureus* CodY have overlapping and the latter has unique regulons that promote virulence (Majerczyk et al., 2010; Molle et al., 2003; Montgomery et al., 2012). Furthermore, *S. aureus* CodY activity is activated by BCAA and GTP *in vitro* and has been co-crystalized with isoleucine and GTP, indicating that *B. subtilis* and *S. aureus* CodY are likely similarly regulated (Han et al., 2016; Majerczyk et al., 2010). Members of the *S. aureus* CodY regulon include *sodA* and *katA*, encoding superoxide dismutase and catalase, respectively, and used to neutralize superoxides and hydrogen peroxides produced by the host immune system (Majerczyk et al., 2010). CodY also represses expression of the *agr* operon, which encodes a regulatory system that responds to population density and enables transcription of virulence genes (Roux et al., 2014), such as capsule and alpha-toxin biosynthesis (Majerczyk et al., 2010). Taken together, (p)ppGpp and CodY enable expression of virulence genes in *S. aureus*.

Mechanisms of persister formation

(p)ppGpp has also been shown to promote antibiotic survival or persistence in bacteria. During antibiotic treatment, a population of bacteria rapidly dies but a small subpopulation of bacteria, called persisters, are able to survive in high concentrations of antibiotics. Persistence, in contrast to resistance, is non-heritable and is characterized by a biphasic kill curve: the rapid kill is represented by a steep downward curve, and the persister population is represented by the plateau, in which the population neither grows nor dies (Figure 4) (Brauner et al., 2016). In a clinical setting, fluctuating antibiotic concentrations, due to drug administration and metabolism in the body, can kill off a majority of the population, leaving persisters. Once antibiotic concentrations drop below

a certain threshold, these persisters can resume growth and are responsible for recalcitrant and chronic infections (Cohen et al., 2013). Further, a persistent population can be a reservoir for new mutations or acquisition of genes that confer resistance to antibiotics (Fridman et al., 2014).

The first instance of persistence was recorded in 1944 by Dr. Joseph Bigger (Bigger, 1944) in the Gram-positive bacterium *Staphylococcus pyogenes* but examinations into the mechanisms of persister formation did not emerge until recently. Many of these mechanisms were demonstrated in *E. coli* and other bacteria, including activation of certain toxins, heterogeneous gene expression, and dormancy.

Toxin activation promotes persistence

High persistence (*hip*) mutants were first isolated by mutagenizing *E. coli* and repeated treatment with a high concentration of ampicillin to generate persisters, plating on ampicillin-containing plates, and recovery of persister colonies by removing ampicillin using penicillinase (Moyed and Bertrand, 1983). Two alleles of *hip*, *hipA7* and *hipA9*, were isolated and did not confer different growth rates nor increased resistance, but increased the number of persisters by at least 100-fold during treatment with cell wall biosynthesis inhibitors (Moyed and Bertrand, 1983). Problems with cloning *hipA* behind strong promoters suggested that the product of *hipA* might be toxic and indeed it encoded a toxin that hinders *E. coli* growth even at low levels of expression, but could be deactivated by its cognate antitoxin, encoded immediately upstream by *hipB* (Black et al., 1991; Korch et al., 2003). It was later revealed that HipA is a serine-threonine kinase that phosphorylates glutamyl-tRNA synthetase, inhibiting aminoacylation of $tRNA^{Glu}$, depleting the cell for Glu-$tRNA^{Glu}$, and activating the stringent response

(Germain et al., 2013; Schumacher et al., 2015). Thus, HipA is a toxin that promotes persistence by activating the stringent response.

E. coli have 12 Type II toxin-antitoxin (TA) pairs (Type II toxins and antitoxins are proteins), including HipAB (Gerdes and Maisonneuve, 2012). Recent work explored the effects of sequentially deleting TA pairs on persistence. Deletion of individual TA pairs did not affect persistence, but accumulating TA deletions resulted in decreased persistence (Maisonneuve et al., 2011). In addition, it was later shown that (p)ppGpp inhibits exopolyphosphatase, stimulating Lon protease to degrade antitoxins, allowing for more toxin production and increased persistence (Maisonneuve et al., 2013). However, the decreased ciprofloxacin persistence in Δ5TA-Δ10TA strains was due to DNA damage-mediated activation of φ80 prophages, not absence of toxins (Harms et al., 2017). Although deletion of 10 TAs does not decrease persistence, deletion of the Lon protease and ability to produce (p)ppGpp still decrease persistence (Harms et al., 2017). How Lon protease and (p)ppGpp mediate persistence is still unclear.

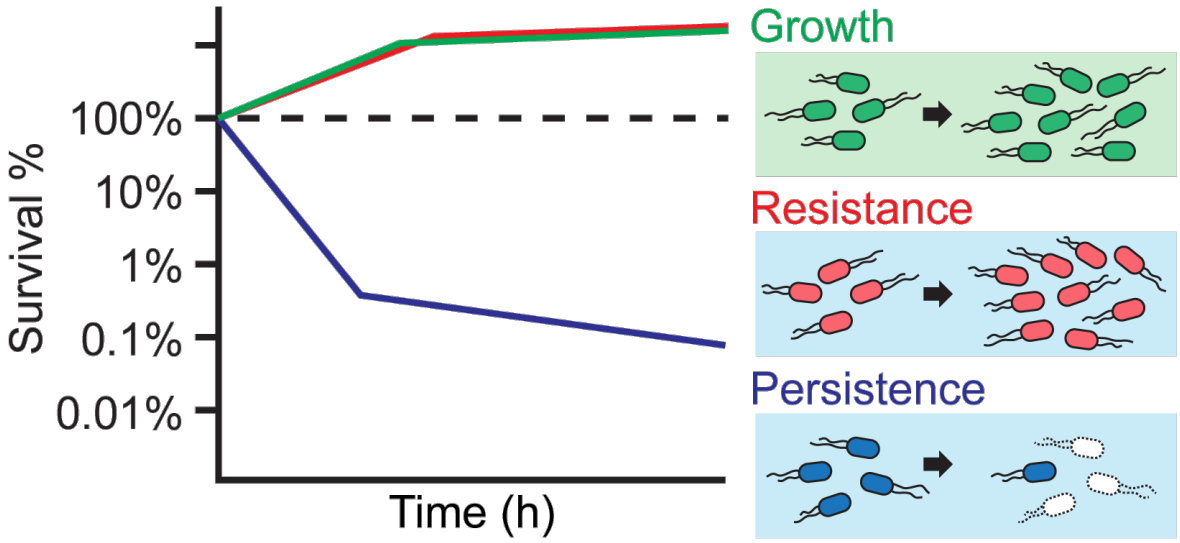

Figure 4. Persistence is a non-heritable trait that results in a subpopulation of bacteria that survive antibiotics. In the presence of growth medium (green background), cells grow until nutrient limitation is reached. In the presence of antibiotics (blue background), resistant bacteria grow, whereas for persisters, a majority of the population die but a subpopulation continues to survive. Dead cells are represented in white with perforated outline.

Another Type II TA, TacT, was shown to increase persistence in *S. enterica*. Non-replicating *S. enterica* persisters were isolated in induced-macrophages and Type II toxins were shown to be overexpressed in these persisters (Helaine et al., 2014). Individual deletions of each of the Type II TAs showed impaired persister formation in macrophages (Helaine et al., 2014). One of these Type II TAs, which encodes TacT, was revealed to be an acetyltransferase that acetylates aminoacylated-tRNAs at the amine of the amino acid, thereby disabling peptidyltransferase activity, stalling translation, and increasing persister formation (Cheverton et al., 2016). In addition to TacT's cognate antitoxin TacA, peptidyl-tRNA hydrolase (Pth) was also identified as an antitoxin of TacT. Pth hydrolyzes peptidyl-tRNAs and acetylated aminoacylated tRNAs, offering a mechanism for resuscitation from the persister state (Cheverton et al., 2016).

Type I TAs (Type I antitoxins are small RNAs that counteracts the toxin at the translational level) also promote persistence in *E. coli* and *Pseudomonas aeruginosa*. In *E. coli*, the GTPase, Obg is involved in critical cellular processes, including ribosome biogenesis and assembly, control of cell division, and chromosome segregation (Kint et al., 2014). It has also been shown that Obg in *E. coli* is an anti-association factor, sequestering the 50S ribosome upon sensing starvation by binding to ppGpp. Obg acts as a checkpoint and prevents translation until starvation is resolved (Feng et al., 2014). Overexpression of *obg* in *E. coli* and *P. aeruginosa* results in increased persistence (Verstraeten et al., 2015). Elevated Obg occurs stochastically in *E. coli*, requires (p)ppGpp for persistence, and activates the transcription of a Type I toxin, *hokB*. HokB is a membrane-associated polypeptide that disrupts membrane potential (Verstraeten et al., 2015). The decreased membrane potential mediates persistence.

Phenotypic heterogeneity contributes to persistence

It was first shown by Balaban *et al*. that persistence could be due to a phenotypic switch wherein a single cell could switch from rapid growth to dormancy and survive antibiotic treatment (Balaban et al., 2004). This led to the characterization of two types of persisters: a) Type I persisters are pre-existing due to back-dilution from stationary phase cells and have increased lag times, and b) Type II persisters are continuously generated in a growing population due to spontaneous switch from rapid growth to slow growth. Thus, wild type *E. coli* comprises of three subpopulations: normal, antibiotic-susceptible, cells (which rapidly die when treated with antibiotic), Type I, and Type II persisters (Balaban et al., 2004). Phenotypic switches between rapid growth to slow growth contributes to the formation of a heterogeneous population and promotes persistence.

Others have also shown that heterogeneous gene expression contributes to persistence. In *E. coli*, there is less accumulation of a fluorescent β-lactam, BOCILLIN, in persisters than in non-persisters (Pu et al., 2016a). Since antibiotic accumulation is affected by porins, which facilitates antibiotic diffusion across the membrane, or efflux pumps, which actively transports antibiotics into or out of the cell, porin and efflux pump deletions were made to determine how BOCILLIN was removed from persister cells. Deletion of an efflux pump, TolC, resulted in massive BOCILLIN accumulation, suggesting increased efflux pump expression may be responsible for decreased BOCILLIN uptake. Indeed, RNA-Seq and qPCR data show that persisters produce higher transcripts for efflux pumps than non-persisters, and the increased efflux pump expression correlates with β-lactam survival (Pu et al., 2016a). Thus, heterogeneous

expression of efflux pumps may be responsible for decreased accumulation of β-lactams and increased persistence in *E. coli*. This work presents a paradoxical "dormant, but active" strategy, whereby cells passively evade antibiotics through mechanisms that promote dormancy (shown in other works), and actively remove antibiotics through efflux pumps (shown in this work) (Pu et al., 2016b).

In *Mycobacteria smegmatis*, the catalase-peroxidase KatG activates the prodrug isoniazid (INH) (Wakamoto et al., 2013). *M. smegmatis* persisters formed in the presence of INH, not because of differences in growth rates, but due to heterogeneous *katG* expression resulting in differential survival in INH. High pulses of *katG* activate INH, resulting in decreasing survival whereas persister formation was observed with low *katG* expression (Wakamoto et al., 2013).

Diauxic shifts and energy depletion lead to persister cell formation

There are several models that support the hypothesis that depletion of energy leads to persister formation. In *E. coli*, carbon source transitions during growth induces persister formation (Amato et al., 2013). During exponential growth, bacteria consume a preferred carbon source until exhaustion, then experience a lag period (called diauxic shift) in which the bacteria adjust their physiology to consume a secondary carbon source. Exponentially-growing *E. coli* that started consuming glucose, but was forced to consume fumarate once glucose was depleted, formed more persisters than if they continued to consume glucose (Amato et al., 2013). During glucose starvation, catabolite repression is turned off and the stringent response is activated (Traxler et al., 2008). After catabolite repression is turned off, adenylyl cyclase produces cyclic AMP (cAMP), which binds to the cAMP receptor protein to activate promoters for carbon

utilization, is increased, there is an increase in persisters. This effect requires ppGpp and a transcription factor, DksA (Amato et al., 2013).

Recent work in *S. aureus* propose that energy depletion by decreasing ATP is responsible for persister formation (Conlon et al., 2016). *S. aureus* persistence appears to be mediated by decreases in ATP, which they observe occurs upon entrance into stationary phase (Conlon et al., 2016). Although the work does not directly address Type I and Type II persister formation, it is important to note that their general observation that ATP levels decrease upon entrance into stationary phase is distinct from Type I persisters, which are pre-existing persisters in a growing population due to back-dilution from stationary phase overnight cultures (Balaban et al., 2004). Reporters for stationary phase, P_{cap5A}-*gfp* promoter for capsular polysaccharide expression and P_{arcA}-*gfp* for arginine deaminase, were activated upon entrance into stationary phase. Cells expressing P_{cap5A}-*gfp* were sorted into dim, middle, and bright and each fraction was treated with ciprofloxacin. Cells with bright GFP, indicating low ATP and entrance into stationary phase, had a greater number of persisters than middle or dim fractions. Furthermore, decreasing ATP levels using arsenate also increased persisters in ciprofloxacin. Thus, the work proposes that exponentially growing *S. aureus* cells randomly experience drops in ATP and prematurely enters stationary phase and become persisters.

Conlon et al. also test the importance of (p)ppGpp in mediating antibiotic tolerance in *S. aureus* and show no differences in antibiotic survival between wild type and *rsh* mutants. This directly contradicts our work in Chapter 3, where we show that (p)ppGpp plays a role in spontaneous and induced persistence. Further, in Chapter 3,

we show that ATP-depletion drugs, CCCP and arsenate, induce (p)ppGpp production in *B. subtilis*. Thus, ATP depletion causes (p)ppGpp to accumulate and GTP levels to drop, all of which promote persistence.

One of the traits that define persisters is dormancy. Much of the existing research support this model, from depletion of ATP which decreases ATP-dependent cellular processes, to increases in the toxin component of TA modules, and increases in (p)ppGpp to inhibit cellular activity (Conlon et al., 2016; Moyed and Bertrand, 1983; Verstraeten et al., 2015). However, there is evidence to suggest that metabolic dormancy is not a requirement for persistence. A cell division and metabolic activity reporter, dilution of accumulated mCherry protein and reductase activity to reduce redox sensor green respectively, was used to separate a population of *E. coli* into metabolically active and dormant populations (Orman and Brynildsen, 2013). FACS was used to separate cells by the cell division or metabolic activity reporter and each fraction was treated with antibiotics. Notably, the fractions containing actively dividing or metabolically active cells contained persisters albeit to a lesser extent than dormant cells. Further, metabolically inactive cells did not all become persisters. These data suggest that a threshold of persistence may occur and that individual events can still dictate whether these cells become persisters.

Importance

The relevance of persistence research is coming to light in the post-antibiotic era. In general, treatment of infections with antibiotics kills a majority of the bacteria and the host immune system can remove the remaining bacteria (Cohen et al., 2013). However, due to the fluctuation of antibiotic concentrations in the body or a compromised host

immune system, bacterial clearance is inefficient, causing the bacteria to regrow once antibiotic concentrations are sub-MIC, resulting in recurrent infections. Further, sublethal or fluctuating antibiotic concentrations may stimulate stress responses and lead to development of resistant bacteria from a persister population (Gullberg et al., 2011).

Persisters are a reservoir for antibiotic resistance to develop. That, coupled with misuse and wrongful prescription of antibiotics, and lack of new antibiotics has given rise to antibiotic resistance. One way to tackle this global threat is to determine the mechanisms of persister formation and thereby decrease persister populations.

Scope of dissertation

Based on the current literature, there are multiple mechanisms for persister formation and no clear agreement on the mechanisms of persistence. To this end, I sought to systematically determine the role of (p)ppGpp on persistence and stress survival.

In this thesis, I discovered that the alarmone (p)ppGpp, apart from its usual role as a modulator of transcription, is required for survival of nutrient downshift, responsible for Type I and Type II persister formation during treatment with bactericidal antibiotics, and prevents killing by bacteriostatic antibiotics.

Literature Cited

Abranches, J., Martinez, A.R., Kajfasz, J.K., Chávez, V., Garsin, D.A., and Lemos, J.A. (2009). The molecular alarmone (p)ppGpp mediates stress responses, vancomycin tolerance, and virulence in *Enterococcus faecalis*. J. Bacteriol. *191*, 2248–2256.

Achila, D., Gulati, M., Jain, N., and Britton, R. a (2012). Biochemical characterization of ribosome assembly GTPase RbgA in Bacillus subtilis. J. Biol. Chem. *287*, 8417–8423.

Agirrezabala, X., Fernández, I.S., Kelley, A.C., Cartón, D.G., Ramakrishnan, V., and Valle, M. (2013). The ribosome triggers the stringent response by RelA via a highly

distorted tRNA. EMBO Rep. 1–6.
Amato, S.M., Orman, M.A., and Brynildsen, M.P. (2013). Metabolic control of persister formation in *Escherichia coli*. Mol. Cell *50*, 475–487.
Arenz, S., Abdelshahid, M., Sohmen, D., Payoe, R., Starosta, A.L., Berninghausen, O., Hauryliuk, V., Beckmann, R., and Wilson, D.N. (2016). The stringent factor RelA adopts an open conformation on the ribosome to stimulate ppGpp synthesis. Nucleic Acids Res. *44*, 6471–6481.
Atkinson, G.C., Tenson, T., and Hauryliuk, V. (2011). The RelA/SpoT homolog (RSH) superfamily: distribution and functional evolution of ppGpp synthetases and hydrolases across the tree of life. PLoS One *6*, e23479.
Balaban, N.Q., Merrin, J., Chait, R., Kowalik, L., and Leibler, S. (2004). Bacterial persistence as a phenotypic switch. Science (80-.). *305*, 1622–1625.
Barker, M.M., Gaal, T., Josaitis, C.A., and Gourse, R.L. (2001). Mechanism of regulation of transcription initiation by ppGpp. I. Effects of ppGpp on transcription initiation *in vivo* and *in vitro*. J. Mol. Biol. *305*, 673–688.
Battesti, A., and Bouveret, E. (2006). Acyl carrier protein/SpoT interaction, the switch linking SpoT-dependent stress response to fatty acid metabolism. Mol. Microbiol. *62*, 1048–1063.
Beljantseva, J., Kudrin, P., Andresen, L., Shingler, V., Atkinson, G.C., Tenson, T., and Hauryliuk, V. (2017). Negative allosteric regulation of *Enterococcus faecalis* small alarmone synthetase RelQ by single-stranded RNA. Proc. Natl. Acad. Sci. *114*, 201617868.
Bigger, J.W. (1944). The bactericidal action of penicillin on *Staphylococcus pyogenes*. Ir. J. Med. Sci. *19*, 585–595.
Bittner, A.N., Kriel, A., and Wang, J.D. (2014). Lowering GTP level increases survival of amino acid starvation but slows growth rate for *Bacillus subtilis* cells lacking (p)ppGpp. J. Bacteriol. *196*, 2067–2076.
Black, D.S., Kelly, A.J., Mardis, M.J., and Moyed, H.S. (1991). Structure and organization of *hip*, an operon that affects lethality due to inhibition of peptidoglycan or DNA synthesis. J. Bacteriol. *173*, 5732–5739.
Boutte, C.C., and Crosson, S. (2011). The complex logic of stringent response regulation in Caulobacter crescentus: starvation signalling in an oligotrophic environment. Mol. Microbiol. *80*, 695–714.
Boutte, C.C., and Crosson, S. (2013). Bacterial lifestyle shapes stringent response activation. Trends Microbiol. *21*, 174–180.
Boutte, C.C., Henry, J.T., and Crosson, S. (2012). ppGpp and polyphosphate modulate cell cycle progression in *Caulobacter crescentus*. J. Bacteriol. *194*, 28–35.
Brauner, A., Fridman, O., Gefen, O., and Balaban, N.Q. (2016). Distinguishing between resistance, tolerance and persistence to antibiotic treatment. Nat. Rev. Microbiol. *14*, 320–330.
Britton, R.A. (2009). Role of GTPases in bacterial ribosome assembly. Annu. Rev. Microbiol. *63*, 155–176.
Brown, A., Fernández, I.S., Gordiyenko, Y., and Ramakrishnan, V. (2016). Ribosome-dependent activation of stringent control. Nature *534*, 1–16.
Cao, M., Kobel, P.A., Morshedi, M.M., Wu, M.F.W., Paddon, C., and Helmann, J.D. (2002). Defining the *Bacillus subtilis* σ^W regulon: a comparative analysis of

promoter consensus search, run-off transcription/macroarray analysis (ROMA), and transcriptional profiling approaches. J. Mol. Biol. *316*, 443–457.

Cashel, M., and Gallant, J. (1969). Two compounds implicated in the function of the RC gene in *Escherichia coli*. Nature *221*, 838–841.

Charity, J.C., Blalock, L.T., Costante-Hamm, M.M., Kasper, D.L., and Dove, S.L. (2009). Small molecule control of virulence gene expression in *Francisella tularensis*. PLoS Pathog. *5*, e1000641.

Cheverton, A.M., Gollan, B., Przydacz, M., Wong, C.T., Mylona, A., Hare, S.A., and Helaine, S. (2016). A *Salmonella* toxin promotes persister formation through acetylation of tRNA. Mol. Cell *63*, 86–96.

Cohen, N.R., Lobritz, M.A., and Collins, J.J. (2013). Microbial persistence and the road to drug resistance. Cell Host Microbe *13*, 632–642.

Conlon, B.P., Rowe, S.E., Gandt, A.B., Nuxoll, A.S., Donegan, N.P., Zalis, E.A., Clair, G., Adkins, J.N., Cheung, A.L., and Lewis, K. (2016). Persister formation in *Staphylococcus aureus* is associated with ATP depletion. Nat. Microbiol. *1*, 1–7.

Corrigan, R.M., Bellows, L.E., Wood, A., and Gründling, A. (2016). ppGpp negatively impacts ribosome assembly affecting growth and antimicrobial tolerance in Gram-positive bacteria. Proc. Natl. Acad. Sci. 201522179.

Cuthbert, B.J., Ross, W., Rohlfing, A.E., Dove, S.L., Gourse, R.L., Brennan, R.G., and Schumacher, M.A. (2017). Dissection of the molecular circuitry controlling virulence in *Francisella tularensis*. Genes Dev. *31*, 1–12.

Czarny, T.L., Perri, A.L., French, S., and Brown, E.D. (2014). Discovery of novel cell wall-active compounds using P_{ywaC}, a sensitive reporter of cell wall stress, in the model Gram-positive bacterium Bacillus subtilis. Antimicrob. Agents Chemother. *58*, 3261–3269.

D'Elia, M.A., Millar, K.E., Bhavsar, A.P., Tomljenovic, A.M., Hutter, B., Schaab, C., Moreno-Hagelsieb, G., and Brown, E.D. (2009). Probing teichoic acid genetics with bioactive molecules reveals new interactions among diverse processes in bacterial cell wall biogenesis. Chem. Biol. *16*, 548–556.

DeNapoli, J., Tehranchi, A.K., and Wang, J.D. (2013). Dose-dependent reduction of replication elongation rate by (p)ppGpp in *Escherichia coli* and *Bacillus subtilis*. Mol. Microbiol. *88*, 93–104.

Feng, B., Mandava, C.S., Guo, Q., Wang, J., Cao, W., Li, N., Zhang, Y., Zhang, Y., Wang, Z., Wu, J., et al. (2014). Structural and functional insights into the mode of action of a universally conserved Obg GTPase. PLoS Biol. *12*, e1001866.

Fridman, O., Goldberg, A., Ronin, I., Shoresh, N., and Balaban, N.Q. (2014). Optimization of lag time underlies antibiotic tolerance in evolved bacterial populations. Nature *513*, 418–421.

Friesen, J.D., Fiil, N.P., Parker, J.M., and Haseltine, W.A. (1974). A new relaxed mutant of *Escherichia coli* with an altered 50S ribosomal subunit. Proc Natl Acad Sci U S A *71*, 3465–3469.

Fung, D.K., Anderson, B.W., Tse, J.L., and Wang, J.D. (2017). Bacillus: Cellular and Molecular Biology (Caister Academic Press).

Gaca, A.O., Colomer-Winter, C., and Lemos, J.A. (2015). Many means to a common end: The intricacies of (p)ppGpp metabolism and its control of bacterial homeostasis. J. Bacteriol. *197*, 1146–1156.

Gerdes, K., and Maisonneuve, E. (2012). Bacterial persistence and toxin-antitoxin loci. Annu. Rev. Microbiol. *66*, 103–123.

Germain, E., Castro-Roa, D., Zenkin, N., and Gerdes, K. (2013). Molecular mechanism of bacterial persistence by HipA. Mol. Cell *52*, 248–254.

Gropp, M., Strausz, Y., Gross, M., and Glaser, G. (2001). Regulation of *Escherichia coli* RelA requires oligomerization of the C-terminal domain. J. Bacteriol. *183*, 570–579.

Gullberg, E., Cao, S., Berg, O.G., Ilbäck, C., Sandegren, L., Hughes, D., and Andersson, D.I. (2011). Selection of resistant bacteria at very low antibiotic concentrations. PLoS Pathog. *7*, 1–9.

Han, A.R., Kang, H.R., Son, J., Kwon, D.H., Kim, S., Lee, W.C., Song, H.K., Song, M.J., and Hwang, K.Y. (2016). The structure of the pleiotropic transcription regulator CodY provides insight into its GTP-sensing mechanism. Nucleic Acids Res. *44*, 9483–9493.

Handke, L.D., Shivers, R.P., and Sonenshein, A.L. (2008). Interaction of *Bacillus subtilis* CodY with GTP. J. Bacteriol. *190*, 798–806.

Harms, A., Fino, C., Sørensen, M.A., Semsey, S., and Gerdes, K. (2017). Prophages and growth dynamics confound experimental results with antibiotic-tolerant persister cells. MBio *8*, 1–18.

Haseltine, W.A., and Block, R. (1973). Synthesis of guanosine tetra- and pentaphosphate requires the presence of a codon-specific, uncharged transfer ribonucleic acid in the acceptor site of ribosomes. Proc. Natl. Acad. Sci. *70*, 1564–1568.

Hauryliuk, V., Atkinson, G.C., Murakami, K.S., Tenson, T., and Gerdes, K. (2015). Recent functional insights into the role of (p)ppGpp in bacterial physiology. Nat. Rev. Microbiol. *13*, 298–309.

Helaine, S., Cheverton, A.M., Watson, K.G., Faure, L.M., Matthews, S.A., and Holden, D.W. (2014). Internalization of *Salmonella* by macrophages induces formation of nonreplicating persisters. Science (80-.). *343*, 204–208.

Helmann, J.D. (2016). Bacillus subtilis extracytoplasmic function (ECF) sigma factors and defense of the cell envelope. Curr. Opin. Microbiol. *30*, 122–132.

Hogg, T., Mechold, U., Malke, H., Cashel, M., and Hilgenfeld, R. (2004). Conformational antagonism between opposing active sites in a bifunctional RelA/SpoT homolog modulates (p)ppGpp metabolism during the stringent response. Cell *117*, 57–68.

Jenvert, R.-M., and Schiavone, L.H. (2007). The flexible N-terminal domain of ribosomal protein L11 from *Escherichia coli* is necessary for the activation of stringent factor. J. Mol. Biol. *365*, 764–772.

Kanjee, U., Ogata, K., and Houry, W.A. (2012). Direct binding targets of the stringent response alarmone (p)ppGpp. Mol. Microbiol. *85*, 1029–1043.

Kint, C., Verstraeten, N., Hofkens, J., Fauvart, M., and Michiels, J. (2014). Bacterial Obg proteins: GTPases at the nexus of protein and DNA synthesis. Crit. Rev. Microbiol. *40*, 207–224.

Korch, S.B., Henderson, T. a., and Hill, T.M. (2003). Characterization of the *hipA7* allele of *Escherichia coli* and evidence that high persistence is governed by (p)ppGpp synthesis. Mol. Microbiol. *50*, 1199–1213.

Krásný, L., and Gourse, R. (2004). An alternative strategy for bacterial ribosome synthesis: *Bacillus subtilis* rRNA transcription regulation. EMBO J. *23*, 4473–4483.

Kriel, A., Bittner, A.N., Kim, S.H., Liu, K., Tehranchi, A.K., Zou, W.Y., Rendon, S., Chen, R., Tu, B.P., and Wang, J.D. (2012). Direct regulation of GTP homeostasis by (p)ppGpp: A critical component of viability and stress resistance. Mol. Cell *48*, 231–241.

Kriel, A., Brinsmade, S.R., Tse, J.L., Tehranchi, A.K., Bittner, A.N., Sonenshein, A.L., and Wang, J.D. (2014). GTP dysregulation in *Bacillus subtilis* cells lacking (p)ppGpp results in phenotypic amino acid auxotrophy and failure to adapt to nutrient downshift and regulate biosynthesis genes. J. Bacteriol. *196*, 189–201.

Li, W., Bouveret, E., Zhang, Y., Liu, K., Wang, J.D., and Weisshaar, J.C. (2016). Effects of amino acid starvation on RelA diffusive behavior in live *Escherichia coli*. Mol. Microbiol. *99*, 571–585.

Liu, K., Bittner, A.N., and Wang, J.D. (2015a). Diversity in (p)ppGpp metabolism and effectors. Curr. Opin. Microbiol. *24*, 72–79.

Liu, K., Myers, A.R., Pisithkul, T., Claas, K.R., Satyshur, K.A., Amador-Noguez, D., Keck, J.L., and Wang, J.D. (2015b). Molecular mechanism and evolution of guanylate kinase regulation by (p)ppGpp. Mol. Cell *57*, 735–749.

Loveland, A.B., Bah, E., Madireddy, R., Zhang, Y., Brilot, A.F., Grigorieff, N., and Korostelev, A.A. (2016). Ribosome-RelA structures reveal the mechanism of stringent response activation. Elife *5*, 1–23.

Maisonneuve, E., Shakespeare, L.J., Girke, M., and Gerdes, K. (2011). Bacterial persistence by RNA endonucleases. Proc. Natl. Acad. Sci. *108*, 13206–13211.

Maisonneuve, E., Castro-Camargo, M., and Gerdes, K. (2013). (p)ppGpp controls bacterial persistence by stochastic induction of toxin-antitoxin activity. Cell *154*, 1140–1150.

Majerczyk, C.D., Dunman, P.M., Luong, T.T., Lee, C.Y., Sadykov, M.R., Somerville, G.A., Bodi, K., and Sonenshein, A.L. (2010). Direct targets of CodY in *Staphylococcus aureus*. J. Bacteriol. *192*, 2861–2877.

Mechold, U., Potrykus, K., Murphy, H., Murakami, K.S., and Cashel, M. (2013). Differential regulation by ppGpp versus pppGpp in Escherichia coli. Nucleic Acids Res. *41*, 6175–6189.

Molle, V., Nakaura, Y., Shivers, R.P., Yamaguchi, H., Losick, R., Fujita, Y., and Sonenshein, A.L. (2003). Additional targets of the *Bacillus subtilis* global regulator CodY identified by chromatin immunoprecipitation and genome-wide transcript analysis. J. Bacteriol. *185*, 1911–1922.

Montgomery, C.P., Boyle-Vavra, S., Roux, A., Ebine, K., Sonenshein, A.L., and Daumb, R.S. (2012). CodY deletion enhances in vivo virulence of community-associated methicillin-resistant *Staphylococcus aureus* clone USA300. Infect. Immun. *80*, 2382–2389.

Moyed, H.S., and Bertrand, K.P. (1983). *hipA*, a newly recognized gene of *Escherichia coli* K-12 that affects frequency of persistance after inhibition of murein synthesis. J. Bacteriol. *155*, 768–775.

Nanamiya, H., Kasai, K., Nozawa, A., Yun, C.-S., Narisawa, T., Murakami, K., Natori, Y., Kawamura, F., and Tozawa, Y. (2008). Identification and functional analysis of novel (p)ppGpp synthetase genes in *Bacillus subtilis*. Mol. Microbiol. *67*, 291–304.

Nguyen, D., Joshi-Datar, A., Lepine, F., Bauerle, E., Olakanmi, O., Beer, K., McKay, G., Siehnel, R., Schafhauser, J., Wang, Y., et al. (2011). Active starvation responses

mediate antibiotic tolerance in biofilms and nutrient-limited bacteria. Science *334*, 982–986.

Nomura, Y., Takabayashi, T., Kuroda, H., Yukawa, Y., Sattasuk, K., Akita, M., Nozawa, A., and Tozawa, Y. (2012). ppGpp inhibits peptide elongation cycle of chloroplast translation system in vitro. Plant Mol. Biol. *78*, 185–196.

Nomura, Y., Izumi, A., Fukunaga, Y., Kusumi, K., Iba, K., Watanabe, S., Nakahira, Y., Weber, A.P.M., Nozawa, A., and Tozawa, Y. (2014). Diversity in guanosine 3',5'-bisdiphosphate (ppGpp) sensitivity among guanylate kinases of bacteria and plants. J. Biol. Chem. *289*, 15631–15641.

Orman, M.A., and Brynildsen, M.P. (2013). Dormancy is not necessary or sufficient for bacterial persistence. Antimicrob. Agents Chemother. *57*, 3230–3239.

Paul, B.J., Barker, M.M., Ross, W., Schneider, D. a, Webb, C., Foster, J.W., and Gourse, R.L. (2004). DksA: A critical component of the transcription initiation machinery that potentiates the regulation of rRNA promoters by ppGpp and the initiating NTP. Cell *118*, 311–322.

Porse, B.T., and Garrett, R. a (1999). Ribosomal mechanics, antibiotics, and GTP hydrolysis. Cell *97*, 423–426.

Potrykus, K., and Cashel, M. (2008). (p)ppGpp: Still magical? Annu. Rev. Microbiol. *62*, 35–51.

Potrykus, K., Murphy, H., Philippe, N., and Cashel, M. (2011). ppGpp is the major source of growth rate control in *E. coli*. Environ. Microbiol. *13*, 563–575.

Pu, Y., Zhao, Z., Li, Y., Zou, J., Ma, Q., Zhao, Y., Ke, Y., Zhu, Y., Chen, H., Baker, M.A.B., et al. (2016a). Enhanced efflux activity facilitates drug tolerance in dormant bacterial cells. Mol. Cell *62*, 284–294.

Pu, Y., Ke, Y., and Bai, F. (2016b). Active efflux in dormant bacterial cells – new insights into antibiotic persistence. Drug Resist. Updat. *30*, 7–14.

Roelofs, K.G., Wang, J., Sintim, H.O., and Lee, V.T. (2011). Differential radial capillary action of ligand assay for high-throughput detection of protein-metabolite interactions. Proc. Natl. Acad. Sci. U. S. A. *108*, 15528–15533.

Rojas, A.M., Ehrenberg, M., Andersson, S.G.E., and Kurland, C.G. (1984). ppGpp inhibition of elongation factors Tu, G and Ts during polypeptide synthesis. Mol. Gen. Genet. *197*, 36–45.

Ross, W., Vrentas, C.E., Sanchez-Vazquez, P., Gaal, T., and Gourse, R.L. (2013). The magic spot: A ppGpp binding site on *E. coli* RNA polymerase responsible for regulation of transcription initiation. Mol. Cell *50*, 420–429.

Ross, W., Sanchez-Vazquez, P., Chen, A.Y., Lee, J.H., Burgos, H.L., and Gourse, R.L. (2016). ppGpp binding to a site at the RNAP-DksA interface accounts for Its dramatic effects on transcription initiation during the stringent response. Mol. Cell *62*, 811–823.

Roux, A., Todd, D.A., Velázquez, J. V., Cech, N.B., and Sonenshein, A.L. (2014). CodY-mediated regulation of the *Staphylococcus aureus* Agr system integrates nutritional and population density signals. J. Bacteriol. *196*, 1184–1196.

Rymer, R.U., Solorio, F.A., Tehranchi, A.K., Chu, C., Corn, J.E., Keck, J.L., Wang, J.D., and Berger, J.M. (2012). Binding mechanism of metal·NTP substrates and stringent-response alarmones to bacterial DnaG-type primases. Structure *20*, 1478–1489.

Schaefer, L., Uicker, W.C., Wicker-Planquart, C., Foucher, A.-E., Jault, J.-M., and Britton, R. a (2006). Multiple GTPases participate in the assembly of the large ribosomal subunit in Bacillus subtilis. J. Bacteriol. *188*, 8252–8258.

Schumacher, M.A., Balani, P., Min, J., Chinnam, N.B., Hansen, S., Vulić, M., Lewis, K., and Brennan, R.G. (2015). HipBA–promoter structures reveal the basis of heritable multidrug tolerance. Nature *524*, 59–64.

Shyp, V., Tankov, S., Ermakov, A., Kudrin, P., English, B.P., Ehrenberg, M., Tenson, T., Elf, J., and Hauryliuk, V. (2012). Positive allosteric feedback regulation of the stringent response enzyme RelA by its product. EMBO Rep. *13*, 835–839.

Smith, I., Paress, P., and Pestkaf, S. (1978). Thiostrepton-resistant mutants exhibit relaxed synthesis of RNA. Proc. Natl. Acad. Sci. *75*, 5993–5997.

Srivatsan, A., Han, Y., Peng, J., Tehranchi, A.K., Gibbs, R., Wang, J.D., and Chen, R. (2008). High-precision, whole-genome sequencing of laboratory strains facilitates genetic studies. PLoS Genet. *4*, 1–14.

Srivatsan, A., Tehranchi, A., MacAlpine, D.M., and Wang, J.D. (2010). Co-orientation of replication and transcription preserves genome integrity. PLoS Genet. *6*, e1000810.

Steinchen, W., Schuhmacher, J.S., Altegoer, F., Fage, C.D., Srinivasan, V., Linne, U., Marahiel, M.A., and Bange, G. (2015). Catalytic mechanism and allosteric regulation of an oligomeric (p)ppGpp synthetase by an alarmone. Proc. Natl. Acad. Sci. U. S. A. *112*, 13348–13353.

Traxler, M.F., Summers, S.M., Nguyen, H.-T., Zacharia, V.M., Hightower, G.A., Smith, J.T., and Conway, T. (2008). The global, ppGpp-mediated stringent response to amino acid starvation in *Escherichia coli*. Mol. Microbiol. *68*, 1128–1148.

Verstraeten, N., Knapen, W.J., Kint, C.I., Liebens, V., Van den Bergh, B., Dewachter, L., Michiels, J.E., Fu, Q., David, C.C., Fierro, A.C., et al. (2015). Obg and membrane depolarization are part of a microbial bet-hedging strategy that leads to antibiotic tolerance. Mol. Cell *59*, 9–21.

Wakamoto, Y., Dhar, N., Chait, R., Schneider, K., Signorino-Gelo, F., Leibler, S., and McKinney, J.D. (2013). Dynamic persistence of antibiotic-stressed mycobacteria. Science (80-.). *339*, 91–95.

Wang, J.D., Sanders, G.M., and Grossman, A.D. (2007). Nutritional control of elongation of DNA replication by (p)ppGpp. Cell *128*, 865–875.

Wendrich, T.M., and Marahiel, M.A. (1997). Cloning and characterization of a relA/spoT homologue from Bacillus subtilis. Mol. Microbiol. *26*, 65–79.

Wendrich, T.M., Blaha, G., Wilson, D.N., Marahiel, M. a, and Nierhaus, K.H. (2002). Dissection of the mechanism for the stringent factor RelA. Mol. Cell *10*, 779–788.

Wimberly, B.T., Guymon, R., McCutcheon, J.P., White, S.W., and Ramakrishnan, V. (1999). A detailed view of a ribosomal active site: the structure of the L11-RNA complex. Cell *97*, 491–502.

Yang, X., and Ishiguro, E.E. (2001). Involvement of the N terminus of ribosomal protein L11 in regulation of the RelA protein of *Escherichia coli*. J. Bacteriol. *183*, 6532–6537.

Zhang, S., and Haldenwang, W.G. (2003). RelA is a component of the nutritional stress activation pathway of the *Bacillus subtilis* transcription factor σ^B. J. Bacteriol. *185*, 5714–5721.

Chapter 2: GTP dysregulation in *Bacillus subtilis* cells lacking (p)ppGpp results in phenotypic amino acid auxotrophy and failure to adapt to nutrient downshift and regulate biosynthesis genes

This chapter is adapted from "Kriel, A., Brinsmade, S.R., Tse, J.L., Tehranchi, A.K., Bittner, A.N., Sonenshein, A.L., and Wang, J.D. (2014) GTP dysregulation in *Bacillus subtilis* cells lacking (p)ppGpp results in phenotypic amino acid auxotrophy and failure to adapt to nutrient downshift and regulate biosynthesis genes. *Journal of Bacteriology*, 196(1): 189-201"

J.T.B. performed the nutrient downshift experiments in Figures 1F and 6 and participated in discussion and editing of the manuscript.

Abstract

The nucleotide (p)ppGpp inhibits GTP biosynthesis in the Gram-positive bacterium *Bacillus subtilis*. Here we examined how this regulation allows cells to grow in the absence of amino acids. We showed that *B. subtilis* cells lacking (p)ppGpp, due to either deletions or point mutations in all three (p)ppGpp synthetase genes, *yjbM*, *ywaC*, and *relA*, strongly require supplementation of leucine, isoleucine, valine, methionine, and threonine and modestly require three additional amino acids. This polyauxotrophy is rescued by reducing GTP levels. Reduction of GTP levels activates transcription of genes responsible for the biosynthesis of the five strongly required amino acids by inactivating the transcription factor CodY, which represses the *ybgE*, *ilvD*, *ilvBHC-leuABCD*, *ilvA*, *ywaA*, and *hom-thrCB* operons, and by a CodY-independent activation of transcription of the *ilvA*, *ywaA*, *hom-thrCB*, and *metE* operons. Interestingly, providing the eight required amino acids does not allow for colony formation of (p)ppGpp^0 cells when transitioning from amino acid-replete medium to amino acid-limiting medium, and we found that this is due to an additional role that (p)ppGpp plays in protecting cells during nutrient downshifts. We conclude that (p)ppGpp allows adaptation to amino acid limitation by a combined effect of preventing death during metabolic transitions and sustaining growth by activating amino acid biosynthesis. This ability of (p)ppGpp to integrate a general stress response with a targeted reprogramming of gene regulation allows appropriate adaptation and is likely conserved among diverse bacteria.

Introduction

Bacteria employ an extensive network of regulatory mechanisms to tune cellular metabolism and gene expression in response to diverse nutritional conditions. The general stress response mechanisms are integrated with specific regulatory programs controlling the expression of biosynthesis genes, and the proper coupling of these processes ensures viability and allows optimal growth under shifting nutrient conditions.

In bacteria, the stringent response, mediated by the nucleotide guanosine penta- or tetra- phosphate, or collectively (p)ppGpp, alerts cells to nutrient limitation and is also involved in regulation of amino acid biosynthesis (Potrykus and Cashel, 2008). *Escherichia coli* cells that cannot produce (p)ppGpp [referred to as (p)ppGpp^0] require approximately eleven amino acids for growth, but the identities of the required amino acids vary depending on the strain background (Murphy and Cashel, 2003; Xiao et al., 1991). In *E. coli*, (p)ppGpp upregulates several amino acid biosynthesis genes directly by binding to RNA polymerase (RNAP) or indirectly by passive redistribution of RNAPs that are released upon (p)ppGpp-mediated inhibition of transcription of stable RNA and other genes (Barker et al., 2001; Paul et al., 2004). However, transcriptome analyses showed that upon isoleucine starvation, amino acid biosynthesis genes are not induced *en masse* (Traxler et al., 2008). Additionally, supplementing the medium with the auxotrophic requirements alone does not allow efficient colony formation of (p)ppGpp^0 cells, an unsolved mystery (Xiao et al., 1991).

In other bacteria, (p)ppGpp is also required for viability in the absence of amino acids. In the Gram-positive bacterium *Bacillus subtilis*, (p)ppGpp is synthesized by three enzymes: RelA, YjbM, and YwaC (Nanamiya et al., 2008; Srivatsan et al., 2008;

Wendrich and Marahiel, 1997). Deleting all three (p)ppGpp synthetase genes results in cells that cannot form colonies on minimal medium containing glucose but can form colonies with supplementation of all twenty amino acids, confirming that these cells are auxotrophic for certain amino acids (Kriel et al., 2012). Deletion of *relA* alone rendered *B. subtilis* cell growth strongly dependent on externally supplemented valine and weakly dependent on leucine, isoleucine, and methionine (Brinsmade and Sonenshein, 2011), the precise auxotrophic requirements of (p)ppGpp^0 cells are unknown.

(p)ppGpp^0 cells have high levels of GTP, and the inability of (p)ppGpp^0 cells to form colonies on minimal medium can be suppressed by mutations in *guaA*, *guaB*, and *gmk*, which encode enzymes in the GTP biosynthesis pathway, and by mutations in *codY*, which encodes the global transcriptional regulator CodY (Kriel et al., 2012). High levels of GTP activate CodY (Brinsmade and Sonenshein, 2011) to repress multiple genes in the biosynthetic pathways for the branched-chain amino acids (BCAA) (isoleucine, leucine, and valine) (Molle et al., 2003), threonine, and arginine (Belitsky and Sonenshein, 2013). In addition, GTP and ATP levels are often inversely correlated, and increased levels of ATP stimulate transcription of the BCAA biosynthetic genes *ilvB* and *ywaA*, both of which initiate with ATP (Krásný et al., 2008). However, the relative contributions of these mechanisms to (p)ppGpp-dependent prototrophy and how the lack of cellular (p)ppGpp can be circumvented by mutations in *codY* and GTP biosynthesis are not understood.

To answer these questions, we determined the precise amino acid requirements in *B. subtilis* (p)ppGpp cells and identified broader amino acid requirements than previously observed. Strong requirements for BCAAs, methionine, and threonine and

mild requirements for three additional amino acids were found. We then systematically characterized the effects of (p)ppGpp, CodY, and GTP levels on global transcription profiles to reveal their relative contributions to the amino acid auxotrophy of (p)ppGpp^0 cells. Finally, we found an apparent residual amino acid requirement when supplementation of all eight defined auxotrophic requirements was insufficient to restore colony formation and this was due to a failure of (p)ppGpp^0 cells to survive a sudden nutrient downshift.

Materials and Methods

Bacterial strains, media, and growth conditions. All *B. subtilis* strains are derivatives of SMY (Schaeffer et al., 1965) and are listed in Table 1. For liquid growth, cells were grown in S7 defined synthetic medium (Vasantha and Freese, 1980) containing 5 mM potassium phosphate (pH 7.0), 10 mM $(NH_4)_2SO_4$, 2 mM $MgCl_2$, 0.7 mM $CaCl_2$, 50 mM $MnCl_2$, 5 mM $FeCl_3$, 1 mM $ZnCl_2$, 2 mM thiamine, and 50 mM 3-(N-morpholino) propanesulfonic acid (MOPS), supplemented with 0.1% (wt/vol) glutamate, 1% (wt/vol) glucose, 0.5% (wt/vol) Casamino Acids (Bacto Casamino Acids, BD223050), and 0.02 mg/ml tryptophan (which is not present in Casamino Acids). Cells were grown at 37 °C with vigorous shaking (250 rpm). For growth on solid medium, cells were plated on 1.5% (wt/vol) agar with Spizizen minimal salts, 1% (wt/vol) glucose, and 0.1% (wt/vol) glutamate. Where indicated, defined solid medium was supplemented with 0.05 mg/ml of each amino acid, with the exception of 0.5 mg/ml aspartic acid and glutamic acid, 0.02 mg/ml tryptophan and tyrosine, and 0.04 mg/ml cysteine (Harwood et al., 1990).

Strain construction. Strain JDW1464 (*relA*^{D264G} *ywaC*^{D87G} *yjbM*^{D72G}) was created by substituting a conserved aspartic acid residue in each of the three (p)ppGpp

synthetases, corresponding to D264 in RelA, D87 in YwaC, and D72 in YjbM, with glycine (Figure 1C). To change these residues, regions of *relA*, *ywaC*, or *yjbM* were first cloned into the EcoRI site of pJW299 (Kriel et al., 2012) to create pJW368, pJW369, and pJW370, respectively. Site-directed mutagenesis was then performed with the QuikChange site-directed mutagenesis kit to create pJW371, pJW372, and pJW373, respectively. The following mutagenic primers were used (capital letters denote sites of mutation): for *relA*, oJW984 (ggacagccaacaaaCcgtaaatttcattga) and oJW985 (tcaatgaaatttacgGtttgttggctgtcc); for *ywaC*, oJW992 (gcacgcc ggcaatgCcgtgaatatgctcctt) and oJW993 (aaggagcatattcacgGcattgccggcgt gc); for *yjbM*, oJW988 (ctaaggccagcaatgCcctgcatggtttcaa) and oJW989 (tt gaaaccatgcaggGcattgctggccttag).

The mutations were introduced into SMY sequentially (*ywaC*, followed by *yjbM*, and lastly *relA*). At each step, plasmid pJW371 (or pJW372 or pJW373) was integrated into the chromosome by transformation (selected for chloramphenicol resistance), followed by subsequent transformation with pSS4332 (expressing I-SceI endonuclease; a kind gift from Scott Stibitz) to introduce a double-strand break that promotes recombination and loss of the integrated plasmid (Janes and Stibitz, 2006). Mutant alleles were confirmed by sequencing.

To reduce expression of *guaB*, pJW305 was created by inserting a 5' fragment of guaB, from 22 bp upstream of ATG to 500 bp into the coding region (includes the ribosome-binding site but not the promoter) between the HindIII and EcoRI sites of pMUTIN4. JDW1391 [$guaB^{down}$ (p)ppGpp^0] was created by integrating pJW305 into the chromosome of Δ*ywaC*::*kan* Δ*yjbM*::*spc* strain, placing *guaB* under tight P_{spac}-dependent (isopropyl- β-D-thiogalactopyranoside [IPTG]-inducible) control. The

guaB^{down} allele was confirmed by sequencing. The *relA* allele was introduced as the last step in strain construction. To deplete *guaB*, *guaB*^{down} cells were grown in medium lacking IPTG.

JDW1392 [*ilvB*^{up} (p)ppGpp^{0}] was created by sequentially transforming deletions of *ywaC*, *yjbM*, and *relA* into SRB107 (*ilvBp4 ilvBp*ΔT2) (Brinsmade et al., 2010). JDW1824 [BCAA^{up} (p)ppGpp^{0}] was created by sequentially transforming deletions of *ywaC*, *yjbM*, and *relA* into SRB194 (*ilvBp4 ilvBp*ΔT2 *ybgEp*ΔCBS3 *ilvDp*ΔCBS) (Brinsmade et al., 2010).

Measurement of intracellular nucleotides by TLC. Nucleotides were extracted, analyzed by thin-layer chromatography (TLC), and measured using a PhosphorImager, as described previously (Wang et al., 2007). Cells were treated for 20 min with arginine hydroxamate (RHX) (0.5 mg/ml) to mimic amino acid starvation by depleting charged arginine-tRNAs or with guanosine (Guo) (1 mM) to increase intracellular GTP pools via the salvage pathway (Kriel et al., 2012).

Microarray-based gene expression profiling. Wild-type, (p)ppGpp^{0}, Δ*codY* (p)ppGpp^{0}, and *guaB*^{down} (p)ppGpp^{0} cells were grown to an optical density at 600 nm (OD_{600}) of ~0.3 and treated for 20 min with RHX (0.5 mg/ml) to induce the stringent response or guanosine (1 mM) to increase GTP levels. Samples were collected by rapidly mixing cultures with equal volumes of methanol at -20 °C. Cells were then pelleted by centrifugation at 4,000 X g for 5 min. RNA was isolated using the Qiagen RNeasy kit. The procedures for reverse transcription, labeling, hybridization, and analysis were performed as described previously. Transcript levels were normalized to a common reference mixture, and data were filtered to include only significantly affected genes

(1,524 genes). For identification of significantly affected genes, significance analysis of microarrays (SAM analysis) was performed as multiclass among all samples (i.e., 12 classes, 3 replicates each); significantly affected genes were selected using a *q* value cutoff of <0.01. Transcript levels of the 1,524 significantly altered genes were hierarchically clustered (centered, average linkage) using the software program Cluster and plotted using the program TreeView.

Results

Loss of (p)ppGpp synthetase activity in B. subtilis results in failure to grow on minimal medium

In *B. subtilis*, (p)ppGpp is synthesized by three enzymes: a large bifunctional enzyme, RelA (Wendrich and Marahiel, 1997), and two small enzymes, YwaC and YjbM (Nanamiya et al., 2008; Srivatsan et al., 2008) (Figure 1A, 1B). We have previously shown that deletion of all three genes (Δ*relA* Δ*ywaC* Δ*yjbM*) from the prototrophic *B. subtilis* strain SMY results in failure to form colonies on minimal medium (Kriel et al., 2012). To confirm the phenotypes we observed are due to loss of (p)ppGpp synthesis activities rather than other potential functions of RelA, YwaC, or YjbM, we inactivated the synthetase activity of each enzyme by mutating a conserved active site residue required for (p)ppGpp synthesis based on the homology to the RelA enzyme from *Streptococcus equisimilis* (SeqRel) (Figure 1C) (Hogg et al., 2004). The mutation of this conserved residue in all three (p)ppGpp synthetases of *B. subtilis* resulted in *relA*^{D264G} *ywaC*^{D87G} *yjbM*^{D72G} strain, which cannot synthesize TLC-detectable (p)ppGpp but the encoded proteins are expected to retain their three-dimensional structure.

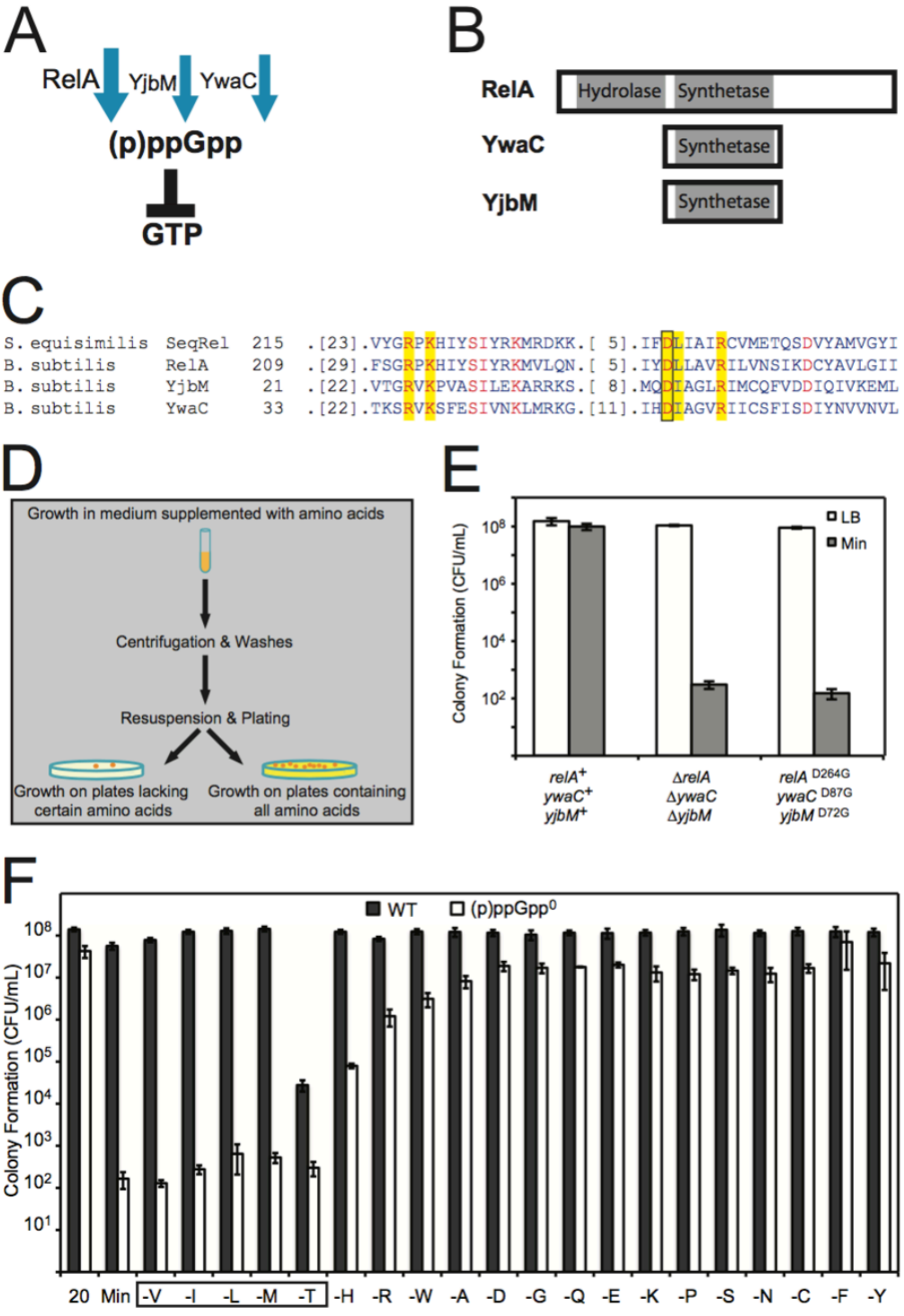

Figure 1. (p)ppGpp synthesis is required for amino acid prototrophy. A. In *B. subtilis*, the enzymes RelA, YwaC, and YjbM synthesize (p)ppGpp. The bifunctional enzyme RelA also hydrolyzes (p)ppGpp. B. Conserved N-terminal (p)ppGpp synthetase and hydrolase domains of YwaC, YjbM, and RelA. C. Sequence alignment showing the conserved residues (red), active site residues (highlighted in yellow), and aspartic acid active site residue (boxed) that when mutated in the *S. equisimilis* RelA protein

abolishes (p)ppGpp synthetase activity without affecting hydrolase activity. The respective conserved aspartic acid residues (RelA^{D264}, YwaC^{D87}, and YjbM^{D72}), aligned using the Conserved Domain Database (Marchler-Bauer et al., 2011), were mutated in each (p)ppGpp synthetase of *B. subtilis* to abolish (p)ppGpp synthetase activity without affecting other potential functions of these proteins. D. Schematic of the plating efficiency assay for determining amino acid auxotrophy. E. Wild-type (*relA*$^{+}$ *ywaC*$^{+}$ *yjbM*$^{+}$), synthetase deletion (Δ*relA* Δ*ywaC* Δ*yjbM*), and synthetase point mutant (*relA*^{D264G} *ywaC*^{D87G} *yjbM*^{D72G}) cells were plated on LB and minimal medium (Min) plates, and colonies were counted the next day. “CFU/ml” indicates CFU per ml of culture, normalized to an OD_{600} of 1. F. (p)ppGpp^{0} cells display strong requirements for valine, leucine, isoleucine, threonine, and methionine (boxed); (p)ppGpp^{0} cells also display weaker requirements for arginine, histidine, and tryptophan. Cells were grown in medium supplemented with Casamino Acids, washed, and then plated on defined medium plates supplemented with all twenty amino acids (denoted by 20) or supplemented with only nineteen amino acids (denoted as “-X” to indicate the amino acid that was not added in the indicated plates). Colonies were counted the next day.

Using a plating assay (Figure 1D) in which cells were grown in liquid medium supplemented with Casamino Acids and then plated on minimal or rich solid media to compare the CFU, we confirmed that loss of (p)ppGpp synthesis, via gene deletions (Δ*relA* Δ*ywaC* Δ*yjbM*) or point mutations (*relA*^{D264G} *ywaC*^{D87G} *yjbM*^{D72G}), renders cells incapable of forming colonies on minimal media (except for spontaneous suppressor mutants, which form at a frequency of ~10^{-5}) (Figure 1E). Therefore, the synthesis of (p)ppGpp, rather than other protein functions, allows cells to grow on minimal media.

B. subtilis (p)ppGpp^0 cells are auxotrophic for multiple amino acids in addition to BCAA

The inability of (p)ppGpp^0 cells to form colonies on minimal medium indicates that they are auxotrophic for certain amino acids. To determine the precise amino acid requirements of (p)ppGpp^0 cells, we examined their ability to form colonies on twenty amino acid dropout plates, each lacking one amino acid, similar to experiments performed in *E. coli* (Xiao et al., 1991). Wild-type SMY forms colonies on any group of nineteen amino acids with the same efficiency as on all twenty amino acids, with the exception of plates lacking threonine, which has decreased plating efficiency (Figure 1F). The partial requirement for threonine may be due to feedback inhibition of Hom (homoserine dehydrogenase) by isoleucine and methionine, both downstream products of threonine (Yeggy and Stahly, 1980). In contrast to wild-type cells, (p)ppGpp^0 cells exhibited strong requirements for BCAA, methionine, and threonine, and moderate requirements for histidine, arginine, and tryptophan (Figure 1F). These requirements are far more stringent than those of Δ*relA* cells, which have a strong requirement for valine and modest requirements for leucine, isoleucine, methionine (Wendrich and Marahiel, 1997).

We previously performed a genetic screen revealing that the requirements for exogenous amino acids in (p)ppGpp^0 cells can be relieved by loss-of-function mutations in the GTP biosynthesis genes *guaA*, *guaB*, and *gmk* and in the transcriptional regulator *codY* (Figure 2A) (Kriel et al., 2012), suggesting that CodY and/or GTP are responsible for the auxotrophy. However, further analysis of these strains was limited by the tryptophan and methionine auxotrophies of the background strain (YB886) due to mutations in the biosynthesis genes *trpC* and *metB* (Yasbin et al., 1980). To comprehensively test the effects of CodY and GTP on (p)ppGpp^0 strain auxotrophies, we used the prototrophic SMY strain (Schaeffer et al., 1965). We constructed a Δ*relA* Δ*ywaC* Δ*yjbM* Δ*codY* strain to eliminate CodY activity. Deletions of *codY* partially suppressed the plating efficiency defect of (p)ppGpp^0 cells on minimal medium (Figure 2B, Min). Plating on amino acid dropout plates revealed that deletion of *codY* relieved the strong requirements for valine, isoleucine, leucine, methionine, and threonine, and the moderate requirement for arginine, but partially relieved the requirements for histidine and tryptophan (Figure 2B). We also reduced expression of *guaB*, encoding the IMP dehydrogenase, which synthesizes XMP from IMP, in (p)pGpp^0 SMY cells (Figure 2A). Because *guaB* was reported to be an essential gene (Kobayashi et al., 2003), we placed it under an IPTG-inducible promoter at its endogenous locus. Reduction in *guaB* expression (*guaB*^{down}), when IPTG was removed from the medium, relieved the requirement for all eight amino acids of (p)ppGpp^0 cells in the SMY background (Figure 2B), indicating that reduction of GTP biosynthesis suppressed all auxotrophies of (p)ppGpp^0 cells.

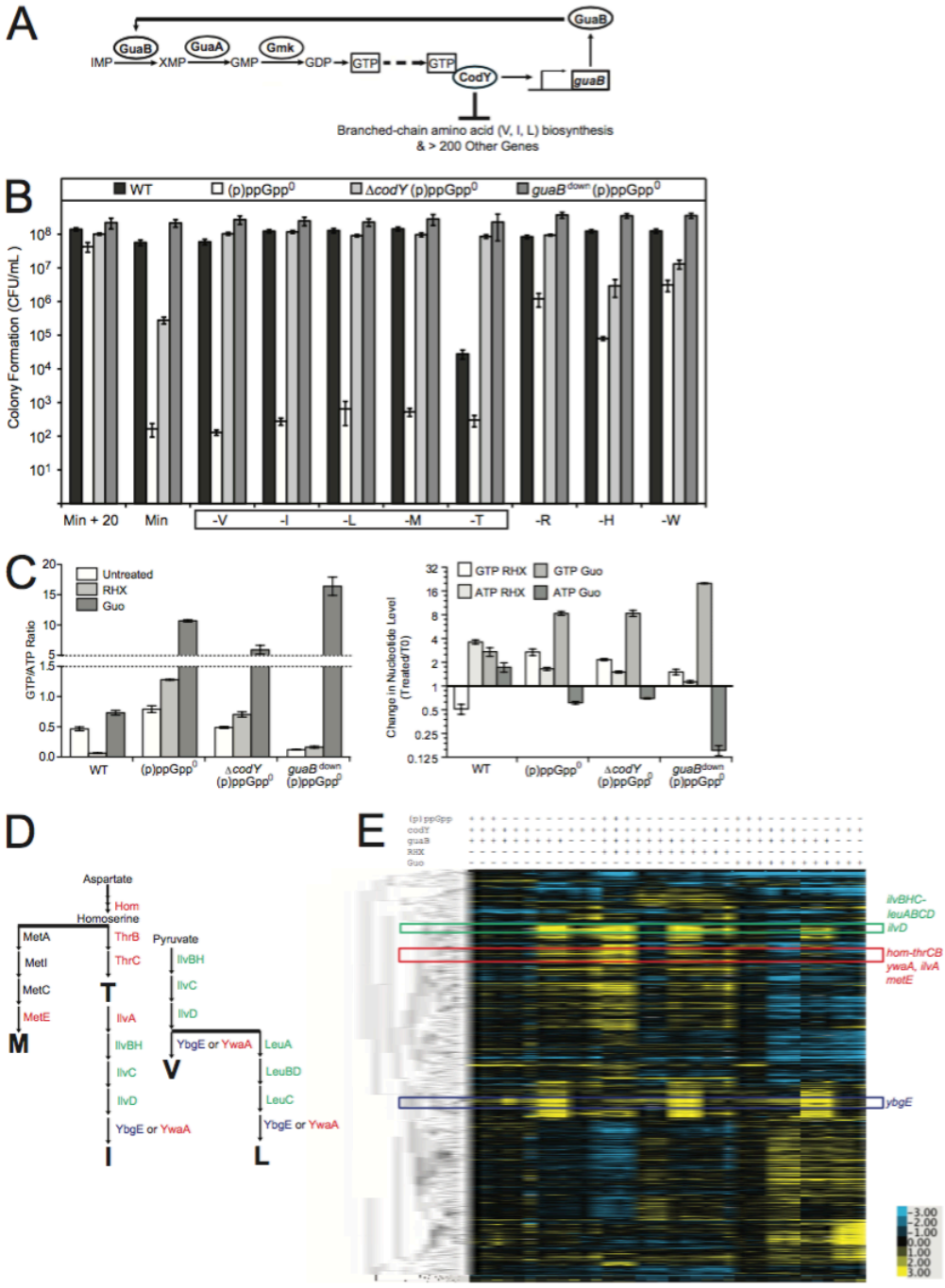

Figure 2. Effects of (p)ppGpp, *guaB*, and *codY* on global transcription profiles of *B. subtilis* cells. A. Schematic of the pathways affected by the (p)ppGpp^0 suppressor mutations. GuaB, GuaA, and Gmk are enzymes in the GTP biosynthesis pathway. GTP activates CodY. CodY activates transcription of *guaB* and represses numerous other genes, including those involved in biosynthesis of BCAA: valine, isoleucine, and leucine. B. Colony formation of WT, (p)ppGpp^0, Δ*codY* (p)ppGpp^0, and *guaB*^{down} (p)ppGpp^0 cells on plates supplemented with all twenty amino acids or plates lacking valine (V), isoleucine (I), leucine (L), methionine (M), threonine (T), arginine (R), histidine (H), or

tryptophan (W). Cells were plated as indicated in Figure 1F. Boxed amino acids indicates strong amino acid requirements. C. GTP/ATP ratios or GTP and ATP levels relative to those for untreated cells at t=0 of wild-type, (p)ppGpp^0, Δ*codY* (p)ppGpp^0, and *guaB*^{down} (p)ppGpp^0 cells. ^{32}P-labeled cells were treated with 0.5 mg/ml RHX or 1 mM Guo for 20 min. Error bars represent standard errors of the means for three independent biological replicates. D. Schematic of the amino acid biosynthesis pathways that lead to the production of the amino acids that are strongly required by (p)ppGpp^0 cells: threonine, methionine, isoleucine, valine, and leucine. E. Hierarchical clustering analysis of transcript levels obtained from microarrays. Rows correspond to the genes; columns correspond to samples with strains and treatments labeled above the heat map for WT [(p)ppGpp$^+$], (p)ppGpp^0 [(p)ppGpp$^-$], Δ*codY* (p)ppGpp^0 (codY$^-$), and *guaB*^{down} (p)ppGpp^0 (guaB$^-$) cells that are either untreated, treated with RHX, or treated with Guo. Three independent experimental replicates are shown. Transcript levels (log_2) are indicated by color such that high levels are yellow and low levels are blue. Genes were hierarchically clustered using the software program Cluster and plotted with TreeView software. Colored boxes correspond to distinct clusters containing the genes involved in synthesis of the amino acids that are strongly required by (p)ppGpp^0 cells, which are indicated with the corresponding colors in panel C. For an expanded view, see Figure S1B in the supplemental material.

Effects of guaB and codY on global transcription profiles in (p)ppGpp^0 cells

To understand whether these strong auxotrophic requirements and their suppressions are due to alteration of gene expression by CodY and/or GTP, we examined gene expression profiles of wild-type, (p)ppGpp^0, *guaB*^{down} (p)ppGpp^0, and Δ*codY* (p)ppGpp^0 strains (Figure S1A) during exponential growth upon addition of arginine hydroxamate (RHX) to induce (p)ppGpp in wild-type cells and upon addition of guanosine, which elevates GTP levels in all three (p)ppGpp-deficient strains (Figure 2C) (Kriel et al., 2012). We found that these strains displayed profound differences in genes significantly altered ($q < 0.01$); biological replicates behaved consistently. We observed some expected changes, including a general decrease in expression of *de novo* purine biosynthesis genes (the *purEKBCSQLFMNHD* operon) in response to guanosine treatment in all cells, likely due to negative feedback regulation of the *de novo* biosynthesis pathway (Ebbole and Zalkin, 1987). We also observed a decrease in expression of ribosomal protein genes upon accumulation of (p)ppGpp, as previously observed (Eymann et al., 2002). In addition, we observed changes in the CodY regulon that are highly consistent with a previous analysis in (p)ppGpp$^+$ cells (Molle et al., 2003). Of particular interest to our study are genes involved in synthesizing amino acids that are strongly required by (p)ppGpp^0 cells (Val, Ile, Leu, Met, and Thr) (Figure 2D). Upon RHX treatment, these genes were strongly induced in wild-type cells but failed to be induced in (p)ppGpp^0 cells. In addition, these genes are located among three distinct clusters on the hierarchical tree of the microarray data (Figure 2E), and their transcription is strongly affected by mutations in *codY* or *guaB* or both. Combining gene

expression profiling with auxotrophic analysis, we found that the regulation of these genes contributes to the strong amino acid requirements.

Hyperrepression of ilvBHC-leuABCD, ilvD, and ybgE by CodY in (p)ppGpp^0 cells

We first examined two clusters on the hierarchical tree (Figure 2E, green and blue) that include BCAA biosynthetic genes known to be strongly and directly repressed by CodY (Molle et al., 2003): the *ilvB* (*ilvBHC-leuABCD*) and *ilvD* operons (green) and *ybgE* (blue) (Figure 3A). CodY is activated by GTP (Brinsmade and Sonenshein, 2011; Handke et al., 2008; Ratnayake-Lecamwasam et al., 2001), so reduction of intracellular GTP, due to either regulation by (p)ppGpp or reduced expression of *guaB*, should inactivate CodY-mediated repression of these genes. Examination of expression profiles of these CodY-regulated BCAA biosynthesis genes verified that they are indeed derepressed in wild-type cells upon (p)ppGpp induction by RHX and in Δ*codY* (p)ppGpp^0 and *guaB*^{down} (p)ppGpp^0 cells (Figure 3B to F). In contrast, *ilvB*, *ilvD*, and *ybgE* expression is strongly inhibited in (p)ppGpp^0 cells, suggesting that their direct repression by CodY underlies the failure to synthesize BCAA in (p)ppGpp^0 cells.

Direct repression by CodY is not the only factor contributing to the regulation of *ilvB* and *ilvD*. An additional CodY-independent effect of ATP and GTP concentrations on transcription was observed previously. Upon amino acid starvation, (p)ppGpp accumulation results in a decrease in the intracellular GTP concentration and a reciprocal increase in the ATP concentration; this increase kinetically stimulates the transcription initiation rates of genes whose initiating nucleotide is ATP, including the *ilvB* operon, and inhibits transcription initiation of genes whose initiating nucleotide is

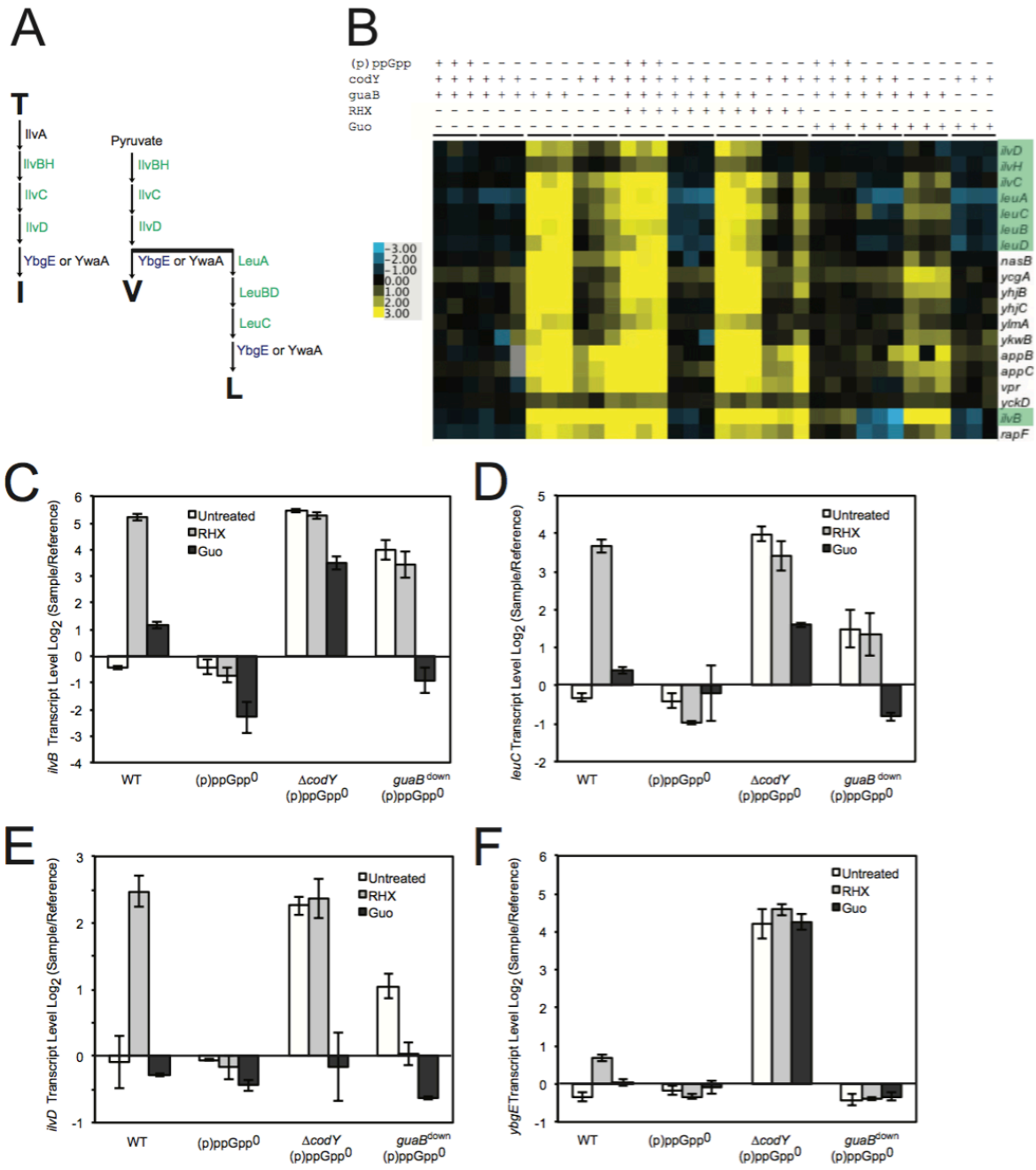

Figure 3. Transcript levels of *ilvBHC-leuABCD*, *ilvD*, and *ybgE* in (p)ppGpp^0 cells and the effects of CodY and GTP. A. Schematic of the BCAA (isoleucine, valine, and leucine) biosynthesis pathways. Genes in two major clusters in the hierarchical tree of the microarray data in Fig. 2D are colored accordingly: the *ilvBHC-leuABCD* and *ilvD* operons are in the green cluster; the *ybgE* operon clusters separately in blue. B. A cluster in which genes in the *ilvB* and *ilvD* operons (green) are located. Transcript levels (log_2) are indicated by color such that high levels are yellow and low levels are blue. C to F. Transcript levels of *ilvB* (C), *leuC* (D), *ilvD* (E), or *ybgE* (F) in wild-type, (p)ppGpp^0, Δ*codY* (p)ppGpp^0, and *guaB*^{down} (p)ppGpp^0 cells both before and after RHX or Guo treatment. Transcript levels were normalized to a common reference, and log_2 ratios are

plotted. Similar trends were obtained for other genes in the *ilvB* operon: *ilvH*, *ilvC*, *leuA*, *leuB*, and *leuD*. For this and all subsequent figures, the averages of three biological replicates and the standard errors of the means are presented for each strain and treatment

GTP, including the *rrn* operons (Krásný and Gourse, 2004; Krásný et al., 2008; Tojo et al., 2008). This mechanism may contribute to the increased transcription of *ilvB* observed in wild-type and *guaB*^{down} (p)ppGpp^{0} cells, and, although less obviously, this mechanism could also contribute to the increased transcription of *ilvB* seen in Δ*codY* (p)ppGpp^{0} cells because deletion of *codY* lowers the GTP levels of (p)ppGpp^{0} cells (Figure 2C), since CodY positively regulates *guaB* expression (Molle et al., 2003). To conclusively demonstrate this mechanism, we tested whether altering GTP and ATP levels can affect transcription of the *ilvB* operon in the absence of both CodY and (p)ppGpp. We treated Δ*codY* (p)ppGpp^{0} cells with guanosine, which increased GTP levels by ~8-fold and reduced ATP levels by ~30% (Figure 2C). We found that genes in the *ilvB* operon were reduced by ~4-fold in Δ*codY* (p)ppGpp^{0} cells (e.g., Figure 3C, 3D), demonstrating an unambiguous CodY-independent response.

Interestingly, *ilvD*, located in the same cluster as members of the *ilvB* operon on the hierarchical map of the microarrays (Figure 3B), was similarly affected, since its expression was reduced by ~6-fold upon guanosine addition even in the absence of CodY (Figure 3E). In contrast, expression of *ybgE*, which is not located close to *ilvB* and *ilvD* in the hierarchical tree of the microarrays (Figure 2D, S3), was not affected by guanosine addition in the absence of CodY (Figure 3F). In summary, the *ilvB* and *ilvD* operons but not *ybgE* are downregulated by GTP accumulation and/or ATP depletion via both CodY-dependent and CodY-independent mechanisms.

To address whether the BCAA requirements of (p)ppGpp^{0} cells are predominantly through direct CodY-mediated repression of *ilvBHC-leuABCD*, *ilvD*, and *ybgE*, we reduced CodY-mediated repression of these BCAA genes in (p)ppGpp^{0} cells

without inactivating CodY itself. The *ilvB*^{up} mutant strain harbors a deletion of the leucine-sensing T box and two point mutations in the high-affinity CodY binding site (Figure 4A), effectively reducing CodY-dependent regulation of the *ilvBHC-leuABCD* operon and increasing its basal expression level. The BCAA^{up} mutant strain contains the alleles above as well as deletions of CodY-binding sites at *ilvD* and *ybgE* (Figure 4A) (Brinsmade et al., 2010). We observed that *ilvB*^{up} (p)ppGpp^0 cells were relieved of the requirement for leucine, while BCAA^{up} (p)ppGpp^0 cells were relieved of the requirements for leucine, valine, and to a lesser extent isoleucine (Figure 4B). These data demonstrate that CodY-mediated repression of *ilvBHC- leuABCD* and *ilvD* contributes to BCAA auxotrophy in (p)ppGpp^0 cells.

Relieving CodY-mediated repression of these genes did not completely relieve the requirements for valine, leucine, and isoleucine to the same extent as deletion of *codY*. Assuming that the BCAA^{up} mutant is fully CodY derepressed for the *ilvB*, *ilvD*, and *ybgE* operons (we cannot rule out the possibility of residual repression by CodY), the further relief of the BCAA requirements observed in Δ*codY* (p)ppGpp^0 cells suggests a contribution of CodY-independent BCAA gene regulation to the auxotrophy. Thus, the additional CodY-independent effect of nucleotide levels on transcription of the *ilvB* and *ilvD* operons and/or regulation of biosynthesis genes that are not affected by the mutations in the BCAA^{up} strain (i.e., *ilvA*, *ywaA*, and *hom-thrCB*) may also play a role in completely relieving the BCAA requirements.

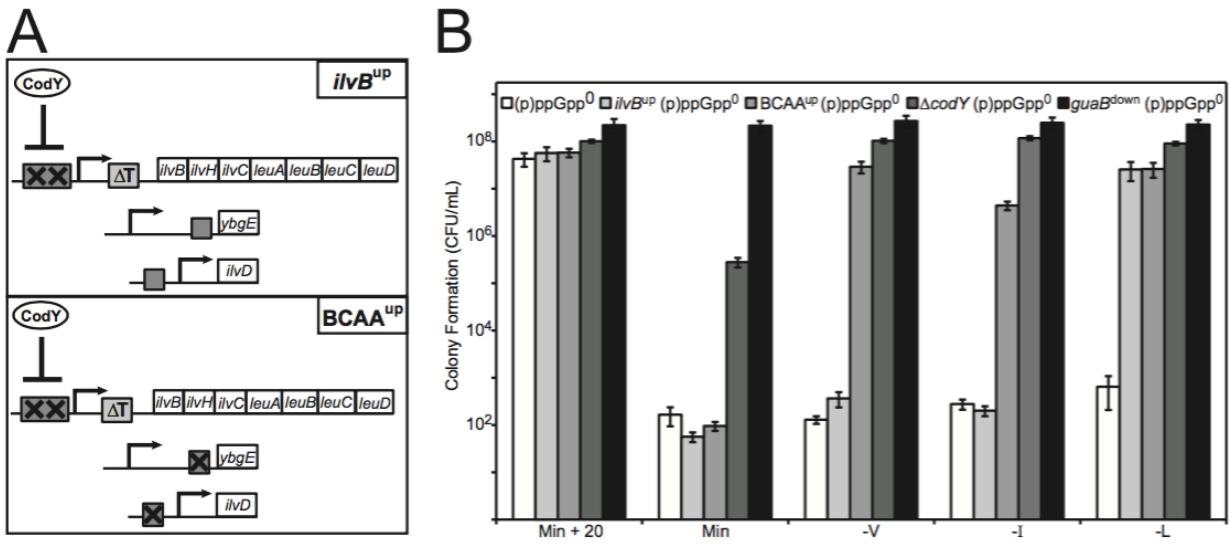

Figure 4. Hyperrepression by CodY causes the branched-chain amino acid requirements of (p)ppGpp^0 cells. A. Alteration of CodY-binding sites in the *ilvB*^{up} and BCAA^{up} mutants. In the *ilvB*^{up} mutant, two point mutations (X) in the high-affinity CodY-binding site (rectangle) at the promoter of the *ilvBHC-leuABCD* operon prevent CodY from binding to the promoter. An additional deletion of the leucine-dependent terminator (T box) increases the basal expression of the *ilvB* operon (rectangle labeled ΔT). In the BCAA^{up} mutant, in addition to the *ilvB* promoter mutations, CodY binding sites (rectangles) in the promoters of *ybgE* and *ilvD* are deleted (X) to prevent CodY from repressing transcription of the *ilvBHC-leuABCD*, *ilvD*, and *ybgE* operons. B. Colony formation of (p)ppGpp^0 (white), *ilvB*^{up} (p)ppGpp^0 (light gray), BCAA^{up} (p)ppGpp^0 (medium gray), Δ*codY* (p)ppGpp^0 (dark gray), and *guaB*^{down} (p)ppGpp^0 (black) cells on dropout plates. Cells were plated as for Figure 1F.

Contribution of CodY and GTP levels to repression of ilvA, ywaA, and hom-thrCB

An additional group of genes involved in biosynthesis of BCAA and threonine, *ywaA*, *ilvA*, and *hom-thrCB* (Figure 5A, 5B), exhibit expression patterns distinct from those of *ilv-leu* (red, Figure 2D). Threonine synthesis requires *hom-thrCB*, while isoleucine requires both threonine and *ilvA* for its synthesis (Figure 5A). Their transcript levels were strongly upregulated in wild-type cells following amino acid starvation, as well as in Δ*codY* (p)ppGpp^0 and *guaB*^{down} (p)ppGpp^0 cells but failed to be upregulated in (p)ppGpp^0 cells (Figure 5C to E). Thus, their misregulation may also contribute to the BCAA and threonine auxotrophies.

ywaA, *ilvA*, and *hom-thrCB* have recently been revealed as *in vitro* targets of CodY (Belitsky and Sonenshein, 2013). In addition, we observe that their transcript levels decrease in Δ*codY* (p)ppGpp^0 cells upon guanosine treatment, indicating that GTP and/or ATP levels can also affect their transcription independently of CodY (Figure 5C to E). Although *ywaA*, *ilvA*, and *hom-thrCB* are regulated by GTP levels via both CodY-dependent and CodY-independent mechanisms similarly to findings for *ilvB* and *ilvD*, the magnitudes of their CodY-dependent and CodY-independent regulatory components are different, with *ywaA*, *ilvA*, and *hom-thrCB* displaying a stronger transcriptional response to guanosine treatment in the absence of (p)ppGpp and CodY.

Repression of methionine biosynthesis genes in (p)ppGpp^0 cells

(p)ppGpp^0 cells also displayed a strong requirement for methionine. We observed that one of the genes required for methionine biosynthesis, *metE*, clustered near *ywaA*, *ilvA*, and *hom-thrCB* (Figure 5B). Specifically, transcript levels of *metE* were upregulated by ~10- to 30-fold upon activation of the stringent response in wild-type cells but not in

(p)ppGpp^0 cells (Figure 5F). Such strong changes in *metE* transcription, as well as changes in *hom* (producing homoserine, a precursor for methionine biosynthesis), are likely sufficient to account for the observed methionine auxotrophy in the absence of (p)ppGpp. The *metE* operon is not known to be a direct target of CodY, and transcript levels of *metE* decrease by ~4-fold in (p)ppGpp^0 Δ*codY* cells following guanosine treatment (Figure 5F), indicating that GTP and/or ATP levels indeed affect *metE* transcription independently of CodY.

We also examined transcript levels of other genes involved in methionine biosynthesis: *metA* and *metIC* (*yjcIJ*). *metA* expression was not significantly affected by (p)ppGpp during starvation. *metIC* was upregulated in wild-type cells during the stringent response, and this upregulation was abolished in (p)ppGpp^0 cells. Upregulation of *metIC* was not restored in either the Δ*codY* or *guaB*^{down} (p)ppGpp^0 strains, suggesting that regulation of *metIC* does not account for the relief of the methionine auxotrophy of (p)ppGpp^0 cells by these mutations.

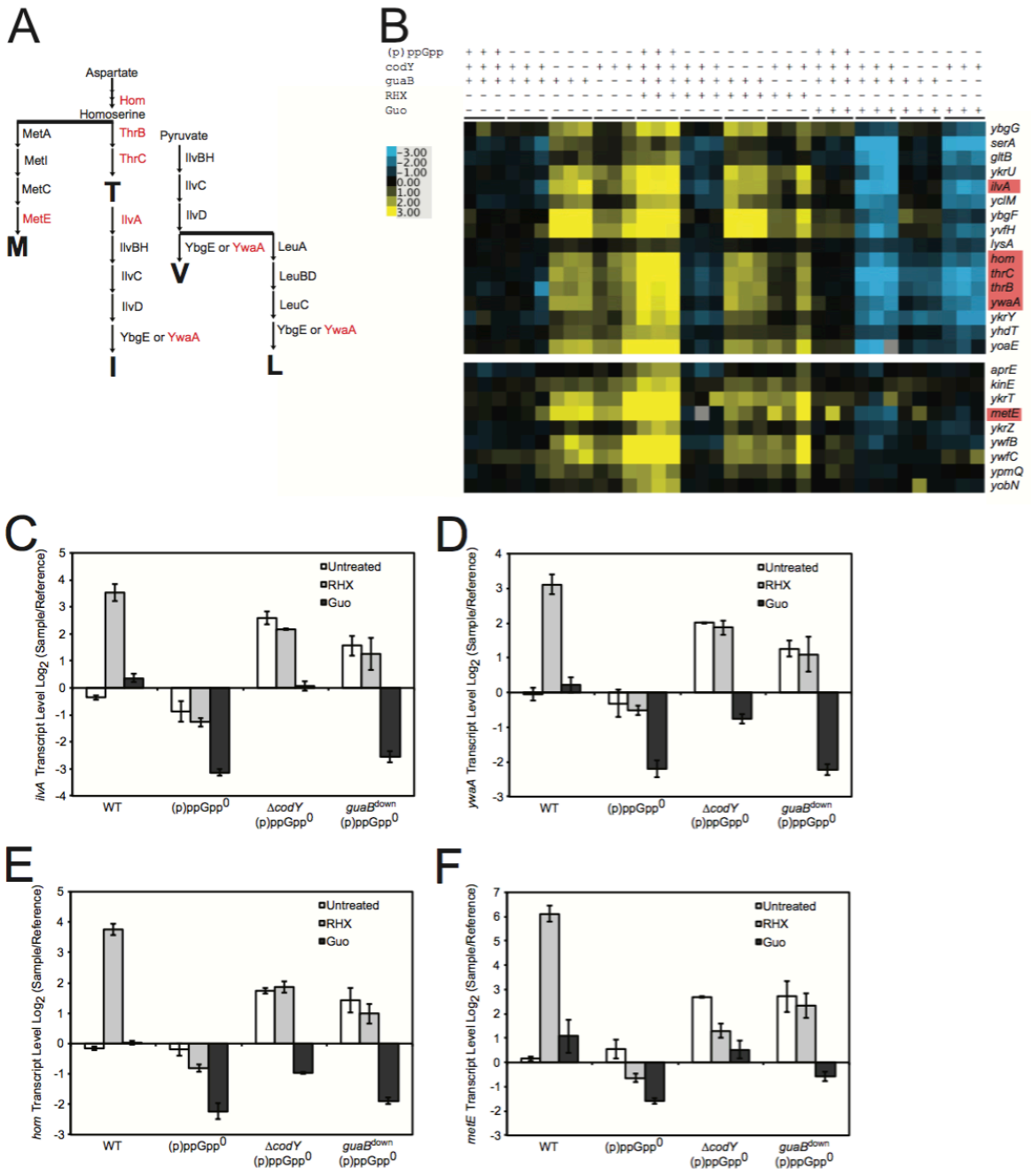

Figure 5. Transcript levels of *ilvA*, *ywaA*, *hom-thrCB*, and *metE* in (p)ppGpp^0 cells and the effects of CodY and GTP. A. Schematic of the amino acid biosynthesis pathways that lead to the production of those amino acids that are strongly required by (p)ppGpp^0 cells: threonine, methionine, isoleucine, valine, and leucine. Proteins involved in the biosynthesis of these amino acids whose genes localized together in clustering analysis of transcriptional profiles, separately from the *ilvB*, *ilvD*, and *ybgE* operons, are highlighted in red. B. A cluster of genes obtained from Figure 2D (red), where the *ilvA*, *ywaA*, *hom-thrCB*, and *metE* operons are located. Transcript levels ($\log_2$) are indicated by color such that high levels are yellow and low levels are blue. C to F. Transcript

levels of *ilvA* (C), *ywaA* (D), *hom* (E), or *metE* (F) both before and after RHX or Guo treatment in wild-type, (p)ppGpp^0, Δ*codY* (p)ppGpp^0, and *guaB*^{down} (p)ppGpp^0 cells. Similar results were obtained for the other genes in the *hom* operon: *thrC* and *thrB*.

Failure to survive nutrient downshift contributes to an apparent complex auxotrophy in (p)ppGpp^0 cells

We have identified strong requirements for five amino acids in (p)ppGpp^0 cells and showed that most of the genes specifically responsible for their synthesis are strongly misregulated in (p)ppGpp^0 cells by elevated GTP levels via a combination of CodY-dependent and CodY-independent mechanisms. We also identified three additional amino acids that are modestly required in (p)ppGpp^0 cells. In theory, if the failure of (p)ppGpp^0 cells to grow on minimal medium stemmed from their inability to produce the eight required amino acids, then supplementing these amino acids in the medium should restore colony formation. To test this prediction, we performed the standard plating assays in which cells were grown in liquid medium supplemented with Casamino Acids and then plated on medium supplemented with all eight amino acids required by (p)ppGpp^0 cells: valine, leucine, isoleucine, methionine, threonine, arginine, histidine, and tryptophan (Figure 6A). However, we found that, similar to results observed for *E. coli* ppGpp^0 cells (Xiao et al., 1991), the *B. subtilis* (p)ppGpp^0 strain could not form colonies on plates supplemented with all auxotrophic requirements (Figure 6B). This suggests that either (p)ppGpp^0 cells have additional auxotrophic requirements or, alternatively, another factor in combination with repression of amino acid biosynthesis genes prevents colony formation of (p)ppGpp^0 cells.

We reasoned that the apparent inability of (p)ppGpp^0 cells to form colonies on medium supplemented with the eight auxotrophic requirements may stem from failure to survive nutrient shift from liquid medium with full amino acid supplementation to only eight amino acids on solid medium. We have previously observed rapid death of

(p)ppGpp^0 cells upon RHX treatment (Kriel et al., 2012), and we reasoned that death could occur in (p)ppGpp^0 cells during nutrient downshift in our plating assay. A prediction from this hypothesis is that when not subjected to nutritional downshift, (p)ppGpp^0 cells should form colonies efficiently on medium supplemented with the eight required amino acids. We tested this prediction by taking colonies on plates with eight amino acids that survived the initial downshift (from step 1, Figure 6A), suspending them in Spizizen buffer, and comparatively plating them on media with twenty amino acids, eight amino acids, and no amino acids (step 2, Figure 6C). We verified that the majority of colonies we picked do in fact form colonies on plates with eight amino acids but do not on minimal medium, indicating that they are not suppressor mutants (Figure 6D). These data confirmed that (p)ppGpp^0 cells are indeed only auxotrophic for eight amino acids, supporting our hypothesis that the inability to withstand nutrient downshift prevents efficient colony formation of (p)ppGpp^0 cells on medium containing only the auxotrophic requirements.

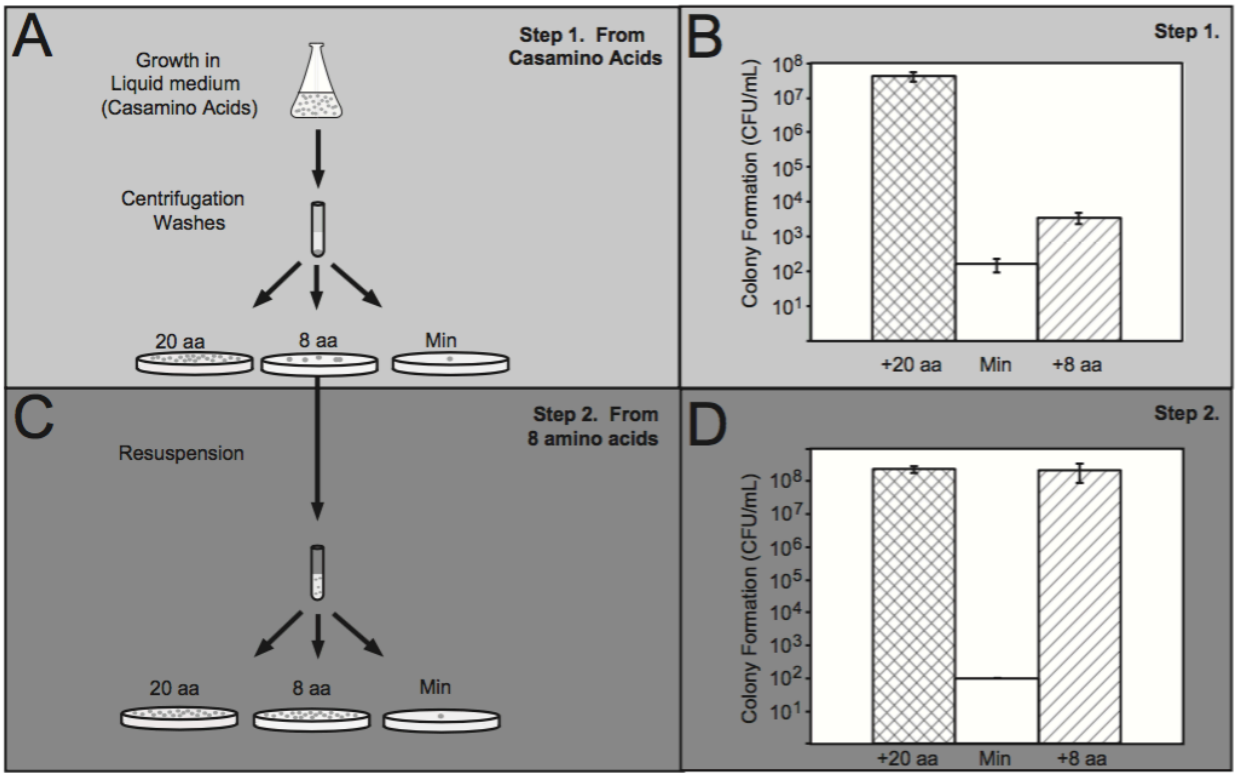

Figure 6. Supplementing required amino acids allows for colony formation of (p)ppGpp^0 cells only in the absence of nutrient downshift. A. Standard plating efficiency assay for determining amino acid auxotrophy involves nutrient downshift (Step 1). Cells were grown in liquid medium supplemented with Casamino Acids and then plated on defined medium supplemented with the auxotrophic requirements of (p)ppGpp^0 cells: valine, isoleucine, leucine, methionine, threonine, histidine, arginine, and tryptophan (8 aa). Cells were also plated on medium supplemented with all twenty amino acids (20 aa) and on medium without amino acid supplementation (Min) for comparison. B. Colony formation (CFU/ml) results from Step 1. C. To determine whether supplementing the required amino acids allows colony formation of (p)ppGpp^0 cells in the absence of nutrient downshift (Step 2), cells that formed colonies on medium supplemented with 8 aa were suspended in buffer and plated directly on medium supplemented with the auxotrophic requirements (8 aa). Cells were also plated on medium supplemented with all twenty amino acids (20 aa) for comparison and on minimal medium without amino acid supplementation (Min) to test for suppressor mutants. D. Colony formation (CFU/ml) results from Step 2.

Discussion

In this study, we document that the inability to produce (p)ppGpp in *B. subtilis* results in high GTP levels and consequently, strong requirements for BCAA, methionine, and threonine and moderate requirements for arginine, histidine, and tryptophan. The BCAA auxotrophy is due primarily to direct repression of transcription of the BCAA biosynthesis genes *ilvBHC-leuABCD* and *ilvD* by GTP-mediated activation of CodY. The threonine auxotrophy is likely due to a combined direct effect of elevated GTP levels and GTP-mediated activation of CodY on transcription of the *hom-thrCB* operon. The methionine auxotrophy is likely due to both the effects on transcription of *hom* and also GTP-mediated downregulation of transcription of *metE*, potentially via initiating nucleotide concentrations. Reducing GTP levels allows cells to adapt to amino acid limitation both by activating transcription of biosynthesis genes and by protecting (p)ppGpp^0 cells against death during nutrient shifts that prevent efficient colony formation on plates supplemented with the auxotrophic requirements. We conclude that (p)ppGpp regulates GTP levels to allow resistance to amino acid limitation by two distinct physiological roles: first by preventing cell death during nutrient downshift and then by transcriptionally enabling amino acid biosynthesis (Figure 7).

Overlapping and differential transcriptional regulation of amino acid biosynthesis genes by CodY and GTP levels accounts for strong auxotrophies of (p)ppGpp^0 cells

The strong requirements for BCAA, threonine, and methionine in (p)ppGpp^0 cells can be explained by the effect of GTP levels on transcription of amino acid biosynthesis genes, via both GTP-dependent activation of the transcriptional regulator CodY and a CodY-independent effect. CodY-dependent repression of *ybgE*, *ilvBHC-leuABCD*, *ilvD*,

ilvA, *ywaA*, and *hom-thrCB* was previously characterized (Belitsky and Sonenshein, 2013; Molle et al., 2003). CodY-independent regulation was previously characterized for *ilvB* and *ywaA*; transcription of these genes initiates with ATP, and their transcription increases in wild-type cells during amino acid starvation in response to elevated ATP levels (Krásný et al., 2008; Tojo et al., 2008). Beyond *ilvB* and *ywaA*, we identified additional targets that are similarly regulated by nucleotide levels in a CodY-independent manner, including the BCAA biosynthesis genes *ilvA* and *ilvD* and the threonine and methionine biosynthesis genes *hom-thrCB* and *metE*, as evidenced by their strong downregulation (~4-fold) in (p)ppGpp^0 Δ*codY* cells upon guanosine addition. Based on the locations of the conserved -10 and -35 regions of the *hom-thrCB* promoter, we predict that the transcription start site (TSS) of this operon is likely to be an A (Helmann, 1995). The TSS of *metE* could not be predicted. It is possible that these genes are activated by increased ATP levels similarly to *ilvB* and *ywaA* (Krásný et al., 2008; Tojo et al., 2008). Additionally, they may also be regulated by GTP levels via an indirect and negative mechanism; i.e., decreased GTP levels reduce transcription of genes initiating with GTP, such as *rrn* operons (Krásný and Gourse, 2004), that engage the majority of cellular RNAP, thus increasing the availability of free RNAP for transcription of all other genes not initiating with GTP via passive redistribution. A similar situation takes place in *E. coli*, in which ppGpp accumulation not only directly activates transcription of amino acid biosynthesis genes (Paul et al., 2005) but also indirectly activates their transcription by inhibiting rRNA transcription, leading to passive redistribution of RNA polymerase to amino acid promoters (Barker et al., 2001). The difference is that in *B. subtilis*, (p)ppGpp does not directly regulate transcription by

binding to RNAP but indirectly regulates transcription by modulating GTP levels. Future *in vitro* and *in vivo* mechanistic analyses are required to test these models.

Our results provide a rough estimation of the relative contributions of these gene regulatory mechanisms to the amino acid auxotrophies of (p)ppGpp^0 cells (Figure 7). We find that hyperrepression of the *ilvB* operon by CodY is responsible for the leucine requirement [Figure 4B, ilvB^{up} (p)ppGpp^0 cells] and that CodY-mediated repression of the *ilvB*, *ybgE*, and *ilvD* operons is collectively responsible for the isoleucine and valine requirements [Figure 4B, BCAA^{up} (p)ppGpp^0 cells], while regulation of *hom-thrCB*, *ilvA*, and *ywaA* expression likely plays an additional role in the isoleucine requirement. The threonine and methionine requirements are likely due to effects of GTP and ATP levels on transcription of *hom-thrCB* and *metE*. However, demonstrating their contribution to threonine and methionine auxotrophies would require characterizing and manipulating their promoters, particularly their transcription start sites.

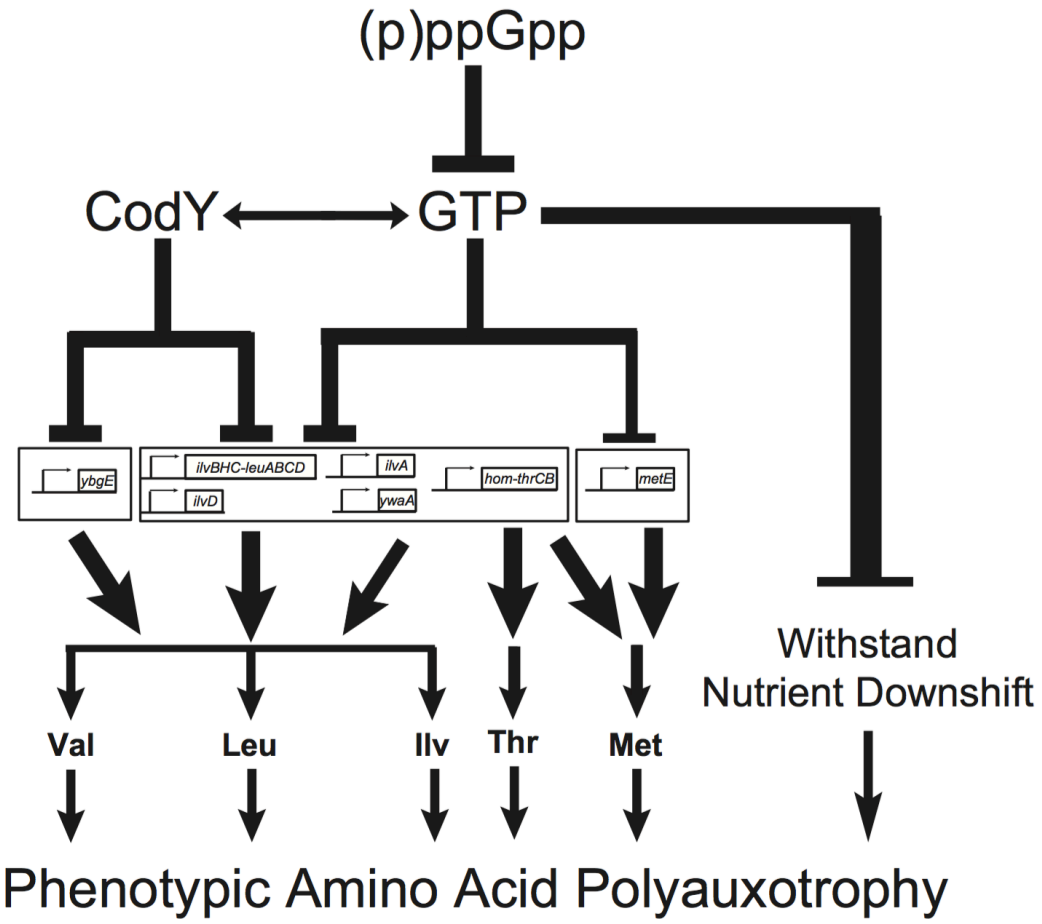

Figure 7. (p)ppGpp decreases GTP levels to upregulate amino acid biosynthesis and protect cellular viability during nutritional downshifts. (p)ppGpp allows growth on minimal medium by decreasing GTP levels. Decreased GTP levels allow increased transcription of various amino acid biosynthesis genes, through both CodY-dependent and CodY-independent mechanisms. Specifically, transcription of *ybgE* is controlled by CodY, transcription of the *ilvB* and *ilvD* operons is controlled primarily by CodY but is also affected by GTP levels, and transcription of *ywaA* and *ilvA* is likely directly regulated by CodY but also controlled by GTP levels. In the absence of (p)ppGpp-mediated regulation of GTP levels, hyperactivity of CodY is primarily responsible for causing the auxotrophies for valine, leucine, and isoleucine. Transcription of the *hom-thrCB* operon is likely directly regulated by CodY but is also strongly affected by GTP levels. Transcription of *metE* is also strongly affected by GTP levels. Thus, the inability of (p)ppGpp^0 cells to properly regulate GTP levels and thus transcription of these operons likely leads to the auxotrophies for threonine and methionine. Additionally, even when all of the amino acid requirements of (p)ppGpp^0 cells are met, these cells still cannot form colonies following a downshift in amino acid availability. Hence, (p)ppGpp-mediated regulation of GTP levels also allows cells to survive nutrient downshifts. This complex regulatory cascade, initiated by the inhibition of GTP biosynthesis by (p)ppGpp, allows cells to rapidly respond to changing nutrient conditions and sustain growth afterwards.

A note of caution is that the regulation of the genes characterized here is within the context of (p)ppGpp^0 cells, whose GTP and ATP levels (especially upon guanosine addition) may lie beyond the range of concentrations typically found in wild-type cells. Due to the different physiological ranges of nucleotide levels in the microarray samples compared to findings for cells in the auxotrophy experiments, these two concepts are not necessarily equivalent, i.e., a larger variation in the microarrays may not necessarily mean a bigger physiological contribution to the auxotrophy on plates. For example, the *metIC* operon is affected by changes in GTP levels in a CodY-independent manner during RHX and decoyinine treatments (Tojo et al., 2010), and indeed we verified that *metIC* is induced upon RHX treatment (Figure S4). However, in Δ*codY* (p)ppGpp^0 cells, addition of guanosine did not result in strong downregulation of this operon. This suggests that *metIC* may be responsive to low GTP levels (during RHX or decoyinine treatment) but not responsive to high GTP levels (during guanosine treatment). These data suggest that different operons may be tunable within different dynamic ranges of nucleotide levels. In wild-type cells, the expression of different amino acid biosynthesis genes is modulated in a complex fashion by the continuum of physiological activities of CodY, GTP, and ATP.

Moderate arginine, histidine, and tryptophan auxotrophies

(p)ppGpp^0 cells exhibit moderate requirements for arginine, histidine, and tryptophan. Both the arginine biosynthesis genes *argG* and *argJ* have recently been revealed as targets of CodY *in vivo* (Brinsmade et al., 2014), and the *argC* operon containing *argJ* has also been identified as a direct target of CodY *in vitro* (Belitsky and

Sonenshein, 2013). We observed moderate but significant upregulation of *argJ* in wild-type cells upon amino acid starvation (~6-fold) that depends on (p)ppGpp (Figure S5). We also observed a mild derepression of *argJ* upon deletion of *codY* in (p)ppGpp^0 cells in our microarray analysis. The CodY-dependent expression changes in *argJ* and *argG* observed here (when glutamate is provided as a nitrogen source) are not as strong as results with ammonium as the nitrogen source (Brinsmade et al., 2014), likely because the *argJ* and *argG* operons are strongly repressed by CodY only when glutamate, a precursor of arginine biosynthesis, is not available. Nonetheless, the observation of a CodY-dependent change in *argJ* transcription, combined with the fact that deletion of CodY rescues the arginine auxotrophy, suggests that CodY-mediated repression of arginine biosynthesis genes causes the partial arginine requirement of (p)ppGpp^0 cells.

In contrast to the arginine auxotrophy, the moderate auxotrophic requirements for histidine and tryptophan are not completely rescued by *codY* deletion and are unlikely due to altered transcription of their biosynthesis genes. Interestingly, the synthesis of these amino acids relies heavily on the precursor of purine biosynthesis, phosphoribosyl pyrophosphate (PRPP). Perhaps PRPP is exhausted in (p)ppGpp^0 cells due to overproduction of GTP, and thus histidine and tryptophan production is compromised, whereas inhibition of *de novo* GTP biosynthesis by (p)ppGpp could free up PRPP for synthesis of these amino acids. Alternatively, these apparent amino acid requirements may stem from the effects of nutrient downshift and not actually constitute *bona fide* amino acid auxotrophies.

Amino acid biosynthesis versus adjusting to nutrient downshift: dual protection by (p)ppGpp

Our results suggest that the inability of (p)ppGpp^0 cells to form colonies does not stem solely from the inability to properly upregulate transcription of amino acid biosynthesis genes. (p)ppGpp accumulation not only affects the transcription of BCAA, threonine, and methionine biosynthesis genes but also protects cells from death during nutrient downshift (Figure 6 and 7). This explains why supplementing all of the amino acid requirements of (p)ppGpp^0 cells does not completely allow colony formation: it relieves the auxotrophic requirements but does not protect cells from nutrient downshift that occurs when switching from growth in twenty amino acids to merely eight (Figure 6B). When not subjected to nutrient downshift, (p)ppGpp^0 cells are capable of forming colonies on medium supplemented with the required amino acids (Figure 6D). Since nutrient downshift is often an intermediate step in auxotrophic analysis, (p)ppGpp allows cells to form colonies on amino acid-limiting medium by acting on two distinct successive processes: surviving nutrient downshift and allowing prototrophy. The failure to survive nutrient downshift when GTP levels are dysregulated in the absence of (p)ppGpp could be due to transcriptional misregulation of genes other than the amino acid biosynthesis genes, e.g., failure to downregulate rRNA and ribosomal protein synthesis at high GTP levels (Krásný and Gourse, 2004), or due to GTP-related metabolic dysregulation via an unknown cause, e.g., posttranscriptional or allosteric regulations.

Similarly to what we found in *B. subtilis*, failure to survive nutrient downshift could also account for the observed inconsistency of polyauxotrophy in *E. coli* (p)ppGpp^0 cells (Xiao et al., 1991). Additionally, in *E. coli* the DksA transcription factor also performs dual functions during amino acid starvation: upregulating transcription of amino acid

biosynthesis genes (Paul et al., 2005) and protecting cells from transcription-replication conflict (Tehranchi et al., 2010). It will be interesting to examine whether components of the stringent response also protect *E. coli* and other bacteria by the sequential effect of ensuring survival during the change of conditions and then engaging the cell's biosynthetic machinery to adapt to the new situation.

Literature Cited

Barker, M.M., Gaal, T., and Gourse, R.L. (2001). Mechanism of regulation of transcription initiation by ppGpp. II. Models for positive control based on properties of RNAP mutants and competition for RNAP. J. Mol. Biol. *305*, 689–702.

Belitsky, B.R., and Sonenshein, A.L. (2013). Genome-wide identification of *Bacillus subtilis* CodY-binding sites at single-nucleotide resolution. Proc. Natl. Acad. Sci. U. S. A. *110*, 7026–7031.

Brinsmade, S.R., and Sonenshein, A.L. (2011). Dissecting complex metabolic integration provides direct genetic evidence for CodY activation by guanine nucleotides. J. Bacteriol. *193*, 5637–5648.

Brinsmade, S.R., Kleijn, R.J., Sauer, U., and Sonenshein, A.L. (2010). Regulation of CodY activity through modulation of intracellular branched-chain amino acid pools. J. Bacteriol. *192*, 6357–6368.

Brinsmade, S.R., Alexander, E.L., Livny, J., Stettner, A.I., Segre, D., Rhee, K.Y., and Sonenshein, A.L. (2014). Hierarchical expression of genes controlled by the *Bacillus subtilis* global regulatory protein CodY. Proc. Natl. Acad. Sci. *111*, 8227–8232.

Ebbole, D.J., and Zalkin, H. (1987). Cloning and characterization of a 12-gene cluster from *Bacillus subtilis* encoding nine enzymes for *de novo* purine nucleotide synthesis. J. Biol. Chem. *262*, 8274–8287.

Eymann, C., Homuth, G., Scharf, C., and Hecker, M. (2002). *Bacillus subtilis* functional genomics: global characterization of the stringent response by proteome and transcriptome analysis. J. Bacteriol. *184*, 2500–2520.

Handke, L.D., Shivers, R.P., and Sonenshein, A.L. (2008). Interaction of *Bacillus subtilis* CodY with GTP. J. Bacteriol. *190*, 798–806.

Harwood, C.R., Cutting, S.M., and Chambert, R. (1990). Molecular biological methods for *Bacillus*.

Helmann, J.D. (1995). Compilation and analysis of *Bacillus subtilis* σ^A-dependent promoter sequences: evidence for extended contact between RNA polymerase and upstream promoter DNA. Nucleic Acids Res. *23*, 2351–2360.

Hogg, T., Mechold, U., Malke, H., Cashel, M., and Hilgenfeld, R. (2004). Conformational antagonism between opposing active sites in a bifunctional RelA/SpoT homolog modulates (p)ppGpp metabolism during the stringent response. Cell *117*, 57–68.

Janes, B.K., and Stibitz, S. (2006). Routine markerless gene replacement in *Bacillus anthracis*. Infect. Immun. *74*, 1949–1953.

Kobayashi, K., Ehrlich, S.D., Albertini, A., Amati, G., Andersen, K.K., Arnaud, M., Asai, K., Ashikaga, S., Aymerich, S., Bessieres, P., et al. (2003). Essential *Bacillus subtilis* genes. Proc. Natl. Acad. Sci. *100*, 4678–4683.

Krásný, L., and Gourse, R. (2004). An alternative strategy for bacterial ribosome synthesis: *Bacillus subtilis* rRNA transcription regulation. EMBO J. *23*, 4473–4483.

Krásný, L., Tiserová, H., Jonák, J., Rejman, D., and Sanderová, H. (2008). The identity of the transcription +1 position is crucial for changes in gene expression in response to amino acid starvation in *Bacillus subtilis*. Mol. Microbiol. *69*, 42–54.

Kriel, A., Bittner, A.N., Kim, S.H., Liu, K., Tehranchi, A.K., Zou, W.Y., Rendon, S., Chen, R., Tu, B.P., and Wang, J.D. (2012). Direct regulation of GTP homeostasis by (p)ppGpp: A critical component of viability and stress resistance. Mol. Cell *48*, 231–

241.
Marchler-Bauer, A., Lu, S., Anderson, J.B., Chitsaz, F., Derbyshire, M.K., DeWeese-Scott, C., Fong, J.H., Geer, L.Y., Geer, R.C., Gonzales, N.R., et al. (2011). CDD: A Conserved Domain Database for the functional annotation of proteins. Nucleic Acids Res. *39*, D225–D229.
Molle, V., Nakaura, Y., Shivers, R.P., Yamaguchi, H., Losick, R., Fujita, Y., and Sonenshein, A.L. (2003). Additional targets of the *Bacillus subtilis* global regulator CodY identified by chromatin immunoprecipitation and genome-wide transcript analysis. J. Bacteriol. *185*, 1911–1922.
Murphy, H., and Cashel, M. (2003). Isolation of RNA polymerase suppressors of a (p)ppGpp deficiency. Methods Enzymol. *371*, 596–601.
Nanamiya, H., Kasai, K., Nozawa, A., Yun, C.-S., Narisawa, T., Murakami, K., Natori, Y., Kawamura, F., and Tozawa, Y. (2008). Identification and functional analysis of novel (p)ppGpp synthetase genes in *Bacillus subtilis*. Mol. Microbiol. *67*, 291–304.
Paul, B.J., Barker, M.M., Ross, W., Schneider, D. a, Webb, C., Foster, J.W., and Gourse, R.L. (2004). DksA: A critical component of the transcription initiation machinery that potentiates the regulation of rRNA promoters by ppGpp and the initiating NTP. Cell *118*, 311–322.
Paul, B.J., Berkmen, M.B., and Gourse, R.L. (2005). DksA potentiates direct activation of amino acid promoters by ppGpp. Proc. Natl. Acad. Sci. *102*, 7823–7828.
Potrykus, K., and Cashel, M. (2008). (p)ppGpp: Still magical? Annu. Rev. Microbiol. *62*, 35–51.
Ratnayake-Lecamwasam, M., Serror, P., Wong, K.W., and Sonenshein, A.L. (2001). *Bacillus subtilis* CodY represses early-stationary-phase genes by sensing GTP levels. Genes Dev. *15*, 1093–1103.
Schaeffer, P., Millet, J., and Aubert, J.P. (1965). Catabolic repression of bacterial sporulation. Proc. Natl. Acad. Sci. *54*, 704–711.
Srivatsan, A., Han, Y., Peng, J., Tehranchi, A.K., Gibbs, R., Wang, J.D., and Chen, R. (2008). High-precision, whole-genome sequencing of laboratory strains facilitates genetic studies. PLoS Genet. *4*, 1–14.
Tehranchi, A.K., Blankschien, M.D., Zhang, Y., Halliday, J. a, Srivatsan, A., Peng, J., Herman, C., and Wang, J.D. (2010). The transcription factor DksA prevents conflicts between DNA replication and transcription machinery. Cell *141*, 595–605.
Tojo, S., Satomura, T., Kumamoto, K., Hirooka, K., and Fujita, Y. (2008). Molecular mechanisms underlying the positive stringent response of the *Bacillus subtilis ilv-leu* operon, involved in the biosynthesis of branched-chain amino acids. J. Bacteriol. *190*, 6134–6147.
Tojo, S., Kumamoto, K., Hirooka, K., and Fujita, Y. (2010). Heavy involvement of stringent transcription control depending on the adenine or guanine species of the transcription initiation site in glucose and pyruvate metabolism in *Bacillus subtilis*. J. Bacteriol. *192*, 1573–1585.
Traxler, M.F., Summers, S.M., Nguyen, H.-T., Zacharia, V.M., Hightower, G.A., Smith, J.T., and Conway, T. (2008). The global, ppGpp-mediated stringent response to amino acid starvation in *Escherichia coli*. Mol. Microbiol. *68*, 1128–1148.
Vasantha, N., and Freese, E. (1980). Enzyme changes during *Bacillus subtilis* sporulation caused by deprivation of guanine nucleotides. J. Bacteriol. *144*, 1119–

1125.
Wang, J.D., Sanders, G.M., and Grossman, A.D. (2007). Nutritional control of elongation of DNA replication by (p)ppGpp. Cell *128*, 865–875.
Wendrich, T.M., and Marahiel, M.A. (1997). Cloning and characterization of a relA/spoT homologue from Bacillus subtilis. Mol. Microbiol. *26*, 65–79.
Xiao, H., Kalman, M., Ikehara, K., Zemel, S., Glaser, G., and Cashel, M. (1991). Residual guanosine 3', 5'-bispyrophosphate synthetic activity of relA null mutants can be eliminated by spoT null mutations. J. Biol. Chem. *266*, 5980–5990.
Yasbin, R.E., Fields, P.I., and Andersen, B.J. (1980). Properties of *Bacillus subtilis* 168 derivatives freed of their natural prophages. Gene *12*, 155–159.
Yeggy, J., and Stahly, D. (1980). Sporulation and regulation of homoserine dehydrogenase in *Bacillus subtilis*. Can. J. Microbiol. *26*, 1386–1391.

Table 1. Strains used in study.

Strain	Genotype	Reference
SMY	Prototroph	Schaeffer *et al*., 1965
JDW1021	SMY Δ*ywaC* Δ*yjbM* Δ*codY* Δ*relA*::*mls*	Kriel *et al*., 2012
JDW1332	SMY Δ*yjbM*::*spc* Δ*ywaC*::kan Δ*relA*::*mls*	Kriel *et al*., 2012
JDW1391	SMY Δ*ywaC*::*kan* Δ*yjbM*::*spc* Δ*relA*::*cm* *guaB*::P_{spac}-*guaB erm*	Kriel *et al*., 2012
JDW1392	SMY *ilvBp4 ilvBp*ΔT2 Δ*yjbM*::*spc* Δ*ywaC*::*kan* Δ*relA*::*mls*	This work
JDW1430	SMY Δ*ywaC* Δ*yjbM*	Kriel *et al*., 2012
JDW1464	SMY *relA*^{D264G} *ywaC*^{D87G} *yjbM*^{D72G}	This work
JDW1824	SMY *ilvBp4 ilvBp*ΔT2 *ybgEp*ΔCBS3 *ilvDp*ΔCBS Δ*yjbM*::*spc* Δ*ywaC*::*kan* Δ*relA*::*mls*	This work
JDW1898	SMY Δ*ywaC*::*kan* Δ*yjbM*::*spc*	Kriel *et al*., 2012
SRB107	SMY *ilvBp4 ilvBp*ΔT2	Brinsmade *et al*., 2010
SRB194	SMY *ilvBp4 ilvBp*ΔT2 *ybgEp*ΔCBS3 *ilvDp*ΔCBS	Brinsmade *et al*., 2010

Table 2. Plasmids used in study.

Plasmid	Genotype	Reference
pJW204	pGEM/Δ*ywaC*::*kan amp cat*	Kriel *et al*., 2012
pJW239	pEX44/Δ*yjbM amp cat*	Kriel *et al*., 2012
pJW265	pEX44/Δ*yjbM*::*spc amp cat*	Kriel *et al*., 2012
pJW299	pEX44/I-SceI site *amp cat*	Kriel *et al*., 2012
pJW300	pJW239/Δ*yjbM I*-SceI site *amp cat*	Kriel *et al*., 2012
pJW305	pMUTIN4/P_{spac}-*guaB erm*	Kriel *et al*., 2012
pJW306	pJW299/Δ*ywaC I*-SceI site *amp cat*	Kriel *et al*., 2012
pJW368	pJW299/*relA I*-SceI site *amp cat*	This work
pJW369	pJW299/*ywaC I*-SceI site *amp cat*	This work
pJW370	pJW299/*yjbM I*-SceI site *amp cat*	This work
pJW371	pJW299/*relA*^{D264G} *I*-SceI site *amp cat*	This work
pJW372	pJW299/*ywaC*^{D87G} *I*-SceI site *amp cat*	This work
pJW373	pJW299/*yjbM*^{D72G} *I*-SceI site *amp cat*	This work
pJW418	pJW299/Δ*codY I*-SceI site *amp cat*	Kriel *et al*., 2012
pSS4332	*oriU* P*amy*-I-SceI *kan*	Jane and Stibitz, 200

Supplemental Figures

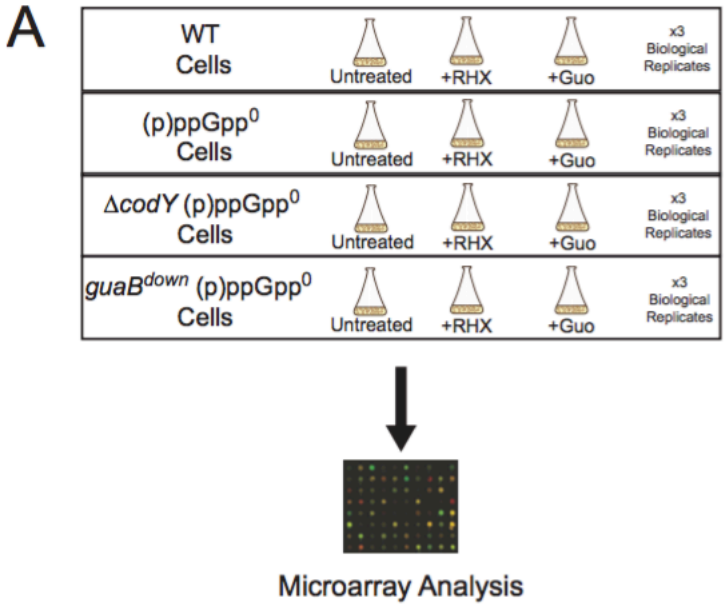

Figure S1. Microarray analysis of wild-type and mutant cells before and after RHX or Guo treatments. (A) Schematic of how cells were collected for microarray analysis. WT, (p)ppGpp^0, Δ*codY* (p)ppGpp^0 and *guaB*^{down} (p)ppGpp^0 cells were grown to an OD_{600} ~ 0.3, and treated for 20 min with arginine hydroxamate (RHX, 0.5 mg/ml) to induce the stringent response by sudden amino acid starvation, or guanosine (Guo, 1 mM) to increase GTP levels. (B) Expanded image of Figure 2D located https://www.ncbi.nlm.nih.gov/pmc/articles/PMC3911124/bin/supp_196_1_189__index.html.

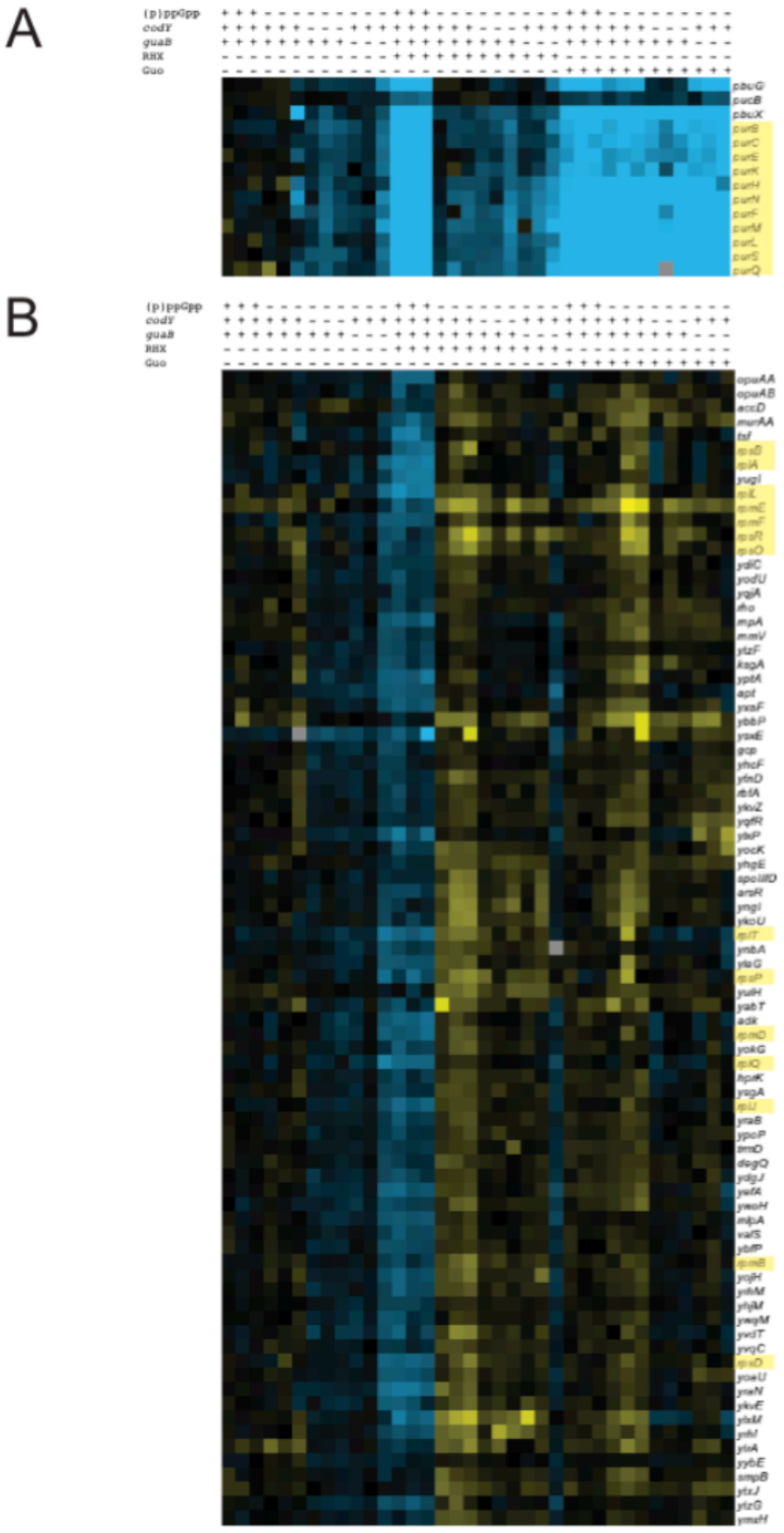
A
(p)ppGpp
codY
guaB
RHX
Guo
pbuG
pucB
pbuX
purS
purC
purE
purK
purH
purN
purF
purM
purL
purQ
B
(p)ppGpp
codY
guaB
RHX
Guo
opuAA
opuAB
accD
murAA
tsf
rplD
rplA
yugI
rplL
rplE
rplF
rplT
rplO
ydiC
yodU
yqgA
rho
mpA
mmiV
ytzF
ksgA
yptA
apt
yxaF
ybbP
yxeE
gcp
yhcF
yfnD
rbfA
ykvZ
yqfR
ybeP
yocK
yhgE
spoIIID
arpR
yngI
ykoU
rplT
ymbA
ybxG
rplP
yuiH
yabT
adk
rplD
yokG
rplQ
hprK
yqgA
rplU
ynaB
ypoP
trmD
degQ
ydgJ
ywfA
ywoH
mfpA
valS
ybiP
rplB
yojH
yhiM
yhjM
ywqM
yvcT
yvqC
rplO
yoaU
ywrN
ykuE
ybxM
ynlI
ylxA
yyfE
smpB
ytxJ
ytzG
ymxH

Figure S2. Hierarchical clustering analysis of transcript levels obtained from transcriptional microarrays. (A) Hierarchical clustering analysis of transcript levels showing a cluster of genes in the *purEKBCSQLFMNHD* operon. (B) Hierarchical clustering analysis of transcript levels showing a cluster of ribosomal protein genes.

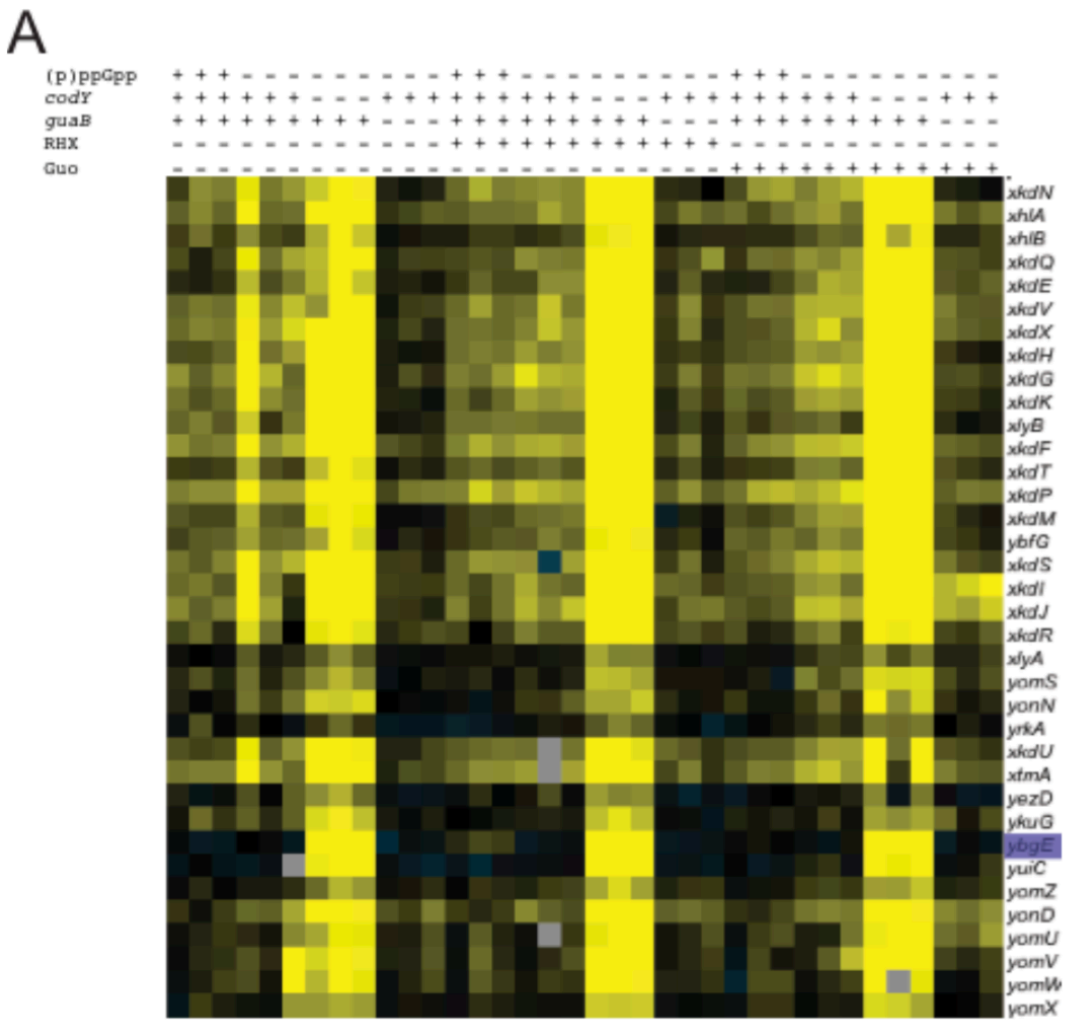

Figure S3. Hierarchical clustering analysis of transcript levels obtained from microarrays showing a cluster of genes regulated by CodY containing *ybgE*.

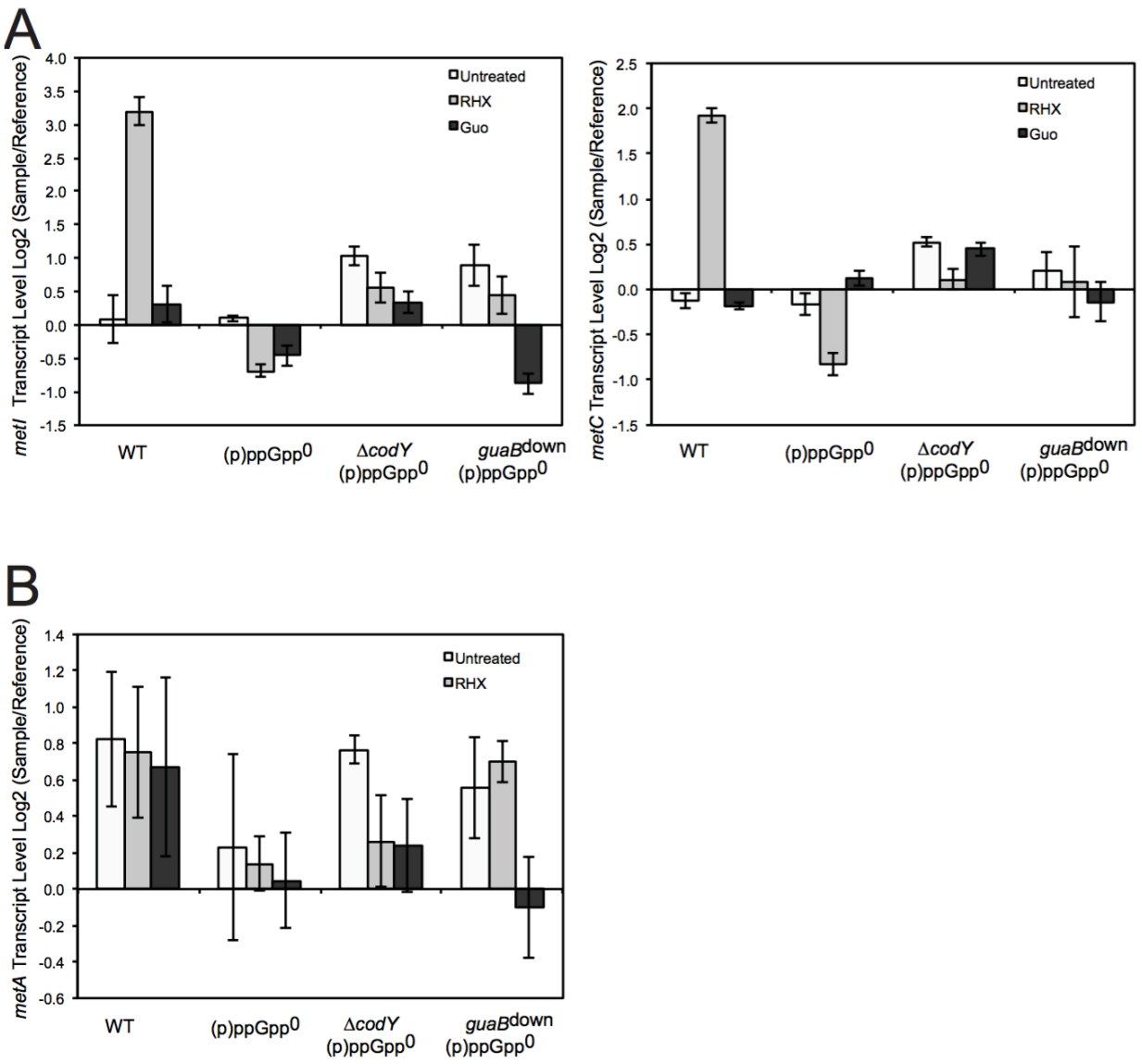

Figure S4. Transcript levels of methionine biosynthesis genes obtained from microarrays. Transcript levels of genes in the *metIC (yjcIJ)* operon (A) and *metA* (B) in wild-type, (p)ppGpp^0, Δ*codY* (p)ppGpp^0 and *guaB*^{down} (p)ppGpp^0 cells both before and after RHX or Guo treatment. Error bars represent standard error of the mean over three independent biological replicates.

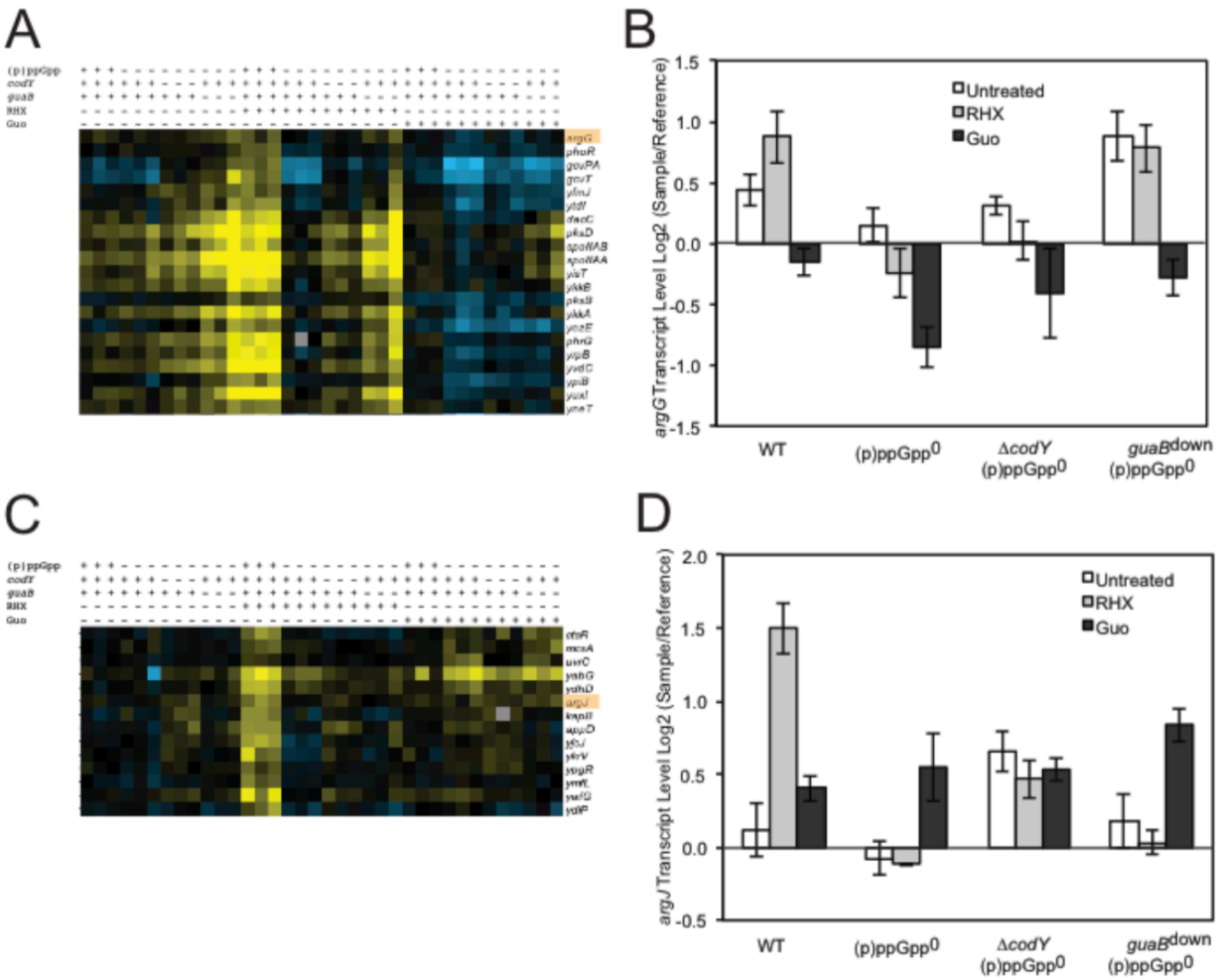

Figure S5. Analysis of transcript levels of arginine biosynthesis genes obtained from transcriptional microarrays. (A, C) Hierarchical clustering analysis of transcript levels showing a cluster of genes containing *argG* (A) and *argJ* (C).
(B, D) Transcript levels of *argG* (B) and *argJ* (D) in wild-type, (p)ppGpp^0, Δ*codY* (p)ppGpp^0 and *guaB*^{down} (p)ppGpp^0 cells both before and after RHX or Guo treatment (in medium with glutamate nitrogen source). Error bars represent standard error of the mean over three independent biological replicates.

Chapter 3: Spontaneous and adaptive persistence by (p)ppGpp-mediated GTP antagonism in Gram-positive bacteria

This chapter is adapted from “Fung, D.K.*, Barra, J.T.*, Schroeder, J.W., Ying, D., and Wang, J.D. (2018) Spontaneous and adaptive persistence by (p)ppGpp-mediated GTP antagonism in Gram-positive bacteria. In editing.”

J.T.B. is co-first author on this manuscript. J.T.B. designed and executed experiments in Figures 1, 2, 4, and 6, and edited the manuscript.

Abstract

A major culprit of antimicrobial treatment failure is dormant, antibiotic-tolerant persisters. The pathways for persister generation in Gram positive bacteria remain poorly understood. Here we show that persisters in the Gram-positive *Bacillus subtilis* can be generated both spontaneously before antibiotic treatment or in response to antibiotic treatment, via the bacterial alarmone (p)ppGpp through its antagonizing effect on GTP. (p)ppGpp accumulates in a rare fraction of unstressed cells, which lowers GTP levels beneath a specific threshold to trigger a phenotypic switch from rapid growth to dormancy. These dormant cells are antibiotic tolerant, and their resuscitation is proceeded by re-accumulation of intracellular GTP. (p)ppGpp can also be induced by sub-lethal concentrations of antibiotic treatment to increase adaptive antibiotic tolerance, via different (p)ppGpp synthetases, implicating the evolutionary advantage of both types of persistence. (p)ppGpp-GTP dichotomy is likely a conserved mechanism of persistence in Gram-positive bacteria.

Introduction

Persisters are phenotypically switched cells that are highly antibiotic tolerant and capable of surviving lethal doses of antibiotic for prolonged period of time. Once treatment is discontinued, persisters can resume growth (Balaban et al., 2004; Bigger, 1944; Harms et al., 2017; Lewis, 2010) thus underlying chronic and recurrent bacterial infections (Cohen et al., 2013; Lewis, 2001; Nguyen et al., 2011; Zhang et al., 2012). Persisters may also evolve antibiotic resistant genetic traits that allow them to grow in the presence of antibiotics, leading to ultimate antimicrobial failure (Levin-Reisman et al., 2017).

Persisters were first proposed to be responsible for antibiotic tolerance in the classical work done by Joseph Bigger (Bigger, 1944). In this work, he suggested several potential pathways of persister formation: they can be induced by drug treatment, or produced spontaneously prior to drug treatment. The source of spontaneous persisters can arise from stationary phase cells that are undergoing growth lag after back-dilution (Type I persisters), or can be generated stochastically via a noise-generating bet-hedging strategy (Type II persisters). However, experimental support for persisters was challenging to obtain, in part due to the difficulty in isolating pure wild type persisters. Experimental support for spontaneous persisters was provided mostly in the form of mutants with elevated frequency of persisters, which have mutations in toxin-antitoxin (TA) modules that allow toxins to turn on dormancy and push the cells over a certain threshold to attain persistence (Balaban et al., 2004; Dorr et al., 2010; Germain et al., 2013; Kaspy et al., 2013; Mok et al., 2015; Schumacher et al., 2015; Verstraeten et al., 2015). In addition to TA modules, the starvation-inducible nucleotide (p)ppGpp

(guanosine tetra- or penta-phosphate) (Potrykus and Cashel, 2008) is recognized as a driver for Type I persisters. (p)ppGpp biosynthesis is essential for the high persistence phenotype observed in *hipA7 E. coli* (Korch et al., 2003), where Type I persistence was first visualized, because the HipA toxin induces (p)ppGpp (Germain et al., 2013; Kaspy et al., 2013; Maisonneuve et al., 2013). However, the role of TA and ppGpp in *E. coli* has recently been challenged (Harms et al., 2017; Shan et al., 2017).

A recent study revealed that persister formation in Gram-positive bacterium *S. aureus* is associated with ATP depletion but not (p)ppGpp (Conlon et al., 2016). However, other studies have alternatively shown that antibiotic tolerance in *E. faecalis* and *S. aureus* are associated with (p)ppGpp biosynthesis (Corrigan et al., 2016; Gaca et al., 2013; Geiger et al., 2014). These studies raise the following critical questions: what are the pathways of persister formation and what is the role of (p)ppGpp on persistence in Gram-positive bacteria?

Here, we apply single-cell analyses to persister formation in the Gram-positive bacterium *B. subtilis*, which shares common features in (p)ppGpp regulation with many Gram-positive pathogens. We report the observation of both spontaneous and antibiotic-induced persister formation (Type I and II persisters), and reveal (p)ppGpp as their common driving factor. Different (p)ppGpp synthetases contribute to formation of stochastic and induced persisters, suggesting that bacteria evolved both bet-hedging and responsive persister development via (p)ppGpp. Finally, our results suggest that cellular GTP depletion by (p)ppGpp is an important mechanism of persistence in Gram-positive bacteria.

Results

(p)ppGpp is both necessary and sufficient for persistence in B. subtilis. To understand the role of the stress-inducible nucleotide (p)ppGpp in antibiotic survival of the Gram-positive bacterium *B. subtilis*, we first determined the minimal inhibitory concentrations (MIC) of bacteriostatic and bactericidal antibiotics that inhibit the growth of *B. subtilis* into turbid culture (Figure 1A). Wild-type cells do not have a significantly different MIC compared to mutants deleted of all three (p)ppGpp synthetase genes- *relA*, *yjbM* and *ywaC* ((p)ppGpp^0 cells) (Figure. 1A, S1), indicating that (p)ppGpp does not significantly promote antibiotic resistance. We next tested the survival of wild type *B. subtilis* to vancomycin (VAN) and ciprofloxacin (CIP) at a range of different concentrations above MIC (Figure. 1B, 1C). In exponentially growing populations, we observed a bi-phasic mode of killing, in which a rapid killing phase is followed by prolonged survival of the remaining population (~0.1-0.01%) (Figure. 1B, 1C) independent of drug concentration, suggesting that they are due to a small fraction of highly tolerant persisters. Importantly, upon regrowth, these cells are re-sensitized to antibiotic killing (Figure. 1D, 1E), confirming that they derived from a phenotypic switch rather than genetically altered cells that are tolerant to antibiotics (Bigger, 1944; Cohen et al., 2013)(Bigger, 1944; Cohen et al., 2013; Maisonneuve and Gerdes, 2014).

When we pretreated the cells with arginine hydroxamate (RHX), an amino acid analog which induces (p)ppGpp accumulation to ~1 mM (Kriel et al., 2012), we observed a dramatic increase (~100-800-fold) in the persister population (to ~10%-80%) in the (p)ppGpp-induced population compared to the non-induced control. In contrast, the (p)ppGpp^0 mutant had a strong reduction (>10-fold compared to (p)ppGpp$^+$) in

antibiotic tolerance (Figure. 1F, 1G), indicating that (p)ppGpp is also necessary for persistence.

It was recently reported that persistence can be induced by treatment with compounds that disrupt ATP synthesis such as CCCP and arsenate in *S. aureus* (Conlon et al., 2016). Interestingly, we consistently observed (p)ppGpp accumulation in CCCP-treated or arsenate-treated *B. subtilis* cells (Figure. 2A). In addition, loss of (p)ppGpp synthesis significantly compromised CCCP's ability to induce antibiotic tolerance (Figure. 2B). CCCP-mediated protection against antibiotics but itself renders cells sensitive to CCCP itself. Thus, ATP synthesis inhibitors promote antibiotic tolerance, at least in part, through (p)ppGpp induction.

(p)ppGpp promotes persistence through antagonizing GTP. We next investigated how (p)ppGpp allows for antibiotic tolerance. Since no difference in MIC was detected between WT and (p)ppGpp^0 (Figure 1A, 1B), the differences in antibiotic survival were unlikely due to differences in antibiotic uptake/efflux or other resistance mechanisms. In agreement with a recent finding that known TA systems are not involved in persistence in Gram-positive pathogen *S. aureus* (Conlon et al., 2016), we also detected no significant differences in CIP and VAN tolerance when comparing wild-type *B. subtilis* and its isogenic mutant with deletion of three known TA systems (Δ3TA) (Figure S2).

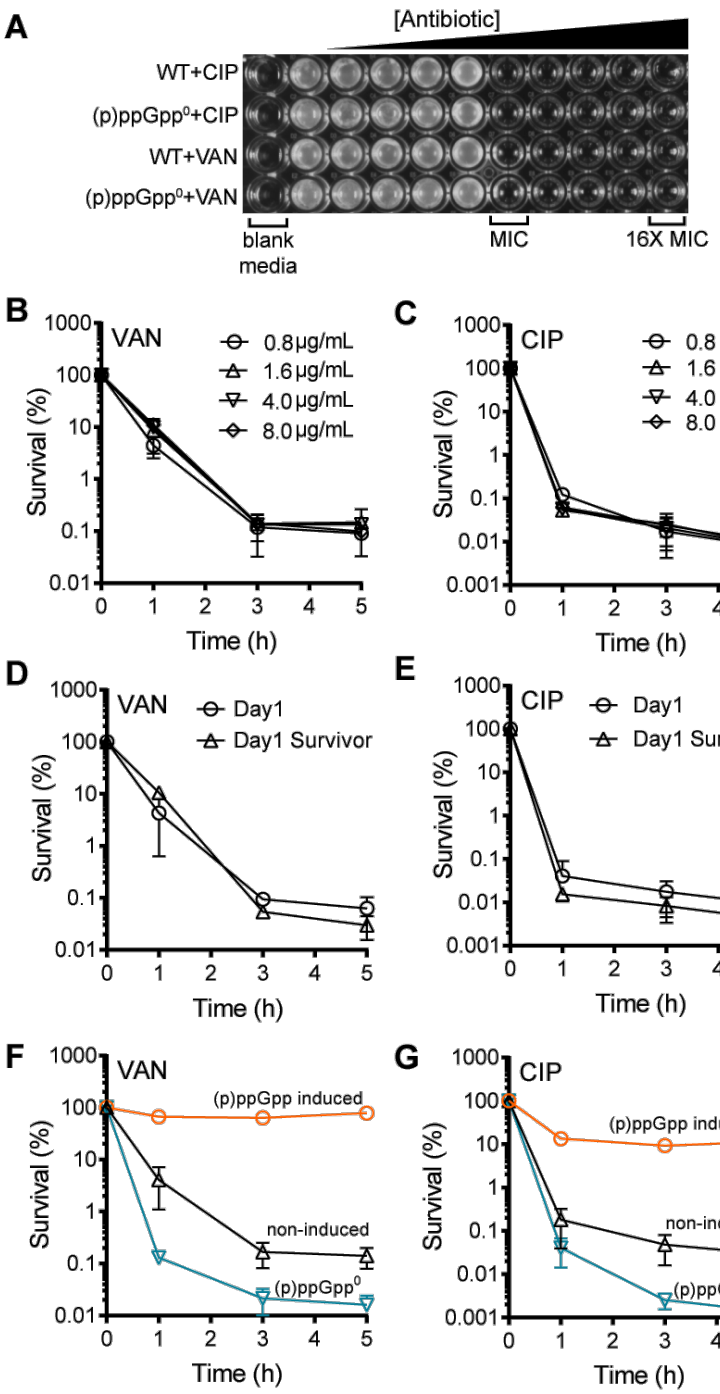

Figure 1. (p)ppGpp mediates persistence to antibiotics. (A) Minimal inhibitory concentrations (MICs) of WT and (p)ppGpp^0 to various antibiotics. Values represent mean ± SD, N = 3. (B and C) Survival of WT cells to increasing concentrations of (B) VAN or (C) CIP ranging from ~4X to 40X MIC for up to 5 h. (D and E) Survival of exponentially-growing WT cells (Day 1, solid lines), or its successor population derived from survivors after 5h treatment (Day 1 survivor, dotted lines), to treatments with (D) VAN or (E) CIP for up to 5 h. (F and G) Survival of WT (black) and (p)ppGpp^0 (blue) to

bactericidal antibiotics with or without pre-induction of (p)ppGpp biosynthesis. Cells were either pre-induced with 0.5 mg/mL RHX for 30 min (orange) or without induction (black and blue), followed by exposure to (F) VAN or (G) CIP for up to 5 h. Each time point represents mean ± SD, N ≥ 3.

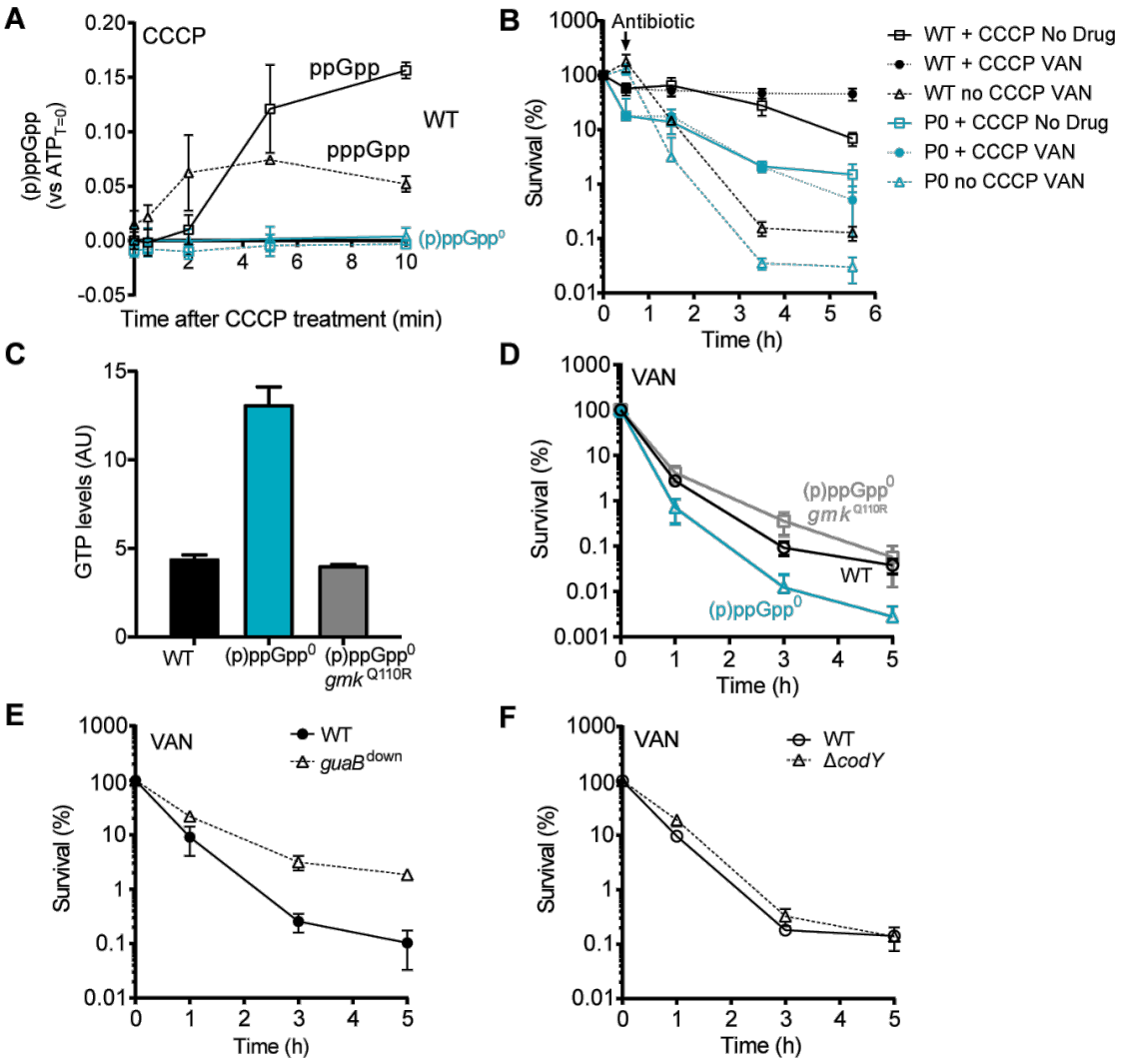

Figure 2. Persistence by (p)ppGpp-mediated GTP down-regulation. (A) Changes in (p)ppGpp levels in response to ATP depletion. Cells were treated with CCCP and measured for changes in nucleotide levels with TLC over time as indicated. N = 2. (B) CCCP promotes persistence in association with (p)ppGpp. WT (black) and (p)ppGpp^0 (blue) cells with or without 30 min CCCP pre-treatment were tested for persister levels with VAN treatment for 5h. N = 2. (C) GTP levels of WT (black), (p)ppGpp^0 (blue), and (p)ppGpp^0 *gmk*^{Q110R} (grey). N = 3. (D) Survival of WT (black), (p)ppGpp^0 (blue), and (p)ppGpp^0 *gmk*^{Q110R} (grey) populations under VAN treatment. N = 3. (E) Survival of WT (solid line) and GuaB-depleted strain (*guaB*^{down}, dashed line) to VAN treatment. N = 3. (F) Survival of WT (solid line) and Δ*codY* (dashed line) to VAN treatment. N = 2. All values represent mean ± SD.

(p)ppGpp plays critical roles in GTP down-regulation in *B. subtilis*, including depletion of GTP during (p)ppGpp production and direct inhibition of GTP biosynthesis by (p)ppGpp (Kriel et al., 2012). Using fluorescence microscopy, intracellular GTP levels were shown to be elevated in the (p)ppGpp^0 mutant when compared to wild type cells (Figure. 2C). We examined whether the loss of antibiotic tolerance in the absence of (p)ppGpp can be compensated by reducing GTP levels. We obtained a (p)ppGpp^0 mutant in the gene *gmk*, encoding guanylate kinase (Experimental Procedures), which brought GTP to a level comparable to WT (Figure. 2C). Lowering GTP levels is sufficient to mediate persistence in the absence of (p)ppGpp (Figure. 2D). In addition, reduction of GTP biosynthesis in the presence of (p)ppGpp biosynthesis further enhanced persistence. We engineered a strain in a (p)ppGpp$^+$ background that controls the expression of *guaB* (encoding IMP dehydrogenase) under an IPTG-inducible promoter. Growing cells without IPTG reduces GTP levels, which increase persistence by more than ten-fold over the wild type cells (Figure. 2E). This effect is independent of the transcription regulator CodY, which mediates a large proportion of transcription changes due to (p)ppGpp accumulation (Kriel et al., 2014; Sonenshein, 2005), as Δ*codY* mutant exhibited similar levels of persister as WT (Figure. 2F).

Development of a single-cell GTP reporter in B. subtilis. To confirm the effect of GTP on persistence, we developed a fluorescent reporter for detecting relative cellular GTP status to visualize the distribution of low GTP cells in a population and determine their connections to persister formation. We constructed two fluorescent reporters, one is transcriptionally fused to the *ilvB* promoter which is strongly activated in response to (p)ppGpp accumulation and reduced intracellular GTP levels (Figure S3A) (Kriel et al.,

2014), another is fused to a ribosomal P1 promoter which is strongly down-regulated by reduced intracellular GTP levels (Krásný and Gourse, 2004). We introduced the two reporters into the same wild-type cells and subjected them to amino acid downshift that triggers (p)ppGpp accumulation, and observed an apparent increase in P_{ilvB} reporter fluorescence, and repression of P_{rrnB} activity (Figure 3A, S3B). The reciprocal expression of the two reporters also indicated that the reporter activities was not due to a general effect on translation.

We tested the P_{ilvB} reporter in multiple (p)ppGpp-inducing conditions and observed a strong and quantitative correlations: during growth transition into stationary phase which triggers starvation-mediated (p)ppGpp accumulation (Figure. 3B), upon carbon starvation, RHX treatment, and amino acid downshift (Figure. 3C). The P_{ilvB} reporter exhibit rapid time-dependent changes (within minutes) in response to (p)ppGpp accumulation (Figure. S3C), as well as dose-dependent responses to different (p)ppGpp inducers (Figure. 3B). Finally, we have confirmed that the observed reporter response was dependent on (p)ppGpp accumulation, as the lack of (p)ppGpp biosynthesis rendered the reporter strain unresponsive to RHX treatment (Figure. S3D). We subsequently utilized this reporter system to study variations in (p)ppGpp-GTP levels in the population and its effect on persister formation.

Spontaneous persisters have reduced GTP levels. Using the P_{ilvB} reporter, we examined GTP levels in single cells using time-lapse microscopy. We found that while the vast majority of cells grown in nutrient-replete medium have only background fluorescence, a few cells display bright fluorescence, indicative of low GTP levels. We performed microscopy to identify individual cells with high (p)ppGpp reporter

fluorescence and subsequently tracked their survival upon antibiotic treatment using time-lapse microscopy. Exponentially-growing cells containing the P_{ilvB} reporter were inoculated onto agarose pads containing growth medium to prevent starvation during the imaging experiment. Cells with high P_{ilvB} activity were identified and monitored for their survival before and after treatment with a lethal concentration of carbenicillin and cell death dye Sytox blue (Figure. 3D, Movie S1). Cells with high reporter fluorescence (i.e. high (p)ppGpp, red cell) were non-dividing before antibiotic treatment, while the rest of the population were actively growing (Figure. 3D, 20 min to 50 min). Upon antibiotic treatment, the bulk of the population was rapidly killed and eventually lysed, while the (p)ppGpp^{High} cells remained viable (Figure. 3D, 90 min to 290 min). We next examined the presence of (p)ppGpp^{High} cells in the population. Using flow cytometry, we found that a small fraction of exponentially growing cells has elevated fluorescence levels (Figure. 3E, orange population) indicative of high (p)ppGpp and reduced GTP levels. We performed fluorescent-activated cell sorting (FACS) to sample this population (Figure. 3F) and tested for their survival to antibiotic treatment. Strikingly, the 0.1% fraction with the highest reporter fluorescence displayed ~80% survival when treated with a lethal dose of antibiotic VAN (Figure. 3F), suggesting that they are almost all persisters. (p)ppGpp induction in response to nutrient downshift can lead to further increase of the (p)ppGpp^{High} sub-population, which leads to a proportional increase in persisters (Figure. S3C-S3E). This altogether demonstrated that persistence is associated with a small population of cells with elevated (p)ppGpp.

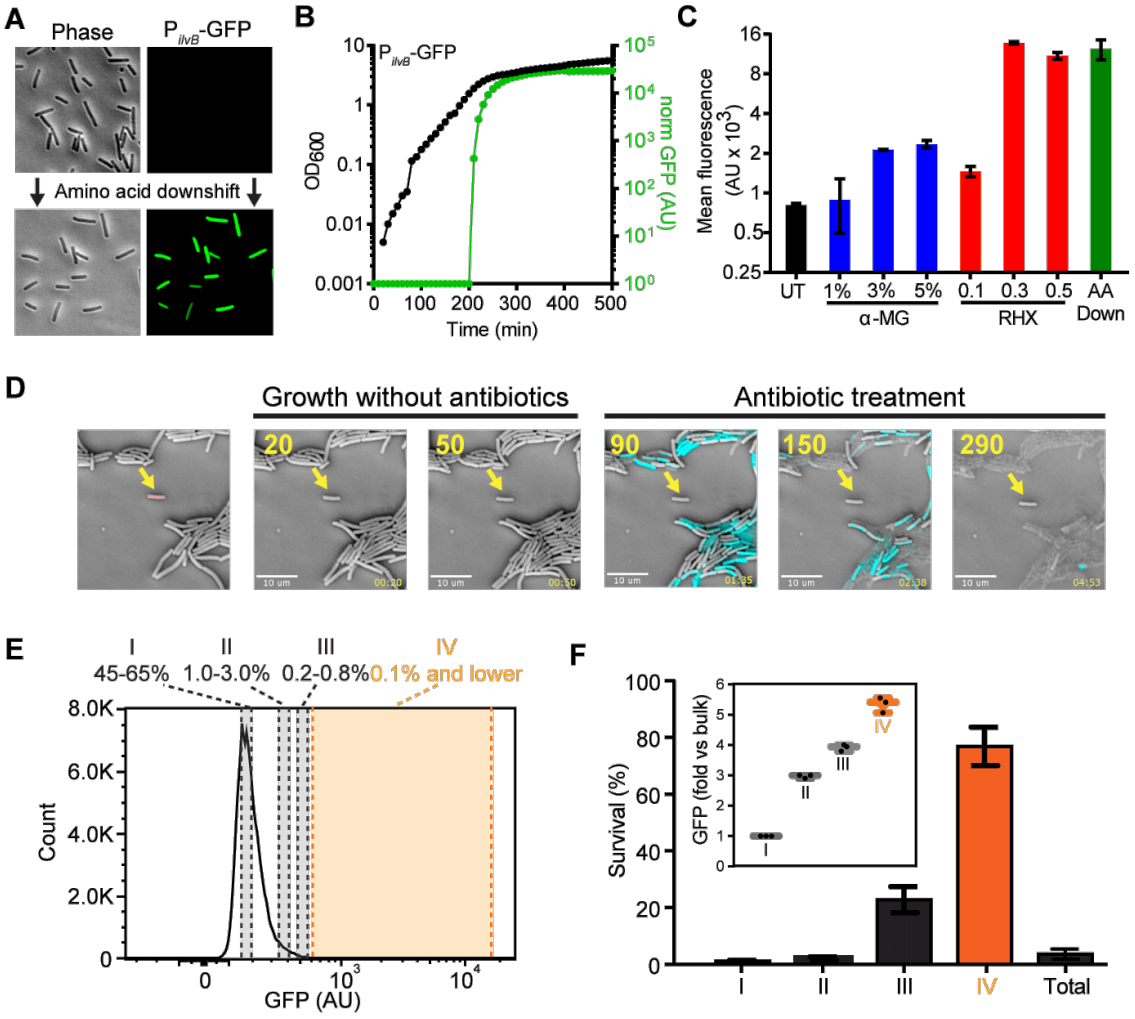

Figure 3. Single-cell GTP antagonism underlies persistence. (A) Representative images of WT cells containing the P_{ilvB} reporter before and after the amino acid downshift. (B) Changes in P_{ilvB} activities (P_{ilvB}-GFP, green) during growth (OD_{600}, black) over time. GFP was normalized to OD_{600}. (C) WT cells were treated with increasing concentrations of alpha-methylglucoside (α-MG, blue), arginine hydroxamate (RHX, red), or amino acid downshift (AA down, green). Single-cell fluorescence was measured after 2h of treatment using fluorescence microscopy. Values represent mean ± SD from N = 2 of n > 200 cells each. (D) Observation of persister survival using time-lapse microscopy (see also Movie S1). Cells under GTP depletion were identified (arrow) using the P_{ilvB} reporter. Antibiotic survival was tested using carbenicillin and Sytox-blue staining for viability. Values in yellow indicate time in min. (E) FACS of exponentially-growing WT cells into different fractions (I to IV) according to P_{ilvB} activities as indicated. (F) VAN survival of sorted populations from (E). Values represent mean ± SD, N > 3.

Stochastic induction of (p)ppGpp leads to entrance of growing cells into persister state. The (p)ppGpp-mediated persisters we observed using our single-cell reporter can have two potential origins: carry-over cells in the inoculum from stationary phase (i.e. Type I persisters), or cells that stochastically enter persister state during active growth (i.e. Type II persisters) (Balaban et al., 2004) (Figure. 4A). To understand whether (p)ppGpp is involved in Type II persistence we performed serial passage experiments, which eliminated Type I but not Type II persisters, and enumerated persister levels in each passage for both wild-type (WT) and (p)ppGpp^0 (P^0) populations (Figure. 4B). We found that the level of persisters stabilized in WT cells after the first passage, indicating that the remaining persisters (~0.06%) are continuously generated Type II persisters (Figure. 4C, black bars). In contrast, the (p)ppGpp^0 mutant had significantly lower (<10-fold) level of persisters across passages (Figure. 4C, blue bars). This suggested that (p)ppGpp is a major contributor (~90%) of Type II persistence (Figure. 4D).

Using WT cells containing the P_{ilvB} reporter and single-cell time-lapse microscopy, we captured the formation of Type II persisters being generated stochastically from growing cells (Figure. 4E, S4A, Movies S2 and S3). Figure. 4F showed four independent trajectories of cells entering persistence from active growth, in which an increase in (p)ppGpp (Figure. 4F, GFP, red curves) is accompanied by cessation of growth (Figure. 4F, cell size, black curves). Notably, changes in (p)ppGpp preceded the changes in growth of these cells, supporting that accumulation of (p)ppGpp is the driving force to the transition. In addition, the level of (p)ppGpp accumulation at the point of transition also appeared to be similar (Figure. 4F, red dotted lines), suggesting that entry into persistence requires accumulation of (p)ppGpp

above a threshold level. We also monitored changes in growth rates and reporter fluorescence for cells in the persistent state, actively growing, or exiting from persister into growing state (Figure. 4G, 4H, S4B-S4E, Movies S4 to S6). Each state has a unique growth rate and GFP fluorescence profile consistent with our observations that persisters have high GFP and low growth rate, whereas rapidly growing cells have low GFP and high growth rate. We also analyzed the changes in specific growth rates associated with (p)ppGpp and observed that WT cells showed immediate growth arrest upon reaching a (p)ppGpp threshold at about 600 AU (Figure. 4I, black line). However, in the (p)ppGpp^0 *gmk*^{Q110R} (P^0*gmk*) mutant, the P$_{ilvB}$ fluorescence, which is dependent on GTP in the absence of (p)ppGpp regulation, assumed an almost linear correlation with growth rate (Figure. 4I, purple line), rather than a rapid switch observed in WT. We also found that the P^0*gmk* mutant exhibits higher variations in single-cell growth rates compared to WT, and the cells slowly enter the persister state from slow growth instead of a rapid transition (Figure. S4F-S4H). Such differences suggest that unlike in WT, persistence in P^0*gmk* likely stems from generally reduced growth rates and increased fluctuations in GTP biosynthesis due to the lack of GTP homeostatic control by (p)ppGpp.

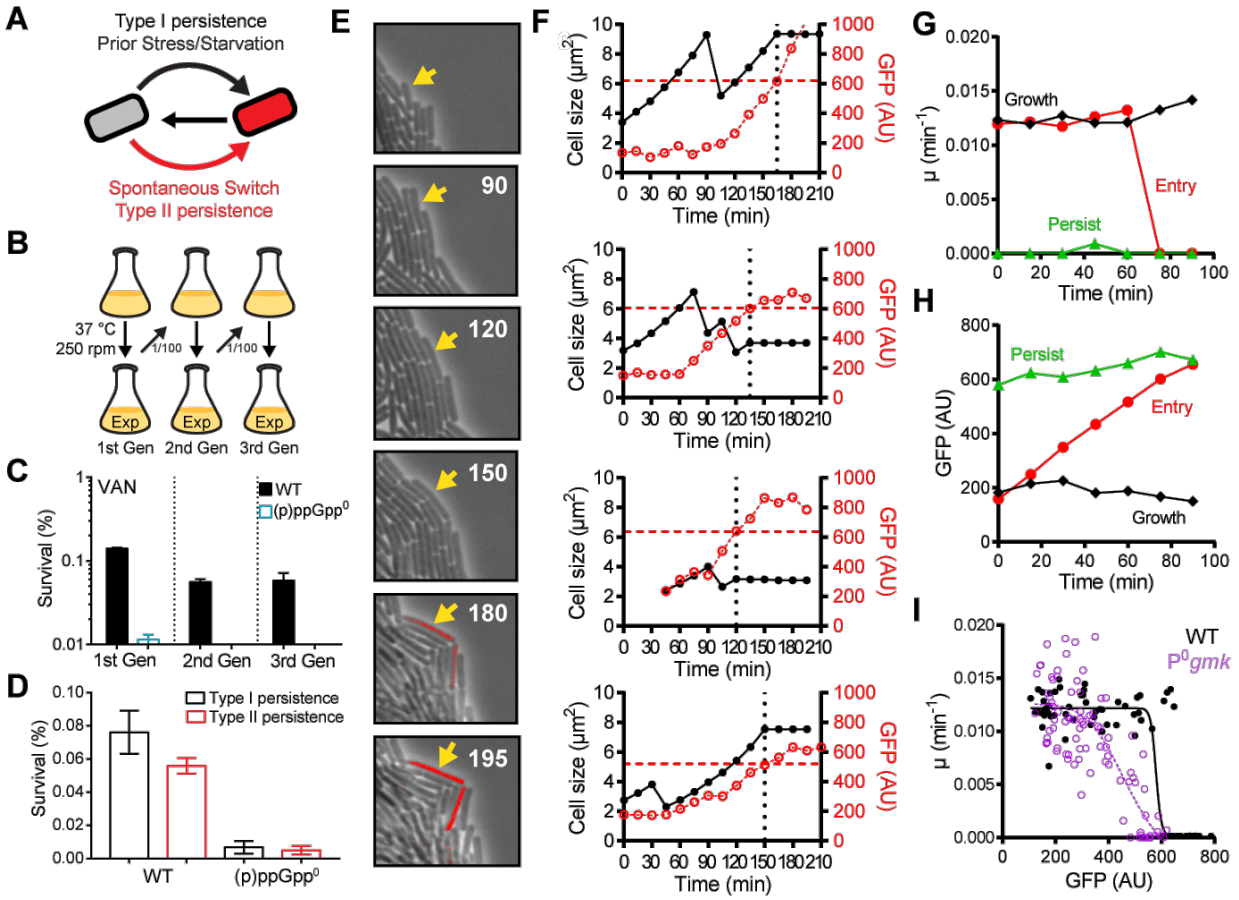

Figure 4. GTP antagonism by (p)ppGpp leads to rapid persister formation. (A) Persistence can be due to the presence of carry-over stressed cells (Type I persistence) or cells that spontaneously enter persistence (Type II persistence). (B and C) Dissociation of Type I or Type II persisters. WT and (p)ppGpp^0 cells were grown to log phase (1st Gen) and sub-cultured (100-fold dilutions) for two additional rounds (2nd Gen and 3rd Gen). (C) Populations from different passages were tested for persister levels with VAN treatment for 5h. Persisters which were eliminated by serial passage were Type I persisters, while Type II persisters remain in 2nd and 3rd Gen. Values represent mean ± SD, N = 3. (D) Levels of Type I and Type II persistence in WT and (p)ppGpp^0 cells calculated from (C). (E) Development of Type II persisters observed during active cell growth (see also Movie S2 and S3, and Figure S4A). Growth and changes in P_{ilvB} activities were monitored over time using time-lapse microscopy. (F) Changes in P_{ilvB} activities (red open circles) and cell size (black solid circles) from four independent events of stochastic entrance into persistence. Red dashed lines indicate P_{ilvB} expression at entrance into persister state and black dotted lines indicate time of entry. (G and H) Representative changes in specific growth rates (μ) (G) and P_{ilvB} activities (H) over time in WT cells during growth and persistence (see also Figure S4B-E and Movies S4-S6). (I) Correlation of single-cell growth rate and P_{ilvB} activities in WT (solid black circles) and (p)ppGpp^0 *gmk*^{Q110R} mutant (open purple circles). Solid (WT) and dashed lines ((p)ppGpp^0 *gmk*^{Q110R}) indicate non-linear regression curves fitted to the respective populations.

Spontaneous persistence is mediated by synthetases RelA and YjbM. In *B. subtilis* and other Firmicutes, (p)ppGpp is synthesized by three different synthetases: a bifunctional synthetase and hydrolase RelA, and two small alarmone synthetases YjbM and YwaC (Figure. 5A). To dissect their roles on stochastic persistence, we utilized flow cytometry to measure single-cell (p)ppGpp levels using the P_{ilvB} reporter in WT and a series of (p)ppGpp synthetase mutants under exponential growth and separated the cells into GFP-low and GFP-high populations (Figure. 5B, 5C). We first measured their median fluorescence, which corresponds to the basal (p)ppGpp levels of the bulk of the population (Figure. 5D). While we could detect an appreciable level of basal (p)ppGpp in WT, such levels were significantly diminished (by ~50%) in the *relA*^{Syn} (synthetase-inactive RelA) or Δ*yjbM* mutant. Furthermore, inactivation of both RelA and YjbM led to almost complete abolishment of basal (p)ppGpp synthesis similar to that of the (p)ppGpp^0 mutant (Figure. 5D). It is noted that the residual P_{ilvB} activity detected in (p)ppGpp^0 is due to leaky expression of the reporter. Interestingly, the allosteric *yjbM*^{F42A} mutant (YjbM with its allosteric pppGpp regulatory site disrupted) (Steinchen et al., 2015) displayed similar defect as the *yjbM* knockout (Figure. 5D), suggesting that its activity is dependent on the allosteric regulation by pppGpp. On the contrary, loss of *ywaC* only had minor impact on the basal (p)ppGpp level (~2%) (Figure. 5D). This suggests that RelA and YjbM are responsible for basal (p)ppGpp synthesis during active growth.

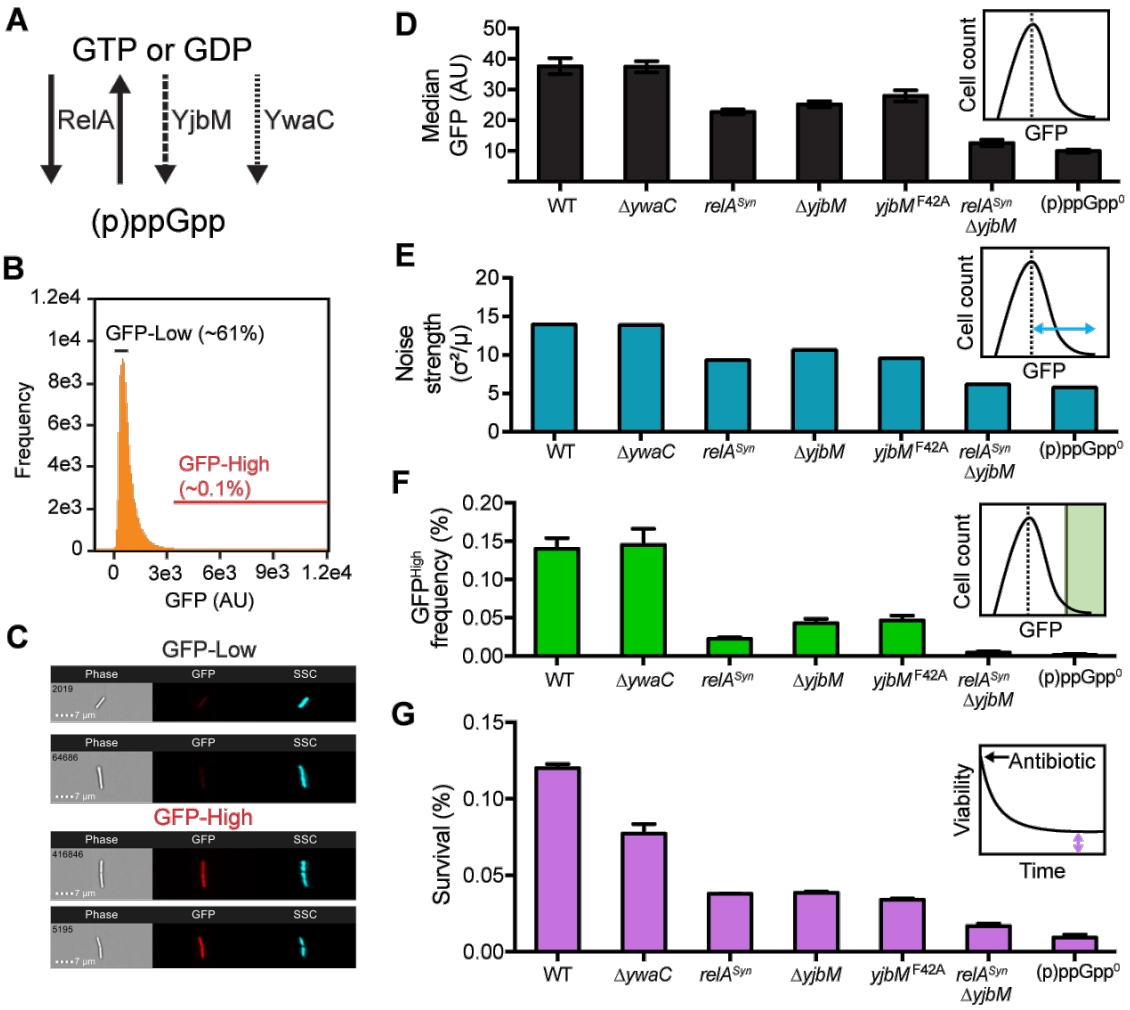

Figure 5. Stochastic persistence is mediated by RelA and YjbM. (A) (p)ppGpp biosynthesis in *B. subtilis* and related Gram-positive bacteria. RelA is a bifunctional enzyme that synthesizes and hydrolyzes (p)ppGpp, while the small alarmone synthetases RelA and YjbM are monofunctional synthetases. RelA is known to be regulated by nutritional stresses while YwaC is controlled at the expression level by membrane stresses. YjbM activity can be induced allosterically by pppGpp. (B and C) Analysis of persister distribution using the P_{ilvB} reporter and flow cytometry. (B) Single-cell distribution of P_{ilvB} activities in WT (~250,000 cells) and identification of GFP-low and GFP-high cells based on FACS sorting experiment in Figure. 3E. (C) Snapshots of GFP-low and GFP-high cells in (B). SSC indicates side-scatter. (D to G) Persister distribution in WT and (p)ppGpp synthetase mutant populations containing the P_{ilvB} reporter (see also Figure. S5). Each population was analyzed for its (D) Median GFP levels, (E) Noise strength (i.e. variability of single-cell GFP levels), (F) Fraction of GFP-high cells, and (G) Survival to VAN treatment for 5h. Values represent mean ± SD from N = 2 of n > 106 cells each.

Next, we measured the heterogeneity of single-cell (p)ppGpp in the form of population variance or amount of noise in both wild-type and synthetase mutant populations (Figure. 5E). We found that the differences in single-cell (p)ppGpp in WT and synthetase mutant populations mirrored their basal (p)ppGpp synthesis in Figure. 5D, in which disruption of either RelA or YjbM led to significant reduction in cell-to-cell variations in (p)ppGpp levels (Figure. 5E). To further understand whether the differences in (p)ppGpp heterogeneity confer changes in persister levels, we analyzed the populations by gating the subpopulation with high (p)ppGpp levels (> 5-fold over basal levels) based on our prior FACS sorting experiment to predict the relative abundance of persisters in different populations before antibiotic treatment (Figure. 5F). We found the predicted frequencies of stochastic persisters were significantly reduced when either RelA (~7-fold) or YjbM (~4-fold) was disrupted, but not YwaC (Figure. 5F). Furthermore, the *relA*^{Syn} Δ*yjbM* double mutant resembled the (p)ppGpp^{0} mutant. To confirm whether the predicted persister levels correlate with survival against antibiotics, we enumerated the levels of persisters in these populations by VAN treatment for 5h. While the survivor frequencies generally agreed with the predicted levels of stochastic persisters, we found that the *relA*^{Syn} Δ*yjbM* mutant contained a significant number of antibiotic survivors over the (p)ppGpp^{0} mutant (Figure. 5G). This discrepancy suggests that there is an additional pathway of persistence in addition to the stochastically generated persisters, and is likely mediated by the other (p)ppGpp synthetase YwaC.

Elevation of (p)ppGpp in response to specific antibiotic promotes persistence. Since the loss of RelA and YjbM should eliminate the generation of stochastic persisters, the resulting persisters detected in the mutant *relA*^{Syn} Δ*yjbM* mutant (Figure. 5F, 5G) likely

emerged in response to antibiotic exposure. To test this hypothesis, we first studied the effect of sub-lethal antibiotics (~0.5x MIC) on (p)ppGpp accumulation in WT cells containing the P_{ilvB} reporter. We found that exposure to specific antibiotics at even sub-lethal concentrations resulted in apparent increase in (p)ppGpp, particularly for cell-wall targeting antibiotics including Bacitracin (BAC), Carbenicillin (CARB) and Vancomycin (VAN) (Figure. 6A). To further examine whether the induction was YwaC-dependent, we performed the same microscopy experiment using a mutant lacking YwaC (Δ*ywaC*), or another mutant with YwaC as the only (p)ppGpp synthetase (*relA*^{Syn} Δ*yjbM*), and found that indeed the induction was mediated by YwaC, as evidenced by higher GFP levels in strains containing YwaC (Figure 6B). After BAC treatment, we observed an increase in GFP fluorescence, with a concomitant decrease in growth rate, in five independent trajectories, indicative of (p)ppGpp production like we showed previously (Figure. 6C, 4F).

To examine the connection between antibiotic-mediated (p)ppGpp induction and persistence, we compared the persister levels in WT and Δ*ywaC* strains treated with antibiotics that can induce (p)ppGpp through YwaC (e.g. VAN), with another antibiotic which cannot induce (p)ppGpp (e.g. CIP). As shown in Figure 6D, we were able to detect a subtle (~2-fold) but reproducible difference in persister levels under VAN treatment but not CIP treatment (Figure 6D, WT vs Δ*ywaC*). Such differences are more apparent when we compare *relA*^{Syn} Δ*yjbM* (with YwaC as the sole (p)ppGpp synthetase) and (p)ppGpp^0 populations (Figure 6D, *relA*^{Syn} Δ*yjbM* vs P^0). This finding suggests that specific antibiotics can lead to higher levels of persister formation due to its ability to induce (p)ppGpp.

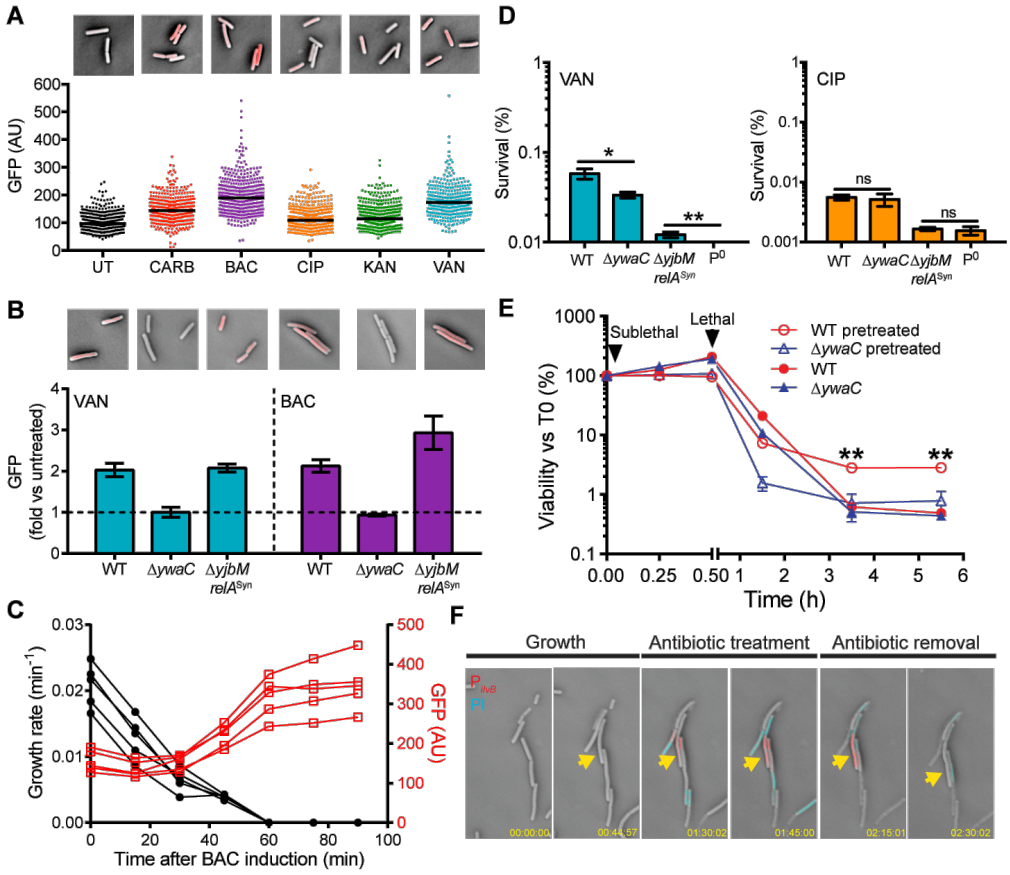

Figure 6. (p)ppGpp accumulation in response to specific antibiotics enables induced persistence. (A) Specific antibiotics induce (p)ppGpp accumulation. WT cells containing P_{ilvB} reporter exposed to sub-lethal concentrations of Carbenicillin (CARB), Ciprofloxacin (CIP), Kanamycin (KAN), Vancomycin (VAN), or Bacitracin (BAC). Single-cell fluorescence was quantitated and normalized to cell size. Horizontal bars represent median fluorescence (n > 300 cells). (B) (p)ppGpp accumulation in response to cell-wall active antibiotics is mediated by YwaC. WT, Δ*ywaC* and *relA*^{Syn} Δ*yjbM* cells subjected to sub-lethal VAN or BAC treatment as in (A). (C) Changes in specific growth rate and P_{ilvB} activities over time for cells that enter persistence after BAC treatment. (D) YwaC promotes persistence to specific antibiotics. Survival of WT, Δ*ywaC*, *relA*^{Syn} Δ*yjbM* and (p)ppGpp^0 (P^0) cells to lethal VAN (blue, (p)ppGpp-inducing) or CIP (orange, non-inducing) treatments and their persister levels. Values represent mean ± SD, N = 3. *p < 0.05, **p < 0.005, ns, not significant (Student's t-test) (E) Sub-lethal BAC increases persistence in a YwaC-dependent manner. WT (red) and Δ*ywaC* (blue) cells were subjected to sub-lethal BAC (open symbols) or without treatment (filled symbols) for 30 min, followed by exposure to lethal BAC treatment for up to 5h. Values represent mean ± SD, N = 3. **p < 0.005 (Student's t-test). (F) Time-lapse microscopy of antibiotic-induced survival upon antibiotic treatment. WT cells containing the P_{ilvB} reporter was allowed to grow in the absence of antibiotic (Growth). Cells were then subjected to treatment with carbenicillin (Antibiotic treatment) followed by antibiotic removal using penicillinase (Antibiotic removal). Cell death was monitored using propidium iodide (cyan).

Since bacteria are normally exposed to increasing concentrations of antibiotics in the environment through diffusion from antibiotic-producing organisms, we speculated that (p)ppGpp induction by antibiotics could enhance their survival through inducible persister formation should such a scenario occur. To test this, we used Bacitracin (BAC) as an example and divided our lethal single-dose antibiotic treatment into two applications: an initial sub-lethal dose for 30 min followed by the remaining dose for the next 5 hours, and studied the survival of wild-type (WT) and Δ*ywaC* populations over time (Figure. 6E). The experiment was done in parallel with populations that received a single lethal treatment. We first confirmed that both WT and Δ*ywaC* were not killed by the sub-lethal dose alone (Figure. 6E, open symbols, first 0.5 hr). In the case of single lethal treatment, we found that both WT and Δ*ywaC* had similar levels of persisters after treatment (Figure. 6E, red solid circles vs blue solid triangles). However, WT populations that received a sub-lethal dose followed by a lethal dose had higher levels (~5-fold) of persisters compared to the single lethal treatment (Figure. 6E, red open circles vs red solid circles). More importantly, the effect of sub-lethal induction was abolished in the Δ*ywaC* mutant (Figure. 6E, blue open triangles). We also found that this YwaC-dependent induction of persistence occurs over a range of sub-lethal antibiotic concentrations (Figure S6).

Discussion

Persisters were proposed more than 70 years ago to be non-dividing cells that spontaneously form in a growing culture and were responsible for failures in treatment of Gram-positive *Staphylococcal* infections (Bigger, 1944). Since then mounting evidence strongly supported Bigger's model, yet little is known regarding the molecular

mechanism of persistence in Gram-positive bacteria. In this study, we revealed a mechanism of persistence in Gram-positive bacteria mediated by GTP depletion due to stochastic or induced accumulation of (p)ppGpp (Figure. 7). We have demonstrated that (p)ppGpp is a mechanism of persistence (Figure. 1), and persisters are a small population of cells with elevated (p)ppGpp (Figure. 3). In addition, (p)ppGpp-regulated persisters can form stochastically through the synthetases RelA and YjbM (Figure. 4, 5), or induced by specific antibiotics or ATP synthesis inhibition (Figure. 2). These findings altogether suggested that in contrast to Gram-negative bacteria, (p)ppGpp regulates persistence through GTP down-regulation in Gram-positive species.

GTP antagonism by (p)ppGpp as a persistence mechanism in Gram-positive bacteria

The key to persistence is growth arrest. A recent study in *S. aureus* suggested that persistence is associated with ATP depletion and not through (p)ppGpp production (Conlon et al., 2016). Here we reveal that ATP depletion through treatment with CCCP or arsenate induces (p)ppGpp production in *B. subtilis* (Figure. 2A). For wild type cells, shortly after ATP depletion, (p)ppGpp levels increase, GTP levels decrease, with a mild decrease in ATP. This mild decrease in ATP is likely explained by the fact that typically, (p)ppGpp production is accompanied by an increase in ATP (Kriel et al., 2012), but depletion of ATP with CCCP or arsenate, results in a net mild decrease in ATP observed on TLCs. Pretreatment of wild type cells with CCCP indeed enhances VAN survival, but this is likely due to the net protective effects of (p)ppGpp production, GTP decrease, and ATP decrease. For (p)ppGpp^0 cells, there is marked decrease in ATP levels during CCCP treatment, indicating that their increased VAN survival is mainly due to lower ATP. All in all, it cannot be ruled out that persister formation by depleting ATP

may be due to (p)ppGpp production and GTP depletion, which we further characterize in this work.

In this work, we reveal that persistence is mediated by (p)ppGpp antagonism of GTP in Gram-positive bacteria. We show that (p)ppGpp accumulation leads to increased antibiotic tolerance and that abolishing (p)ppGpp biosynthesis leads to significantly reduced antibiotic survival without detectable changes in resistance (Figure. 1A to 1G), which supports that (p)ppGpp is both sufficient and necessary for persistence. Furthermore, we showed that persistence is inversely-correlated with GTP levels (Figure. 2C and 2D), and genetic depletion of GTP can restore persistence in the absence of (p)ppGpp biosynthesis (Figure. 2D) or even increase persistence over WT levels (Figure. 2F). These findings altogether support that (p)ppGpp promotes persistence through GTP down-regulation.

Our finding that GTP biosynthesis is a persistence effector downstream of (p)ppGpp corroborates our previous reports that (p)ppGpp directly inhibits GTP biosynthesis (Kriel et al., 2012; Liu et al., 2015), as well as the effect of GTP homeostasis on growth can be uncoupled from (p)ppGpp (Bittner et al., 2014). In *B. subtilis*, GTP is utilized as the initiating nucleotide (iNTP) for rRNA transcription and is rate-limiting for rRNA synthesis (Krásný and Gourse, 2004). Thus, regulation of GTP by (p)ppGpp provides a general control of cellular translation capacity through ribosome synthesis, which is critical to growth regulation (Ehrenberg et al., 2013). Furthermore, high (p)ppGpp levels can independently inhibit additional targets involved in translation (Rojas et al., 1984) and ribosome assembly, such as Obg (Buglino et al., 2002) and Era (Corrigan et al., 2016), which collectively leads to reduced translation.

(p)ppGpp reduction of GTP likely regulates survival and energy conservation processes as well. Rapid reduction in cellular GTP (from ~ 3 mM to ~0.2 mM as estimated by our previous study (Liu et al., 2015)) in response to (p)ppGpp induction may also directly inhibit other biogenesis processes such as cell division, potentially by disrupting FtsZ polymerization which is a GTP-dependent process estimated to be sensitive to GTP modulation at high μM range (Adams and Errington, 2009; Erickson et al., 2010; Mukherjee et al., 2006; Small and Addinall, 2003) or by decreasing deposition of new cell wall material by CpgA, a GTPase (Absalon et al., 2008). Similarly, activity of the replicative DNA primase DnaG is subjected to GTP-dependent control in addition to direct (p)ppGpp interaction (Rymer et al., 2012; Wang et al., 2007), leading to reversible inhibition of replication elongation and energy conservation (DeNapoli et al., 2013). Since antibiotic lethality stems from deleterious disruption of key cellular processes including cell wall biosynthesis, DNA replication, and translation (Kohanski et al., 2007), it is plausible that GTP depletion involves preventive attenuation of antibiotic-targeted processes which contributes to persistence.

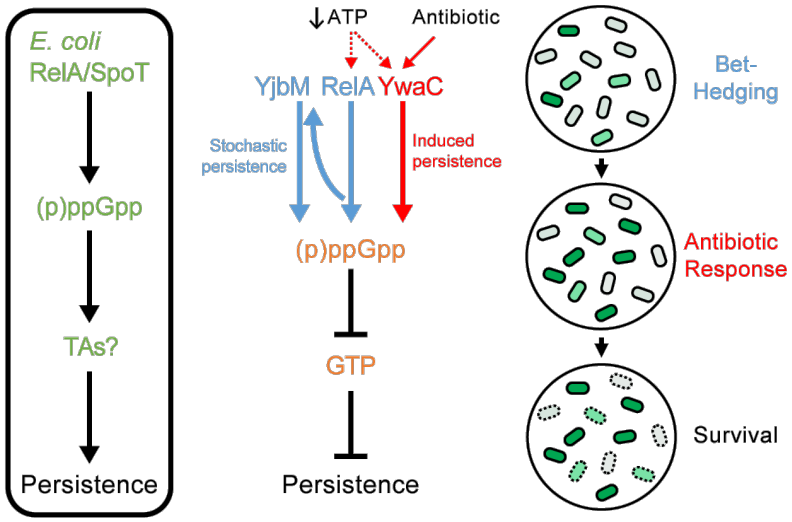

Figure 7. Stochastic and responsive persistence mediated by (p)ppGpp and GTP. In contrast to Gram-negative bacteria (e.g. *E. coli*) which may persistence through (p)ppGpp and toxin-antitoxin systems (TAs) (black box), persistence in Gram-positive bacteria (e.g. *B. subtilis*) is regulated by (p)ppGpp-mediated GTP depletion (orange). Down-regulation of GTP by (p)ppGpp contributes to both stochastic formation of persisters during active growth through (p)ppGpp synthetases RelA and YjbM (stochastic persistence, blue), or in response to specific antibiotics through YwaC (induced persistence, red). Furthermore, inhibition of ATP synthesis also leads to (p)ppGpp accumulation and induction of persistence, potentially through RelA or YwaC (dotted red arrows). Overall, the two pathways of persister formation mediated by (p)ppGpp enables both bet-hedging and responsive strategies of survival against either unpredictable or gradually emerging threats in different environments.

Alternatively, reduction in GTP can lead to changes in gene expression through the transcriptional regulator CodY (Richardson et al., 2015; Sonenshein, 2005), or indirectly through increased availability of free RNA polymerase (Tojo et al., 2008), or elevated ATP levels which function as iNTP for specific promoters (Krásný et al., 2008). We have experimentally excluded the role of CodY in persistence (Figure. 2F), however it is still possible that expression of specific stress response genes during GTP depletion through CodY-independent mechanisms are involved in persistence. Furthermore, elevation of ATP upon (p)ppGpp-mediated GTP depletion (Figure. S3C) could indirectly support energy-dependent survival mechanisms (e.g. antibiotic efflux) (Pu et al., 2016). In light of the expanded view that persisters in Gram-negative bacteria adopt both passive dormancy (Balaban et al., 2004; Cheverton et al., 2016; Keren et al., 2004; Maisonneuve et al., 2013) and active responses (Nguyen et al., 2011; Orman and Brynildsen, 2013; Pu et al., 2016) to survive lethal antibiotic stresses, it would be interesting to speculate that such mechanisms may also be in play under GTP control in Gram-positive bacteria.

Finally, robust regulation of cellular GTP levels by (p)ppGpp has been shown to be largely limited to *B. subtilis* and other *Firmicutes* (Gaca et al., 2015). This is attributed to the presence of structurally-divergent GTP biosynthesis enzymes that are potently inhibited by direct (p)ppGpp interaction (Kriel et al., 2012; Liu et al., 2015). This evolutionarily-distinct feature of GTP control by (p)ppGpp, along with the diverse functions of GTP in gene expression and metabolism in these species (Krásný and Gourse, 2004; Krásný et al., 2008; Kriel et al., 2014; Richardson et al., 2015), suggests that regulation of GTP-mediated persistence by (p)ppGpp is a distinct mechanism in

Gram-positive bacteria. This is in contrast to persistence regulated by (p)ppGpp through toxin-antitoxin systems in Gram-negative species, although there is decreasing support for the model, in light of the discovery of prophages in the toxin-deleted strains (Germain et al., 2013; Harms et al., 2017; Korch et al., 2003; Maisonneuve et al., 2013; Shan et al., 2017). Considering the role of (p)ppGpp on bacterial virulence (Dalebroux et al., 2010), and reports that RelA mutants with increased (p)ppGpp levels provide fitness advantages during persistent infections by pathogenic *Firmicutes* such as *E. faecium* (Honsa et al., 2017) and *S. aureus* (Gao et al., 2010), targeting the stringent response is increasingly appealing as a strategy to improve infection control.

(p)ppGpp heterogeneity and stochastic persistence

Another important question regarding persistence is the origins and formation of a small number of persisters in the population. By utilizing our developed single-cell (p)ppGpp-responsive reporter, we showed that persistence stems from (p)ppGpp heterogeneity in the population and is enriched in populations with elevated (p)ppGpp levels (Figure. 3E, 3F). Furthermore, persisters can form spontaneously in an actively growing population (Figure. 4) and is dependent on the (p)ppGpp synthetases RelA and YjbM (Figure. 5). The finding that (p)ppGpp level heterogeneity is formed by the synthetases RelA and YjbM suggests that stochastic persistence involves combined (p)ppGpp synthesis from the two enzymes. This is supported by our observation that disruption of either RelA or YjbM led to significant reduction in the frequencies of cells with high (p)ppGpp levels (Figure. 5F). Furthermore, disruption of the allosteric pppGpp activation site in YjbM (Steinchen et al., 2015) resulted in (p)ppGpp biosynthesis and persistence similar to a *yjbM* deletion mutant (Figure. 5). As YjbM preferentially

synthesizes ppGpp over pppGpp (Steinchen et al., 2015), allosteric activation of YjbM is likely mediated by pppGpp synthesized by RelA. This functional interaction enables cross-stimulation and cooperative activities between synthetases, enhancing each enzyme's (p)ppGpp synthesis capacity.

Another interesting finding from our single-cell study is that there appears to be a threshold concentration of (p)ppGpp (or depletion of GTP) required for persistence entry (Figure. 4F). This threshold concentration of (p)ppGpp is approximately in the low mM range based on quantitative estimation from this work (Figure. S3) and our previous study (Kriel et al., 2012). From the biochemistry perspective, such level of (p)ppGpp is sufficient for regulation of a number of known (p)ppGpp-interacting targets, including GuaB ($K_i \approx 50$ μM) (Kriel et al., 2012), Gmk ($K_i \approx 13.5$ μM) (Kriel et al., 2012; Liu et al., 2015), and HprT ($IC_{50} \approx 11$ μM) (Kriel et al., 2012) which are (p)ppGpp-inhibited enzymes responsible for GTP biosynthesis. This agrees with our findings that persistence is mediated by GTP downregulation (Figure. 2). Furthermore, while the (p)ppGpp^0 *gmk*^{Q110R} mutant has similar GFP (Figure. 4I) and persister levels (Figure. 2D) as the WT, persistence entry in WT assumes a rapid growth arrest rather than a gradual transition in (p)ppGpp^0 *gmk*^{Q110R} (Figure. 4I, S4). This suggests that entry into persistence by (p)ppGpp-mediated GTP downregulation enables a rapid transition or switch into persistence for WT but (p)ppGpp^0 *gmk*^{Q110R} solely relies on slow growth and low GTP. This rapid switch is likely due to the robust regulation of multiple GTP biosynthesis enzymes and other targets of cellular metabolism by (p)ppGpp and a quick drop in GTP. Furthermore, we also found that (p)ppGpp^0 *gmk*^{Q110R} displayed increased cell-to-cell variability in growth rate compared to WT (Figure. S4). This suggests that

(p)ppGpp tightly and robustly minimizes fluctuations in growth rates, perhaps through modulation of GTP biosynthesis at basal (p)ppGpp levels or through homeostatic control of GTP concentrations (Bittner et al., 2014).

Responsive persistence by induced diversification of (p)ppGpp

Apart from spontaneous persistence, we showed that specific antibiotics, notably cell-wall biosynthesis inhibitors, induced (p)ppGpp production by YwaC, indicating an induced diversification mechanism of antibiotic survival. YwaC expression is under the control of extracytoplasmic function (ECF) sigma factors σ^M and σ^W (Cao et al., 2002; D'Elia et al., 2009; Eiamphungporn and Helmann, 2008; Geiger and Wolz, 2014; Rietkötter et al., 2008). However, previous studies were mainly focused on its role in a collective population response. By utilizing the (p)ppGpp-responsive reporter, we revealed that even sub-lethal concentrations of these antibiotics can trigger a measurable increase in (p)ppGpp (Figure. 6A), and more importantly, a significant diversification of single-cell (p)ppGpp levels that enables persister formation (Figure. 6B, 6D). This heterogeneous response to antibiotics can be due to a number of factors including cell-to-cell variations in growth and division cycle or variability in membrane stress responses which determines the degree of *ywaC* transcription and consequently (p)ppGpp biosynthesis. This induced persistence by YwaC is another survival mechanism, in addition to spontaneous persistence as a bet-hedging strategy, to ensure survival in the face of an uncertain environment.

Methods and Materials

Bacterial strains and strain construction. LB and LB-agar were used for cloning and maintenance of strains. For selection in *B. subtilis*, media was supplemented with the

following antibiotics when required: spectinomycin (80 µg/mL), chloramphenicol (5 µg/mL), kanamycin (10 µg/mL), and tetracycline (10 µg/mL). Combination of lincomycin (12.5 µg/mL) and erythromycin (0.5 µg/mL) was used to select for MLS resistance. Carbenicillin (100 µg/mL) was used for selection in *E. coli*.

B. subtilis (p)ppGpp biosynthesis mutants were constructed by transformations of integration plasmids containing an I-sceI endonuclease cut site and regions of homology upstream and downstream of specific synthetase genes (pJW300 for Δ*yjbM*, pJW306 for Δ*ywaC*, and pJW371 for *relA*^{D264G} or *relA*^{Syn}) followed by transformation of pSS4332 for marker-less recombination (Janes and Stibitz, 2006). Successful recombination was verified by PCR.

For the construction of (p)ppGpp^{0} mutant, Δ*ywaC* Δ*yjbM* was transformed with Δ*relA*::*mls* PCR product from genomic DNA using oligos oJW418/oJW419 and selected for MLS resistance (Kriel et al., 2012).

Construction of integration plasmid for YjbM^{F42A} was done by site-directed mutagenesis of pJW370 by PCR using oligos oJW2309/oJW2310. The *gmk*^{Q110R} allele was generated from a suppressor screen on guanosine-containing plates and differentiated from *hprT* suppressors by absence of growth on 8-azaguanine plates (Van Diggelen et al., 1979).

B. subtilis toxin deletion mutant (Δ3TA) was constructed by serial transformation of PCR products from the *B. subtilis* knockout collection (BGSC) and Cre recombinase-mediated removal of the lox-site flanked *erm*^{R} cassette with pDR244-*cre* and selection for the loss of MLS resistance (Koo et al., 2017).

Construction of fluorescence reporters was done by fusion of PCR products containing respective promoter regions (oJW1935/oJW1936 for P_{ilvB} or oJW2083/oJW2084 for P_{rrnB}) with coding regions of fluorescence proteins (oJW1995/oJW1996 for GFP or oJW2805/oJW2806 for mCherry) using ligase cycling reaction (LCR) (Kok et al., 2014). In the case of P_{ilvB}-GFP or P_{ilvB}-mCherry fusions, the construct was cloned into pDR110 flanked by *amyE.* In the case of P_{rrnB}-GFPns (unstable GFP sequence from Griffith *et al.* (Griffith and Grossman, 2008)), DNA fragments of GFP^{ns} (oJW1995/oJW2020), flanking regions of *lacA* (oJW1990/oJW2414 and oJW2413/oJW2082), and lox-site flanked erm^R cassette (oJW2133/oJW2134) were amplified by PCR. The resulting PCR products were fused by LCR followed by amplification using PCR to generate linear recombination fragment of *lacA*::P_{rrnB}-GFPns. Chromosome integration of reporter constructs was done by transformation and selection for SPEC or MLS resistance. Removal of the lox-site flanked erm^R cassette with was done by transformation with pDR244-*cre* and selected for the loss of MLS resistance. All mutants and constructs were verified by DNA sequencing.

Growth conditions

Bacillus subtilis strains were grown in S7 defined medium (Vasantha and Freese, 1980); MOPS was used at 50 mM rather than 100 mM, supplemented with 0.1% glutamate, 1% glucose, and 0.5% casamino acids. Growth of YB886 strain background was supplemented with 20 µg/mL tryptophan and 50 µg/mL methionine (Harwood et al., 1990). Cell cultures were grown at 37 °C from overnight plates with vigorous shaking. Cultures in logarithmic phase (OD_{600} = 0.1-0.3) were treated with antibiotics or inducers, such as arginine hydroxamate (RHX, 0.5 mg/mL), carbonyl cyanide m-chlorophenyl

hydrazone (CCCP, 5 μM), sodium azide (NaN_3, 4 mM), or arsenate (2.5 mM). Isopropyl β-D-1-thiogalactopyranoside (IPTG) was added to a final concentration of 0.5 mM to induce *guaB* expression from an IPTG-inducible promoter (P_{spac}).

For microscopy experiments, the following inducers and concentrations were used: RHX: 0.1/0.3/0.5 mg/mL; α-methylglucoside (α-MG): 1%/3%/5%; CCCP: 5 μM; NaN_3: 4 mM; Arsenate: 2.5 mM; CARB: 0.5 μg/mL; BAC: 80 μg/mL; CIP: 0.125 μg/mL; KAN: 0.625 μg/mL; VAN: 0.25 μg/mL) along with non-induction controls. For nutrient downshift experiments, cells grown in S7 media supplemented with casamino acids were washed twice with S7 minimal media and re-suspended in an equal volume of S7 minimal media followed by 30-min incubation under the same condition.

Minimum inhibitory concentration (MIC) determination

MICs for chloramphenicol (CAM), tetracycline (TET), kanamycin (KAN), ciprofloxacin (CIP), norfloxacin (NOR), rifampicin (RIF), and vancomycin (VAN) were determined using the microdilution method (Cockerill, F.R., Wikler, M.A., Alder, J., Dudley, M.N., Eliopoulos, G.M., Ferraro, M.J., Hardy, D.J., Hect, D.W., Hindler, J.F., Patel, J.B., Powell, M., Swenson, J.M., Thomson, R.B., Traczewski, M.M., Turnidge, J.D., Weinstein, M.P., and Zimmer, 2012). Logarithmic phase cells were back-diluted to a final titer of ≈ $5X10^5$ CFU/mL into 96-well plates containing two-fold serial dilutions of respective antibiotics in S7 defined medium. After 16-20 hours of incubation at 37 °C with shaking, the MIC was determined as the lowest drug concentration that prevented visible growth.

Persister assay

Cells were harvested from young, overnight LB-agar plates (< 10 h), back-diluted into fresh S7 defined media at OD_{600} = 0.005, and grown at 37 °C with vigorous shaking. Cells were grown to logarithmic phase (OD_{600} ≈ 0.1-0.3) and subsequently treated with bactericidal concentrations of antibiotics (CIP, 4 μg/mL; VAN, 4 μg/mL; KAN, 8 μg/mL; BAC, 384 μg/mL). To determine cell viability, culture aliquots were taken at T=0 and at designated times after treatment, plated onto Luria-Broth (LB) agar, and incubated at 37 °C overnight. Viability at different time points was determined as CFU/mL/OD_{600} and relative survival (vs T_0) was calculated. For experiments involving pre-induction of cells with (p)ppGpp-inducing agents, cells were grown to OD_{600} ≈ 0.1 and divided into two: one containing the inducing agent (RHX, 0.5 mg/mL; BAC, 64 μg/mL; CCCP, 5 μM; NaN_3, 4 mM; arsenate, 2.5 mM) and other as non-induction control. The cultures were grown for an additional 30 min under the same conditions (T=0.5 hr) and subjected to the persister assay, as described above. In the case of BAC treatment, the final antibiotic concentrations were identical for both induced and non-induced populations.

Measurement of intracellular nucleotides by thin-layer chromatography

To measure intracellular nucleotides, cells were first harvested from overnight plates, back-diluted to OD_{600} = 0.005, and grown in low-phosphate S7 defined medium (0.1X phosphate, 0.5 mM)), supplemented with casamino acids. Once cultures reached OD_{600} ≈ 0.05, 1 mL cells were labeled with 50 μCi of ^{32}P orthophosphate (900 mCi/mmol; Perkin Elmer) or 2-3 generations before treatment or sampling. At OD_{600} ≈ 0.15, RHX, CCCP, or arsenate were added and samples were collected at regular time points for nucleotide extraction. Nucleotides were extracted by incubating 100 μL cells with 20 μL of 2 N formic acid for at least 20 minutes. Samples were spotted on PEI cellulose thin-

layer chromatography (TLC) plates (Selecto) and developed in 1.5 M or 0.85 M potassium phosphate monobasic (KH_2PO_4, pH 3.4) buffer to separate (p)ppGpp or GTP, respectively. TLC plates were exposed on storage phosphor screens (GE Healthcare) and scanned on a Typhoon imager (GE Healthcare). Intensities of nucleotide spots were quantified using ImageQuant software (Molecular Dynamics) and normalized to the number of phosphates in the corresponding nucleotide and ATP level at T=0 for comparison between samples.

Fluorescence plate assay

To monitor GFP expression from P_{ilvB}-GFP reporter during growth in liquid culture, cells were grown to $OD_{600} \approx 0.1$-0.3 in S7 defined medium and then diluted to $OD_{600} = 0.005$ into fresh S7 defined medium. 200 µL of the diluted cultures were transferred into wells of 96-well black plate with flat clear bottom and transparent lid. The plate was incubated at 37°C with constant shaking for up to 18h in a Biotek Synergy2 microplate reader. Measurement of OD_{600} and GFP signals of individual wells was performed every 10 min using absorbance monochromator (for OD_{600}), and excitation (485/20) and emission filters (528/20) for GFP.

Fluorescence microscopy

To monitor (p)ppGpp induction using fluorescence reporters, cells were grown to $OD_{600} \approx 0.1$ followed by 30-min induction with RHX, α-MG, CCCP, NaN_3, Arsenate, CARB, BAC, CIP, KAN, or VAN (concentrations were listed under growth conditions) along with non-induction controls. All imaging samples were spotted on 1.5% agarose pads made with the same growth medium, and immediately imaged with Olympus IX-83 inverted microscope (Olympus) using 60X phase contrast objective with fluorescence filters

(excitation: 470/20 nm, dichroic mirror: 485 nm, emission: 515/50 nm for GFP; excitation: 575/20 nm, dichroic mirror: 595 nm, emission: 645/90 nm for mCherry; and excitation: 427/10 nm, dichroic mirror: 595 nm, emission: 472/30 nm for Sytox blue). Single-cell time-lapse imaging was performed at 37°C using temperature-controlled imaging chamber (Tokai Hit) coupled with automatic stage and microscope control as described previously (Young et al., 2011). For imaging persister survival, 5 μg/mL CARB and 25 nM Sytox blue (Molecular Probes) at final concentrations were used. Microscopy image analysis and cell parameters (cell size and fluorescence intensity) measurements were done using Metamorph software (Molecular Devices). Single cell growth rate (μ) at each frame was calculated using the equation: $\mu = \frac{1}{A}\frac{\Delta A}{\Delta t}$, where A is the cell area, ΔA is the change in cell area and Δt is the change in time (in min).

Flow cytometry and cell sorting

Flow cytometry was performed in UWCCC flow cytometry core. Cells for flow cytometry analysis were grown under same experimental conditions as described above. For flow cytometry analysis, cells were immediately fixed with 0.4% paraformaldehyde for 15 min at room temperature, washed 3x with 1x phosphate buffered saline (PBS), and kept at 4°C until analysis. Fixation was verified by viability plating and microscopy. Flow cytometry analysis was performed using BD LSRFortessa flow cytometer (BD Biosciences) with a 70-μm nozzle. Cell populations were detected using both forward and side scatter (FSC and SSC). Single-cell fluorescence was measured using 488 nm laser and detection filters for GFP (530/30 nm, 505LP dichroic filter). Approximately two million events were counted for each sample and. FACS analysis was performed using BD FACSAria cell sorter (BD Biosciences) with a 70-μm nozzle at room temperature

using 488 nm laser and detection filters for GFP (525/50 nm, 505LP dichroic filter). At least 5,000 cells were obtained from the rarest gate for each sample. Cell recovery rate was estimated to be > 90% based on viability counting on LB plates. Aliquots of gated populations were subjected to persister assay as described above. Flow-cytometry data were analyzed using FlowJo X software (FlowJo, LLC). Smallest allowed gate was used for forward and side scatter to reduce variations in fluorescence signals due to size variation. Identical gating strategies were used for different samples.

Literature Cited

Absalon, C., Hamze, K., Blanot, D., Frehel, C., Carballido-Lopez, R., Holland, B.I., van Heijenoort, J., and Séror, S.J. (2008). The GTPase CpgA is implicated in the deposition of the peptidoglycan sacculus in *Bacillus subtilis*. J. Bacteriol. *190*, 3786–3790.

Adams, D.W., and Errington, J. (2009). Bacterial cell division: assembly, maintenance and disassembly of the Z ring. Nat. Rev. Microbiol. *7*, 642–653.

Balaban, N.Q., Merrin, J., Chait, R., Kowalik, L., and Leibler, S. (2004). Bacterial persistence as a phenotypic switch. Science (80-.). *305*, 1622–1625.

Bigger, J.W. (1944). The bactericidal action of penicillin on *Staphylococcus pyogenes*. Ir. J. Med. Sci. *19*, 585–595.

Bittner, A.N., Kriel, A., and Wang, J.D. (2014). Lowering GTP level increases survival of amino acid starvation but slows growth rate for *Bacillus subtilis* cells lacking (p)ppGpp. J. Bacteriol. *196*, 2067–2076.

Buglino, J., Shen, V., Hakimian, P., and Lima, C.D. (2002). Structural and biochemical analysis of the Obg GTP binding protein. Structure *10*, 1581–1592.

Cao, M., Kobel, P.A., Morshedi, M.M., Wu, M.F.W., Paddon, C., and Helmann, J.D. (2002). Defining the *Bacillus subtilis* σ^W regulon: a comparative analysis of promoter consensus search, run-off transcription/macroarray analysis (ROMA), and transcriptional profiling approaches. J. Mol. Biol. *316*, 443–457.

Cheverton, A.M., Gollan, B., Przydacz, M., Wong, C.T., Mylona, A., Hare, S.A., and Helaine, S. (2016). A *Salmonella* toxin promotes persister formation through acetylation of tRNA. Mol. Cell *63*, 86–96.

Cockerill, F.R., Wikler, M.A., Alder, J., Dudley, M.N., Eliopoulos, G.M., Ferraro, M.J., Hardy, D.J., Hect, D.W., Hindler, J.F., Patel, J.B., Powell, M., Swenson, J.M., Thomson, R.B., Traczewski, M.M., Turnidge, J.D., Weinstein, M.P., and Zimmer, B.L. (2012). Methods for dilution antimicrobial susceptibility tests for bacteria that grow aerobically.

Cohen, N.R., Lobritz, M.A., and Collins, J.J. (2013). Microbial persistence and the road to drug resistance. Cell Host Microbe *13*, 632–642.

Conlon, B.P., Rowe, S.E., Gandt, A.B., Nuxoll, A.S., Donegan, N.P., Zalis, E.A., Clair, G., Adkins, J.N., Cheung, A.L., and Lewis, K. (2016). Persister formation in *Staphylococcus aureus* is associated with ATP depletion. Nat. Microbiol. *1*, 1–7.

Corrigan, R.M., Bellows, L.E., Wood, A., and Gründling, A. (2016). ppGpp negatively impacts ribosome assembly affecting growth and antimicrobial tolerance in Gram-positive bacteria. Proc. Natl. Acad. Sci. 201522179.

D'Elia, M.A., Millar, K.E., Bhavsar, A.P., Tomljenovic, A.M., Hutter, B., Schaab, C., Moreno-Hagelsieb, G., and Brown, E.D. (2009). Probing teichoic acid genetics with bioactive molecules reveals new interactions among diverse processes in bacterial cell wall biogenesis. Chem. Biol. *16*, 548–556.

Dalebroux, Z.D., Svensson, S.L., Gaynor, E.C., and Swanson, M.S. (2010). ppGpp conjures bacterial virulence. Microbiol. Mol. Biol. Rev. *74*, 171–199.

DeNapoli, J., Tehranchi, A.K., and Wang, J.D. (2013). Dose-dependent reduction of replication elongation rate by (p)ppGpp in *Escherichia coli* and *Bacillus subtilis*. Mol. Microbiol. *88*, 93–104.

Van Diggelen, O.P., Donahue, T.F., and Shin, S. (1979). Basis for differential cellular

sensitivity to 8-azaguanine and 6-thioguanine. J. Cell. Physiol. *98*, 59–72.
Dorr, T., Vulic, M., and Lewis, K. (2010). Ciprofloxacin causes persister formation by inducing the TisB toxin in Escherichia coli. PLoS Biol. *8*, 29–35.
Ehrenberg, M., Bremer, H., and Dennis, P.P. (2013). Medium-dependent control of the bacterial growth rate. Biochimie *95*, 643–658.
Eiamphungporn, W., and Helmann, J.D. (2008). The Bacillus subtilis σ^M regulon and its contribution to cell envelope stress responses. Mol. Microbiol. *67*, 830–848.
Erickson, H.P., Anderson, D.E., and Osawa, M. (2010). FtsZ in bacterial cytokinesis: Cytoskeleton and force generator all in one. Microbiol. Mol. Biol. Rev. *74*, 504–528.
Gaca, Anthony O, Kajfasz, J.K., Miller, J.H., Liu, K., Wang, J.D., Abranches, J., and Lemos, A. (2013). Basal levels of (p)ppGpp in Enterococcus faecalis: The magic beyond the stringent response. MBio *4*, 1–10.
Gaca, A.O., Colomer-Winter, C., and Lemos, J.A. (2015). Many means to a common end: The intricacies of (p)ppGpp metabolism and its control of bacterial homeostasis. J. Bacteriol. *197*, 1146–1156.
Gao, W., Chua, K., Davies, J.K., Newton, H.J., Seemann, T., Harrison, P.F., Holmes, N.E., Rhee, H.W., Hong, J.I., Hartland, E.L., et al. (2010). Two novel point mutations in clinical *Staphylococcus aureus* reduce linezolid susceptibility and switch on the stringent response to promote persistent infection. PLoS Pathog. *6*.
Geiger, T., and Wolz, C. (2014). Intersection of the stringent response and the CodY regulon in low GC Gram-positive bacteria. Int. J. Med. Microbiol. *304*, 150–155.
Geiger, T., Kästle, B., Gratani, F.L., Goerke, C., and Wolz, C. (2014). Two small (p)ppGpp synthases in *Staphylococcus aureus* mediate tolerance against cell envelope stress conditions. J. Bacteriol. *196*, 894–902.
Germain, E., Castro-Roa, D., Zenkin, N., and Gerdes, K. (2013). Molecular mechanism of bacterial persistence by HipA. Mol. Cell *52*, 248–254.
Griffith, K.L., and Grossman, A.D. (2008). Inducible protein degradation in *Bacillus subtilis* using heterologous peptide tags and adaptor proteins to target substrates to the protease ClpXP. Mol. Microbiol. *70*, 1012–1025.
Harms, A., Fino, C., Sørensen, M.A., Semsey, S., and Gerdes, K. (2017). Prophages and growth dynamics confound experimental results with antibiotic-tolerant persister cells. MBio *8*, 1–18.
Harwood, C.R., Cutting, S.M., and Chambert, R. (1990). Molecular biological methods for *Bacillus*.
Honsa, E.S., Cooper, V.S., Mhaissen, M.N., Frank, M., Shaker, J., Iverson, A., Rubnitz, J., Hayden, R.T., Lee, R.E., Rock, C.O., et al. (2017). RelA mutant *Enterococcus faecium* with multiantibiotic tolerance arising in an immunocompromised host. MBio *8*, 1–12.
Janes, B.K., and Stibitz, S. (2006). Routine markerless gene replacement in *Bacillus anthracis*. Infect. Immun. *74*, 1949–1953.
Kaspy, I., Rotem, E., Weiss, N., Ronin, I., Balaban, N.Q., and Glaser, G. (2013). HipA-mediated antibiotic persistence via phosphorylation of the glutamyl-tRNA-synthetase. Nat. Commun. *4*, 1–7.
Keren, I., Shah, D., Spoering, A., Kaldalu, N., and Lewis, K. (2004). Specialized persister cells and the mechanism of multidrug tolerance in *Escherichia coli*. J. Bacteriol. *186*, 8172–8180.

Kohanski, M. a., Dwyer, D.J., Hayete, B., Lawrence, C. a., and Collins, J.J. (2007). A Common Mechanism of Cellular Death Induced by Bactericidal Antibiotics. Cell *130*, 797–810.

Kok, S. De, Stanton, L.H., Slaby, T., Durot, M., Holmes, V.F., Patel, K.G., Platt, D., Shapland, E.B., Serber, Z., Dean, J., et al. (2014). Rapid and reliable DNA assembly via ligase cycling reaction. ACS Synth. Biol. *3*, 97–106.

Konkol, M.A., Blair, K.M., and Kearns, D.B. (2013). Plasmid-encoded ComI inhibits competence in the ancestral 3610 strain of *Bacillus subtilis*. J. Bacteriol. *195*, 4085–4093.

Koo, B.M., Kritikos, G., Farelli, J.D., Todor, H., Tong, K., Kimsey, H., Wapinski, I., Galardini, M., Cabal, A., Peters, J.M., et al. (2017). Construction and Analysis of Two Genome-Scale Deletion Libraries for Bacillus subtilis. Cell Syst. *4*, 291–305.e7.

Korch, S.B., Henderson, T. a., and Hill, T.M. (2003). Characterization of the *hipA7* allele of *Escherichia coli* and evidence that high persistence is governed by (p)ppGpp synthesis. Mol. Microbiol. *50*, 1199–1213.

Krásný, L., and Gourse, R. (2004). An alternative strategy for bacterial ribosome synthesis: *Bacillus subtilis* rRNA transcription regulation. EMBO J. *23*, 4473–4483.

Krásný, L., Tiserová, H., Jonák, J., Rejman, D., and Sanderová, H. (2008). The identity of the transcription +1 position is crucial for changes in gene expression in response to amino acid starvation in *Bacillus subtilis*. Mol. Microbiol. *69*, 42–54.

Kriel, A., Bittner, A.N., Kim, S.H., Liu, K., Tehranchi, A.K., Zou, W.Y., Rendon, S., Chen, R., Tu, B.P., and Wang, J.D. (2012). Direct regulation of GTP homeostasis by (p)ppGpp: A critical component of viability and stress resistance. Mol. Cell *48*, 231–241.

Kriel, A., Brinsmade, S.R., Tse, J.L., Tehranchi, A.K., Bittner, A.N., Sonenshein, A.L., and Wang, J.D. (2014). GTP dysregulation in *Bacillus subtilis* cells lacking (p)ppGpp results in phenotypic amino acid auxotrophy and failure to adapt to nutrient downshift and regulate biosynthesis genes. J. Bacteriol. *196*, 189–201.

Levin-Reisman, I., Ronin, I., Gefen, O., Braniss, I., Shoresh, N., and Balaban, N.Q. (2017). Antibiotic tolerance facilitates the evolution of resistance. Science (80-.). *355*, 826–830.

Lewis, K. (2001). Riddle of biofilm resistance. Antimicrob. Agents Chemother. *45*, 999–1007.

Lewis, K. (2010). Persister cells. Annu. Rev. Microbiol. *64*, 357–372.

Liu, K., Myers, A.R., Pisithkul, T., Claas, K.R., Satyshur, K.A., Amador-Noguez, D., Keck, J.L., and Wang, J.D. (2015). Molecular mechanism and evolution of guanylate kinase regulation by (p)ppGpp. Mol. Cell *57*, 735–749.

Maisonneuve, E., and Gerdes, K. (2014). Molecular Mechanisms Underlying Bacterial Persisters. Cell *157*, 539–548.

Maisonneuve, E., Castro-Camargo, M., and Gerdes, K. (2013). (p)ppGpp controls bacterial persistence by stochastic induction of toxin-antitoxin activity. Cell *154*, 1140–1150.

Mok, W.W.K., Park, J.O., Rabinowitz, J.D., and Brynildsen, M.P. (2015). RNA futile cycling in model persisters derived from MazF accumulation. MBio *6*, 1–13.

Mukherjee, A., Jackson, S. a, Leclerc, J.E., and Cebula, T. a (2006). Exploring

genotypic and phenotypic diversity of microbes using microarray approaches. Toxicol. Mech. Methods *16*, 121–128.

Nguyen, D., Joshi-Datar, A., Lepine, F., Bauerle, E., Olakanmi, O., Beer, K., McKay, G., Siehnel, R., Schafhauser, J., Wang, Y., et al. (2011). Active starvation responses mediate antibiotic tolerance in biofilms and nutrient-limited bacteria. Science *334*, 982–986.

Orman, M.A., and Brynildsen, M.P. (2013). Dormancy is not necessary or sufficient for bacterial persistence. Antimicrob. Agents Chemother. *57*, 3230–3239.

Potrykus, K., and Cashel, M. (2008). (p)ppGpp: Still magical? Annu. Rev. Microbiol. *62*, 35–51.

Pu, Y., Zhao, Z., Li, Y., Zou, J., Ma, Q., Zhao, Y., Ke, Y., Zhu, Y., Chen, H., Baker, M.A.B., et al. (2016). Enhanced efflux activity facilitates drug tolerance in dormant bacterial cells. Mol. Cell *62*, 284–294.

Richardson, A.R., Somerville, G.A., and Sonenshein, A.L. (2015). Regulating the intersection of metabolism and pathogenesis in Gram-positive bacteria. Microbiol. Spectr. *3*, 1–27.

Rietkötter, E., Hoyer, D., and Mascher, T. (2008). Bacitracin sensing in *Bacillus subtilis*. Mol. Microbiol. *68*, 768–785.

Rojas, A.M., Ehrenberg, M., Andersson, S.G.E., and Kurland, C.G. (1984). ppGpp inhibition of elongation factors Tu, G and Ts during polypeptide synthesis. Mol. Gen. Genet. *197*, 36–45.

Rymer, R.U., Solorio, F.A., Tehranchi, A.K., Chu, C., Corn, J.E., Keck, J.L., Wang, J.D., and Berger, J.M. (2012). Binding mechanism of metal·NTP substrates and stringent-response alarmones to bacterial DnaG-type primases. Structure *20*, 1478–1489.

Schumacher, M.A., Balani, P., Min, J., Chinnam, N.B., Hansen, S., Vulić, M., Lewis, K., and Brennan, R.G. (2015). HipBA–promoter structures reveal the basis of heritable multidrug tolerance. Nature *524*, 59–64.

Shan, Y., Gandt, A.B., Rowe, S.E., Deisinger, J.P., Conlon, B.P., and Lewis, K. (2017). ATP-dependent persister formation in *Escherichia coli*. MBio *8*, 1–14.

Small, E., and Addinall, S.G. (2003). Dynamic FtsZ polymerization is sensitive to the GTP to GDP ratio and can be maintained at steady state using a GTP-regeneration system. Microbiology *149*, 2235–2242.

Sonenshein, A.L. (2005). CodY, a global regulator of stationary phase and virulence in Gram-positive bacteria. Curr. Opin. Microbiol. *8*, 203–207.

Steinchen, W., Schuhmacher, J.S., Altegoer, F., Fage, C.D., Srinivasan, V., Linne, U., Marahiel, M.A., and Bange, G. (2015). Catalytic mechanism and allosteric regulation of an oligomeric (p)ppGpp synthetase by an alarmone. Proc. Natl. Acad. Sci. U. S. A. *112*, 13348–13353.

Tojo, S., Satomura, T., Kumamoto, K., Hirooka, K., and Fujita, Y. (2008). Molecular mechanisms underlying the positive stringent response of the *Bacillus subtilis ilv-leu* operon, involved in the biosynthesis of branched-chain amino acids. J. Bacteriol. *190*, 6134–6147.

Vasantha, N., and Freese, E. (1980). Enzyme changes during *Bacillus subtilis* sporulation caused by deprivation of guanine nucleotides. J. Bacteriol. *144*, 1119–1125.

Verstraeten, N., Knapen, W.J., Kint, C.I., Liebens, V., Van den Bergh, B., Dewachter, L., Michiels, J.E., Fu, Q., David, C.C., Fierro, A.C., et al. (2015). Obg and membrane depolarization are part of a microbial bet-hedging strategy that leads to antibiotic tolerance. Mol. Cell *59*, 9–21.

Wang, J.D., Sanders, G.M., and Grossman, A.D. (2007). Nutritional control of elongation of DNA replication by (p)ppGpp. Cell *128*, 865–875.

Zhang, Y., Yew, W.W., and Barer, M.R. (2012). Targeting persisters for tuberculosis control. Antimicrob. Agents Chemother. *56*, 2223–2230.

Table 3. Strains used in study.

Strain	Genotype	Reference
JDW2144	NCIB 3610 *comI*^{Q12L} (unauthorized loss of pAS32, personal communication D. Kearns)	(Konkol et al., 2013)
JDW2231	3610 *comI*^{Q12L} Δ*ywaC* Δ*yjbM* Δ*relA*::*mls*	This work
JDW2528	3610 *comI*^{Q12L} Δ*ywaC* Δ*yjbM* Δ*relA*::*mls* *gmk*^{Q110R}	This work
JDW2914	3610 *comI*^{Q12L} Δ*codY*	This work
JDW3031	3610 *comI*^{Q12L} *guaB*::P$_{spac}$-*guaB erm* (*guaB*^{down})	This work
JDW2911	3610 *comI*^{Q12L} Δ*txpA* ΔyonT Δ*ydcE*::*erm* (Δ3TA)	This work
JDW2961	3610 *comI*^{Q12L} P$_{ilvB}$-mCherry	This work
JDW2963	3610 *comI*^{Q12L} *lacA*::P$_{rrnB}$-GFP^{unstable} (ADSA) P$_{ilvB}$-mCherry (B.s. optimized)	This work
JDW2921	3610 *comI*^{Q12L} P$_{ilvB}$-GFP	This work
JDW2927	3610 *comI*^{Q12L} Δ*ywaC* Δ*yjbM* Δ*relA*::*mls* P$_{ilvB}$-GFP	This work
JDW2931	3610 *comI*^{Q12L} Δ*ywaC* P$_{ilvB}$-GFP	This work
JDW2923	3610 *comI*^{Q12L} Δ*yjbM* P$_{ilvB}$-GFP	This work
JDW2935	3610 *comI*^{Q12L} *relA*^{D264G} P$_{ilvB}$-GFP	This work
JDW2941	3610 *comI*^{Q12L} Δ*yjbM relA*^{D264G} P$_{ilvB}$-GFP	This work
JDW2949	3610 *comI*^{Q12L} *yjbM*^{F42A} P$_{ilvB}$-GFP	This work

Table 4. Plasmids used in study.

Plasmid	Genotype	Reference
pJW239	pEX44/Δ*yjbM amp cat*	Kriel *et al*., 2012
pJW299	pEX44/I-SceI site *amp cat*	Kriel *et al*., 2012
pJW300	pJW239/Δ*yjbM* I-SceI site *amp cat*	Kriel *et al*., 2012
pJW305	pMUTIN4/ P$_{spac}$-*guaB'-lacZ erm*	Kriel *et al*., 2012
pJW306	pJW299/Δ*ywaC* I-SceI site *amp cat*	Kriel *et al*., 2012
pJW370	pJW299/*yjbM* I-SceI site *amp cat*	Kriel *et al*., 2014
pJW371	pJW299/*relA*^{D264G} I-SceI site *amp cat*	Kriel *et al*., 2014
pJW558	pDR110/*amyE*::P$_{ilvB}$-GFPmut2	This work
pJW561	pDR110/*amyE*::P$_{ilvB}$-mCherry (B.s. optimized)	This work
pJW562	pJW370/*yjbM*^{F42A} I-SceI site *amp cat*	This work
pSS4332	*oriU* P$_{amy}$-I-sceI *kan*	Jane and Stibitz, 2006
pDR244	*cre* + Ts origin	BGSC, Gross lab

Supplemental Information

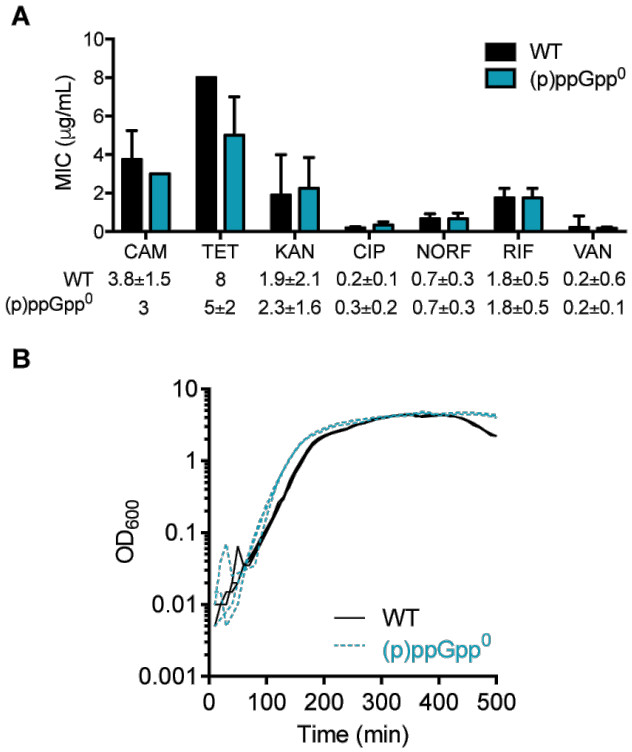

Figure S1, related to Figure 1. (p)ppGpp mediated persistence is not due to changes in MIC or growth rate. (A) Minimal inhibitory concentrations (MICs) of WT and (p)ppGpp^0 to various antibiotics. Values represent mean ± SD, N = 3. (B) Growth of WT (solid lines) and (p)ppGpp^0 (broken lines) over time. N= 3.

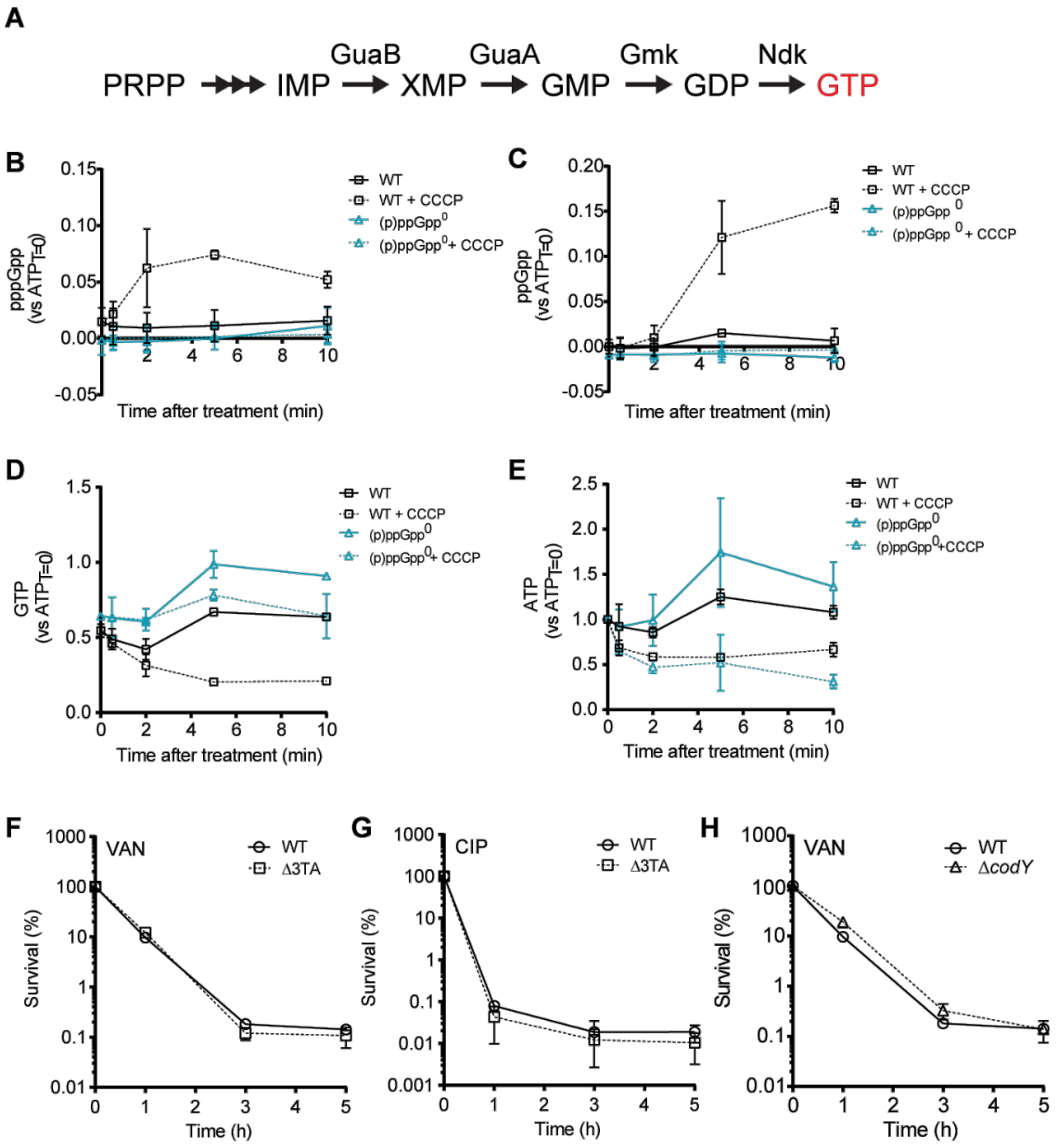

Figure S2, related to Figure 2. Persistence by GTP downregulation. (A) Schematic of *de novo* purine and downstream GTP biosynthesis. The *pur* operon encodes enzymes responsible for the conversion of PRPP to IMP, which further leads to downstream GTP biosynthesis. Gmk and GuaB are directly inhibited by (p)ppGpp which results in reduction in GTP levels during (p)ppGpp accumulation. (B to E) Changes in nucleotide levels in response to ATP depletion. WT and (p)ppGpp^0 cells were treated with CCCP and measured for changes in (B) pppGpp, (C) ppGpp, (D) GTP, or (E) ATP levels with TLC over time as indicated. N = 2. (F and G) Disruption of known TA systems does not affect persistence in B. subtilis. Survival of WT and TA mutant lacking all known TA systems (Δ3TA). Cells were subjected to (F) VAN or (G) CIP treatment for 5h. Values represent mean ± SD, N = 3. (H) Survival of WT (solid line) and Δ*codY* (dashed line) to VAN treatment. N = 2. All values represent mean ± SD.

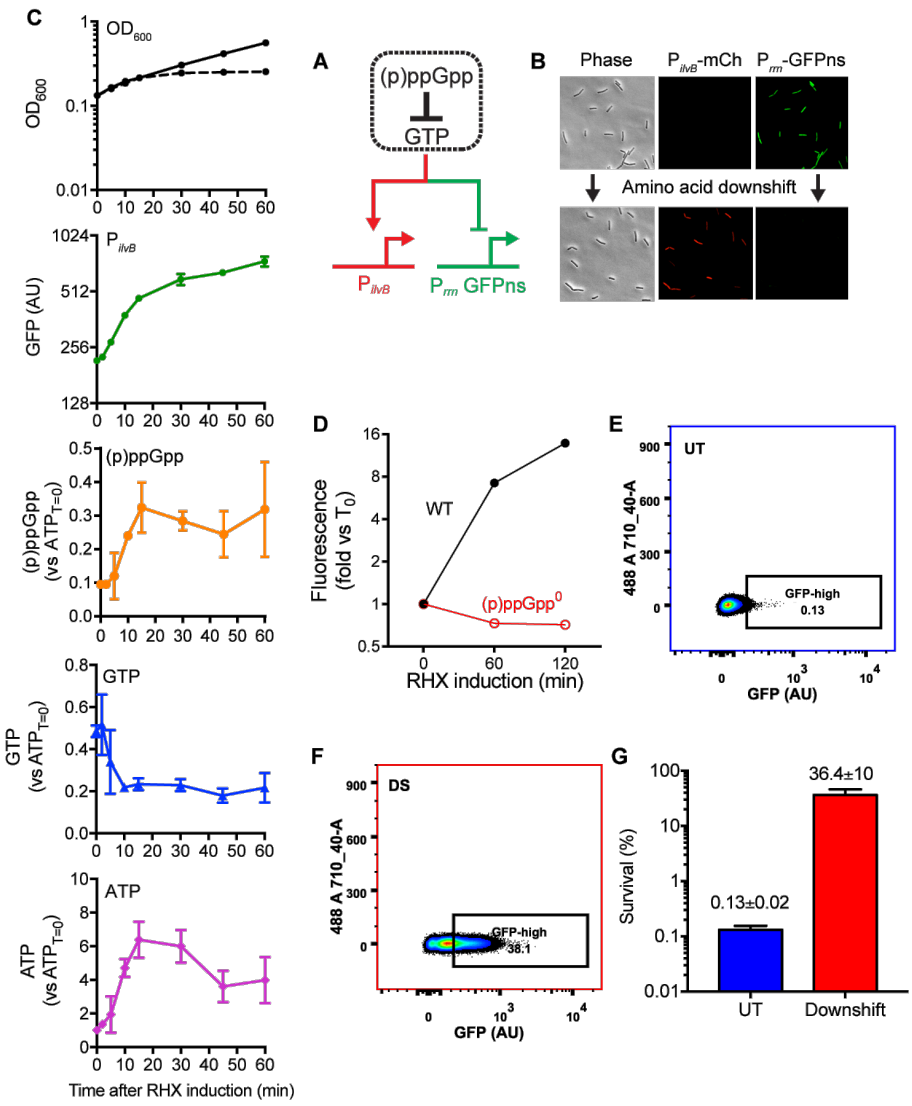

Figure S3, related to Figure 3. P_{ilvB} activities to chemical and physiological induction of (p)ppGpp. (A) Design of single-cell GTP reporter in *B. subtilis*. Depletion of GTP during (p)ppGpp accumulation derepresses the activity of *ilvB* promoter (i.e. expression of P_{ilvB}-FP), as well as inhibition of ribosomal RNA synthesis (i.e. inhibition of P_{rrnB}-GFPns expression). (B) Representative images of WT cells containing both reporters before and after the amino acids downshift. (C) WT cells were grown to log phase and treated with 0.5 mg/mL RHX followed by measurement of growth (OD_{600}), P_{ilvB} activities (GFP) and relative abundance of various intracellular nucleotides as indicated. Fluorescence measurement was performed using fluorescence microscopy and nucleotide levels were determined using TLC. Each time point represents mean ± SD, N = 2. (D) Reporter activities in wild-type (WT) and (p)ppGpp-null mutant ((p)ppGpp^0) in response to (p)ppGpp induction by 0.3 mg/mL RHX. Each time point represents mean fluorescence from n > 500 cells each. (E to G) Flow-cytometry analysis and persister assay of WT populations (E) before (UT) and (F) after amino acids downshift (DS) using the P_{ilvB} reporter (~$1.5x10^6$ cells each). Fraction of GFP-high cells was gated and counted based on FACS sorting analysis as shown in Figure 3E. Numbers indicate the proportion of GFP-high cells in the population. (G) Survival of populations from (E) and (F) to VAN treatment for 5h. Values represent mean ± SD, N = 2.

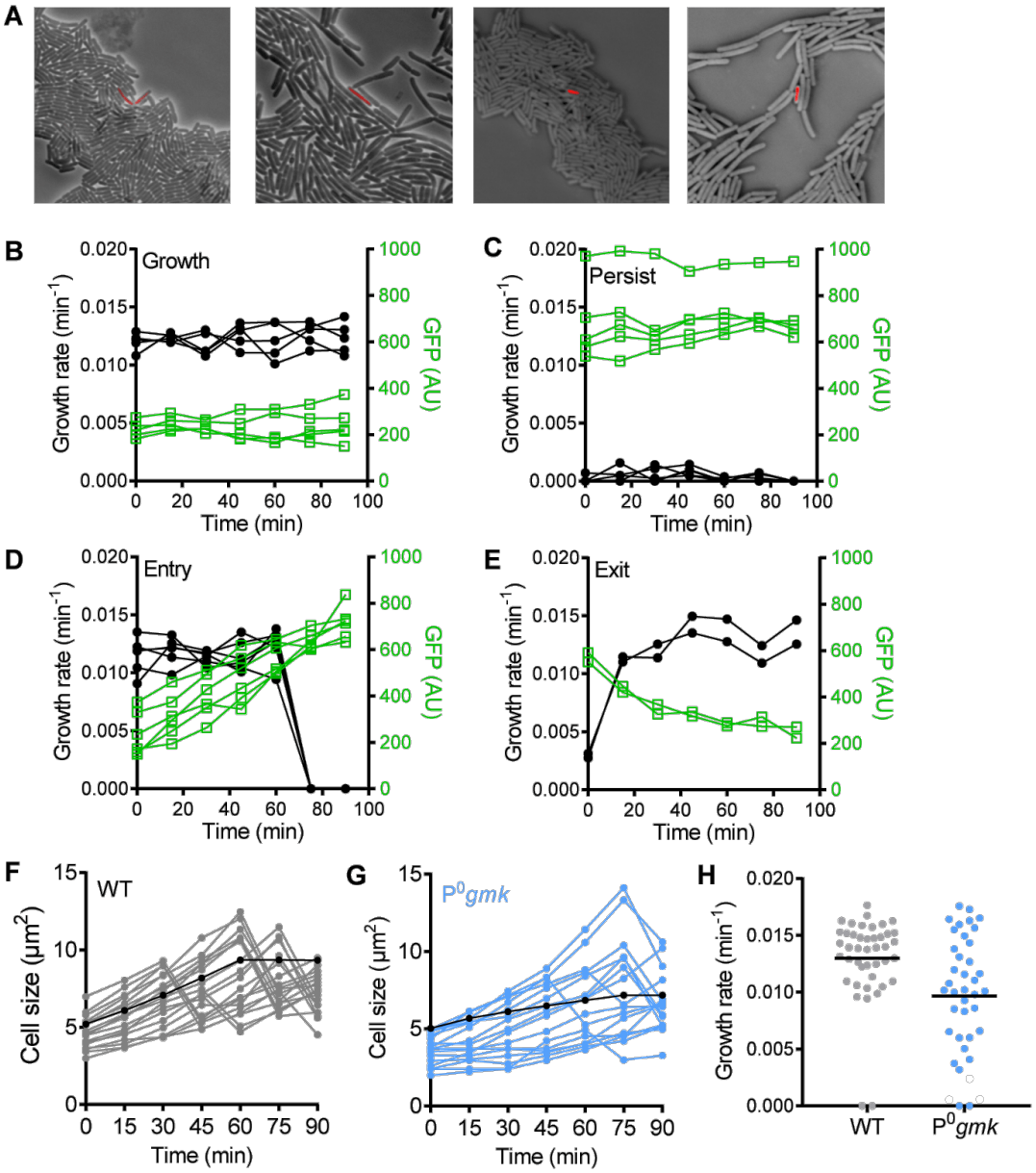

Figure S4, related to Figure 4. Stochastic development of (p)ppGpp-induced persisters and transitions between growth and persistence. (A) Snapshots of stochastic development of (p)ppGpp-induced persisters from single-cell time-lapse microscopy in WT cells containing the P_{ilvB} reporter. (B to E) Changes in growth rate and P_{ilvB} reporter fluorescence in WT during active growth (Growth) (B), persistence (Persist) (C), entry into persistence (Entry) (D), or exit from persistence (Exit) (E). (F to H) Variations in growth of wild-type and (p)ppGpp^0 *gmk*^{Q110R} cells. Single-cell growth of (F) wild-type (WT, grey) and (G) (p)ppGpp^0 *gmk*^{Q110R} mutant (P^0*gmk*, blue). Both strains were grown in parallel and subjected to time-lapse microscopy and quantitation as described. The black lines indicate a rare persistence entry event in either strain. (H) Specific growth rates obtained from (F) and (G). Data shown are from n > 40 cells for each strain. Black bars indicate the mean.

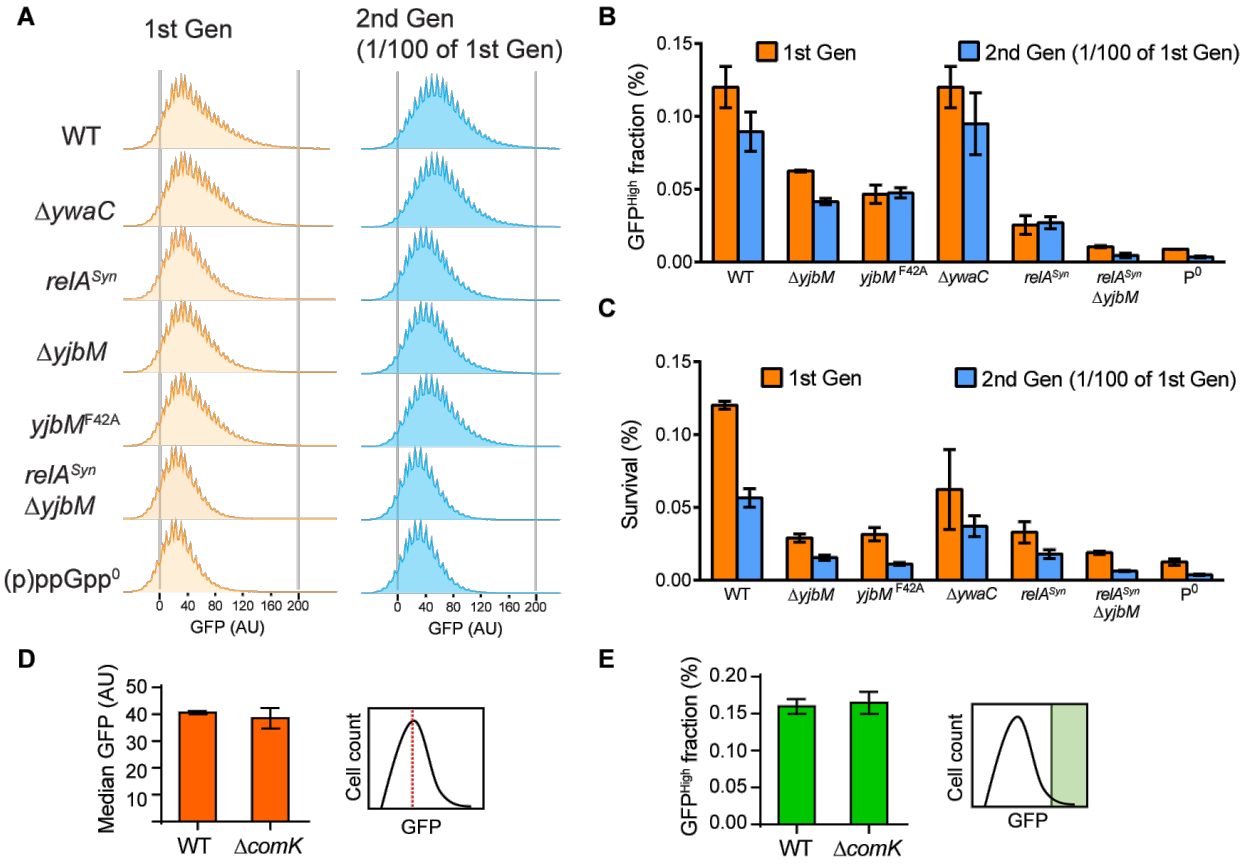

Figure S5, related to Figure 5. Analysis of persister distribution using flow cytometry. (A) Flow cytometry analysis of wild-type and (p)ppGpp biosynthesis mutants containing the P_{ilvB} reporter (~1.5x10^6 cells each). Cells were grown to exponential phase (1st Gen, orange) and re-inoculate (1/100 dilution) into fresh media and re-grew to exponential phase (2nd Gen, cyan). Both generations were analyzed by flow cytometry. (B) Levels of GFP-high cells from data obtained in (A). (C) Survival of the same populations tested after VAN treatment for 5h. Values represent mean ± SD from N = 2 of n > 10^6 cells each. (D and E) Persistence is independent of competence. (D) Median P_{ilvB} activity and (E) Frequency of GFP-high cells in WT and Δ*comK* populations measured using flow cytometry. Values represent mean ± SD from N = 2 of n > 10^6 cells each.

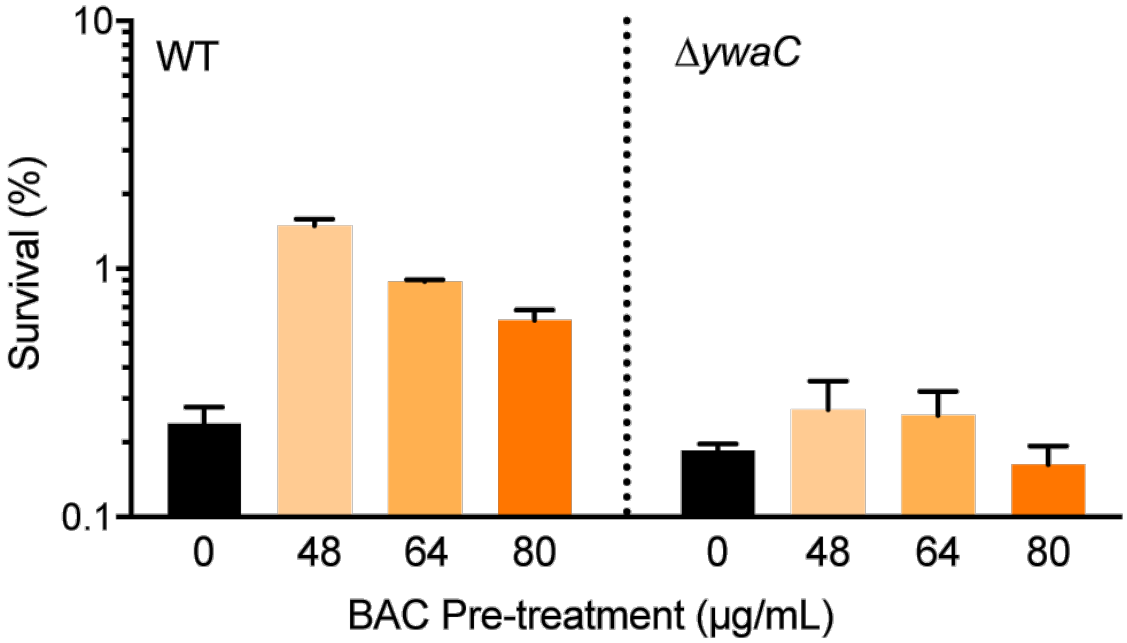

Figure S6, related to Figure 6. Effects of sub-lethal antibiotic concentrations on induced persistence. Sub-lethal BAC induction and antibiotic treatment in WT and Δ*ywaC* populations were carried out as described in Figure. 6E. Values represent mean ± SD, N = 2.

Chapter 4: (p)ppGpp protects *Bacillus subtilis* against chloramphenicol-mediated death by lowering GTP levels

Barra, J.T., Liu, K., Bittner, A.N., Pensinger, D.A., MacGilvray, M.E., Jain, N., Britton, R.A., and Wang, J.D.

J.T.B. designed and executed experiments in Figures 1-4, and 5A and edited the manuscript. This work is unpublished.

Abstract

A major culprit of antimicrobial treatment failure is dormant, antibiotic-tolerant persisters. The pathways for persister generation in Gram positive bacteria remain poorly understood. We recently showed that (p)ppGpp-GTP antagonism mediates persistence to bactericidal antibiotics in *Bacillus subtilis*. Here we show that (p)ppGpp also protects *B. subtilis* against bacteriostatic antibiotics, such as chloramphenicol. In the absence of (p)ppGpp, cell viability is severely decreased when treated with chloramphenicol. Decreasing GTP in (p)ppGpp null cells enables tunable chloramphenicol survival. Finally, abolishing (p)ppGpp regulation of GTP biosynthesis enzymes potentiates chloramphenicol killing, suggesting that (p)ppGpp plays a key role in lowering GTP to protect cells against bacteriostatic antibiotics. *B. subtilis* uses RelA to produce (p)ppGpp in response to chloramphenicol, a secondary metabolite, which may be an evolved trait to allow survival in the soil, which is fraught with many antibiotic secondary metabolites.

Introduction

Antibiotic tolerance, or persistence, is the ability of bacteria to survive bactericidal antibiotic treatment. The phenomenon is characterized by biphasic killing, where a majority of the bacterial population rapidly dies in the presence of an antibiotic but a subpopulation survives (Balaban et al., 2004; Maisonneuve and Gerdes, 2014). This survival phenotype is non-heritable, since re-introduction of this subpopulation of survivors, or persisters, to an antibiotic results in sensitivity similar to the original population (Fung et al., 2018; Maisonneuve and Gerdes, 2014). These survivors are responsible for many recalcitrant infections and biofilms in both clinical and industrial settings. Our previous work highlighted the importance of the alarmone (p)ppGpp and its antagonistic effects on GTP levels in promoting persistence (Fung et al., 2018). We observed that (p)ppGpp is necessary and sufficient to promote persistence, and without (p)ppGpp, decreasing GTP levels mediates persistence. Further, we discovered that basal levels of (p)ppGpp produced from two synthetases, RelA and YjbM, encourage formation of spontaneous persisters, whereas YwaC specifically responds to cell wall-targeting antibiotics to produce (p)ppGpp to increase persister formation (Czarny et al., 2014; Fung et al., 2018). Most persistence work utilizes bactericidal antibiotics, which demonstrates the typical biphasic kill curve. Another class of clinically relevant antibiotic are bacteriostatic antibiotics, such as chloramphenicol and tetracycline.

Bacteriostatic antibiotics prevent the growth of the bacteria and have successfully been used in clinical settings to treat endocarditis, meningitis, and osteomyelitis (infection of heart tissue, meninges, and bone, respectively) (Pankey and Sabath, 2004). In certain instances, bacteriostatic antibiotics are advantageous over bactericidal

antibiotics because the latter relies on actively growing bacteria to function, yet most intracellular bacteria in the host are growth arrested (Brauner et al., 2016; Pankey and Sabath, 2004). Thus bacteriostatic antibiotics can arrest cell growth, which allows the host immune system to remove the bacteria from the cytosol (Cohen et al., 2013; Pankey and Sabath, 2004). Such is the case with *Listeria monocytogenes*: when *L. monocytogenes* infect macrophages and chloramphenicol is introduced to induce growth arrest, the bacteria are internalized by autophagic vacuoles, suggesting that host cells are able to clear infections once cells stop growing (Rich et al., 2003). Despite its relevance in the clinical setting, little is known about how bacteria tolerate bacteriostatic antibiotics. Past work may offer insight into the importance of the alarmone (p)ppGpp. When *B. subtilis* is treated with bacteriostatic antibiotics like chloramphenicol and tetracycline, (p)ppGpp levels increase, suggesting that (p)ppGpp may play a role in mediating growth arrest when treated with bacteriostatic antibiotics (Rhaese et al., 1975). In addition, a transcriptome analysis of *B. subtilis* treated with chloramphenicol revealed that transcription of genes encoding transport proteins, carbohydrate metabolism enzymes, and translation proteins are upregulated (Lin et al., 2005). Clearly, induction of (p)ppGpp during chloramphenicol treatment may be an adaptive response to bacteriostatic antibiotics.

Here, we determined the importance of (p)ppGpp in protecting cells against bacteriostatic antibiotics. We show that without (p)ppGpp, the bacteriostatic antibiotic, chloramphenicol, is bactericidal. The ribosome-associated (p)ppGpp synthetase, RelA, is necessary and sufficient to produce (p)ppGpp in response to chloramphenicol treatment. Without (p)ppGpp, decreasing GTP levels protects against chloramphenicol

in a dose-dependent manner. In fact, GTP is the primary mediator of chloramphenicol tolerance. Removal of (p)ppGpp regulation of GTP biosynthesis enzymes, results in increased GTP levels and killing by chloramphenicol.

Materials and Methods

Strain Construction. *B. subtilis* strains were generated using natural transformation, using previously described techniques (Harwood et al., 1990).

Construction of (p)ppGpp^0. The (p)ppGpp synthetases were sequentially deleted in the *B. subtilis* NCIB 3610 *coml*^{Q12L} background (Konkol et al., 2013), as previously described (Kriel et al., 2012). Briefly, *yjbM* was deleted by integrating plasmid pJW300 into the chromosome through transformation (with selection on CAM plates), followed by transformation with pSS4332 (which expresses I-SceI endonuclease (Janes and Stibitz, 2006)) which introduces a double-strand break that promotes recombination and loss of integrated plasmids. This process was repeated to delete *ywaC*, using the plasmid pJW306. *relA* was deleted by PCR-amplifying the *relA*::*mls* locus from JDW168 and integrating it into the Δ*yjbM* Δ*ywaC* background. Absence of *yjbM* and *ywaC* were confirmed using colony PCR and the (p)ppGpp^0 phenotype was confirmed by plating onto S7+glucose (minimal) medium (Kriel et al., 2012).

Construction of (p)ppGpp^0 gmk^{Q110R}. The (p)ppGpp^0 *gmk*^{Q110R} was obtained as previously described (Fung et al., 2018). Briefly, (p)ppGpp^0 (JDW2231) was grown on S7+glucose medium. The surviving colonies were screened for suppressor mutations in HprT and Gmk by selection on plates containing S7+CAS+0.5 mM 8-azaguanine

(Kornberg and Baker, 1992) and S7+CAS+0.1 mM guanosine (Kriel et al., 2012) to differentiate mutations in HprT or Gmk, respectively. Survivors of guanosine but not 8-azaguanine were sequenced to identify the mutant *gmk* allele.

Construction of (p)ppGpp^0 guaB mutants. All (p)ppGpp^0 *guaB* mutants were obtained as previously indicated (Kriel et al., 2012).

Construction of (p)ppGpp^0 ΔcodY mutant. The (p)ppGpp^0 Δ*codY* was constructed as previously indicated (Kriel et al., 2012). It was discovered that JDW1021 still contained kanamycin resistance from pSS4332, so successive rounds of passaging on LB and selection on LB+Kan plates was done to detect loss of plasmid.

Construction of guaB^{down}. The *guaB*^{down} strain was constructed as previously indicated (Kriel et al., 2012).

Construction of ecgmk ecgpt. The *ecgmk* strain was constructed as previously indicated (Liu et al., 2015a). The plasmid pJW468 was constructed by inserting the *E. coli gpt* coding sequence with an RBS between the HindIII and SphI cut sites into pDR90. This allows for an IPTG-inducible *E. coli gpt*. The plasmid was integrated into the *amyE* locus of the *ecgmk* strain. Loss of AmyE activity was confirmed by iodine testing of colonies patched on LB+starch agar (5 g starch/ 500 mL LB agar).

Growth Conditions and Media. Unless stated otherwise, *Bacillus subtilis* strains were grown in S7 defined medium (Vasantha and Freese, 1980); MOPS was used at 50 mM

rather than 100 mM, supplemented with 0.1% glutamate, 1% glucose, and 0.5% casamino acids. When appropriate, amino acids were supplemented in the medium for auxotrophies (Harwood et al., 1990). Cell cultures were grown at 37 °C with shaking until logarithmic phase (0.2-0.4 OD_{600}) was reached. Cultures were then treated with antibiotics or other treatments. When applicable, isopropyl β-D-1-thiogalactopyranoside (IPTG) was added to a final concentration of 0.5 mM to induce gene expression from an IPTG-inducible promoter.

Antibiotic Tolerance Assay. To test antibiotic tolerance, cells were harvested from young overnight plates (plates less than 10 hours old) and back-diluted to OD_{600} = 0.005. Cells were grown to logarithmic phase (0.2-0.4 OD_{600}) and untreated samples (T=0) were serially diluted and plated onto Luria-Broth (LB) agar plates to determine CFU/mL/OD_{600} prior to treatment. After, cells were treated with a final concentration of 12 μg/mL CAM (3X MIC). This concentrations were determined to be several fold higher than the determined MICs (Fung et al., 2018). At each hour for up to three hours, samples were serially diluted and plated onto LB agar. LB agar plates were incubated at 37 °C overnight. CFU/mL/OD_{600} were determined. Relative CFU/mL/OD was calculated by dividing the CFU/mL/OD_{600} at a specific time point by CFU/mL/OD_{600} at T=0.

Measurement of Intracellular Nucleotides by TLC. Measurement of nucleotides was performed as described (Wang et al., 2007). Nucleotides were quantified using ImageQuant software (Molecular Dynamics). Obtained intensities were normalized to

the number of phosphates in the corresponding nucleotide. Nucleotide levels are normalized to ATP level at T=0.

HprT and Gpt Enzymatic Assay. Enzyme inhibition assays were performed as indicated (Biazus et al., 2009; Kriel et al., 2012). The *B. subtilis* HprT data is reproduced from Figure 2E in Kriel *et al*. (2012) for comparison purposes. Briefly, reactions were performed at 25 °C and contained 100 mM Tris-HCl (pH 7.4) buffer, 1.2 mM $MgCl_2$, 1 mM PRPP, 50 µM guanine, 20 nM HprT, and 0-100 µM of pppGpp. Reactions were initiated by adding PRPP and the absorbance at 257 nm (for detection of GMP) was monitored for 10 minutes using a temperature-controlled spectrophotometer (Shimadzu UV-2401PC). The initial velocities of the reaction at each pppGpp concentration were determined. The percent activity was determined by dividing the initial velocity of the reaction at a specific pppGpp concentration by the initial velocity of the reaction without pppGpp. Data was fitted using GraphPad Prism version 5.02 for Windows (GraphPad Software, San Diego, CA, USA, www.graphpad.com).

Measurement of Protein Synthesis by ^{35}S-methionine Incorporation. Cells were grown to mid-exponential phase in S7 defined medium supplemented with 19 amino acids and 0.1X methionine (5 µg/mL), and 0.2 ml of culture was pulse-labeled with 10 µCi of ^{35}S-methionine (1000 Ci/mmole, MP Biomedicals) for 2 min. After initial measurements (T=0) were obtained, cells were split into untreated or CAM (12 µg/mL)-treated cultures and added to ^{35}S-methionine at regular time intervals. To stop the incorporation, ice-cold 20% trichloroacetic acid (TCA) was mixed with labeled samples and incubated on

ice for 30 min. Samples were filtered on glass-fiber filters (GF/C, Whatman) with vacuum and washed with ice-cold 5% TCA. Filters were dried and incubated in scintillation fluid. The amount of radioactivity incorporated, measured as counts per minute (CPM), was determined using a liquid scintillation counter. The change in protein synthesis activity was determined by dividing the CPM at a certain time point by CPM at T=0.

Sucrose Density Centrifugation for Ribosome Profiles. Cells were grown to mid-exponential phase (OD_{600} = 0.2-0.4) in LB and 600 mL of cells were harvested by centrifugation. Add treatments (such as 12 µg/mL CAM) when appropriate. These conditions closely match treatment conditions for antibiotic tolerance assays. Cell pellets were stored at -80 °C until needed. To lyse cells, pellets were resuspended in ice cold lysis buffer (10 mL BufferA, 10 µL 1M DTT, 1 EDTA-free protease inhibitor cocktail tablets (Roche), 50 µL Tween 20, 1 mM DTT; Buffer A: 10 mM Tris-HCl, pH 7.5, 10 mM $MgCl_2$, 60 mM KCl), 4 µL DNAse (~3 kunit/µL RNase free DNAase set, Qiagen), and lysed by passing cells through the French press three times at 1200-1400 psi. Cells were clarified by centrifuging at 16,000 X g for 20 minutes at 4 °C. The OD_{260} was obtained and the lysate was stored at -80 °C until ultracentrifugation. For centrifugation, prepare a 18-43% sucrose gradient using Buffer B (20mM Tris HCl pH 7.5, 10 mM $MgCl_2$, 50 mM NH_4Cl, 1 mM DTT, 50% sucrose). Layer cell lysate (up to 30 OD_{260}) on top and spin at 21,000 rpm (~88000 g) for 14 hours (these are specifications for 36 mL samples, spun using a Surespin 630 rotor) at 4 ^{o}C. Once the cell lysate is separated,

monitor the ribosome profile using a Biorad FPLC by monitoring UV absorbance at 254 nm.

Results

RelA is necessary and sufficient for chloramphenicol survival

Our previous work determined the MIC of chloramphenicol (CAM) to be 3 μg/mL (Fung et al., 2018). To determine whether (p)ppGpp protects cells against bacteriostatic antibiotics like chloramphenicol, we treated wild type and (p)ppGpp^0 cells with 12 μg/mL CAM (4X MIC). To our surprise, CAM kills about 99.9% of (p)ppGpp^0 cells by 2 hours of treatment, whereas, as expected, wild type cells neither grow nor die (Figure 1A). This bacteriostatic to bactericidal transition appears to be a general response for bacteriostatic antibiotics, since tetracycline and arginine hydroxamate also kills (p)ppGpp^0 but not wild type (Figure S1) (Kriel et al., 2012). CAM killing is also dose-dependent since lower, sub-MIC CAM concentrations kill cells less than at a higher concentration (Figure 1B).

Since (p)ppGpp is required for chloramphenicol survival, we determined which of the three (p)ppGpp synthetases were necessary for (p)ppGpp production. *B. subtilis* contains a bifunctional RelA which can synthesize and hydrolyze (p)ppGpp (Hogg et al., 2004) and two smaller monofunctional synthetases, YjbM and YwaC (Nanamiya et al., 2008; Srivatsan et al., 2008). To test the importance of RelA synthesis activity, one of the catalytic residues were mutated, forming RelA^{D264G} (Hogg et al., 2004; Kriel et al., 2014). The mutation is necessary because RelA cannot be deleted if other (p)ppGpp synthetases are present, since the hydrolase activity prevents toxic build-up of

(p)ppGpp (Srivatsan et al., 2008). Mutation of RelA synthetase resulted in cell death similar to (p)ppGpp^0, indicating that RelA is necessary to survive CAM treatment (Figure 1A). YjbM, along with RelA, cooperate to produce basal levels of (p)ppGpp and was recently shown to be stimulated by pppGpp (Fung et al., 2018; Steinchen et al., 2015), whereas YwaC responds to cell wall damage (Czarny et al., 2014; Fung et al., 2018). We inactivated the synthetase domains of YjbM and YwaC and treated the strain with CAM. The mutated YjbM and YwaC neither grew nor died, indicating that a functional RelA was sufficient for CAM survival (Figure 1A). Thus, RelA is necessary and sufficient for CAM survival.

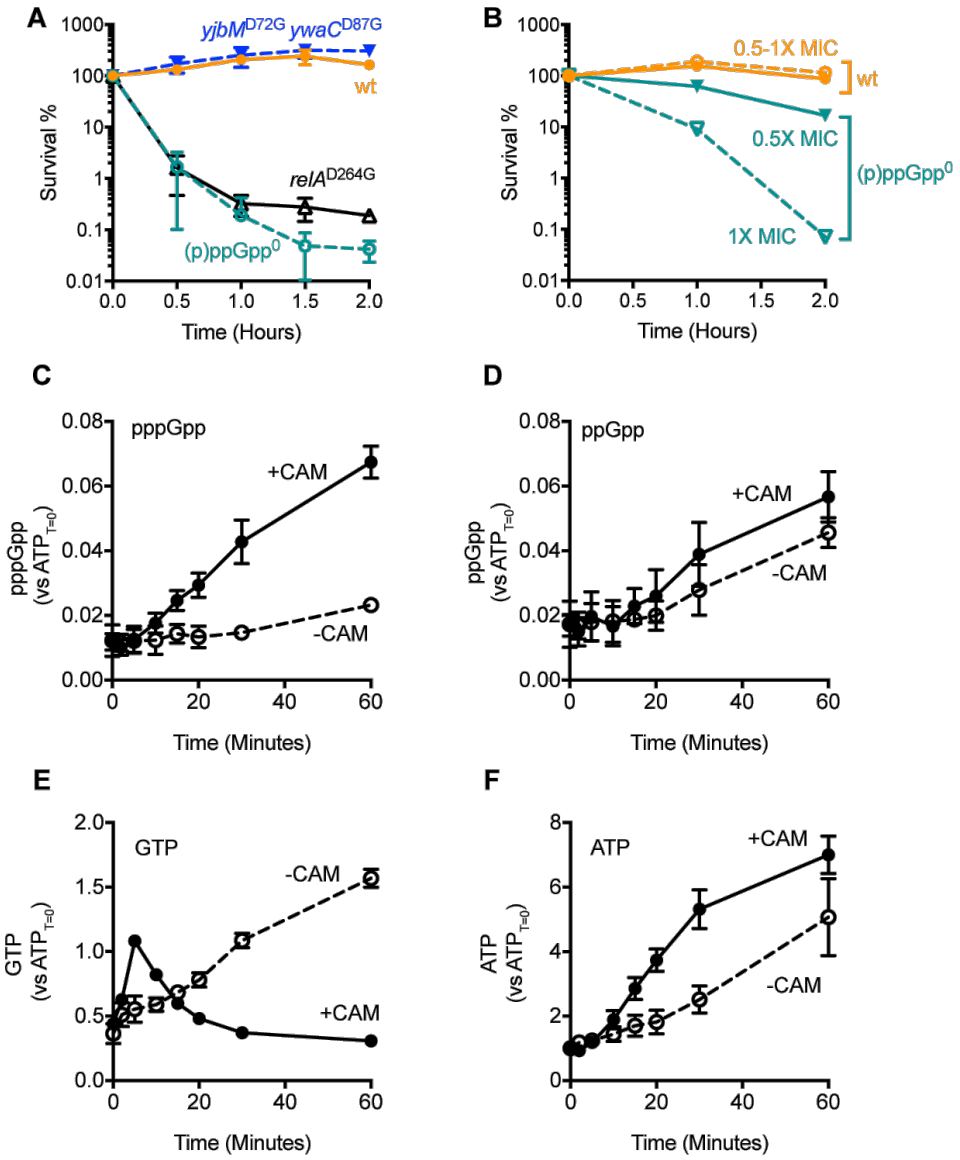

Figure 1. RelA produces (p)ppGpp during chloramphenicol treatment, which protects cells from a bacteriostatic to bactericidal switch. A. Exponentially growing *B. subtilis* SMY wild type, (p)ppGpp^0, *relA*^{D264G}, and *yjbM*^{D72G} *ywaC*^{D87G} were treated with 12 µg/mL CAM (4X MIC) for up to two hours. Percent survival was determined by dividing the number of tolerant CFU/mL/OD at each time point by the number of CFU/mL/OD at T=0 and converted to a percentage. Values are N=3 ± SD. B. Wild type and (p)ppGpp^0 cells were treated with 3 µg/mL and 1.5 µg/mL CAM and percent survival was determined (N=1). C to F. Radiolabeled wild type cells were treated with (closed circles) and without (open circles) 12 µg/mL CAM and nucleotides were extracted at T=0 to 60 minutes. pppGpp (C), ppGpp (D), GTP (E), and ATP (F) levels were determined and normalized against ATP$_{T=0}$. Values for N=2 ± SD are plotted.

CAM induces (p)ppGpp production in wild type cells. The difference between wild type and (p)ppGpp^0 survival during CAM treatment (Figure 1A, 1B) prompted us to examine (p)ppGpp levels in wild type cells in the presence and absence of CAM. As shown in Figure 1C and 1D, (p)ppGpp levels start to increase 10 minutes after addition of CAM and were three-fold higher than the untreated control at 60 minutes of CAM treatment. This agrees with previous reports of CAM-induced (p)ppGpp production in *B. subtilis* (Rhaese et al., 1975). It should be noted that the ability to produce (p)ppGpp coincides with CAM survival: the *relA*^{D264G} synthetase mutant cannot produce (p)ppGpp in response to CAM and are nonviable, whereas the *yjbM*^{D72G} *ywaC*^{D87G} are able to survive (Figure S2). We also observed that GTP levels increased immediately after addition of CAM, followed by a rapid decrease after 10 minutes of CAM treatment. This decrease in GTP levels is likely due to downstream inhibitory effects of (p)ppGpp on GTP biosynthesis and consumption of GTP in (p)ppGpp biosynthesis (Figure 1E). ATP levels increase after CAM addition, similarly to RHX treatment (Fung et al., 2018; Wang et al., 2007), likely because (p)ppGpp inhibits GuaB, pushing *de novo* purine synthesis towards ATP (Figure 1F) (Kriel et al., 2012). Further, it is possible that the increased ATP can activate promoters with ATP as an initiating nucleotide and transcribe genes necessary for survival (Krásný et al., 2008). Taken together, our data suggested that CAM-induced elevation of (p)ppGpp levels, which was accompanied by a decrease in GTP and increase in ATP, is analogous to that of amino acid starvation (Kriel et al., 2012) which prepares wild type, but not (p)ppGpp^0 cells, to survive otherwise lethal CAM stress.

Decreasing GTP levels in (p)ppGpp^0 cells is sufficient to restore antibiotic tolerance to wild type levels. Our previous work showed that (p)ppGpp regulates GTP homeostasis and loss of this regulation in (p)ppGpp^0 cells results in high GTP levels that is correlated to cell death (Kriel et al., 2012). Decreasing GTP levels in (p)ppGpp^0 cells alleviated the effects of high GTP levels (Bittner et al., 2014; Fung et al., 2018; Kriel et al., 2012). To test the hypothesis that lowering GTP levels in (p)ppGpp^0 cells results in increased antibiotic tolerance, we treated (p)ppGpp^0 *gmk*^{Q110R} (Fung et al., 2018), a mutant with a defective GTP biosynthesis enzyme, guanylate kinase, with CAM and studied their tolerance over time (Figure 2A). The (p)ppGpp^0 *gmk*^{Q110R} strain, which has lower GTP levels than the parental (p)ppGpp^0 strain, tolerated the antibiotics similar to the wild type. This result suggested that regulating GTP levels downstream of (p)ppGpp mediates antibiotic tolerance. It should be worth noting that the CAM tolerance experiments were conducted in different *B. subtilis* strain backgrounds, which appear to yield different percentages of killing. The strain backgrounds are indicated in figure legends.

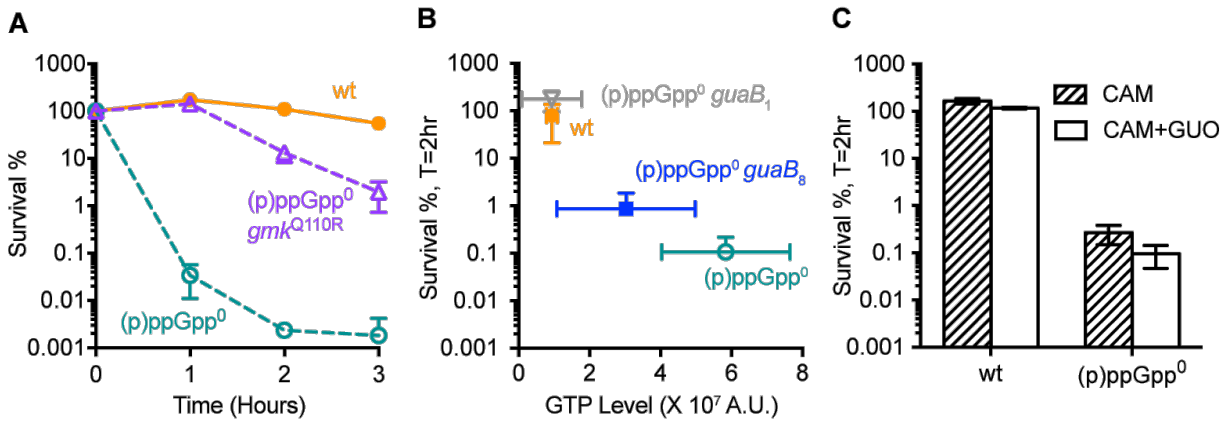

Figure 2. (p)ppGpp protects against chloramphenicol-mediated killing by decreasing GTP levels. A. Exponential phase *B. subtilis* 3610 *comI*^{Q12L} wild type, (p)ppGpp^0, and (p)ppGpp^0 *gmk*^{Q110R} were treated with 12 µg/mL CAM for three hours. Percent survival was determined by dividing the number of tolerant CFU/mL/OD at each time point by the number of CFU/mL/OD at T=0 and converted to a percentage. Values are N=3 ± SD. B. Exponential phase *B. subtilis* YB886 wild type, (p)ppGpp^0, and (p)ppGpp^0 *guaB* mutants were treated with 12 µg/mL CAM for two hours. Their survival was correlated with steady state GTP levels obtained by ^{32}P-orthophosphate labeling. Values are N≥3 ± SD. C. Exponential phase *B. subtilis* SMY wild type and (p)ppGpp^0 were treated with 12 µg/mL CAM or 12 µg/mL CAM and 1 mM GUO. Values are N≥3 ± SD.

Our previous work yielded (p)ppGpp^0 strains with various *guaB* alleles that conferred different GTP levels that correlate with amino acid stress survival and growth rate (Bittner et al., 2014; Kriel et al., 2012). Since CAM killing results in a large survival range, with wild type and (p)ppGpp^0 as extremes, we used the (p)ppGpp^0 *guaB* strains, to test the hypothesis that different GTP levels correlate with CAM killing. Treatment of (p)ppGpp^0 *guaB$_1$* and (p)ppGpp^0 *guaB$_8$* strains results in a range of CAM survival (Figure 2B) and tolerance was inversely proportional to their respective GTP levels, *i.e.* high GTP levels in (p)ppGpp^0 cells resulted in 0.01% survival, while intermediate GTP levels in (p)ppGpp^0 *guaB$_8$* led to 1% survival, and low GTP levels in (p)ppGpp^0 *guaB$_1$* or WT cells resulted in no change in CFU/mL/OD (Figure 2B). Decreased ATP levels have been associated with increased antibiotic tolerance in *S. aureus* (Conlon et al., 2016), so we examined CAM survival with respect to ATP levels and showed that there was no apparent correlation (Figure S3). These results suggest that GTP levels mediate CAM survival in a dose-dependent manner, in which high GTP levels led to antibiotic lethality, and low GTP levels promote antibiotic tolerance.

Since we observed that decreased GTP levels in (p)ppGpp^0 cells increased CAM tolerance, we wanted to test the hypothesis that increased GTP levels results in decreased tolerance. We chemically dysregulated GTP levels in WT and (p)ppGpp^0 cells by addition of 1 mM guanosine (GUO), which has been shown to trigger accumulation of cellular GTP (Kriel et al., 2012). Both WT and (p)ppGpp^0 cells were treated with CAM in the presence or absence of GUO. As expected, WT cells remained completely tolerant under both treatment conditions since (p)ppGpp biosynthesis is present to regulate GTP homeostasis (Kriel et al., 2012). In contrast, addition of GUO

further potentiated the lethality of CAM treatment in (p)ppGpp^0 cells by about 3-fold when compared to the CAM treatment alone (Figure 2C). This result further supports that GTP is a downstream mediator of (p)ppGpp-regulated antibiotic tolerance.

Our previous work showed that decreasing GTP levels by depleting *guaB* (*guaB*^{down}) promoted tolerance to ciprofloxacin and vancomycin when compared to wild type (Fung et al., 2018). Depleting *guaB*, followed by treatment with CAM, showed that cells neither grew nor died, like wild type (Figure S4A). For bactericidal antibiotics, *guaB*^{down} resulted in hypertolerant cells that survived better than wild type cells. If *guaB*^{down} were hypertolerant when treated with CAM, they would be growing, which would indicate resistance (Brauner et al., 2016) (Figure 4), but that is not the case (Figure S4B). Thus, we can rationalize the static growth for *guaB*^{down} when treated with CAM.

Increased tolerance to antibiotics is often associated with lower growth rate (Maisonneuve et al., 2013). To rule out the possibility that decreased GTP levels lower growth rate and thus increase tolerance (Bittner et al., 2014), we correlated the growth rate of all tested strains with CAM tolerance (Figure S5). Since several strains with slow growth rates were still susceptible to CAM treatment, it is unlikely that the CAM tolerance we observe with lower GTP levels is solely due to lower growth rate.

Disruption of (p)ppGpp-mediated GTP biosynthesis regulation potentiates CAM killing in wild type cells. The presence of (p)ppGpp controls GTP biosynthesis (Kriel et al., 2012). It is possible that if we abolish the inhibitory effects of (p)ppGpp on GTP biosynthesis, then we can increase GTP levels in WT cells and render them sensitive to CAM

treatment similar to (p)ppGpp^0 cells. To test this hypothesis, we first constructed a strain called *ecgmk ecgpt* (Figure 3A), in which the endogenous *B. subtilis gmk* (gmk_{Bs}) was replaced with the (p)ppGpp-insensitive *E. coli gmk* (gmk_{Ec}) (Liu et al., 2015a). This strain also carries the IPTG-inducible *E. coli gpt* (gpt_{Ec}), which encodes xanthine-guanine phosphoribosyltransferase (Gpt), a mildly (p)ppGpp-resistant *E. coli* variant of HprT ($HprT_{Bs}$ IC_{50} = ~10 $\pm$ 1 μM, Gpt_{Ec} IC_{50} = 78 $\pm$ 7 μM) (Figure 3B) (Kriel et al., 2012). The presence of Gpt in *ecgmk ecgpt* decreased the inhibitory effects of (p)ppGpp on GTP biosynthesis. To determine whether dysregulating GTP levels sensitizes cells to CAM, we treated *ecgmk* and *ecgmk ecgpt* with CAM and CAM+GUO. The *ecgmk ecgpt* strain exhibited a 10-fold decrease in tolerance during CAM+GUO treatment when compared to CAM alone (Figure 3C). Both *ecgmk* and *ecgmk ecgpt* treated with GUO alone resulted in growth (data not shown). These results indicated that lethality of CAM treatment can be potentiated in (p)ppGpp$^+$ cells by abolishing (p)ppGpp regulation of GTP biosynthesis and dysregulating GTP levels, further supporting the role of GTP as a mediator of CAM survival.

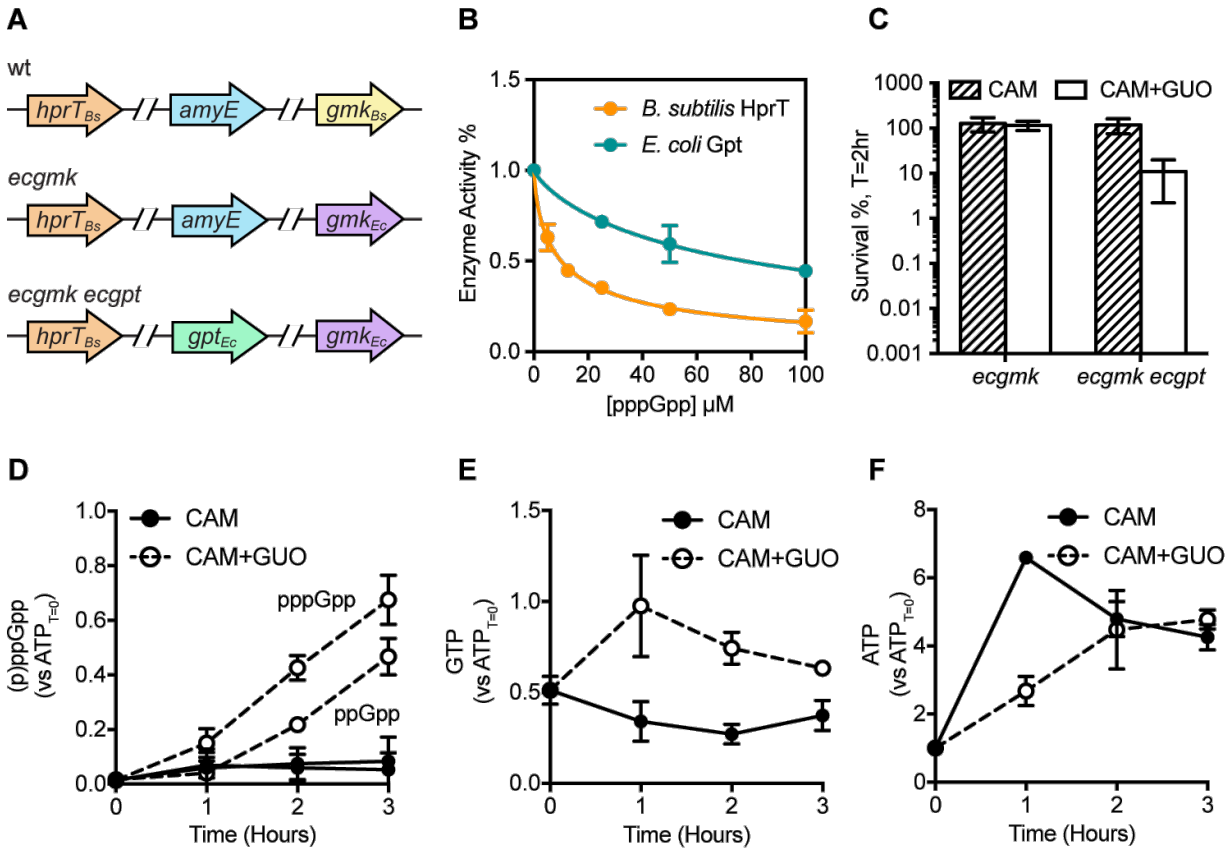

Figure 3. Manipulating GTP levels in wild type cells potentiates CAM killing. A. Schematic of gene content for *B. subtilis* SMY strains wild type, *ecgmk*, and *ecgmk ecgpt*. Genes that are the same color are the same in each strain. B. pppGpp inhibition of *B. subtilis* HprT and *E. coli* Gpt. Values are N=3 ± SD. C. Exponential phase *B. subtilis* SMY *ecgmk* and *ecgmk ecgpt* were treated with 12 µg/mL CAM or 12 µg/mL CAM and 1 mM GUO. Percent survival was determined by dividing the number of tolerant CFU/mL/OD at each time point by the number of CFU/mL/OD at T=0 and converted to a percentage. Values are N≥3 ± SD. D to F. Exponential phase *ecgmk ecgpt* was radiolabeled with ^{32}P-orthophosphate and treated with 12 µg/mL CAM or 12 µg/mL CAM and 1 mM GUO. Nucleotides were extracted and (p)ppGpp (D), GTP (E), and ATP (F) levels were determined over time. Values are N=3 ± SD.

To determine whether GTP levels were dysregulated despite the presence of (p)ppGpp during treatment of *ecgmk ecgpt* with CAM and CAM+GUO treatment, we quantified cellular nucleotide pools by radiolabeling the cells with ^{32}P-orthophosphate, followed by nucleotide separation, and visualization with TLC. After treatment of *ecgmk ecgpt* with CAM+GUO for three hours, pppGpp and ppGpp levels increased about 12-fold and 6-fold, respectively, when compared to CAM alone (Figure 3D). Interestingly, relative GTP levels increased after one hour of treatment, but then decreased after the second hour (Figure 3E), whereas ATP levels fluctuated in an opposite pattern (Figure 3F). The observed increase in GTP levels supported the hypothesis that although *ecgmk ecgpt* is producing pppGpp, the (p)ppGpp-insensitive *E. coli* Gmk and Gpt continued to synthesize GTP, upon GUO addition, to levels similar to that of untreated wild type cells (Figure 1E). The initial increase of GTP levels during CAM+GUO treatment after one hour (Figure 3E) is likely responsible for the observed decrease in tolerance (Figure 3C). Perhaps this three-fold excess of GTP, as also reported in our previous work (Kriel et al., 2012), is sufficient to induce a 10-fold decrease in tolerance when *ecgmk ecgpt* is under CAM+GUO treatment. Conversely, there are no appreciable differences between nucleotide levels in *ecgmk* cells treated with CAM or CAM+GUO (Figure S6A-C). Taken together, our results have demonstrated that increased GTP levels in a (p)ppGpp^{+} strain can lead to CAM-induced lethality.

Decreased CAM and CAM+GUO survival in (p)ppGpp^{0} cells is independent of the CodY regulon. One of the major binding partners of GTP is the master regulator CodY, which represses the transcription of branched-chain amino acid biosynthesis genes at high

GTP levels (Ratnayake-Lecamwasam et al., 2001) and regulates genes involved in metabolism (Belitsky and Sonenshein, 2013). Our previous work showed that high GTP levels in (p)ppGpp^0 cells resulted in CodY hyperactivity, which consequently led to repression of amino acid biosynthesis genes necessary to survive amino acid starvation (Kriel et al., 2014). To rule out the possibility that increased GTP levels in (p)ppGpp^0 cells results in hyper-repression of the CodY regulon and thus decreased CAM tolerance, we tested the tolerance of the (p)ppGpp^0 Δ*codY* strain under CAM and CAM+GUO treatment. Our results indicate that (p)ppGpp^0 and (p)ppGpp^0 Δ*codY* strains have identical responses to CAM and CAM+GUO treatments (Figure 4A, 4B), indicating that the inability of (p)ppGpp^0 cells to survive CAM is independent of the CodY regulon and that CodY is not inhibiting transcription of genes essential for CAM survival.

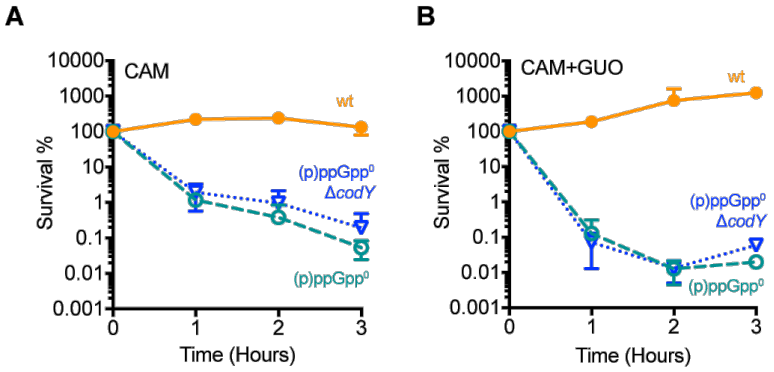

Figure 4. CodY hyperactivity does not affect CAM survival. Exponential phase *B. subtilis* SMY wild type, (p)ppGpp^0, and (p)ppGpp^0 Δ*codY* cells were treated with A. 12 µg/mL CAM and B. 12 µg/mL CAM and 1 mM GUO. Percent survival was determined by dividing the number of tolerant CFU/mL/OD at each time point by the number of CFU/mL/OD at T=0 and converted to a percentage. Values are N=3 ± SD.

Absence of (p)ppGpp does not appear to affect protein synthesis. (p)ppGpp and its inhibition of GTP biosynthesis has pleiotropic effects on bacterial physiology, including translation and ribosome biogenesis. Translation is driven by GTPases that couple GTP hydrolysis with delivery of aminoacylated tRNAs to the A-site (EF-Tu), ribosome translocation and movement of A-site and P-site tRNAs on the mRNA template (EF-G), and translation termination upon detection of a stop codon (RF3) (Seo et al., 2006; Steitz, 2008). Since each amino acid addition and subsequent translocation consumes two GTPs, actively translating ribosomes require large amounts of GTP and a decrease in GTP levels upon (p)ppGpp induction, coupled with inhibition of translation GTPases by (p)ppGpp (Nomura et al., 2012; Rojas et al., 1984), must rapidly reduce translation. Further, GTP levels control the transcription of ribosomal RNAs and ribosomal proteins, so reduced GTP levels upon (p)ppGpp production decreases the concentration of substrates for ribosome production (Krásný and Gourse, 2004). Conversely, (p)ppGpp^0 cells cannot decrease GTP levels or inhibit translation-associated GTPases, and as a result, may not be able to decrease translation. To test the hypothesis that (p)ppGpp^0 cells cannot decrease protein synthesis, we measured ^{35}S-methionine incorporation rates in wild type and (p)ppGpp^0 cells grown in $S7_{50}$ + 19 amino acids + 0.1X methionine (5 μg/mL) with and without 12 μg/mL of CAM treatment. The data indicates that wild type and (p)ppGpp^0 cells were both able to decrease translation at 12 μg/mL and 100 μg/mL CAM (Figure 5A, Figure S7), suggesting that (p)ppGpp^0 is not defective in halting translation. This response might be because CAM specifically inhibits peptidyl transferase activity and prevents the A-site tRNA from being translocated into the P-site and so can subsequently shut down translation in both strains.

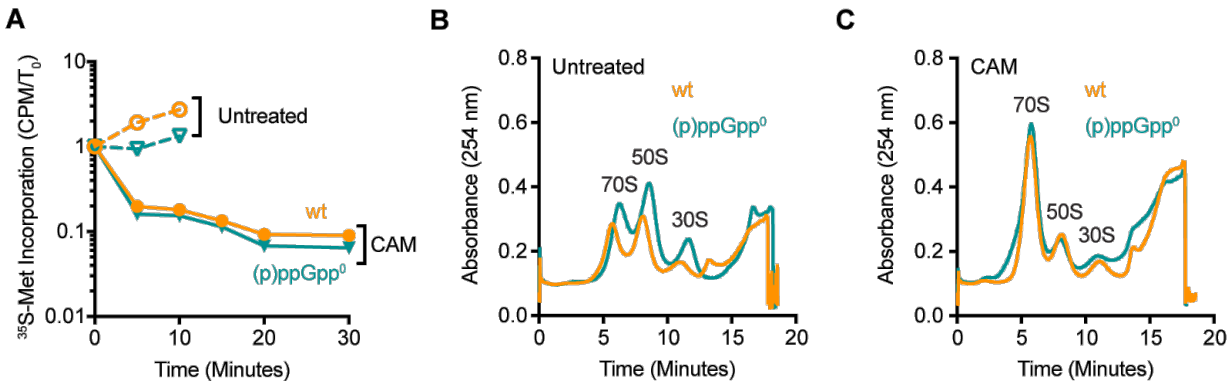

Figure 5. Loss of (p)ppGpp does not appear to affect GTP-dependent processes. A. Exponential phase *B. subtilis* 3610 *comI*^{Q12L} were treated with and without 12 µg/mL CAM and at regular intervals, were pulse-labeled with ^{35}S-methionine for two minutes. The labeling was stopped with addition of 20% TCA. The labeled proteins were extracted onto filters with 5% TCA and counts per minute (CPM) were determined using a liquid scintillation counter. Values are represented as the ratio of CPM at a certain time point to CPM at T=0. Values are N=1. Exponential phase 3610 *comI*^{Q12L} wild type and (p)ppGpp^0 cells were harvested at T=0 (B) or after 12 µg/mL CAM treatment at T=10 minutes (C) and lysed to extract RNA. A total of 30 OD_{260} was layered on top of a 18-43% sucrose gradient and ultracentrifuged to separate the ribosome subunits. After centrifugation, the samples were monitored using UV readings at 254 nm from the bottom of the tube (T=0), with the densest sucrose. The time readings from T=0 to 18 minutes represent reading the centrifuged samples from the bottom to the top of the tube.

Absence of (p)ppGpp may not affect ribosome biogenesis. (p)ppGpp and GTP have been shown to regulate the activity of ribosome assembly GTPases (raGTPases) according to nutrient availability. In *S. aureus*, (p)ppGpp was shown to bind to and inhibit raGTPases, such as RsgA, Era, and several others (Corrigan et al., 2016). When GTP hydrolysis is decreased, either by depleting raGTPases or inhibiting the hydrolysis step, the population of assembled subunits is decreased, depending on which ribosomal precursors are bound by the raGTPases (Britton, 2009). Further, (p)ppGpp can interact with the GTPase Obg and premature 50S ribosomes during starvation and sequester the ribosomes until nutrients are available (Feng et al., 2014). Thus, it is possible that without (p)ppGpp, cells may not be able to properly assemble ribosomes. Wild type and (p)ppGpp^0 cells with and without 10 minutes of 12 μg/mL CAM treatment were harvested, lysed, and their contents were subjected to sucrose density centrifugation. In the untreated samples, wild type and (p)ppGpp^0 cells have similar profiles, with an accumulation of 50S ribosomes, which indicates that they both may have defects in assembly (Figure 5B). Interestingly, when treated with CAM, the wild type and (p)ppGpp^0 profiles align well and the defects in 50S assembly are gone (Figure 5C). Since there are no major differences in the profiles, we concluded that wild type and (p)ppGpp^0 cells do not have ribosome assembly defects during CAM treatment. It should be noted that an ideal profile should look like Figure 5C and the experiment is worth repeating.

Discussion

With the increased prevalence of antibiotic resistance and tolerance in both clinical and industrial settings, it is important to determine the underlying mechanisms that bacteria employ to survive antibiotics. In this work, we have shown that both (p)ppGpp and GTP promote chloramphenicol (CAM) tolerance in *Bacillus subtilis*. In fact, we argue that regulation of GTP levels, the downstream effect of (p)ppGpp (Kriel et al., 2012), is the primary determinant of tolerance (Fung et al., 2018). From our work, we emphasize several important conclusions: 1) (p)ppGpp controls intracellular GTP levels as a stress survival strategy in Firmicutes and 2) (p)ppGpp protects against CAM-induced lethality.

Control of intracellular GTP levels by (p)ppGpp is a stress survival strategy in Firmicutes. Our previous work showed that (p)ppGpp tunes GTP levels to balance optimum growth and protects against stresses such as bactericidal antibiotics and amino acid downshift (Bittner et al., 2014; Fung et al., 2018; Kriel et al., 2014). In this work, we show that (p)ppGpp promotes CAM tolerance in *B. subtilis* by modulating intracellular GTP levels. One of the major effects of modulating GTP level is change in CodY regulatory activity (Handke et al., 2008; Kriel et al., 2014). CodY is a repressor activated by GTP levels in the millimolar range (Handke et al., 2008) and its regulon consists of amino acid biosynthesis, flagellar, and other genes utilized for adaptation to nutrient poor conditions (Belitsky and Sonenshein, 2013). Surprisingly, deletion of *codY* in (p)ppGpp^0 cells did not ameliorate CAM-induced lethality, suggesting that hyperactivity of CodY is not repressing genes essential for (p)ppGpp^0 survival of CAM and other antibiotics (Fung et al., 2018). In other CodY-containing pathogenic bacteria, CodY is known to repress virulence factors, toxins, and other genes used for survival in

a nutrient-poor environment (Geiger and Wolz, 2014; Majerczyk et al., 2010; Richardson et al., 2015). Since GTP pools regulate CodY activity and is linked to the stringent response in *B. subtilis* and the CodYs are homologs(Geiger and Wolz, 2014; Ratnayake-Lecamwasam et al., 2001), this paradigm is likely applicable to *S. aureus* (Geiger and Wolz, 2014), and it is possible that expression of the CodY regulon is independent of antibiotic tolerance in these bacteria (Conlon et al., 2016).

In the absence of (p)ppGpp, different intracellular GTP levels correlate with different degrees of cell death (Figure 2), indicating that there is a GTP level threshold at which cells can no longer tolerate CAM treatment, as we predicted in our previous work (Fung et al., 2018). On the other hand, even in the presence of (p)ppGpp, disrupting GTP homeostasis renders cells sensitive to CAM (Figure 3), suggesting that GTP is a key determinant of antibiotic tolerance. It is thus possible that (p)ppGpp prevents GTP over-accumulation during antibiotic treatment to protect cells against antibiotics (Fung et al., 2018). Given that (p)ppGpp potently inhibits the GTP biosynthesis enzyme guanylate kinase in Firmicutes (Liu et al., 2015a), it is possible that Gram-positive pathogens use a similar mechanism, at least in part, to tolerate antibiotics.

(p)ppGpp protects cells from CAM-induced lethality. In this study, we observed that wild type *B. subtilis* produces (p)ppGpp upon CAM treatment (Figure 1C), suggesting that (p)ppGpp induction is important for adaptation to antibiotic treatment (Fung et al., 2018; Gaca et al., 2013; Geiger et al., 2014; Nguyen et al., 2011). We speculate that production of (p)ppGpp in response to CAM may be due to inhibition of ribosome progression, analogous to the response during amino acid starvation (Brown et al.,

2016; Kriel et al., 2012). Consequently, in the absence of (p)ppGpp, (p)ppGpp^0 cells cannot adapt to CAM treatment and is killed by the drug (Figure 1A, 1B). This observation is in line with our previous work in which (p)ppGpp^0 cells lose viability upon amino acids starvation or arginine hydroxamate treatment, which also inhibits translation (Kriel et al., 2012). It appears that any antibiotic or condition that induces (p)ppGpp production is able to kill (p)ppGpp^0 cells, while wild type cells are static in growth. Altogether, these findings suggest that susceptibility of (p)ppGpp cells to killing by CAM or other stresses is likely mediated by a common or partially over-lapping pathway.

CAM-induced lethality is likely related to GTP toxicity, where, in the absence of (p)ppGpp, high GTP levels kill cells through an unknown mechanism (Kriel et al., 2012). It is likely that (p)ppGpp acts as a sink to keep GTP levels low and maintain GTP levels at a particular threshold to allow for survival (Liu et al., 2015a). Over this threshold, high GTP levels start to kill cells, as seen in (p)ppGpp^0 cells treated with CAM (Figure 1A, 1B) or *ecgmk ecgpt* cells treated with CAM and GUO (Figure 3C), despite the presence of (p)ppGpp. This suggests that GTP is an important determinant of antibiotic tolerance.

How does maintaining GTP homeostasis protect cells from CAM-induced lethality? We have ruled out the effects of GTP-induced hyper-repression of the CodY regulon (Figure 4A, 4B) and altered growth rate on decreased CAM tolerance (Figure S5). We also examined whether (p)ppGpp^0 cells fail to inhibit translation or have altered ribosome profiles during CAM treatment (Figure 5A, 5C). Preliminary data indicate that (p)ppGpp^0 behaves similarly to wild type cells: they inhibit translation upon CAM treatment (likely because CAM inhibits the peptidyltransferase center and physically

prevents the ribosome from progressing) and their ribosome profiles align well, suggesting that (p)ppGpp^0 may not have problems in either process, though both of these experiments warrant repetition.

To obtain clues into the mechanisms of CAM-mediated killing, our next steps will involve determining the transcriptome of wild type and (p)ppGpp^0 cells during chloramphenicol treatment. In *B. subtilis*, GTP concentrations directly affect the transcription of promoters (Krásný and Gourse, 2004; Kriel et al., 2014), so it is possible that without (p)ppGpp, increased GTP levels adversely alter the transcriptome for (p)ppGpp^0 cells or transcripts required for CAM adaptation are not expressed. Previous work examining the global changes in gene expression in *B. subtilis* during treatment with translation inhibitors may provide insight into the types of changes we will observe (Lin et al., 2005). Lin *et al* showed that there were large changes in expression of genes encoding transport proteins, genes involved in protein synthesis, and genes involved in carbohydrate metabolism. Notably, they observed that during CAM treatment, transcription of *ysbAB*, which encodes antiholins and inhibits murein hydrolase activity, is upregulated, which might indicate that *B. subtilis* is actively preventing cell lysis from occurring (Lin et al., 2005). During arginine hydroxamate treatment, wild type and (p)ppGpp^0 cells have opposing *ysbAB* expression levels, indicating that (p)ppGpp might differentially regulate *ysbAB* transcription (Kriel et al., 2012). Examination of transcript levels for the associated murein hydrolase, encoded by *ywbH*, indicates that it is upregulated in (p)ppGpp^0 but not wild type cells. Further, preliminary data from the lab shows that (p)ppGpp^0 cells lyse after three hours of CAM treatment, since they can be stained with propidium iodide (data not shown). Perhaps erroneous regulation of *ysbAB*

and *ywbH* is leading to cell lysis and CAM-mediated cell death, but that remains to be verified, perhaps through overexpression of antiholins to compensate for decreased transcription. Decrease in cell envelope integrity has also been observed in *E. coli* (p)ppGpp^0 during treatment with a fatty acid synthesis inhibitor (Vadia et al., 2017).

(p)ppGpp induction is dependent on the bacterium's niche. Finally, a striking observation is that without (p)ppGpp, CAM turns from a bacteriostatic antibiotic into a bactericidal antibiotic (Figure 1A, 1B). This response is not limited to CAM, as our preliminary data with TET also shows cell death in (p)ppGpp^0 cells (Figure S1). The CAM and TET-mediated killing may be related to the fact that (p)ppGpp is induced during treatment with these antibiotics (Figure 1C to 1F) (Rhaese et al., 1975). Interestingly, several studies have shown that treatment of *E. coli* with CAM actually has opposite effects to that of *B. subtilis*, since CAM treatment causes (p)ppGpp levels to drop in *E. coli* (Cashel, 1969; Gallant and Margason, 1972). What could be the cause of this discrepancy? RelA in *B. subtilis* and *E. coli* are 39% identical and both produce (p)ppGpp during amino acid starvation (Liu et al., 2015b). However, the natural habitat of *B. subtilis* and *E. coli* are not the same, since *B. subtilis* primarily lives in the soil, whereas *E. coli* live in the intestinal tracts. The soil environment can be considered a chemical warzone, since many bacteria and fungi secrete natural products, such as antibiotics, to provide themselves with growth advantages and decrease fitness of surrounding microorganisms (Katz and Baltz, 2016). As such, it is possible that *B. subtilis* has evolved to produce (p)ppGpp in response to natural products like CAM and TET and promote its survival, but *E. coli* has not. The differential response to environmental signals, dependent on the bacterium's lifestyle, is also observed in

Caulobacter crescentus, a freshwater oligotroph, whose natural habitat are nutrient-poor bodies of water. Since it is accustomed to living in nutrient-poor environments, *C. crescentus* does not produce (p)ppGpp in response to amino acid starvation alone. Instead, it must sense drops in carbon or nitrogen and amino acids in order to synthesize (p)ppGpp (Boutte and Crosson, 2011, 2013). *B. subtilis* and *E. coli* may have different responses to CAM as a product of their natural habitat. The differences in (p)ppGpp induction between these two organisms warrant exploration, and can be achieved by simply treating *E. coli* (p)ppGpp^0 cells with CAM and SHX to examine if there are decreases in cell viability.

Literature Cited

Balaban, N.Q., Merrin, J., Chait, R., Kowalik, L., and Leibler, S. (2004). Bacterial persistence as a phenotypic switch. Science (80-.). *305*, 1622–1625.

Belitsky, B.R., and Sonenshein, A.L. (2013). Genome-wide identification of *Bacillus subtilis* CodY-binding sites at single-nucleotide resolution. Proc. Natl. Acad. Sci. U. S. A. *110*, 7026–7031.

Biazus, G., Schneider, C.Z., Palma, M.S., Basso, L. a., and Santos, D.S. (2009). Hypoxanthine-guanine phosphoribosyltransferase from Mycobacterium tuberculosis H37Rv: Cloning, expression, and biochemical characterization. Protein Expr. Purif. *66*, 185–190.

Bittner, A.N., Kriel, A., and Wang, J.D. (2014). Lowering GTP level increases survival of amino acid starvation but slows growth rate for *Bacillus subtilis* cells lacking (p)ppGpp. J. Bacteriol. *196*, 2067–2076.

Boutte, C.C., and Crosson, S. (2011). The complex logic of stringent response regulation in Caulobacter crescentus: starvation signalling in an oligotrophic environment. Mol. Microbiol. *80*, 695–714.

Boutte, C.C., and Crosson, S. (2013). Bacterial lifestyle shapes stringent response activation. Trends Microbiol. *21*, 174–180.

Brauner, A., Fridman, O., Gefen, O., and Balaban, N.Q. (2016). Distinguishing between resistance, tolerance and persistence to antibiotic treatment. Nat. Rev. Microbiol. *14*, 320–330.

Britton, R.A. (2009). Role of GTPases in bacterial ribosome assembly. Annu. Rev. Microbiol. *63*, 155–176.

Brown, A., Fernández, I.S., Gordiyenko, Y., and Ramakrishnan, V. (2016). Ribosome-dependent activation of stringent control. Nature *534*, 1–16.

Cashel, M. (1969). The control of ribonucleic acid synthesis in *Escherichia coli*. J. Biol. Chem *244*, 3133–3141.

Cohen, N.R., Lobritz, M.A., and Collins, J.J. (2013). Microbial persistence and the road to drug resistance. Cell Host Microbe *13*, 632–642.

Conlon, B.P., Rowe, S.E., Gandt, A.B., Nuxoll, A.S., Donegan, N.P., Zalis, E.A., Clair, G., Adkins, J.N., Cheung, A.L., and Lewis, K. (2016). Persister formation in *Staphylococcus aureus* is associated with ATP depletion. Nat. Microbiol. *1*, 1–7.

Corrigan, R.M., Bellows, L.E., Wood, A., and Gründling, A. (2016). ppGpp negatively impacts ribosome assembly affecting growth and antimicrobial tolerance in Gram-positive bacteria. Proc. Natl. Acad. Sci. 201522179.

Czarny, T.L., Perri, A.L., French, S., and Brown, E.D. (2014). Discovery of novel cell wall-active compounds using P_{ywaC}, a sensitive reporter of cell wall stress, in the model Gram-positive bacterium Bacillus subtilis. Antimicrob. Agents Chemother. *58*, 3261–3269.

Feng, B., Mandava, C.S., Guo, Q., Wang, J., Cao, W., Li, N., Zhang, Y., Zhang, Y., Wang, Z., Wu, J., et al. (2014). Structural and functional insights into the mode of

action of a universally conserved Obg GTPase. PLoS Biol. *12*, e1001866.

Fung, D.K., Barra, J.T., Schroeder, J.W., Ying, D., and Wang, J.D. (2018). Spontaneous and adaptive persistence by (p)ppGpp-mediated GTP antagonism in Gram-positive bacteria. Ed.

Gaca, Anthony O, Kajfasz, J.K., Miller, J.H., Liu, K., Wang, J.D., Abranches, J., and Lemos, A. (2013). Basal levels of (p)ppGpp in Enterococcus faecalis: The magic beyond the stringent response. MBio *4*, 1–10.

Gallant, J., and Margason, G. (1972). On the turnover of ppGpp in *Escherichia coli* . J. Biol. Chem. *247*, 6055–6058.

Geiger, T., and Wolz, C. (2014). Intersection of the stringent response and the CodY regulon in low GC Gram-positive bacteria. Int. J. Med. Microbiol. *304*, 150–155.

Geiger, T., Kästle, B., Gratani, F.L., Goerke, C., and Wolz, C. (2014). Two small (p)ppGpp synthases in *Staphylococcus aureus* mediate tolerance against cell envelope stress conditions. J. Bacteriol. *196*, 894–902.

Handke, L.D., Shivers, R.P., and Sonenshein, A.L. (2008). Interaction of *Bacillus subtilis* CodY with GTP. J. Bacteriol. *190*, 798–806.

Harwood, C.R., Cutting, S.M., and Chambert, R. (1990). Molecular biological methods for *Bacillus*.

Hogg, T., Mechold, U., Malke, H., Cashel, M., and Hilgenfeld, R. (2004). Conformational antagonism between opposing active sites in a bifunctional RelA/SpoT homolog modulates (p)ppGpp metabolism during the stringent response. Cell *117*, 57–68.

Janes, B.K., and Stibitz, S. (2006). Routine markerless gene replacement in *Bacillus anthracis*. Infect. Immun. *74*, 1949–1953.

Katz, L., and Baltz, R.H. (2016). Natural product discovery: past, present, and future. J. Ind. Microbiol. Biotechnol. *43*, 155–176.

Konkol, M.A., Blair, K.M., and Kearns, D.B. (2013). Plasmid-encoded ComI inhibits competence in the ancestral 3610 strain of *Bacillus subtilis*. J. Bacteriol. *195*, 4085–4093.

Kornberg, A., and Baker, T.A. (1992). DNA Replication. (New York, NY: W.H. Freeman and Co.).

Krásný, L., and Gourse, R. (2004). An alternative strategy for bacterial ribosome synthesis: *Bacillus subtilis* rRNA transcription regulation. EMBO J. *23*, 4473–4483.

Krásný, L., Tiserová, H., Jonák, J., Rejman, D., and Sanderová, H. (2008). The identity of the transcription +1 position is crucial for changes in gene expression in response to amino acid starvation in *Bacillus subtilis*. Mol. Microbiol. *69*, 42–54.

Kriel, A., Bittner, A.N., Kim, S.H., Liu, K., Tehranchi, A.K., Zou, W.Y., Rendon, S., Chen, R., Tu, B.P., and Wang, J.D. (2012). Direct regulation of GTP homeostasis by (p)ppGpp: A critical component of viability and stress resistance. Mol. Cell *48*, 231–241.

Kriel, A., Brinsmade, S.R., Tse, J.L., Tehranchi, A.K., Bittner, A.N., Sonenshein, A.L., and Wang, J.D. (2014). GTP dysregulation in *Bacillus subtilis* cells lacking

(p)ppGpp results in phenotypic amino acid auxotrophy and failure to adapt to nutrient downshift and regulate biosynthesis genes. J. Bacteriol. *196*, 189–201.

Lin, J.T., Connelly, M.B., Amolo, C., Otani, S., and Yaver, D.S. (2005). Global transcriptional response of *Bacillus subtilis* to treatment with subinhibitory concentrations of antibiotics that inhibit protein synthesis. Antimicrob. Agents Chemother. *49*, 1915–1926.

Liu, K., Myers, A.R., Pisithkul, T., Claas, K.R., Satyshur, K.A., Amador-Noguez, D., Keck, J.L., and Wang, J.D. (2015a). Molecular mechanism and evolution of guanylate kinase regulation by (p)ppGpp. Mol. Cell *57*, 735–749.

Liu, K., Bittner, A.N., and Wang, J.D. (2015b). Diversity in (p)ppGpp metabolism and effectors. Curr. Opin. Microbiol. *24*, 72–79.

Maisonneuve, E., and Gerdes, K. (2014). Molecular Mechanisms Underlying Bacterial Persisters. Cell *157*, 539–548.

Maisonneuve, E., Castro-Camargo, M., and Gerdes, K. (2013). (p)ppGpp controls bacterial persistence by stochastic induction of toxin-antitoxin activity. Cell *154*, 1140–1150.

Majerczyk, C.D., Dunman, P.M., Luong, T.T., Lee, C.Y., Sadykov, M.R., Somerville, G.A., Bodi, K., and Sonenshein, A.L. (2010). Direct targets of CodY in *Staphylococcus aureus*. J. Bacteriol. *192*, 2861–2877.

Nanamiya, H., Kasai, K., Nozawa, A., Yun, C.-S., Narisawa, T., Murakami, K., Natori, Y., Kawamura, F., and Tozawa, Y. (2008). Identification and functional analysis of novel (p)ppGpp synthetase genes in *Bacillus subtilis*. Mol. Microbiol. *67*, 291–304.

Nguyen, D., Joshi-Datar, A., Lepine, F., Bauerle, E., Olakanmi, O., Beer, K., McKay, G., Siehnel, R., Schafhauser, J., Wang, Y., et al. (2011). Active starvation responses mediate antibiotic tolerance in biofilms and nutrient-limited bacteria. Science *334*, 982–986.

Nomura, Y., Takabayashi, T., Kuroda, H., Yukawa, Y., Sattasuk, K., Akita, M., Nozawa, A., and Tozawa, Y. (2012). ppGpp inhibits peptide elongation cycle of chloroplast translation system in vitro. Plant Mol. Biol. *78*, 185–196.

Pankey, G.A., and Sabath, L.D. (2004). Clinical relevance of bacteriostatic versus bactericidal mechanisms of action in the treatment of Gram-positive bacterial infections. Clin. Infect. Dis. *38*, 864–870.

Ratnayake-Lecamwasam, M., Serror, P., Wong, K.W., and Sonenshein, A.L. (2001). *Bacillus subtilis* CodY represses early-stationary-phase genes by sensing GTP levels. Genes Dev. *15*, 1093–1103.

Rhaese, H.J., Dichtelmüller, H., and Grade, R. (1975). Accumulation of guanosine tetraphosphate and pentaphosphate in response to inhibition of protein synthesis in Bacillus subtilis. Eur. J. Biochem. *56*, 385–392.

Rich, K.A., Burkett, C., and Webster, P. (2003). Cytoplasmic bacteria can be targets for autophagy. Cell. Microbiol. *5*, 455–468.

Richardson, A.R., Somerville, G.A., and Sonenshein, A.L. (2015). Regulating the

intersection of metabolism and pathogenesis in Gram-positive bacteria. Microbiol. Spectr. *3*, 1–27.

Rojas, A.M., Ehrenberg, M., Andersson, S.G.E., and Kurland, C.G. (1984). ppGpp inhibition of elongation factors Tu, G and Ts during polypeptide synthesis. Mol. Gen. Genet. *197*, 36–45.

Seo, H.-S., Abedin, S., Kamp, D., Wilson, D.N., Nierhaus, K.H., and Cooperman, B.S. (2006). EF-G-dependent GTPase on the ribosome. Conformational change and fusidic acid inhibition. Biochemistry *45*, 2504–2514.

Srivatsan, A., Han, Y., Peng, J., Tehranchi, A.K., Gibbs, R., Wang, J.D., and Chen, R. (2008). High-precision, whole-genome sequencing of laboratory strains facilitates genetic studies. PLoS Genet. *4*, 1–14.

Steinchen, W., Schuhmacher, J.S., Altegoer, F., Fage, C.D., Srinivasan, V., Linne, U., Marahiel, M.A., and Bange, G. (2015). Catalytic mechanism and allosteric regulation of an oligomeric (p)ppGpp synthetase by an alarmone. Proc. Natl. Acad. Sci. U. S. A. *112*, 13348–13353.

Steitz, T. (2008). A structural understanding of the dynamic ribosome machine. Nat. Rev. *9*, 242–253.

Vadia, S., Tse, J.L., Lucena, R., Yang, Z., Kellogg, D.R., Wang, J.D., and Levin, P.A. (2017). Fatty acid availability sets cell envelope capacity and dictates microbial cell size. Curr. Biol. *27*, 1757–1767.

Vasantha, N., and Freese, E. (1980). Enzyme changes during *Bacillus subtilis* sporulation caused by deprivation of guanine nucleotides. J. Bacteriol. *144*, 1119–1125.

Wang, J.D., Sanders, G.M., and Grossman, A.D. (2007). Nutritional control of elongation of DNA replication by (p)ppGpp. Cell *128*, 865–875.

Table 5. Strains used in study.

Strain	JDW Strain	Genotype	Reference
NCIB 3610 *comI*^{Q12L}	JDW2144	*comI*^{Q12L}	Konkol *et al*., 2014
SMY		Prototroph	Schaeffer *et al*., 1965
YB886		*trpC2 metB10 xin-1 SPβ*$^{-}$	Yasbin *et al*., 1980
(p)ppGpp^{0}	JDW2231	NCIB 3610 *comI*^{Q12L} Δ*yjbM* Δ*ywaC relA*::*mls*	This work
(p)ppGpp^{0}	JDW1965	SMY Δ*yjbM* Δ*ywaC relA*::*mls*	Kriel *et al*., 2012
relA^{D264G}	JDW1445	SMY *relA*^{D264G}	Kriel *et al*., 2012
Δ*ywaC* Δ*yjbM*	JDW1430	SMY Δ*ywaC* Δ*yjbM*	Kriel *et al*., 2012
(p)ppGpp^{0}	JDW755	YB886 Δ*yjbM* Δ*ywaC*::*kan* *relA*::*mls*	Kriel *et al*., 2012
(p)ppGpp^{0} *gmk*^{Q110R}	JDW2528	NCIB 3610 *comI*^{Q12L} Δ*yjbM* Δ*ywaC relA*::*mls gmk*^{Q110R}	Fung *et al*.
(p)ppGpp^{0} *guaB*$_{1}$	JDW1920	YB886 Δ*yjbM* Δ*ywaC*::*kan* Δ*relA*::*mls guaB*(-65T>C)	Kriel *et al*, 2012
(p)ppGpp^{0} *guaB*$_{2}$	JDW1922	YB886 Δ*yjbM* Δ*ywaC*::*kan* Δ*relA*::*mls* guaB(218A>G)	Kriel *et al*., 2012
(p)ppGpp^{0} *guaB*$_{3}$	JDW1925	YB886 Δ*yjbM* Δ*ywaC*::*kan* Δ*relA*::*mls* guaB(361T>C)	Kriel *et al*., 2012
(p)ppGpp^{0} *guaB*$_{4}$	JDW1928	YB886 Δ*yjbM* Δ*ywaC*::*kan* Δ*relA*::*mls guaB*(416C>T)	Kriel *et al*, 2012
(p)ppGpp^{0} *guaB*$_{5}$	JDW1929	YB886 Δ*yjbM* Δ*ywaC*::*kan* Δ*relA*::*mls* guaB(761A>G)	Kriel *et al*., 2012
(p)ppGpp^{0} *guaB*$_{6}$	JDW1932	YB886 Δ*yjbM* Δ*ywaC*::*kan* Δ*relA*::*mls* guaB(857C>T)	Kriel *et al*., 2012
(p)ppGpp^{0} *guaB*$_{7}$	JDW1933	YB886 Δ*yjbM* Δ*ywaC*::*kan* Δ*relA*::*mls* guaB(943G>A)	Kriel *et al*, 2012
(p)ppGpp^{0} *guaB*$_{8}$	JDW1935	YB886 Δ*yjbM* Δ*ywaC*::*kan* Δ*relA*::*mls* guaB(1276G>A)	Kriel *et al*., 2012
(p)ppGpp^{0} *guaB*$_{9}$	JDW1936	YB886 Δ*yjbM* Δ*ywaC*::*kan* Δ*relA*::*mls* guaB(1330G>A)	Kriel *et al*., 2012
(p)ppGpp^{0} *guaB*$_{10}$	JDW1937	YB886 Δ*yjbM* Δ*ywaC*::*kan* Δ*relA*::*mls* guaB(1448C>T)	Kriel *et al*., 2012
(p)ppGpp^{0} *gmk*^{G83S}	jDW1841	YB886 Δ*yjbM ywaC*::*kan* *relA*::*mls gmk*(G83S)	This work
(p)ppGpp^{0} *pyk*^{G318E}	JDW1857	YB886 Δ*yjbM ywaC*::*kan* *relA*::*mls pyk*(G318E)	This work
(p)ppGpp^{0} *hprT* A insert @ 14	JDW1850	YB886 Δ*yjbM ywaC*::*kan* *relA*::*mls hprT* (A insertion @ 14)	This work
ecgmk	JDW2108	SMY *bsugmk*::*ecgmk*	Liu *et al*., 2015

ecgmk ecgpt	JDW2121	SMY bsugmk::ecgmk *amyE*::$P_{hyperspac}$-*ecgpt*	This work
guaB^{down}	JDW1397	YB886 *guaB*::pJW305 (*guaB*'-*lacZ erm* P_{spac}-*guaB*)	Kriel *et al*., 2012
(p)ppGpp^0 Δ*codY*	JDW2222	SMY Δ*yjbM* Δ*ywaC* Δ*codY* *relA*::*mls*	Kriel *et al*., 2014, also this work

Table 6. Plasmids used in study.

Plasmid Number	Genotype	Reference
pEX44	*spoVG-lacZ amp cat*	(Comella and Grossman, 2005)
pJW299	pEX44/I-*Sce*I site *amp cat*	Kriel *et al*., 2012
pJW300	pJW239/Δ*yjbM I-Sce*I *site amp cat*	Kriel *et al*., 2012
pJW305	*guaB'-lacZ erm* P_{spac}-*guaB*	Kriel *et al*., 2012
pJW306	pJW299/Δ*ywaC I-SceI site amp cat*	Kriel *et al*., 2012
pJW371	pJW299/ *relA*^{D264G}	Kriel *et al*., 2012
pJW418	pJW299/Δ*codY I-SceI site amp cat*	Kriel *et al*., 2012
pJW468	pDR90/$P_{hyperspac}$-*ecogpt*	This work
pSS4332	*oriU* P_{amy}-I-*Sce*I *kan*	Jane and Stibitz, 2006

Supplementary Figures

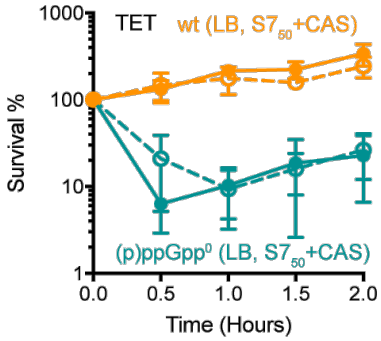

Figure S1. (p)ppGpp protects cells from a bacteriostatic to bactericidal switch during tetracycline treatment, regardless of media (LB vs $S7_{50}$+CAS). Exponentially growing *B. subtilis* SMY wild type and (p)ppGpp^0 were treated with 0.5 µg/mL TET (0.06X MIC) (Fung et al., 2018) for up to two hours. Percent survival was determined by dividing the number of tolerant CFU/mL/OD at each time point by the number of CFU/mL/OD at T=0 and converted to a percentage. Values are N=3 $\pm$ SD.

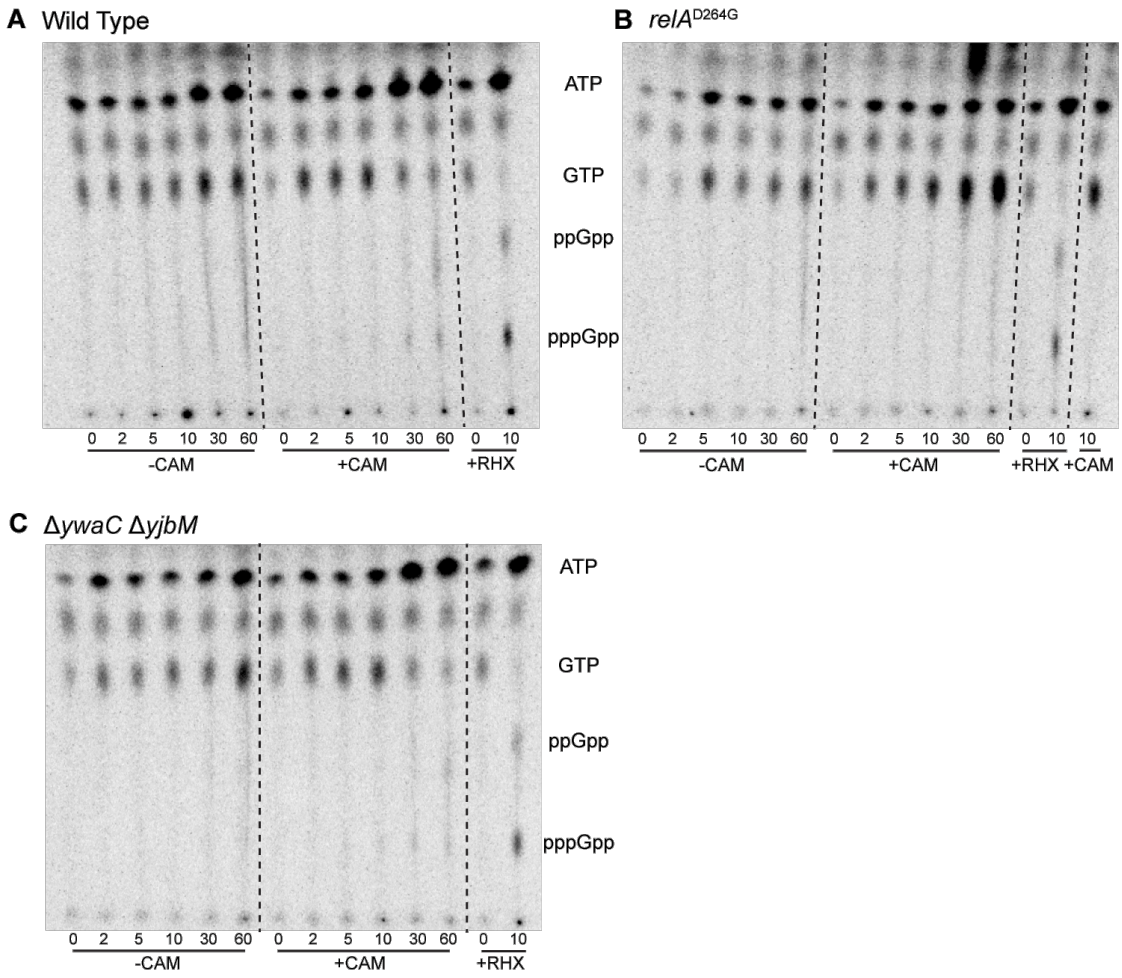

Figure S2. A functional RelA synthetase domain is required to produce detectable (p)ppGpp during CAM treatment. *B. subtilis* SMY A. wild type, B. *relA*^{D264G}, and C. Δ*ywaC* Δ*yjbM* were radiolabeled with ^{32}P-orthophosphate at OD_{600} = ~0.05 and were treated with and without 12 µg/mL CAM once OD_{600} reached 0.15-0.2. Wild type cells were also treated with 0.5 mg/mL arginine hydroxamate as a control. Samples were collected between 0-60 minutes and spotted onto thin layer chromatography plates.

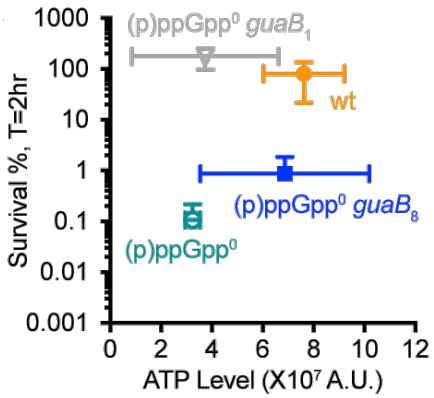

Figure S3. CAM tolerance of (p)ppGpp^0 *guaB* suppressors is not correlated with ATP levels. Correlation between survival of (p)ppGpp^0 *guaB* suppressors after 2 hours of CAM treatment and ATP levels after 20 minutes of CAM treatment.

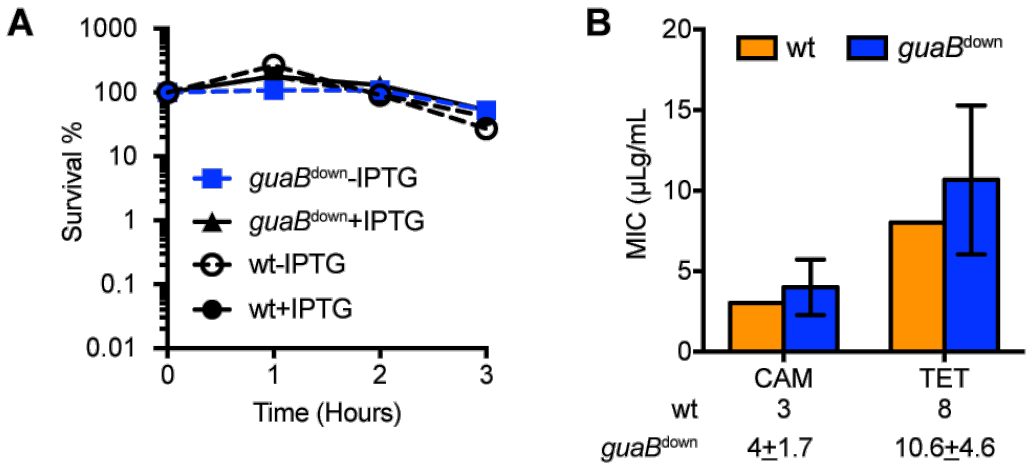

Figure S4. Depletion of *guaB* does not promote antibiotic hypertolerance for chloramphenicol and does not affect resistance. A. Exponentially growing YB886 and an IPTG-inducible *guaB* strain (YB886 *guaB*::pJW305 (*guaB*'-*lacZ erm* P_{spac}-*guaB*)) (Kriel et al., 2012) were grown in the presence or absence of IPTG and treated with 12 µg/mL CAM. Expression of *B. subtilis guaB* was induced using 0.5 mM IPTG. Cell survival was determined as a ratio of number of CFU at a given time point to CFU at T=0. Cell samples were obtained every hour for three hours. Experiments were done at N=1. B. To determine whether *guaB*^{down} is more resistant to antibiotics than the wild type, MIC assays for *guaB*^{down} and wild type strains were done for CAM and TET. *guaB*^{down} was grown in the absence of IPTG. Values are N=3 $\pm$ SD, whereas wild type experiments were done N=1, but coincide well with previously determined MICs (Fung et al., 2018).

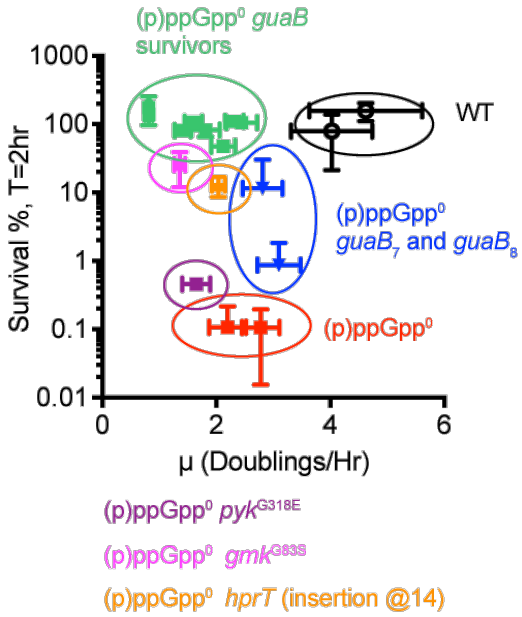

Figure S5. CAM tolerance is not correlated with growth rate. Growth rate measurements of *B. subtilis* YB886 strains were determined using a Synergy 2 plate reader as described (Bittner et al., 2014), with at least six replicates. Growth rate was correlated with 12 μg/mL CAM tolerance after two hours.

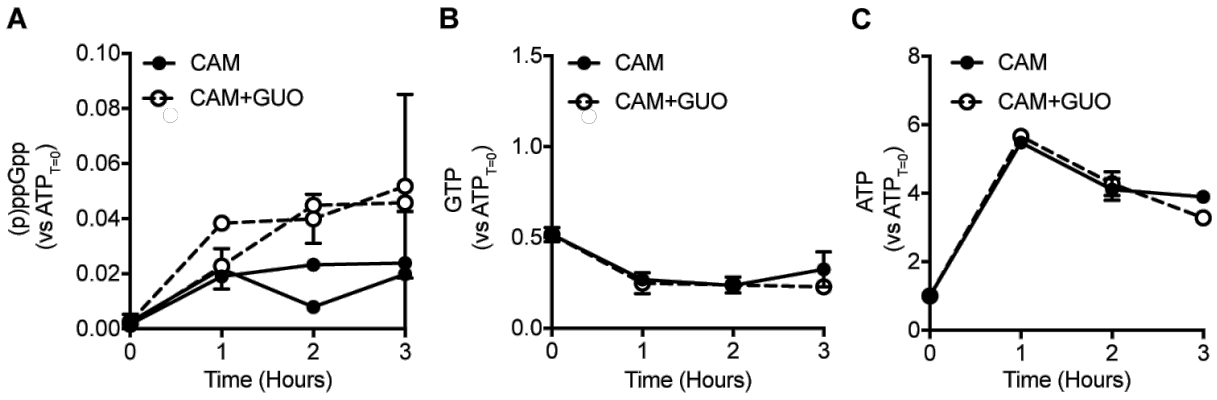

Figure S6. Nucleotide levels in *ecgmk* do not significantly change under CAM and CAM+GUO treatment. ^{32}P-labeled orthophosphate was incorporated into early-exponential phase *ecgmk* cells. Cells were treated with 12 µg/mL CAM or 12 µg/mL CAM and 1 mM GUO when mid-exponential phase was reached. At each time point, nucleotides were extracted and visualized using TLC plates. A. (p)ppGpp, B. GTP, and C. ATP densities were calculated, normalized to ATP levels at T=0, and plotted as shown. Experiments were done at N=2 and SD values are plotted. Compare to Figure 2D-2F.

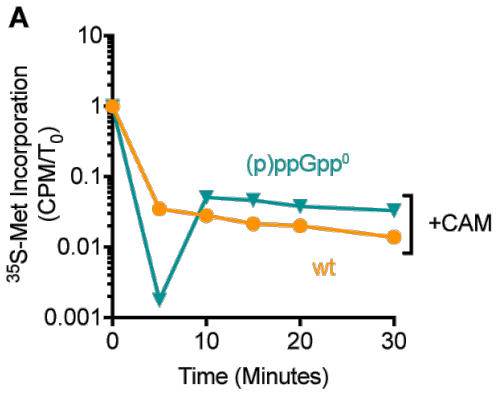

Figure S7. Loss of (p)ppGpp does not appear to affect translation stalling. Exponential phase *B. subtilis* 3610 *comI*^{Q12L} wild type and (p)ppGpp^0 were treated with and without 100 µg/mL CAM and at regular intervals and pulse-labeled with ^{35}S-methionine for two minutes. The labeling was stopped with addition of 20% TCA. The labeled proteins were extracted onto filters with 5% TCA and counts per minute (CPM) were determined using a liquid scintillation counter. Values are represented as the ratio of CPM at a certain time point to CPM at T=0. Values are N=1.

Chapter 5: Summary and Future Directions

In this thesis, I have demonstrated the importance of the alarmone (p)ppGpp in promoting stress survival. Decades of research have established the importance of (p)ppGpp as a regulator of transcription during the stringent response through direct interaction with the *E. coli* RNAP (Ross et al., 2013, 2016). Yet, these binding sites are not present in *B. subtilis* RNAP (Ross et al., 2013, 2016; Vrentas et al., 2008) and (p)ppGpp instead regulates stable RNA transcription indirectly by manipulating GTP levels (Krásný and Gourse, 2004). Our lab previously discovered that during amino acid starvation, (p)ppGpp binds to GTP biosynthesis enzymes, instead of RNAP, to alter the transcriptome and more importantly, maintain GTP homeostasis (Kriel et al., 2012, 2014). With this work, we have expanded upon the protective role of (p)ppGpp. In addition to modulating the *Bacillus subtilis* transcriptome, I have shown that (p)ppGpp controls the formation of spontaneous and antibiotic-induced persisters, and protects cells from bacteriostatic antibiotics. More importantly, I have demonstrated the major contribution of survival is through regulation of intracellular GTP level.

Control of GTP levels by (p)ppGpp dictates stress survival

A theme that encompasses my work in this thesis is that GTP, antagonized by the alarmone (p)ppGpp, is the primary determinant of stress survival. Through spontaneous production or during treatment with arginine hydroxamate (Kriel et al., 2012), nutrient downshift (Chapter 2, Figure. 2) (Kriel et al., 2012), cell wall-targeting antibiotics (Chapter 3, Figure. 6), bacteriostatic antibiotics (Chapter 4, Figure. 2, 3), and ATP synthesis inhibitors (Chapter 3, Figure. 2, S2), (p)ppGpp is produced by wild type *B. subtilis* to protect them against these assaults. (p)ppGpp production is always

accompanied by GTP decrease. Our discovery that (p)ppGpp inhibits GTP biosynthesis enzymes allows us to decouple the regulation using a strain that cannot produce (p)ppGpp [(p)ppGpp^0] (Kriel et al., 2012). Decoupling (p)ppGpp and GTP levels showed us that lowering GTP is indeed the key for survival. Decreasing GTP levels, through generation of suppressors or depletion of *guaB*, allowed cells to survive nutrient downshift and antibiotics similar to cells with (p)ppGpp (Chapter 3, Figure. 2; Chapter 4, Figure 2) (Bittner et al., 2014; Kriel et al., 2012).

Based on our observations, low GTP levels is sufficient to restore (p)ppGpp^0 phenotypes to wild type levels. Both (p)ppGpp and GTP can control cellular processes in *B. subtilis*, such as replication elongation ((p)ppGpp inhibits primase, GTP is a substrate for RNA primers) (Rymer et al., 2012), transcription of stable RNAs and alter the transcriptome through CodY-dependent and CodY-independent mechanisms (GTP is an iNTP for stable RNA synthesis and CodY is activated with GTP levels at the mM level) (Krásný and Gourse, 2004; Sonenshein, 2005) (Chapter 2), translation and ribosome assembly ((p)ppGpp inhibits the GTPases, GTP is a substrate for GTPases and must be hydrolyzed for the GTPases to function) (Cherfils and Zeghouf, 2013; Corrigan et al., 2016; Kanjee et al., 2012; Rojas et al., 1984). Although (p)ppGpp is dispensable, our work examining the single-cell growth rates for wild type and (p)ppGpp^0 *gmk*^{Q110R} provides insights into the advantages of (p)ppGpp (Chapter 3, Figure. 4, S4). (p)ppGpp converts an environmental cue into a signal for the cell to rapidly shutdown cellular processes in a switch-like mechanism. If the entire population can sense the stress, then the shutdown affects the entire population (RHX pre-induction promotes persister formation, at P_{ilvB}-GTP^{on} growth rate rapidly drops). On the

other hand, the growth rates of (p)ppGpp^0 *gmk*^{Q110R} are dispersed and the P_{ilvB}-GTP^{on} signal and growth rate behaves linearly, rather than as a switch. This altered behavior indicates that (p)ppGpp^0 *gmk*^{Q110R} cells are not as efficient at shutting down growth as wild type cells, which results in fitness disadvantages and may explain (p)ppGpp^0 *gmk*^{Q110R} cell death at T=3 hr during chloramphenicol treatment (Chapter 4, Figure. 2). Thus, GTP levels dictate stress survival and (p)ppGpp ensures rapid adaptation to a changing environment.

Persisters as a reservoir for antibiotic resistance

Our work showed that (p)ppGpp-GTP antagonism promoted the formation of persisters, a subpopulation of antibiotic-tolerant bacteria. Although not much is known about how these persisters resuscitate or escape persistence, we know that persisters can regrow once the antibiotic is removed or drops to sub-MIC level (Chapter 3, Figure. 6) (Cohen et al., 2013) and this is a source of bacteria for chronic infections. Another problem is that persisters can act as a reservoir for the emergence of antibiotic resistant bacteria. A recent study examined the role of persistence in acquisition of resistance (Levin-Reisman et al., 2017). In this work, *E. coli* was exposed to several cycles of treatment with high concentrations of ampicillin for several hours, followed by antibiotic removal, and recovery in media with sub-MIC ampicillin. Using this method, they isolated several mutants (*metG*, encoding a methionyl-tRNA synthetase; *prsA*, encoding a ribose-phosphate pyrophosphokinase) that promoted persistence by extending lag time (Fridman et al., 2014; Levin-Reisman et al., 2017). Continued exposure of these populations eventually gave rise to resistant mutants with insertions in the promoter of

ampC, encoding a β-lactamase, to promote expression. They argue that resistance was a second mutational event that occurred after establishing persistence. In support of this, all resistant mutants also harbor mutations that allow persistence. Further, through various computational models, they observe that persistence helps to maintain resistance mutations in a population (Levin-Reisman et al., 2017).

Levin-Reisman *et al*. suggest that persisters are derived from various sources (*metG*, *prsA*), but they all gave rise to insertions in the *ampC* promoter (that enhanced its expression) when cells were treated with ampicillin. For this reason, they suggest that these persistence and resistance factors may have co-evolved. Similarly, the expression of the fumarate reductase operon and *ampC* together enhanced persister formation during norfloxacin treatment (multidrug tolerance), better than *ampC* alone, suggesting that the two factors may have co-evolved to promote persistence (Kim et al., 2016). Our work shows that (p)ppGpp increases persistence through spontaneous and induced persister formation (Chapter 3). Using a similar experimental design as Levin-Reisman *et al*., it may be possible to isolate resistant mutants after successive rounds of antibiotic treatment and perhaps determine the identity of mutated genes that may have co-evolved with (p)ppGpp-mediated persistence. (Levin-Reisman et al., 2017; Siu et al., 2003). It would also be interesting to determine the mechanisms that allow the bacteria to become resistant (e.g. what mutagenic pathways are activated and fidelity pathways are deactivated in order for the resistance mutation to arise and whether these pathways are antibiotic-dependent).

Future Directions

Determining the mechanism of (p)ppGpp-GTP protection against bactericidal and bacteriostatic antibiotics

From this thesis and our previous work, we have highlighted the importance of (p)ppGpp inhibition of GTP levels on stress survival. We have shown that (p)ppGpp regulation of GTP levels maintains GTP homeostasis in the cell, allows for survival of nutrient downshift, and protection against bactericidal and bacteriostatic antibiotics. During each of these stresses, the ability to decrease GTP levels in (p)ppGpp^0 cells compensates for the lack of (p)ppGpp. Further, abolishing the regulation of GTP levels by (p)ppGpp in wild type cells shows that we can potentiate chloramphenicol killing if we can increase GTP levels in cells. Clearly, GTP is a main regulator of stress survival in *B. subtilis*. How do decreased GTP levels promote stress survival? We have described the role of GTP during transcription: decreases in GTP levels decrease ribosomal RNA transcription and deactivates the repressor CodY, thereby activating the CodY regulon (Krásný and Gourse, 2004; Ratnayake-Lecamwasam et al., 2001). With high GTP levels and CodY hyperrepression, there is an apparent amino acid auxotrophy leading to the inability to grow in minimal media (Chapter 2), but treatment of (p)ppGpp^0 Δ*codY* with antibiotics does not drastically increase survival.

Previous work has shown that (p)ppGpp binds to and inhibits *E. coli* translation factors, such as EF-Tu, EF-G, and RF3 (Kanjee et al., 2012; Rojas et al., 1984). Several ribosome assembly GTPases, such as RsgA, RbgA, and Era, were also identified as (p)ppGpp targets in *S. aureus* (Britton, 2009; Corrigan et al., 2016). In addition to being inhibited by (p)ppGpp, GTPase function is controlled by its GTP hydrolysis activity. In

the absence of (p)ppGpp, GTP levels are high so it is possible that (p)ppGpp^0 cells still have functional GTPases during nutrient downshift or treatment with (p)ppGpp-inducing antibiotic. Preliminary data from my thesis work in Chapter 4, showed that there were no differences in translation rate and ribosome assembly for wild type cells and (p)ppGpp^0 cells with dysregulated GTP levels, though the experiments should be repeated to verify the results (Figure 5). It is also possible that small changes in translation rate and ribosome assembly cannot be detected using techniques that examine changes in the entire population but rather require single cell techniques. Another possibility is that the survivors of CAM treatment are the cells with normal ribosomes and that is what is reflected in the translation assay and ribosome profiles. To discern that possibility, FACS can be used to sort out the (p)ppGpp^0 cells with different GTP levels (which correlate with CAM survival) and ribosome profiles can be obtained for each fraction.

It is still possible that absence of (p)ppGpp and its ability to decrease GTP is affecting transcription of genes necessary for survival. As demonstrated in Chapter 2, full supplementation of auxotrophic amino acids to (p)ppGpp^0 cells was insufficient for survival of nutrient downshift, indicating that lack of (p)ppGpp and/or inability to lower GTP is still problematic for the cell. Many of these problems are ameliorated by decreasing GTP. Thus, future work will include using RNA-Seq to determine how the transcriptome is altered with and without (p)ppGpp during nutrient downshift and antibiotic treatment. With RNA-Seq, it is possible to discover new transcripts, including regulatory RNAs, that are upregulated or downregulated due to (p)ppGpp production/GTP downregulation. A major effect of (p)ppGpp is decreased growth rate, so it is possible that many of the downregulated transcripts will be related to growth:

enzymes involved in metabolizing glucose or other energy sources, building the cell wall, cell division, etc. (Durfee et al., 2008; Traxler et al., 2008; Yamaguchi et al., 2015). It is also possible that defense and/or repair mechanisms are upregulated in wild type cells but not in (p)ppGpp^0 cells, hence the decrease in viability during stress. This was demonstrated in *E. coli*, where (p)ppGpp^0 cells could not activate the RpoS regulon (Durfee et al., 2008; Traxler et al., 2008) or Δ*dksA* cells have higher transcription of SOS response genes, indicating that these cells have a higher DNA damage response (Tehranchi et al., 2010). Since (p)ppGpp has pleiotropic effects on the cell, it is likely that more than one mechanism is involved in promoting survival.

Determining the mechanism of (p)ppGpp production during inhibition of ATP biosynthesis

Our work in Chapter 3 showed that inhibition of ATP biosynthesis using inhibitors such as carbonyl cyanide *m*-chlorophenyl hydrazone (CCCP), arsenate, and sodium azide, induced (p)ppGpp production and decreased GTP, but had minimal changes in ATP levels. We also showed that in (p)ppGpp^0 cells, ATP levels are decreased during treatment with CCCP and arsenate, which coincides with increased antibiotic survival. These results indicate that during treatment with ATP biosynthesis inhibitors, cells survive antibiotic treatments primarily by producing (p)ppGpp and decreasing GTP, while maintaining ATP levels, whereas cells without (p)ppGpp rely solely on decreased ATP. These data highlight the fact that multiple mechanisms may be in play to protect cells from antibiotics, (p)ppGpp production, decreased GTP, and decreased ATP.

This work reveals that inhibition of ATP promotes (p)ppGpp synthesis, a novel mechanism of (p)ppGpp induction. Preliminary microscopy data from Appendix I shows that (p)ppGpp is produced primarily through RelA, the ribosome-associated (p)ppGpp synthetase. Since RelA senses uncharged tRNAs at the ribosome, it is possible that ATP depletion results in uncharged tRNAs, since ATP is required for aminoacylation of tRNAs (Nelson and Cox, 2012). Initial attempts to examine tRNA charging states in cells with and without CCCP treatment have yielded inconclusive results so further troubleshooting will be required. In addition, we generated a mutated RelA that cannot detect the charging state of a tRNA, based off of residues that likely interact with the tRNA aminoacylation site (3'-OH in the terminal adenosine) found in *E. coli* (Brown et al., 2016). Future work using this strain will not only address whether the ability to sense tRNA charging affects (p)ppGpp production during CCCP treatment, but also allow us to examine whether uncharged tRNAs are required for 1) stochastic (p)ppGpp production from RelA (Chapter 3), 2) chloramphenicol-mediated production of (p)ppGpp, and many other (p)ppGpp-inducing conditions.

Another possibility is that ATP-dependent transporters are inactivated during treatment with CCCP or the other ATP depleting drugs, leading to starvation and RelA activation. From our previous work, arginine hydroxamate treatment, which induces (p)ppGpp and decreases GTP, led to increased transcription of *appA*, *appB*, and *appF*, all of which encode ATP-dependent oligopeptide transporters (Kriel et al., 2012). Decreased ATP will render these, and other ATP-dependent transporters inactive, provided that these transporters are present in the membrane (Koide and Hoch, 1994). These proteins transport a variety of compounds across the membrane, including

peptides and osmolytes, the latter of which provides protection against high-osmolarity environments (Hoffmann and Bremer, 2017; Holtmann and Bremer, 2004). It is possible that shutdown of these transporters renders cells incapable of transporting amino acid precursors, thereby leading to starvation.

Finally, decreasing ATP by collapsing the proton gradient means that *B. subtilis* cannot rely on the electron transport chain for generating ATP but instead generates ATP solely from glycolysis. ATP decrease can also affect the phosphotransferase system (PTS), the system that transports and phosphorylates glucose or other carbohydrates so that it is maintained in the cell (Fouet et al., 1989), since one of the enzymes, HPr, can be phosphorylated by an ATP-dependent kinase at serine 46 in *S. pyogenes* and *B. subtilis* (Deutscher and Saier, 1983; Fouet et al., 1989; Reizer et al., 1984). If ATP drops low enough or that Hpr is not phosphorylated, then it is possible that the cells cannot bring in glucose, used for *de novo* amino acid synthesis and become starved (Nelson and Cox, 2012), and instead must rely on shuttling in other carbon sources (Reizer et al., 1998). This can be tested by determining whether there are defects in glucose transport or tracking the fate of ^{13}C-labeled glucose in CCCP-treated cells.

Concluding Remarks

In the past several years, we have made great strides in understanding the role of (p)ppGpp in protecting Gram-positive bacteria against nutrient downshift and antibiotics. There is still a lot we do not know, including the binding targets of (p)ppGpp, how (p)ppGpp dynamics in the cell that allow for resuscitation from a dormant state, and

much more. Needless to say, the unexplored territory will lead to many more interesting discoveries in the future.

Literature Cited

Bittner, A.N., Kriel, A., and Wang, J.D. (2014). Lowering GTP level increases survival of amino acid starvation but slows growth rate for *Bacillus subtilis* cells lacking (p)ppGpp. J. Bacteriol. *196*, 2067–2076.

Britton, R.A. (2009). Role of GTPases in bacterial ribosome assembly. Annu. Rev. Microbiol. *63*, 155–176.

Brown, A., Fernández, I.S., Gordiyenko, Y., and Ramakrishnan, V. (2016). Ribosome-dependent activation of stringent control. Nature *534*, 1–16.

Cherfils, J., and Zeghouf, M. (2013). Regulation of small GTPases by GEFs, GAPs, and GDIs. Physiol. Rev. *93*, 269–309.

Cohen, N.R., Lobritz, M.A., and Collins, J.J. (2013). Microbial persistence and the road to drug resistance. Cell Host Microbe *13*, 632–642.

Corrigan, R.M., Bellows, L.E., Wood, A., and Gründling, A. (2016). ppGpp negatively impacts ribosome assembly affecting growth and antimicrobial tolerance in Gram-positive bacteria. Proc. Natl. Acad. Sci. 201522179.

Deutscher, J., and Saier, M.H. (1983). ATP-dependent protein kinase-catalyzed phosphorylation of a seryl residue in HPr, a phosphate carrier protein of the phosphotransferase system in *Streptococcus pyogenes*. Proc. Natl. Acad. Sci. *80*, 6790–6794.

Durfee, T., Hansen, A., Zhi, H., Blattner, F.R., and Jin, D.J. (2008). Transcription profiling of the stringent response in Escherichia coli. J. Bacteriol. *190*, 1084–1096.

Fouet, A., Arnaud, M., Klier, A., and Rapoport, G. (1989). Genetics of the phosphotransferase system of *Bacillus subtilis*. FEMS Microbiol. Rev. *63*, 175–182.

Fridman, O., Goldberg, A., Ronin, I., Shoresh, N., and Balaban, N.Q. (2014). Optimization of lag time underlies antibiotic tolerance in evolved bacterial populations. Nature *513*, 418–421.

Hoffmann, T., and Bremer, E. (2017). Guardians in a stressful world: The Opu family of compatible solute transporters from *Bacillus subtilis*. Biol. Chem. *398*, 193–214.

Holtmann, G., and Bremer, E. (2004). Thermoprotection of *Bacillus subtilis* by exogenously provided glycine betaine and structurally related compatible solutes: Involvement of Opu transporters. J. Bacteriol. *186*, 1683–1693.

Kanjee, U., Ogata, K., and Houry, W.A. (2012). Direct binding targets of the stringent response alarmone (p)ppGpp. Mol. Microbiol. *85*, 1029–1043.

Kim, J., Cho, D., Heo, P., Jung, S., Park, M., Oh, E., Sung, J., and Kim, P. (2016). Fumarate-mediated persistence of Escherichia coli against antibiotics. Antimicrob. Agents Chemother. *60*, 2232–2240.

Koide, A., and Hoch, J.A. (1994). Identification of a second oligopeptide transport system in *Bacillus subtilis* and determination of its role in sporulation. Mol. Microbiol. *13*, 417–426.

Krásný, L., and Gourse, R. (2004). An alternative strategy for bacterial ribosome synthesis: *Bacillus subtilis* rRNA transcription regulation. EMBO J. *23*, 4473–4483.

Kriel, A., Bittner, A.N., Kim, S.H., Liu, K., Tehranchi, A.K., Zou, W.Y., Rendon, S., Chen, R., Tu, B.P., and Wang, J.D. (2012). Direct regulation of GTP homeostasis by (p)ppGpp: A critical component of viability and stress resistance. Mol. Cell *48*, 231–241.

Kriel, A., Brinsmade, S.R., Tse, J.L., Tehranchi, A.K., Bittner, A.N., Sonenshein, A.L.,

and Wang, J.D. (2014). GTP dysregulation in *Bacillus subtilis* cells lacking (p)ppGpp results in phenotypic amino acid auxotrophy and failure to adapt to nutrient downshift and regulate biosynthesis genes. J. Bacteriol. *196*, 189–201.

Levin-Reisman, I., Ronin, I., Gefen, O., Braniss, I., Shoresh, N., and Balaban, N.Q. (2017). Antibiotic tolerance facilitates the evolution of resistance. Science (80-.). *355*, 826–830.

Nelson, D., and Cox, M. (2012). Lehninger Principles of Biochemistry (W.H. Freeman).

Ratnayake-Lecamwasam, M., Serror, P., Wong, K.W., and Sonenshein, A.L. (2001). *Bacillus subtilis* CodY represses early-stationary-phase genes by sensing GTP levels. Genes Dev. *15*, 1093–1103.

Reizer, J., Novotny, M.J., Hengstenberg, W., and Saier, M.H. (1984). Properties of ATP-dependent protein kinase from *Streptococcus pyogenes* that phosphorylates a seryl residue in HPr, a phosphocarrier protein of the phosphotransferase system. J. Bacteriol. *160*, 333–340.

Reizer, J., Hoischen, C., Rivolta, C., Rabus, R., Karamata, D., Jr, M.H.S., and Hillen, W. (1998). A novel protein kinase that controls carbon catabolite repression in bacteria. Mol. Microbiol. *27*, 1157–1169.

Rojas, A.M., Ehrenberg, M., Andersson, S.G.E., and Kurland, C.G. (1984). ppGpp inhibition of elongation factors Tu, G and Ts during polypeptide synthesis. Mol. Gen. Genet. *197*, 36–45.

Ross, W., Vrentas, C.E., Sanchez-Vazquez, P., Gaal, T., and Gourse, R.L. (2013). The magic spot: A ppGpp binding site on *E. coli* RNA polymerase responsible for regulation of transcription initiation. Mol. Cell *50*, 420–429.

Ross, W., Sanchez-Vazquez, P., Chen, A.Y., Lee, J.H., Burgos, H.L., and Gourse, R.L. (2016). ppGpp binding to a site at the RNAP-DksA interface accounts for Its dramatic effects on transcription initiation during the stringent response. Mol. Cell *62*, 811–823.

Rymer, R.U., Solorio, F.A., Tehranchi, A.K., Chu, C., Corn, J.E., Keck, J.L., Wang, J.D., and Berger, J.M. (2012). Binding mechanism of metal·NTP substrates and stringent-response alarmones to bacterial DnaG-type primases. Structure *20*, 1478–1489.

Siu, L.K., Lu, P., Chen, J., Lin, F.M., and Chang, S. (2003). High-level expression of ampC β-lactamase due to insertion of nucleotides between -10 and -35 promoter sequences in Escherichia coli clinical isolates: Cases not responsive to extended-spectrum-cephalosporin treatment. Antimicrob. Agents Chemother. *47*, 2138–2144.

Sonenshein, A.L. (2005). CodY, a global regulator of stationary phase and virulence in Gram-positive bacteria. Curr. Opin. Microbiol. *8*, 203–207.

Tehranchi, A.K., Blankschien, M.D., Zhang, Y., Halliday, J. a, Srivatsan, A., Peng, J., Herman, C., and Wang, J.D. (2010). The transcription factor DksA prevents conflicts between DNA replication and transcription machinery. Cell *141*, 595–605.

Traxler, M.F., Summers, S.M., Nguyen, H.-T., Zacharia, V.M., Hightower, G.A., Smith, J.T., and Conway, T. (2008). The global, ppGpp-mediated stringent response to amino acid starvation in *Escherichia coli*. Mol. Microbiol. *68*, 1128–1148.

Vrentas, C.E., Gaal, T., Berkmen, M.B., Rutherford, S.T., Haugen, S.P., Vassylyev, D.G., Ross, W., and Gourse, R.L. (2008). Still looking for the magic spot: The crystallographically defined binding site for ppGpp on RNA Polymerase is inlikely to

be responsible for rRNA transcription regulation. J. Mol. Biol. *377*, 551–564.
Yamaguchi, T., Iida, K., Shiota, S., Nakayama, H., and Yoshida, S. (2015). Elevated guanosine 5’-diphosphate 3’-diphosphate level inhibits bacterial growth and interferes with FtsZ assembly. FEMS Microbiol. Lett. *362*, 1–7.

Appendix I: RelA senses ATP depletion in *Bacillus subtilis*

Barra, J.T., Yang, J., Fung, D.K., and Wang, J.D.

J.T.B. designed and executed all experiments and edited the manuscript.

Abstract

The alarmone (p)ppGpp is produced when bacteria encounter stressful environments, including nutrient limitation and antibiotic exposure. Recent work from our lab showed that (p)ppGpp maintains GTP homeostasis by antagonizing GTP levels through inhibition of GTP biosynthesis enzymes and consuming GTP as a substrate. Successful regulation of GTP levels is critical for amino acid starvation and antibiotic survival (persistence). Recent reports suggest that decreasing ATP levels also promote persistence. Since GTP and ATP levels are linked, we investigated the possibility that perturbations in ATP level will result in (p)ppGpp production. First, using a (p)ppGpp reporter, we showed that (p)ppGpp is produced when ATP is depleted and is synthesized exclusively using RelA. RelA is dispersed in the cytosol during vegetative growth but upon starvation, RelA uses the ribosome as a sensing platform and produces (p)ppGpp. Using genetics and our (p)ppGpp reporter, we show that after ATP depletion, RelA indeed produces (p)ppGpp when bound to the ribosome. We conclude that RelA senses fluctuations in GTP and ATP levels and produces (p)ppGpp to survive nucleotide imbalance.

Introduction

Persistence is the phenomenon by which a majority of a bacterial population succumbs to bactericidal antibiotic, whereas a subpopulation is able to survive or persist in the antibiotic for an extended period of time. Our most recent work discussed in Chapter 3 showed that (p)ppGpp and its antagonism on GTP levels results in increased persister formation. We also showed that RelA and YjbM produce basal levels of (p)ppGpp to continuously produce persisters during growth, whereas YwaC produces (p)ppGpp specifically in response to sublethal concentrations of cell wall targeting antibiotics, such as bacitracin, and allows for adaptation to lethal concentrations of antibiotics (Fung et al.). Recent work from another group indicated that ATP, not (p)ppGpp, is the determinant of persister formation in *S. aureus* (Conlon et al., 2016). We treated *B. subtilis* with ATP-depleting drugs, such as CCCP and arsenate, and using radiolabeled bacteria and TLCs, examined induced nucleotides and showed that both drugs induce (p)ppGpp (Fung et al.). (p)ppGpp production and subsequent decrease in GTP due to CCCP and arsenate treatment, indeed protects cells against bactericidal antibiotics. In the absence of (p)ppGpp, ATP levels and GTP levels are decreased drastically when cells are treated with CCCP, indicating depletion of ATP and GTP are likely protecting (p)ppGpp^0 cells against bactericidal antibiotics. This new observation that ATP-depleting drugs induced (p)ppGpp production led us to ask new questions, which are addressed in this section.

Materials and Methods

Bacterial strains and strain construction. *B. subtilis* (p)ppGpp biosynthesis mutants were constructed by transformations with integration plasmids containing an I-sceI endonuclease cut site and regions of homology upstream and downstream of specific synthetase genes (pJW300 for Δ*yjbM*, pJW306 for Δ*ywaC*, and pJW371 for *relA*^{D264G}) followed by transformation of pSS4332 for marker-less recombination (Janes and Stibitz, 2006). Successful recombination was verified by PCR. For the construction of (p)ppGpp^0 mutant, Δ*ywaC* Δ*yjbM* was transformed with Δ*relA*::*mls* PCR product from genomic DNA using oligos oJW418/oJW419 and selected for MLS resistance (Kriel et al., 2012).

Construction of Δ*rplK* was achieved by transforming NCIB 3610 *comI*^{Q12L} (JDW2144) with genomic DNA extracted from *B. subtilis* 168 Δ*rplK from the Bacillus* knock-out collection at the *Bacillus* Genetic Stock Center (Koo et al., 2017). Positive transformants were resistant to erythromycin and thiostrepton and verified using PCR.

Construction of *relA*-TGS* using CRISPR-mediated recombination (Burby and Simmons, 2017). Golden Gate cloning was used to insert a *relA*-targeting guide RNA into the CRISPR array of pPB41. Mutagenic PCR was used to mutate Q472A, K474A, K476A, R478A, K482A, and K483A, all of which are located in the TGS domain of *B. subtilis* RelA and are homologous to residues identified in *E. coli* RelA that interact with tRNAs (Brown et al., 2016). Gibson Assembly was used to assemble the mutated TGS domain into pPB41 and this fragment served as a recombination template for CRISPR-mediated recombination after transformation of the plasmid into *B. subtilis* (Burby and Simmons, 2017).

Construction of P_{ilvB}-*gfp* fluorescence reporter was described previously (Fung et al.). Briefly, the reporter was constructed by fusion of PCR products containing respective promoter regions (oJW1935/oJW1936 for P_{ilvB}) with coding regions of fluorescence proteins (oJW1995/oJW1996 for GFP) using ligase cycling reaction (LCR) (Kok et al., 2014). In the case of P_{ilvB}-GFP, the construct was cloned into pDR110 flanked by *amyE.* Chromosome integration of reporter constructs was done by transformation and selection for SPEC. All mutants and constructs were verified by DNA sequencing.

Growth conditions. Bacillus subtilis strains were grown in S7 defined medium (Vasantha and Freese, 1980); MOPS was used at 50 mM rather than 100 mM, supplemented with 0.1% glutamate, 1% glucose, and 0.5% casamino acids. Cell cultures were grown at 37 °C from overnight plates with vigorous shaking. Cultures in logarithmic phase (OD_{600} = 0.1-0.3) were treated with antibiotics or inducers, such as arginine hydroxamate (RHX, 0.5 mg/mL), carbonyl cyanide m-chlorophenyl hydrazone (CCCP, 5 μM), sodium azide (NaN_3, 4 mM), arsenate (2.5 mM), or trimethoprim (TMP, 0.5 μg/mL).

For microscopy experiments, the following inducers and concentrations were used: CCCP: 5 μM; NaN_3: 4 mM; Arsenate: 2.5 mM, along with non-induction controls.

Minimum inhibitory concentration (MIC) determination. MICs for CCCP, NaN_3, and arsenate were determined using the microdilution method (Cockerill, F.R., Wikler, M.A., Alder, J., Dudley, M.N., Eliopoulos, G.M., Ferraro, M.J., Hardy, D.J., Hect, D.W., Hindler, J.F., Patel, J.B., Powell, M., Swenson, J.M., Thomson, R.B., Traczewski, M.M., Turnidge, J.D., Weinstein, M.P., and Zimmer, 2012). Logarithmic phase cells were back-diluted to a final titer of ≈ $5X10^5$ CFU/mL into 96-well plates containing two-fold serial dilutions of respective drugs in S7 defined medium. After 16-20 hours of

incubation at 37 °C with shaking, the MIC was determined as the lowest drug concentration that prevented visible growth.

Persister assay. Cells were harvested from young, overnight LB-agar plates (< 10 h), back-diluted into fresh S7 defined media at OD_{600} = 0.005, and grown at 37 °C with vigorous shaking. Cells were grown to logarithmic phase (OD_{600} ≈ 0.1-0.3) and subsequently treated with CCCP at 5-40 μM or RHX at 0.5 mg/mL. To determine cell viability, culture aliquots were taken at T=0 and at designated times after treatment, plated onto Luria-Broth (LB) agar, and incubated at 37 °C overnight. Viability at different time points was determined as CFU/mL/OD_{600} and relative survival (vs T_0) was calculated.

Fluorescence microscopy. To monitor (p)ppGpp induction using fluorescence reporters, cells were grown to OD_{600} ≈ 0.1 followed by 30-min induction with CCCP, NaN_3, or Arsenate, along with non-induction controls. All imaging samples were spotted on 1.5% agarose pads made with the same growth medium, and immediately imaged with Olympus IX-83 inverted microscope (Olympus) using 60X phase contrast objective with fluorescence filters (excitation: 470/20 nm, dichroic mirror: 485 nm, emission: 515/50 nm for GFP).

Results and Discussion

ATP-depleting drugs activate the P_{ilvB}-gfp reporter, indicating that (p)ppGpp is produced. To determine if ATP-depleting drugs induce (p)ppGpp in *B. subtilis*, we treated wild type and (p)ppGpp^0 cells containing the P_{ilvB}-gfp reporter with carbonyl cyanide *m*-chlorophenyl hydrazone (CCCP), sodium azide (NaN_3), and arsenate. To deplete ATP, CCCP was used to collapse the proton motive force which decreases protons to be

shuttled through ATP synthase to generate ATP (Lamsa et al., 2012). NaN_3 inhibits heme-containing respiratory enzymes, such as cytochrome c oxidase (Lichstein and Soule, 1944; Ortiz de Montellano et al., 1988). Arsenate, which is used in a previous report to decrease ATP levels (Conlon et al., 2016), competes with phosphate in a number of reactions due to their structural and chemical similarities. In particular, arsenate competes with phosphate as the substrate for glyceraldehyde-3-phosphate dehydrogenase so that glyceraldehyde-3-phosphate is converted to 1-arsenato-3-phospho-D-glycerate, instead of 1,3-bisphosphoglycerate. Normally, the 1,3-bisphosphoglycerate is converted to 3-phosphoglycerate, generating an ATP in the process, but the arsenic-containing product rapidly hydrolyzes to arsenate and 3-phosphoglycerate, resulting in loss of the ATP-generating step (Hughes, 2002). The drug concentrations we used to treat the cells were at the MIC because our goal was not to kill the cells but to induce (p)ppGpp production (Appendix Figure 1A). We showed that all three drugs induce (p)ppGpp production in wild type cells but not (p)ppGpp^0 cells (Appendix Figure 1B). These data are supported by TLC data that we reported in our previous work (Fung et al.).

The MIC for arsenate was determined to be 20 mM, but the reporter was not activated at that concentration. Rather, gradually decreasing the arsenate concentration from 10 mM to 2.5 mM showed that the reporter activity was increased. Thus for TLC and induction experiments, we used 2.5 mM arsenate (Fung et al.). Arsenate is a strong inhibitor that not only affects ATP levels but also competes with phosphates. It is possible that at the MIC, *B. subtilis* is actually killed, rather than inhibited (the MIC data cannot distinguish between the two fates).

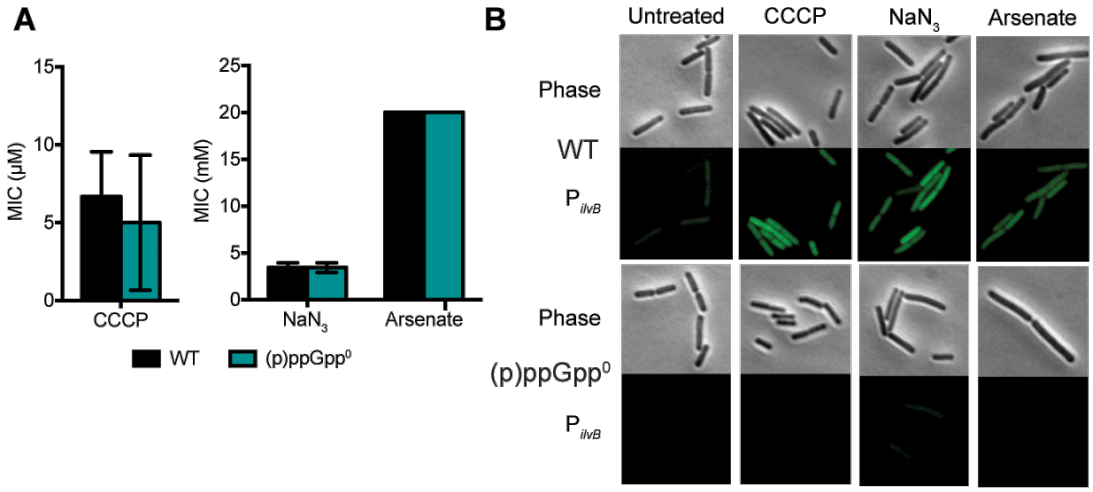

Appendix Figure 1. ATP-depleting drugs induce (p)ppGpp production. A. The MICs for CCCP, NaN_3, and arsenate were determined for *B. subtilis* 3610 *comI*^{Q12L} wild type and (p)ppGpp^0. The determined MICs were used to induce (p)ppGpp production. B. Both wild type and (p)ppGpp^0 P_{ilvB}-*gfp* strains were treated with 5 μM CCCP, 4 mM NaN_3, or 2.5 mM arsenate for 30 minutes and examined under the microscope for GFP fluorescence.

CCCP induces (p)ppGpp production using RelA, the ribosome-associated (p)ppGpp synthetase. We discovered that CCCP, NaN_3, and arsenate all induce (p)ppGpp in *B. subtilis*. We chose to continue our studies with CCCP because its mechanism of inhibition is specific in that it targets the proton motive force, unlike arsenate, which competes with phosphates and its uptake is likely affected by phosphate concentrations in the medium, at least for methicillin-resistant *S. aureus* ((Fung et al.). Since CCCP targets the electron transport chain, at the periphery of the cell, we hypothesized that σ^W and σ^M can sense the stress and activate transcription of *ywaC*, which produces (p)ppGpp in response to cell wall damaging agents (Czarny et al., 2014; D'Elia et al., 2009; Fung et al.).

Using (p)ppGpp synthetase mutants containing the P_{ilvB} reporter, we treated wild type, *relA*^{D264G}, *relA*^{D264G} Δ*yjbM*, Δ*yjbM*, and Δ*ywaC* with 5 μM CCCP and showed that contrary to our hypothesis, Δ*ywaC* still activated the reporter, whereas the *relA*^{D264G}, with a mutation in the active site of the synthetase domain, had decreased fluorescence (Appendix Figure 2A, 2B). Since YjbM produces basal levels of (p)ppGpp, we deleted *yjbM* in the *relA*^{D264G} Δ*yjbM* strain, which resulted in further decrease in fluorescence (Fung et al.; Nanamiya et al., 2008). From this experiment, we showed that intact (p)ppGpp synthesis activity from RelA is essential for CCCP-induced (p)ppGpp production.

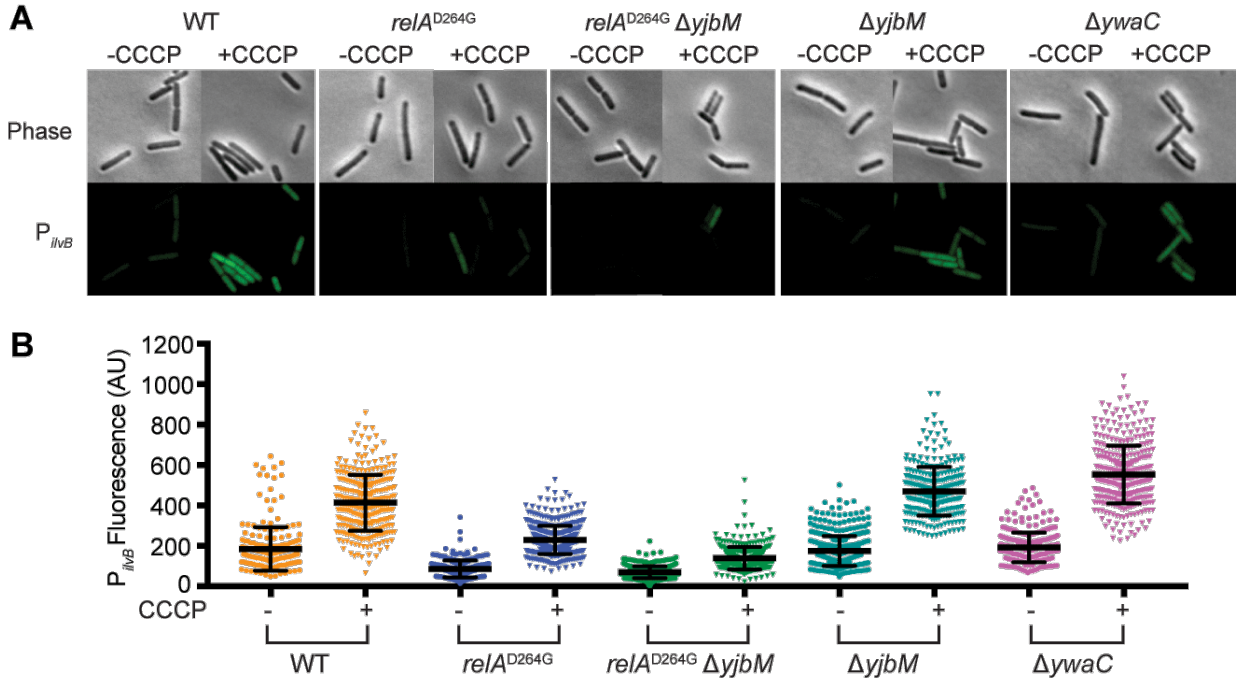

Appendix Figure 2. RelA synthesis activity is required for (p)ppGpp production in response to CCCP treatment. A. *B. subtilis* 3610 *comI*^{Q12L} wild type, *relA*^{D264G}, *relA*^{D264G} Δ*yjbM*, Δ*yjbM*, and Δ*ywaC*, all containing the P_{ilvB}-*gfp* reporter, were treated with 5 μM CCCP for 30 minutes and imaged using fluorescence microscopy. Cellular fluorescence was quantified using Metamorph. Values graphed are mean ± SD, n > 200 cells. Data is a culmination of 7 independent experiments.

RelA binding to the ribosome appears to be required for (p)ppGpp production during CCCP treatment. The L11 protein, encoded by *rplK*, is required for the stringent response, in which RelA uses the ribosome to sense uncharged tRNAs (Figure 1). Deletion of *rplK* or mutation in the N-terminal domain of L11 results in cells that cannot produce (p)ppGpp (Wimberly et al., 1999; Yang and Ishiguro, 2001). To determine whether RelA is producing (p)ppGpp in response to CCCP while bound to the ribosome, we generated a Δ*rplK* mutant containing the P_{ilvB}-*gfp* reporter.

We examined *B. subtilis* wild type, (p)ppGpp^0, and Δ*rplK* strains under the microscope for reporter activity. After treatment with 5 μM CCCP for 30 minutes, we observed that (p)ppGpp^0, as expected, and Δ*rpl*K strains do not have reporter activity (Appendix Figure 3A, 3B). However, Δ*rplK* strains have very slow growth rate (Zhang et al., 2001) and absence of the ribosomal protein may negatively affect translation and interfere with GFP formation. To determine whether Δ*rplK* has problems with translation, we treated the cells with 0.5 μg/mL trimethoprim (TMP), which inhibits dihydrofolate reductase and has been shown to decrease GTP levels in *E. coli* (Kaplan and Silman, 1973). TMP inhibits the formation of tetrahydrofolate, a precursor for nucleotides, thymine synthesis, and one-carbon metabolism. For our purposes, we used it to decrease GTP levels to activate the P_{ilvB} reporter (Fung et al.). If Δ*rplK* does not have problems with translating GFP, then we should see a signal from P_{ilvB}-*gfp*. As expected, the reporter turned on for the wild type strain, and our positive control (p)ppGpp^0, which indicates that 0.5 μg/mL TMP was sufficient to turn on the reporter even in a strain that cannot produce (p)ppGpp (Appendix Figure 3B). For the Δ*rplK* strain, treatment with TMP took about 2 hours for the P_{ilvB} reporter to exhibit a signal,

indicating that increasing treatment time may compensate for problems with decreased growth rate. We treated Δ*rplK* again with CCCP for 2 and 4 hours and saw that the signal is still lower than the signal for (p)ppGpp^0, indicating that the P_{ilvB} reporter does not turn on during CCCP treatment (Appendix Figure 3A). These data suggest that without L11, RelA cannot bind to the ribosome and produce (p)ppGpp in response to CCCP treatment.

There are several experimental caveats to consider before concluding that RelA requires the ribosome to produce (p)ppGpp. First is that removal of L11 from the ribosome causes severe growth rate defects. Although we show that Δ*rplK* can still produce GFP from the P_{ilvB} reporter, it will be better to use L11-NTD mutant, such as L11^{P22A}, which can still insert into the ribosome but cannot produce (p)ppGpp during the stringent response (Wimberly et al., 1999; Yang and Ishiguro, 2001; Zhang et al., 2001). Although L11 is a tertiary binding protein (reviewed in (Shajani et al., 2011)), using this mutant will at least ensure that the ribosomes still have an L11 protein and minimize defects associated with loss of L11. Initial attempts to make this mutation at the endogenous locus using ligase cycling reaction (LCR) or CRISPR have failed. For transformation with the LCR fragment, selection for thiostrepton-resistant mutants, which selects for mutants that have acquired the L11-NTD mutations, were not successful, indicating that more troubleshooting is required. Thiostrepton is an antibiotic that binds at the interface of 23S rRNA and L11-NTD and mutations in the rRNA or L11-NTD will render cells resistant to thiostrepton (Wimberly et al., 1999; Yang and Ishiguro, 2001).

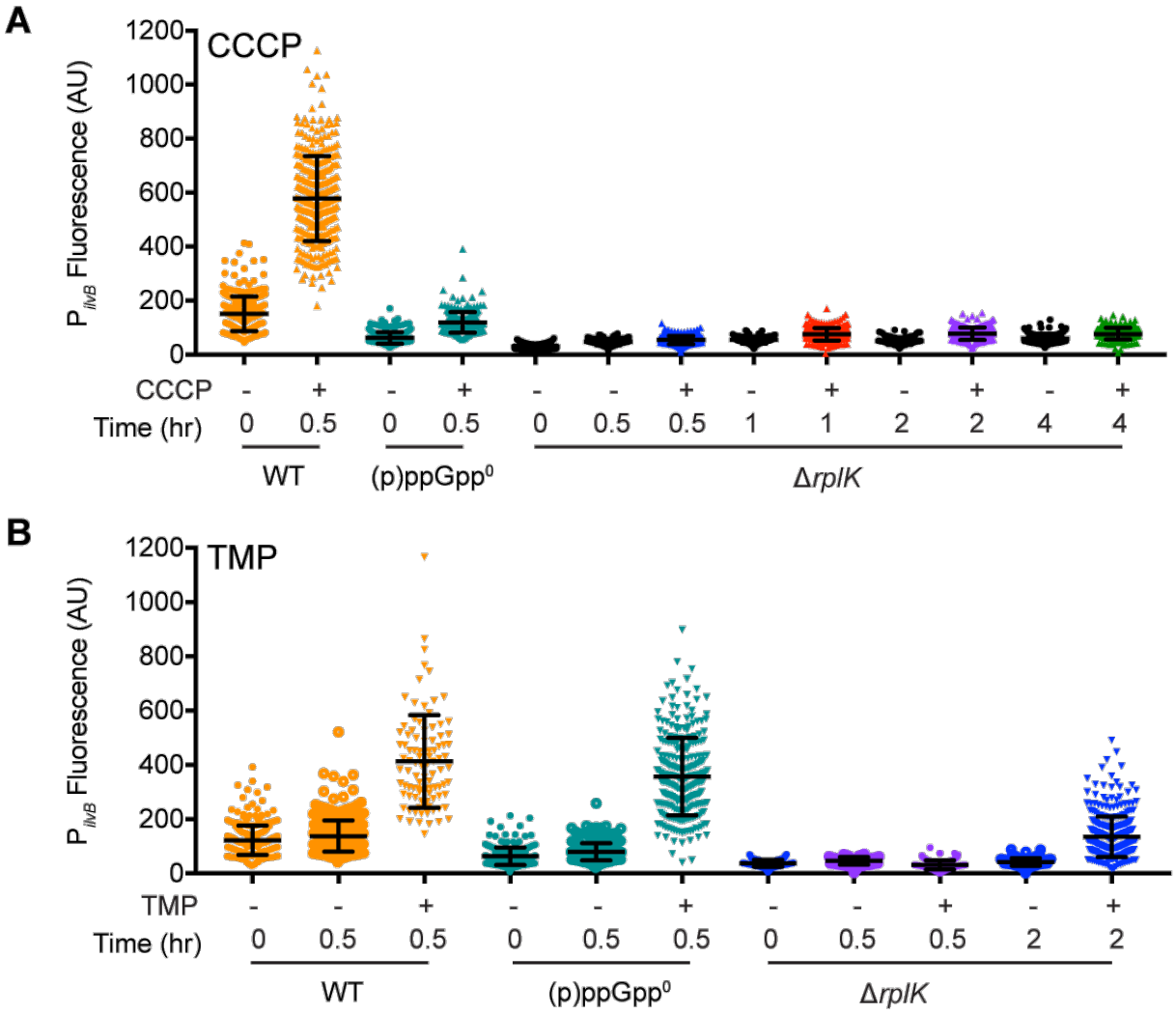

Appendix Figure 3. RplK is required for (p)ppGpp production from RelA. *B. subtilis* 3610 *comI*^{Q12L} wild type, (p)ppGpp^0, and Δ*rplK* with the P$_{ilvB}$-*gfp* reporter were treated with A. 5 μM CCCP or B. 0.5 μg/mL trimethoprim (TMP) at various time points and imaged with fluorescence microscopy. Cellular fluorescence was quantified using Metamorph. Values graphed are mean ± SD, n = 80-300 cells.

Attempts at generating the CRISPR plasmid for recombining the mutation into the endogenous *rplK* locus were also not successful. Using Golden Gate cloning to insert a guide RNA targeting the *rplK* codon encoding Pro22 always resulted in deletion of a CRISPR repeat in the CRISPR array (Appendix Figure 4). Since the *B. subtilis* L11 protein is homologous to the *E. coli* L11 protein (68% identical), and *E. coli* is used to carry the newly constructed plasmid, perhaps the CRISPR plasmid is unstable in *E. coli* unless the guide RNA is deleted. Nevertheless, more troubleshooting is required in order to make the *rplK*^{P22A} mutant.

Reference sequence of *rplK* guide RNA in CRISPR array of CRISPR plasmid pPB41

Sequence of attempted insertion of *rplK* guide RNA into CRISPR plasmid pPB41 results in deletion

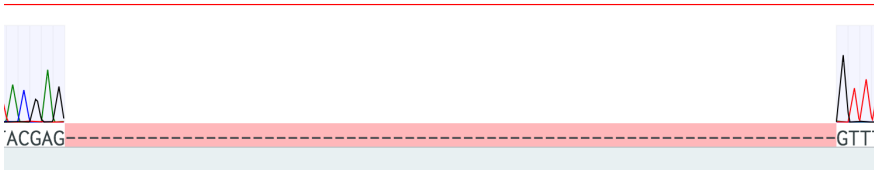

Appendix Figure 4. Attempted cloning of *rplK* guide RNA into CRISPR array of pPB41 (Burby and Simmons, 2017) results in deletion of CRISPR repeat after retrieval from *E. coli* host. Upper panel is the reference sequence of pPB41 containing the *rplK* guide RNA that will be transcribed from a CRISPR array. Lower panel is one of many sequenced fragments resulting in deletion of an entire CRISPR repeat, including the guide RNA.

RelA-TGS domain is critical for arginine hydroxamate survival, but not CCCP. Recently, a cryo-EM structure of RelA bound to the ribosome revealed new insights into the mechanisms of RelA activation and proposed a mechanism of detecting uncharged tRNAs (Brown et al., 2016). In this work, the authors proposed that the ThrRS GTPase SpoT (TGS) domain of RelA (Figure 1) is capable of sensing the aminoacylation state of tRNAs; if the tRNA was charged, then the attached amino acid sterically hinders binding of RelA-TGS. Six key residues on the *E. coli* RelA-TGS were proposed to interact with the terminal end of the tRNA: R487, R489, K491, H493, K498, and R497, which were Q472, K474, K476, R478, K482, and K483 in *B. subtilis*. Using CRISPR-mediated recombination (Burby and Simmons, 2017), we generated a *relA*-TGS* mutant in which all 6 residues were mutated into alanines. We hypothesized that this mutant would not be able to sense the charging state of tRNAs, making it like a (p)ppGpp^0. Treatment of *relA*-TGS* and *relA*-TGS* Δ*yjbM* Δ*ywaC* containing the P_{ilvB}-*gfp* reporter with 5 μM CCCP showed that the reporter was turned on, indicating that (p)ppGpp is likely to be produced, despite the mutation in the TGS domain (Appendix Figure 5A). This observation is supported by kill curve data, since wild type and *relA*-TGS* are not killed by 5 μM CCCP, similar to our previous work (Fung et al.), but any loss of (p)ppGpp synthesis ability results in decreased survival (Appendix Figure 5B). Although the RelA-TGS domain does not appear to be crucial for (p)ppGpp synthesis in response to CCCP, it is critical for survival in response to arginine hydroxamate (RHX), which inhibits the arginyl-tRNA synthetase and induces the stringent response (Appendix Figure 5C).

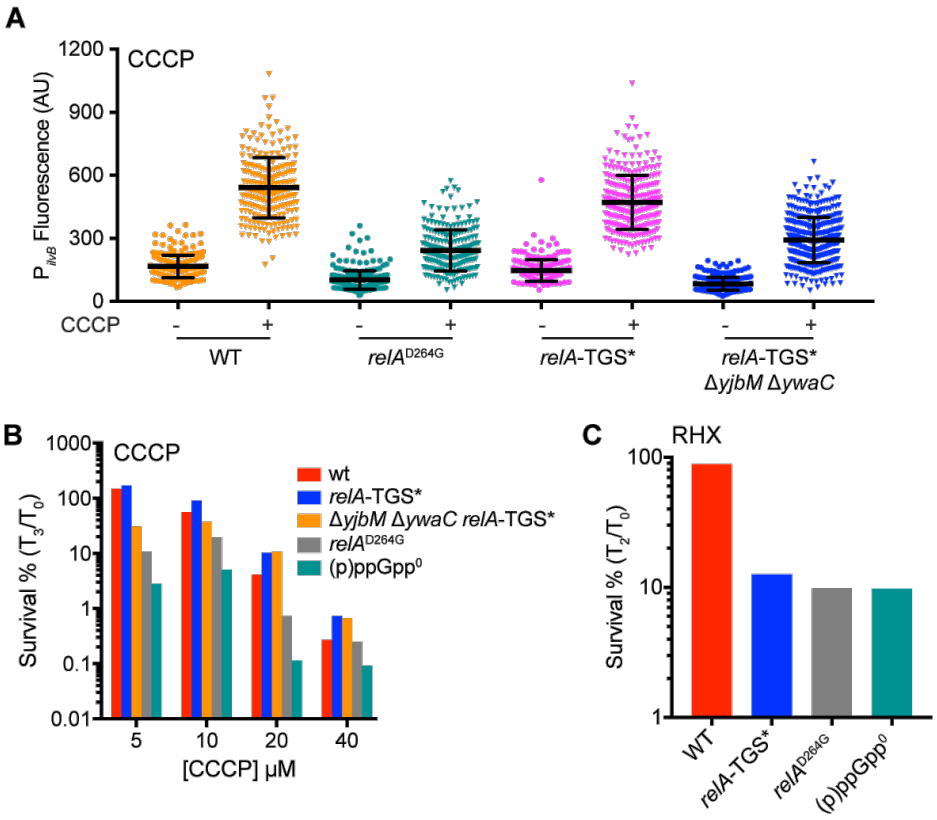

Appendix Figure 5. The RelA-TGS* mutant survives CCCP treatment but is susceptible to arginine hydroxamate. A. *B. subtilis* 3610 *comI*^{Q12L} wild type, *relA*^{D264G}, *relA*-TGS*, and Δ*yjbM* Δ*ywaC relA*-TGS* containing the P$_{ilvB}$-*gfp* reporter was treated with 5 μM CCCP for 30 minutes and imaged with fluorescence microscopy. Cellular fluorescence was quantified using Metamorph. Values graphed are mean ± SD, n > 240 cells. B. Treatment of wild type, *relA*-TGS*, Δ*yjbM* Δ*ywaC relA*-TGS*, *relA*^{D264G}, and (p)ppGpp^0 with 5-40 μM CCCP for 3 hours. Values are N=1. C. Treatment of *B. subtilis* 3610 *comI*^{Q12L} (JDW2901) wild type, *relA*-TGS*, *relA*^{D264G} (JDW2144 background), and (p)ppGpp^0 (JDW2144 background) with 0.5 mg/mL arginine hydroxamate (RHX) for 2 hours. Values are N=1.

The *relA*-TGS* mutant is a powerful tool for differentiating between the stresses that activate (p)ppGpp production: arginine hydroxamate (Chapter 2), chloramphenicol (Chapter 4), CCCP, and arsenate (Chapter 3) (Fung et al.; Kriel et al., 2012; Rhaese et al., 1975). Up until this point, we have always considered RHX and chloramphenicol to induce (p)ppGpp production through the same mechanism, ultimately resulting in ribosome stalling. However, treatment of *relA*-TGS* with chloramphenicol did not result in killing, whereas RHX-treated cells were killed, indicating that these two phenotypes are distinguishable from one another. It is possible that more mutations in the *relA*-TGS* domain will result in phenotypes that resemble (p)ppGpp^0. These residues include P399, K400, H420, and K426 on *B. subtilis relA*, which are hypothesized to stack with the 3'-CCA on tRNAs (Brown et al., 2016). It is possible that the mutations we made in *relA*-TGS* were insufficient to abolish tRNA sensing and these additional mutations are required.

Our data suggest that RelA needs to bind to the ribosome before producing (p)ppGpp in response to CCCP treatment (Appendix I). We hypothesize that CCCP decreases ATP levels, which decreases charged tRNA pools because ATP is required to activate the amino acid (Nelson and Cox, 2012). In the end, CCCP and arsenate would be activating the stringent response because of the decreases in charged tRNA. Initial attempts at examining the tRNA charged states using acid urea PAGE gels were unsuccessful. Optimization of cell harvesting and acid urea PAGE gel protocols are needed in the future.

Another possibility is that ATP depletion is altering the activity of ATP-dependent amino acid transporters, decreasing nutrient transport and thereby creating a starvation

condition (Hoffmann and Bremer, 2017; Koide and Hoch, 1994). We can determine if there are problems with amino acid transport into the cell, we can increase *de novo* synthesis of amino acids by overexpressing amino acid biosynthesis operons or by deleting CodY, a master regulator and repressor of branched chain amino acid biosynthesis genes (Shivers and Sonenshein, 2004).

Literature Cited

Brown, A., Fernández, I.S., Gordiyenko, Y., and Ramakrishnan, V. (2016). Ribosome-dependent activation of stringent control. Nature *534*, 1–16.

Burby, P.E., and Simmons, L.A. (2017). MutS2 promotes homologous recombination in *Bacillus subtilis*. J. Bacteriol. *199*, 1–13.

Cockerill, F.R., Wikler, M.A., Alder, J., Dudley, M.N., Eliopoulos, G.M., Ferraro, M.J., Hardy, D.J., Hect, D.W., Hindler, J.F., Patel, J.B., Powell, M., Swenson, J.M., Thomson, R.B., Traczewski, M.M., Turnidge, J.D., Weinstein, M.P., and Zimmer, B.L. (2012). Methods for dilution antimicrobial susceptibility tests for bacteria that grow aerobically.

Conlon, B.P., Rowe, S.E., Gandt, A.B., Nuxoll, A.S., Donegan, N.P., Zalis, E.A., Clair, G., Adkins, J.N., Cheung, A.L., and Lewis, K. (2016). Persister formation in *Staphylococcus aureus* is associated with ATP depletion. Nat. Microbiol. *1*, 1–7.

Czarny, T.L., Perri, A.L., French, S., and Brown, E.D. (2014). Discovery of novel cell wall-active compounds using P_{ywaC}, a sensitive reporter of cell wall stress, in the model Gram-positive bacterium Bacillus subtilis. Antimicrob. Agents Chemother. *58*, 3261–3269.

D'Elia, M.A., Millar, K.E., Bhavsar, A.P., Tomljenovic, A.M., Hutter, B., Schaab, C., Moreno-Hagelsieb, G., and Brown, E.D. (2009). Probing teichoic acid genetics with bioactive molecules reveals new interactions among diverse processes in bacterial cell wall biogenesis. Chem. Biol. *16*, 548–556.

Fung, D.K., Barra, J.T., Schroeder, J.W., Ying, D., and Wang, J.D. Spontaneous and adaptive persistence by (p)ppGpp-mediated GTP antagonism in Gram-positive bacteria.

Hoffmann, T., and Bremer, E. (2017). Guardians in a stressful world: The Opu family of compatible solute transporters from *Bacillus subtilis*. Biol. Chem. *398*, 193–214.

Hughes, M.F. (2002). Arsenic toxicity and potential mechanisms of action. Toxicol. Lett. *133*, 1–16.

Kaplan, R., and Silman, N. (1973). The effect of trimethoprim on RNA synthesis in relaxed and stringent Escherichia coli strains. Biochem. J. *35*, 326–330.

Koide, A., and Hoch, J.A. (1994). Identification of a second oligopeptide transport system in *Bacillus subtilis* and determination of its role in sporulation. Mol. Microbiol. *13*, 417–426.

Kok, S. De, Stanton, L.H., Slaby, T., Durot, M., Holmes, V.F., Patel, K.G., Platt, D.,

Shapland, E.B., Serber, Z., Dean, J., et al. (2014). Rapid and reliable DNA assembly via ligase cycling reaction. ACS Synth. Biol. *3*, 97–106.

Koo, B.M., Kritikos, G., Farelli, J.D., Todor, H., Tong, K., Kimsey, H., Wapinski, I., Galardini, M., Cabal, A., Peters, J.M., et al. (2017). Construction and Analysis of Two Genome-Scale Deletion Libraries for Bacillus subtilis. Cell Syst. *4*, 291–305.e7.

Kriel, A., Bittner, A.N., Kim, S.H., Liu, K., Tehranchi, A.K., Zou, W.Y., Rendon, S., Chen, R., Tu, B.P., and Wang, J.D. (2012). Direct regulation of GTP homeostasis by (p)ppGpp: A critical component of viability and stress resistance. Mol. Cell *48*, 231–241.

Lamsa, A., Liu, W.-T., Dorrestein, P.C., and Pogliano, K. (2012). The *Bacillus subtilis* cannibalism toxin SDP collapses the proton motive force and induces autolysis. Mol. Microbiol. *84*, 486–500.

Lichstein, H.C., and Soule, M.H. (1944). Studies of the effect of sodium azide on microbic growth and respiration: The action of sodium azide on microbic growth. J. Bacteriol. *47*, 221–230.

Nanamiya, H., Kasai, K., Nozawa, A., Yun, C.-S., Narisawa, T., Murakami, K., Natori, Y., Kawamura, F., and Tozawa, Y. (2008). Identification and functional analysis of novel (p)ppGpp synthetase genes in *Bacillus subtilis*. Mol. Microbiol. *67*, 291–304.

Nelson, D., and Cox, M. (2012). Lehninger Principles of Biochemistry (W.H. Freeman).

Ortiz de Montellano, P., David, S., Ator, M., and Tew, D. (1988). Mechanism-based inactivation of horseradish peroxidase by sodium azide. Formation of meso-azidoprotoporphyrin IX. Biochemistry *27*, 5470–5476.

Rhaese, H.J., Dichtelmüller, H., and Grade, R. (1975). Accumulation of guanosine tetraphosphate and pentaphosphate in response to inhibition of protein synthesis in Bacillus subtilis. Eur. J. Biochem. *56*, 385–392.

Shajani, Z., Sykes, M.T., and Williamson, J.R. (2011). Assembly of bacterial ribosomes. Annu. Rev. Biochem. *80*, 501–526.

Shivers, R.P., and Sonenshein, A.L. (2004). Activation of the Bacillus subtilis global regulator CodY by direct interaction with branched-chain amino acids. Mol. Microbiol. *53*, 599–611.

Wimberly, B.T., Guymon, R., McCutcheon, J.P., White, S.W., and Ramakrishnan, V. (1999). A detailed view of a ribosomal active site: the structure of the L11-RNA complex. Cell *97*, 491–502.

Yang, X., and Ishiguro, E. (2001). Involvement of the N terminus of ribosomal protein L11 in regulation of the RelA protein of *Escherichia coli*. J. Bacteriol. *183*, 6532–6537.

Zhang, S., Scott, J.M., and Haldenwang, W.G. (2001). Loss of ribosomal protein L11 blocks stress activation of the *Bacillus subtilis* transcription factor σ^B. J. Bacteriol. *183*.

Appendix Table 1. Strains used in study.

Strain	JDW Strain	Genotype	Reference
NCIB 3610 *comI*^{Q12L}	JDW2144	NCIB 3610 *comI*^{Q12L}	Konkol *et al*., 2014
Wild type P$_{ilvB}$-*gfp*	KCF045	NCIB 3610 *comI*^{Q12L} *amyE*::P$_{ilvB}$-GFP*mut2*^{A206K}	Fung, Barra *et al*.
(p)ppGpp^0	JDW2231	NCIB 3610 *comI*^{Q12L} Δ*yjbM* Δ*ywaC relA*::*mls*	Fung, Barra *et al*.
(p)ppGpp^0 P$_{ilvB}$-*gfp*	KCF057	NCIB 3610 *comI*^{Q12L} Δ*yjbM* Δ*ywaC relA*::*mls amyE*::P$_{ilvB}$-GFP*mut2*^{A206K}	Fung, Barra *et al*.
relA^{D264G}	JDW2721	NCIB 3610 *comI*^{Q12L} Δ*yjbM* Δ*ywaC relA*^{D264G}	Fung, Barra *et al*.
relA^{D264G} P$_{ilvB}$-*gfp*	KCF067	NCIB 3610 *comI*^{Q12L} Δ*yjbM* Δ*ywaC relA*::*mls amyE*::P$_{ilvB}$-GFP*mut2*^{A206K}	Fung, Barra *et al*.
relA^{D264G} Δ*yjbM* P$_{ilvB}$-*gfp*	KCF079	NCIB 3610 *comI*^{Q12L} Δ*yjbM* *relA*^{D264G} *amyE*::P$_{ilvB}$-GFP*mut2*^{A206K}	Fung, Barra *et al*.
Δ*yjbM* P$_{ilvB}$-*gfp*	KCF076	NCIB 3610 *comI*^{Q12L} Δ*yjbM* *amyE*::P$_{ilvB}$- GFP*mut2*^{A206K}	Fung, Barra *et al*.
Δ*ywaC* P$_{ilvB}$-*gfp*	KCF070	NCIB 3610 *comI*^{Q12L} Δ*ywaC* *amyE*::P$_{ilvB}$-*gfp-spec*	Fung, Barra *et al*.
Δ*rplK*::erm	JDW2553	168 Δ*rplK*::*erm*	BGSC, Koo *et al*., 2017
Δ*rplK*::*erm* P$_{ilvB}$-*gfp*	JLT265	NCIB 3610 *comI*^{Q12L} Δ*rplK*::*erm* *amyE*::P$_{ilvB}$- GFP*mut2*^{A206K}	This work
relA-TGS*	JLT328	NCIB 3610 *comI*^{Q12L} *relA*-TGS*	This work
relA-TGS* P$_{ilvB}$-*gfp*	JLT333	NCIB 3610 *comI*^{Q12L} *relA*-TGS* *amyE*::P$_{ilvB}$- GFP*mut2*^{A206K}	This work
Δ*yjbM* Δ*ywaC* *relA*-TGS*	JLT330	NCIB 3610 *comI*^{Q12L} Δ*yjbM* Δ*ywaC relA*-TGS*	This work
Δ*yjbM* Δ*ywaC* *relA*-TGS* P$_{ilvB}$-*gfp*	JLT336	NCIB 3610 *comI*^{Q12L} Δ*yjbM* Δ*ywaC relA*-TGS* *amyE*::P$_{ilvB}$-GFP*mut2*^{A206K}	This work

Appendix Table 2. Plasmids used in study.

Plasmid No.	Genotype	Marker	Reference
pJW299	pEX44/I-SceI site *amp cat*	Cam^R	Kriel *et al*., 2012
pJW300	pJW239/Δ*yjbM* I-SceI site *amp cat*	Cam^R	Kriel *et al*., 2012
pJW306	pJW299/Δ*ywaC* I-SceI site *amp cat*	Cam^R	Kriel *et al*., 2012
pJW370	pJW299/*yjbM* I-SceI site *amp cat*	Cam^R	Kriel *et al*., 2014

pJW371	pJW299/*relA*^{D264G} I-SceI site *amp cat*	Cam^R	Kriel *et al*., 2014
pJW558	P_{ilvB}-GFPmut2^{A206K}	Sp^R	Fung, Barra, *et al.*
pPB41	CRISPR editing plasmid	Amp^R /Sp^R	Burby and Simmons, 2016
pJY01	pPB41/*relA* gRNA *relA*-TGS* recombination template	Amp^R /Sp^R	This work
pSS4332	*oriU* P_{amy}-I-sceI *kan*	Kan^R	Jane and Stibitz, 2006
pDR244	*cre* + Ts origin	Sp^R	BGSC, Koo *et al*., 2017

Appendix II: Fatty acid availability sets cell envelope capacity and dictates microbial cell size

This chapter is adapted from "Vadia, S., Tse, J.L., Lucena, R., Yang, Z., Kellogg, D.R., Wang, J.D., and Levin, P.A. (2017) Fatty acid availability sets cell envelope capacity and dictates microbial cell size. *Current Biology*, 27(12): 1757-1767."

J.T.B. designed and executed the (p)ppGpp level determination experiments in this manuscript.

Introduction and Results

In this work, we determined the role of nutrient availability, or biosynthetic capacity, on cell size control in *E. coli*. Cells grown in nutrient poor media tend to be smaller and have slower growth rates, and the volume of cell material added to *E. coli* cells changes with carbon availability. Here, we examined the contribution of RNA, protein, and fatty acid biosynthesis to *E. coli* cell size by comparing cell size during treatment with sub-lethal concentrations of rifampicin, chloramphenicol, and cerulenin to cell size during growth in different carbon sources. Of the three antibiotics, treatment with different cerulenin concentrations, which inhibits β-ketoacyl-ACP synthase I (FabB), yielded cells with different sizes and showed a proportional relationship between cell size and fatty acid biosynthesis, a phenotype that is conserved in the evolutionarily distinct *B. subtilis* and *S. cerevisiae*. Defects in cell size during cerulenin treatment could be compensated with oleic acid addition, indicating restoring a component of the plasma membrane corrected for cell size. A genetic approach to examine the impact of fatty acid synthesis on cell size utilized a *fadR* overexpression construct, where FadR, a transcriptional regulator of fatty acid synthesis, was overproduced. Interestingly, overproduction of FadR increased cell size and decreased growth rate, but did not significantly impact the ppGpp to GTP ratio (Appendix Figure 1A, 1B), supporting the model that fatty acid synthesis affects cell size independently of ppGpp levels.

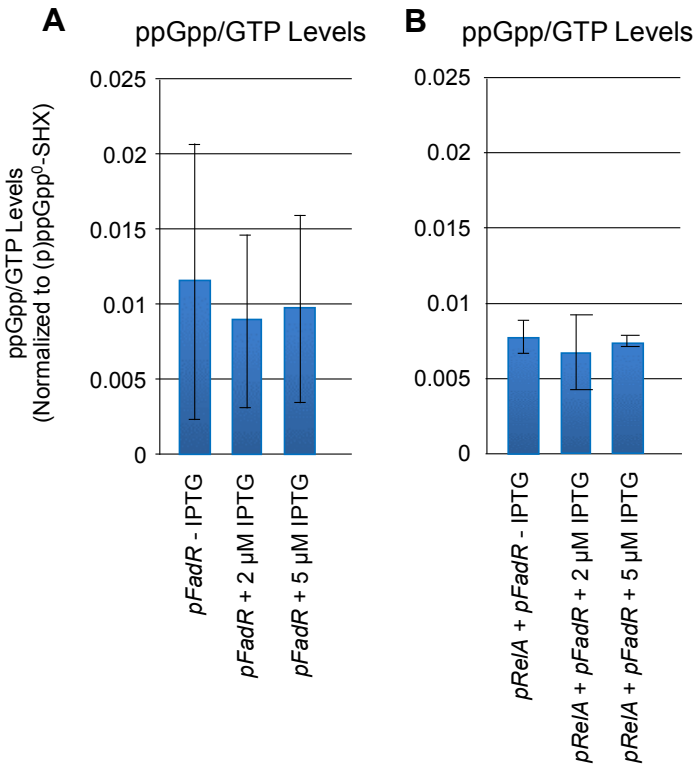

Appendix Figure 1. Induction of *fadR* does not significantly impact ppGpp levels. MG1655 *E. coli* strains harboring *pFadR* or *pFadR* and *pRelA* were grown in low-phosphate MOPS media with or without 2 or 5 µM IPTG and appropriate antibiotics and labeled with ^{32}P-orthophosphate. Once early logarithmic phase was reached, nucleotides were extracted to determine steady-state ppGpp and GTP levels. (A) ppGpp/GTP levels in MG1655-*pFadR* cultured with or without inducer, 2 or 5 µM IPTG. (B) ppGpp/GTP levels in MG1655-*pFadR*/*pRelA* cultured with or without inducer, 2 or 5 µM IPTG. Error bars indicate standard deviations from n = 2. Nucleotides separated using 1.5 M KH_2PO_4 pH 3.4 buffer. Intensities determined using ImageQuant. Plotted ratios are expressed as ppGpp-background/GTP-background – ppGpp for (p)ppGpp^0-serine hydroxamate-background/GTP-background.

Another important observation is that inhibiting fatty acid biosynthesis leads to increases in ppGpp production through SpoT, the bifunctional (p)ppGpp synthetase in *E. coli*. ppGpp production is associated with smaller cell size and lower growth rate. To determine if ppGpp affects cell size upstream or downstream of fatty acid biosynthesis, FadR and RelA, the monofunctional (p)ppGpp synthetase, were overproduced, with the goal of examining whether FadR overproduction will correct for the cell size defect in cells with increased ppGpp. Expression of *fadR* and *relA* yielded cells that were larger than cells expressing *relA* alone, indicating that ppGpp downregulates fatty acid synthesis.

Even without (p)ppGpp, cell size and nutrient availability/growth rate remain coupled. However, (p)ppGpp is required to protect cells against cerulenin, which causes defects in the cell membrane. We observed a striking 10,000-fold decrease in (p)ppGpp^0 cell viability, while the wild type cells neither grew nor died. Further, (p)ppGpp^0 cells stained positive with propidium iodide, indicating that the cell membrane has been compromised in (p)ppGpp^0 cells. This response is reminiscent of chloramphenicol killing (p)ppGpp^0 cells observed in Chapter 4.

Materials and Methods

Thin layer chromatography of radiolabeled E. coli. Strains were grown from single colonies in low-phosphate MOPS (Teknova) at 37 °C with shaking (1X MOPS, 1 mM KH_2PO_4, 0.2% glucose, 0.4% casamino acids) and appropriate antibiotics to early logarithmic phase, then diluted to OD_{600} = 0.005, at which time ^{32}P-orthophosphate was introduced to label the cells. Once cells reached early logarithmic phase again, samples were collected for nucleotide extraction using 2M ice cold formic acid. Nucleotides were

measured using thin layer chromatography and quantified using ImageQuant software (Molecular Dynamics). Intensities were normalized to the number of phosphates in the corresponding nucleotide. ppGpp levels are normalized to GTP level at steady state with signals from steady-state (p)ppGpp^0 cells subtracted.

Appendix III: (p)ppGpp determination in clinically-isolated methicillin-resistant *Staphylococcus aureus*

This chapter consists of unpublished work done in a collaboration with Dr. Warren Rose (University of Wisconsin-Madison, School of Pharmacy) and Dr. Andrew Berti (Wayne State University).

J.T.B. designed and executed the (p)ppGpp level determination experiments.

Introduction

Staphylococcus aureus is a Gram-positive pathogen that causes diseases that range in severity from superficial skin infections to life-threatening septicemia. Alarmingly, methicillin-resistant *S. aureus* (MRSA) is responsible for most hospital-acquired infections. In particular, the MRSA USA300 strain, unlike non-MRSA strains, has three plasmids and five mobile genetic elements, all of which contain virulence factors and resistance genes that have contributed to its pathogenesis and successful evasion of antibiotics (Diep et al., 2006). Determining the mechanisms of persistence in MRSA will aid in drug development.

Recently, the Rose lab isolated daptomycin-resistant MRSA strains from chronic MRSA patients treated with daptomycin for 28 days (Berti *et al*., unpublished). Whole genome sequencing indicated that mutations occurred in the *S. aureus rsh*, encoding a Rel/SpoT homolog (RSH). Individual mutations consisted of L68F (hydrolase), A80V (hydrolase), S171F (hydrolase), and G548S (linker between TGS and ZFD) (Appendix Figure 1, domain designations based on alignment with *B. subtilis* and *E. coli* primary sequence (Brown et al., 2016)). Since these mutants occur in the hydrolase domain, we hypothesized that they are persisters because of attenuated hydrolase activity and will thus have higher basal (p)ppGpp level.

Results

S. aureus RSH and B. subtilis RSH are homologous. An alignment of the *S. aureus* RSH with the *B. subtilis* RelA and *S. equisilimus* Rel shows a similarity of 80% and 70%, respectively, so conclusions about the hydrolase domain in *B. subtilis* and *S.*

equisilimus can be applied to the *S. aureus* RSH. A crystal structure obtained of the first 385 amino acids of *S. equisilimus* Rel (Rel_{Seq}) (Hogg et al., 2004) indicated several important amino acids in the hydrolase domain, which when mutated, results in defective hydrolase activity. One of these amino acids is S164, which maps to S171 in *S. aureus* RSH. Neither of the other mutations were implicated in Hogg *et al*., suggesting that they might be novel mutations (Appendix Figure 1). However, the hypothesis that decreased hydrolase activity induces persistence is not novel (Gao et al., 2010).

Mupirocin is not suitable to induce (p)ppGpp in MRSA. With hindsight, we know that one of the plasmids in USA300 harbors the *ileS* gene, which confers resistance to mupirocin, an isoleucyl-tRNA synthetase inhibitor (Corrigan et al., 2016; Diep et al., 2006). Before this, we tried to use it to examine steady state levels of (p)ppGpp in MRSA. From the MRSA literature, several mupirocin concentrations were used to induce (p)ppGpp: 0.01, 0.05, and 0.25 µg/mL mupirocin. Treatment of MRSA with mupirocin concentrations and low-phosphate Tris-minimal succinate media with casamino acids (TMS) were used to determine the best mupirocin concentration for the experiments. J01 and J01*rsh*(L68F) with and without the various mupirocin concentrations and plotted their growth curves (Appendix Figure 2A, 2B). The growth curve showed that 0.05 µg/mL and 0.25 µg/mL mupirocin inhibited growth in low phosphate TMS broth, but not 0.01 µg/mL. The sub-inhibitory 0.01 µg/mL to induce ppGpp.

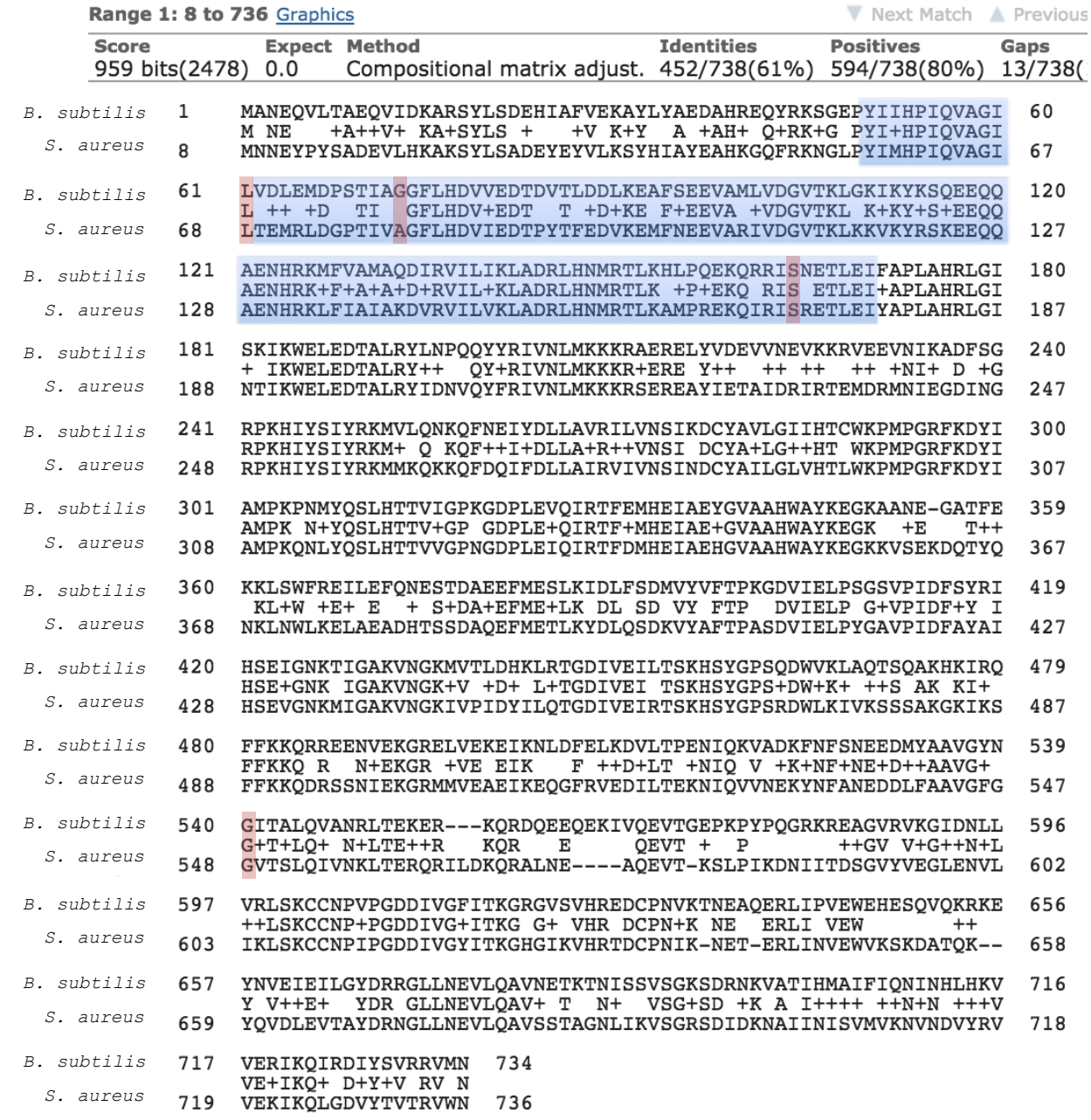

Appendix Figure 1. Alignment of *B. subtilis* and *S. aureus* RSH proteins. Highlighted in blue is the hydrolase domain. Highlighted in red are mutations found in the *rsh* mutants isolated from this study.

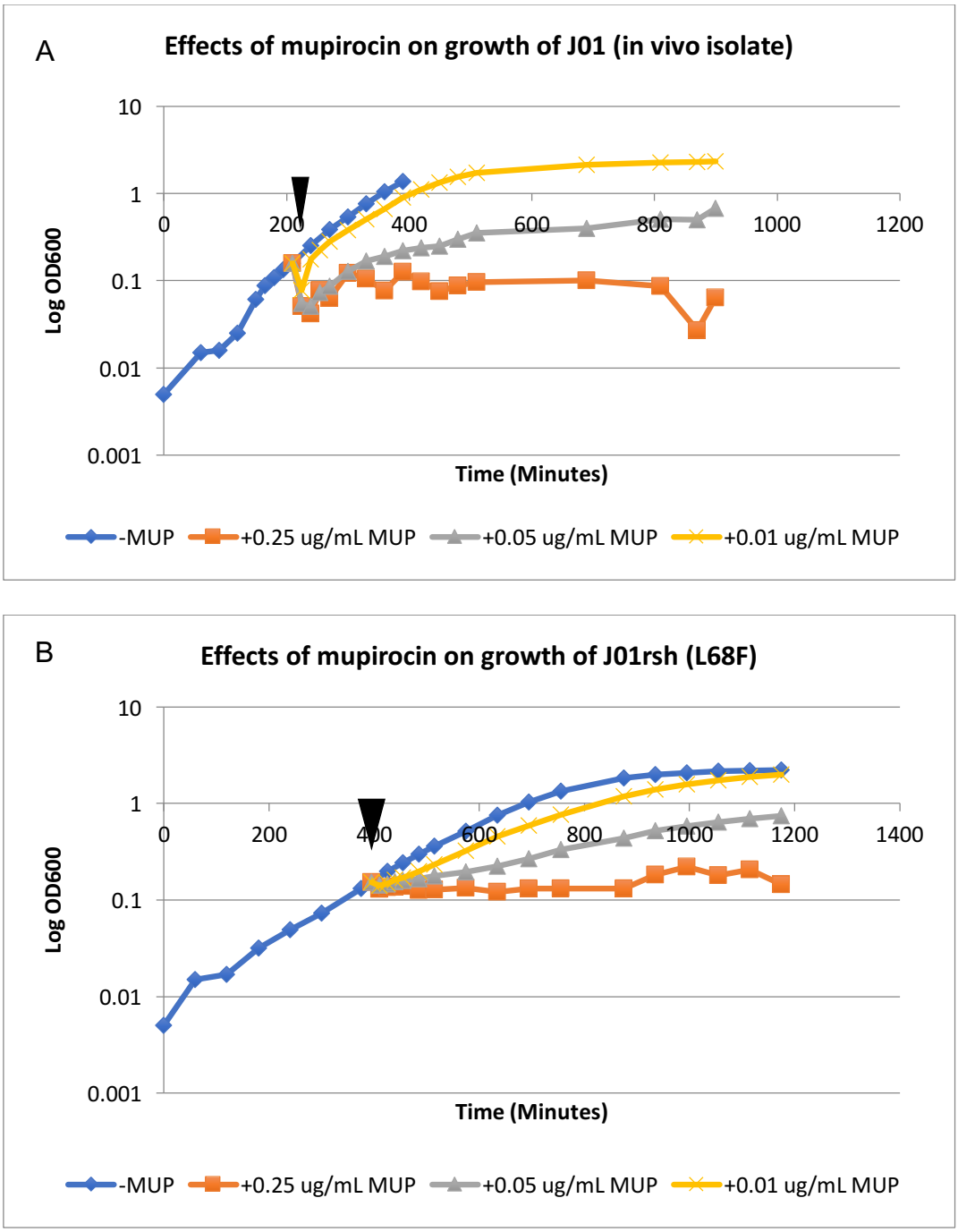

Appendix Figure 2. MRSA J01 and J01 *rsh* (L68F) growth curves to determine mupirocin treatment concentration. A. J01 and B. J01 *rsh* (L68F) cells were grown in low-phosphate TMS broth and treated with 0.01-0.25 µg/mL mupirocin.

(p)ppGpp determination experiments yield contradictory results. To examine (p)ppGpp levels of J01 and J01 *rsh* (L68F), the strains were radiolabeled with ^{32}P-orthophosphate, grown in low-phosphate TMS, treated with 0.01 µg/mL of mupirocin, and (p)ppGpp accumulation was observed every hour for five hours. Results show (p)ppGpp production in J01 treated with and without 0.01 µg/mL mupirocin. Production of (p)ppGpp regardless of inducer suggests that either the mupirocin concentration is not high enough or the later time points are from starvation (OD ~ 0.2 at T=0) (Appendix Figure 3). J01 *rsh* (L68F) without mupirocin showed increasing (p)ppGpp levels but addition of mupirocin showed no increase in (p)ppGpp and very little GTP. Because the stringent response is usually a fast response, we decided to lower the time points. Note that mupirocin is not a good drug to use for this strain.

Shorter time points do not clarify the (p)ppGpp induction data. During the short-term experiment, we see (p)ppGpp in wild type (J01) strains with and without mupirocin treatment (Appendix Figure 4A). In untreated cells, we see accumulation of pppGpp by 60 minutes, likely due to starvation. In J01rsh(L68F) strains, ppGpp is apparent with and without mupirocin (Appendix Figure 4B). In light of our recent work with USA300 strain, it is possible that these MRSA strains have high basal levels of ppGpp, since the spot is always visible. Perhaps the persistent ppGpp aids in resilience to antibiotics and other treatments.

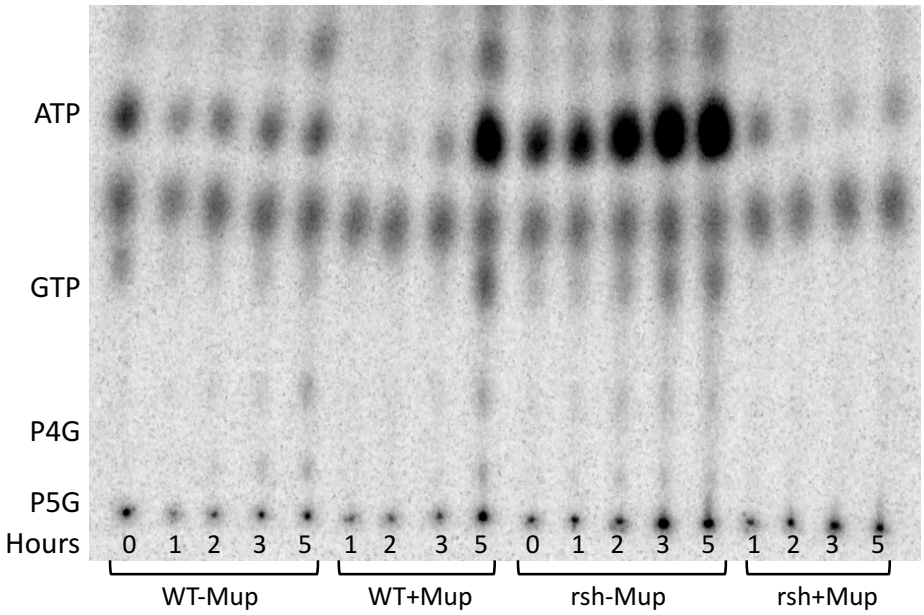

Appendix Figure 3. (p)ppGpp is produced at steady-state/stationary phase, but not during mupirocin treatment.

A Wild type (J01)

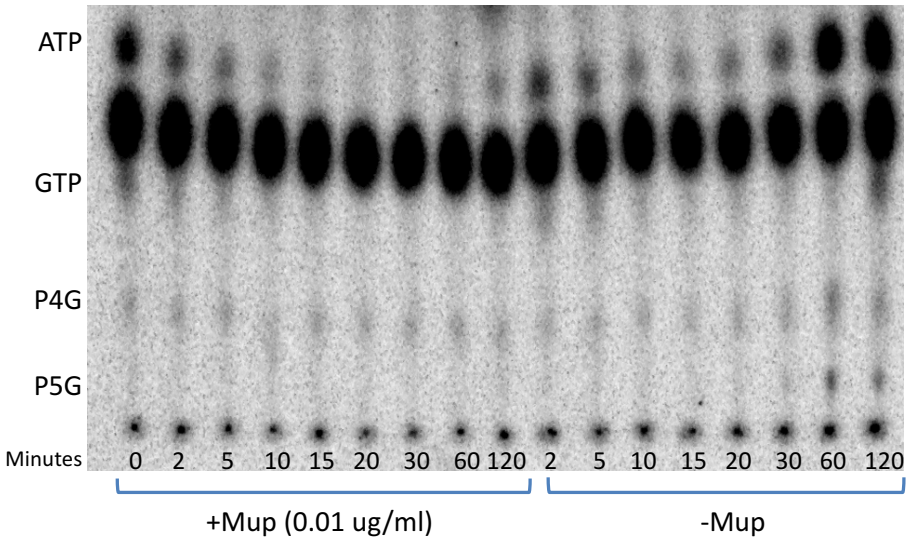

B J01*rsh* (L68F)

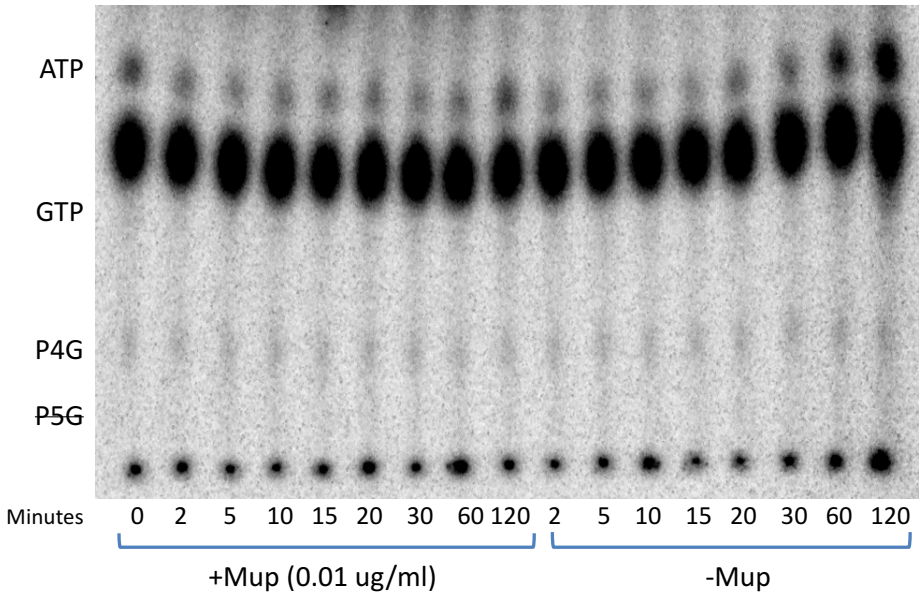

Appendix Figure 4. Nucleotide levels of J01 and J01 *rsh* (L68F) treated with mupirocin from 0-120 minutes.

Conclusions and Troubleshooting

The inconsistent results in this work motivated us to seek alternative approaches to handling these MRSA strains. First, these strains should be grown with a media used by the Wolz group, who works with *S. aureus*, because there is existing data with which we can compare our data (Geiger et al., 2014). Second, as noted above, USA300 is resistant to mupirocin, which means that all of the data is questionable. The growth curve data suggest that a higher mupirocin concentration (0.25 µg/mL) inhibits growth, so future work can either use that concentration or arginine hydroxamate can be used as an alternative. All in all, we are in our infancy working with *S. aureus* and need to work to refine our protocols.

Materials and Methods

Measurement of intracellular nucleotides by thin-layer chromatography

To measure intracellular nucleotides, single *S. aureus* colonies were taken from TSA plates and grown in TSB overnight. The following day, the cultures were back-diluted 1:100 into low-phosphate Tris-minimal succinate media with casamino acids (TMS) (see below) containing ^{32}P-orthophosphate (50 µCi of ^{32}P orthophosphate (900 mCi/mmol; Perkin Elmer) per 1 mL cells). At OD_{600} ≈ 0.15, mupirocin (0.01-0.25 µg/mL) were added and samples were collected at regular time points for nucleotide extraction. Nucleotides were extracted by incubating 100 µL cells with 20 µL of 2 N formic acid for at least 20 minutes. Samples were spotted on PEI cellulose thin-layer chromatography (TLC) plates (Selecto) and developed in 1.5 M or 0.85 M potassium phosphate monobasic (KH_2PO_4, pH 3.4) buffer to separate (p)ppGpp or GTP, respectively. TLC plates were exposed on storage phosphor screens (GE Healthcare) and scanned on a Typhoon

imager (GE Healthcare). Intensities of nucleotide spots were quantified using ImageQuant software (Molecular Dynamics) and normalized to the number of phosphates in the corresponding nucleotide and ATP level at T=0 for comparison between samples.

Literature Cited

Brown, A., Fernández, I.S., Gordiyenko, Y., and Ramakrishnan, V. (2016). Ribosome-dependent activation of stringent control. Nature *534*, 1–16.

Corrigan, R.M., Bellows, L.E., Wood, A., and Gründling, A. (2016). ppGpp negatively impacts ribosome assembly affecting growth and antimicrobial tolerance in Gram-positive bacteria. Proc. Natl. Acad. Sci. 201522179.

Diep, B.A., Gill, S.R., Chang, R.F., Phan, T.H., Chen, J.H., Davidson, M.G., Lin, F., Lin, J., Carleton, H. a., Mongodin, E.F., et al. (2006). Complete genome sequence of USA300, an epidemic clone of community-acquired meticillin-resistant Staphylococcus aureus. Lancet *367*, 731–739.

Gao, W., Chua, K., Davies, J.K., Newton, H.J., Seemann, T., Harrison, P.F., Holmes, N.E., Rhee, H.W., Hong, J.I., Hartland, E.L., et al. (2010). Two novel point mutations in clinical *Staphylococcus aureus* reduce linezolid susceptibility and switch on the stringent response to promote persistent infection. PLoS Pathog. *6*.

Geiger, T., Kästle, B., Gratani, F.L., Goerke, C., and Wolz, C. (2014). Two small (p)ppGpp synthases in *Staphylococcus aureus* mediate tolerance against cell envelope stress conditions. J. Bacteriol. *196*, 894–902.

Hogg, T., Mechold, U., Malke, H., Cashel, M., and Hilgenfeld, R. (2004). Conformational antagonism between opposing active sites in a bifunctional RelA/SpoT homolog modulates (p)ppGpp metabolism during the stringent response. Cell *117*, 57–68.

Appendix Table 3. Strains associated with study.

Strain	Genotype
JDW2802	MRSA US300-derived *in vivo* patient isolate, DapS (J01)
JDW2803	MRSA US300-derived *in vivo* patient isolate, DapR (J03)
JDW2804	MRSA US300-derived *in vivo* patient isolate, DapS (J01) *rsh* (L68F)
JDW2805	MRSA US300-derived *in vivo* patient isolate, DapR (J03) *rsh* (L68F)

TMS recipe for culturing methicillin-resistant *Staphylococcus aureus*
Adapted from Rose Lab

25X Tris minimal salts stock (in 100 ml distilled water):
- 14.5 g NaCl
- 9.25 g KCl
- 2.75 g NH_4CL
- 0.36 g Na_2SO_4
- 0.68 g KH_2PO_4

Recipe for TMS media (in 950 mL distilled water):
- 40 ml 25X Tris minimal salts stock
- 12.1 g Tris base (**NOT** Tris HCl!)
- 16.6 g succinate
- 10.0 g casamino acids
  - pH ~9 prior to adjustment
  - adjust pH to 7.4 (using 12 M HCl) and autoclave.

To 1L sterile TMS media, add the following filter-sterilized solutions:
- 2 ml Tryptophan @ 10 mg/ml
- 1 ml Cysteine (22 mg/ml)
- 1 ml Thiamine (16.9 mg/ml)
- 1 ml Nicotinic Acid (1.23 mg/ml)
- 1 ml Pantothenic acid (0.5 mg/ml)
- 1 ml biotin (0.01 mg/ml)
- 1 ml $MgCl_2$ (95.3 mg/ml)
- 1 ml $CaCl_2$ (11.1 mg/ml)

- ABerti: for this, I usually measure out the mg quantities of each trace element (20 mg for tryptophan!), resuspend them all together in 10 ml water and filter-sterilize the suspension into the autoclaved TMS media. Should make 1 L final volume.

-JTse: Alternatively, make stocks of these solutions and add to TMS accordingly
-Notes: Dissolve biotin in 10% KOH and 90% ddH2O. Dissolve tryptophan in 10% KOH and 90% ddH2O. Dissolve cysteine in 1 M HCl. All other components can be dissolved in water.

- To make TMS iron-replete, supplement with 50 µM FeCl2
- To make low-phosphate media (for P-32 experiments), add 0.068 g of KH2PO4 instead of 0.68 g into the 25X Tris minimal salts stock.

Appendix 4: Unpublished Persistence Data

J.T.B. designed, executed, and analyzed all of the experiments in this section. The data is organized by chronological order with references to Excel files and by antibiotic.

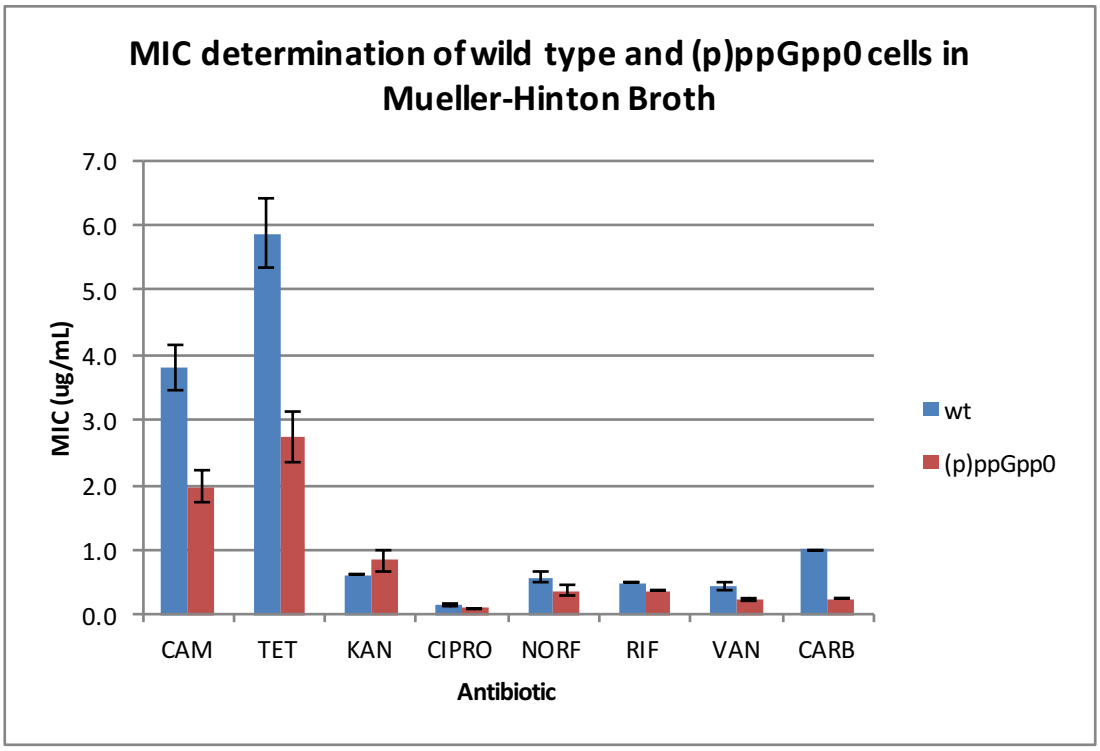

Appendix Figure 1. MIC determination for wild type and (p)ppGpp^0 cells in Mueller-Hinton broth
Purpose: To compare the MICs for wt and (p)ppGpp^0 on Mueller-Hinton Broth, the standard broth for determining MICs, according to the Clinical and Laboratory Standards Institute.

Conditions:

Growth Media	Mueller-Hinton broth
Strain Background	3610 *comI*^{Q12L}
O/N Method	Microdilution method
Kill Curve end point	Not kill curve
Treatment OD	Back-dilute to 1X10^6 cfu/mL
N	2-15

Conclusions: No difference in MIC. Two-fold difference is not enough to be considered resistant.

File Name: Average MIC-MuellerHinton, Graphed tab
Chart tab contains literature MIC values

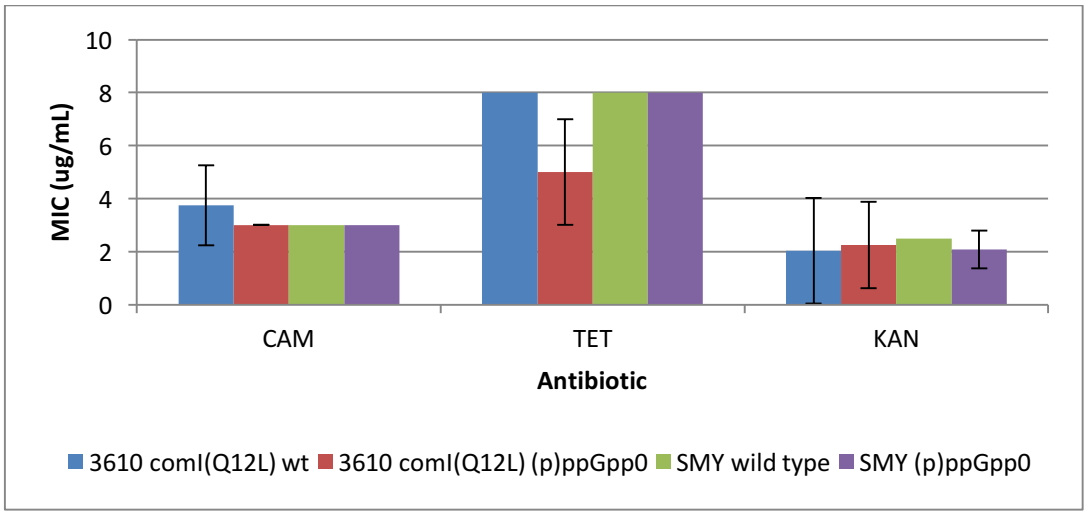

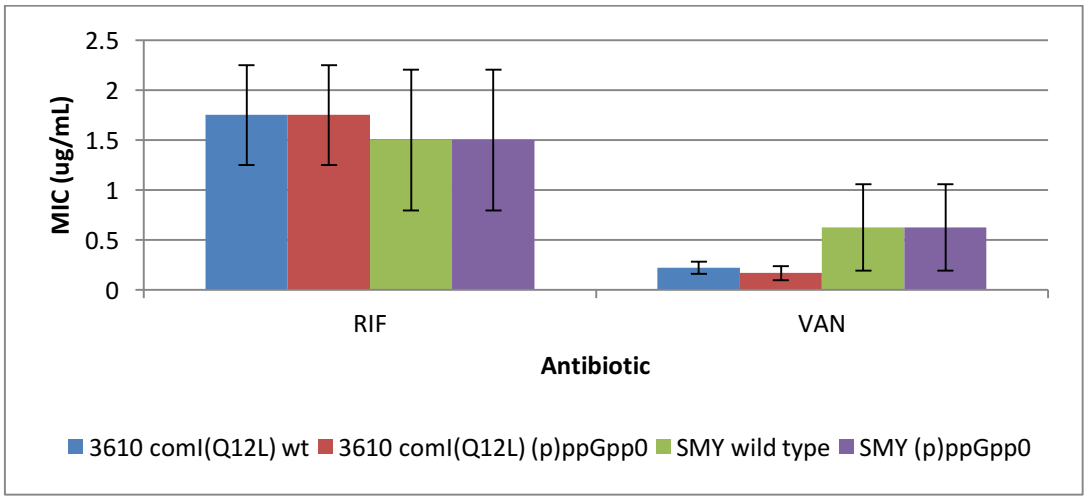

Appendix Figure 2. Comparison of MICs for 3610 *comI*^{Q12L} and SMY wild type and (p)ppGpp^{0} cells in S750+CAS

Purpose: To compare the MICs for wt and (p)ppGpp^{0} and across strain backgrounds.

Conditions:

Growth Media	S750+CAS
Strain Background	3610 *comI*^{Q12L} and SMY
O/N Method	Microdilution method
Kill Curve end point	Not kill curve
Treatment OD	Back-dilute to 1X10^{6} cfu/mL
N	4-8

Conclusions: No difference in MIC, regardless of strain background.

File Name: Average MIC-MinCAA, Graphed tab
Chart tab contains literature MIC values

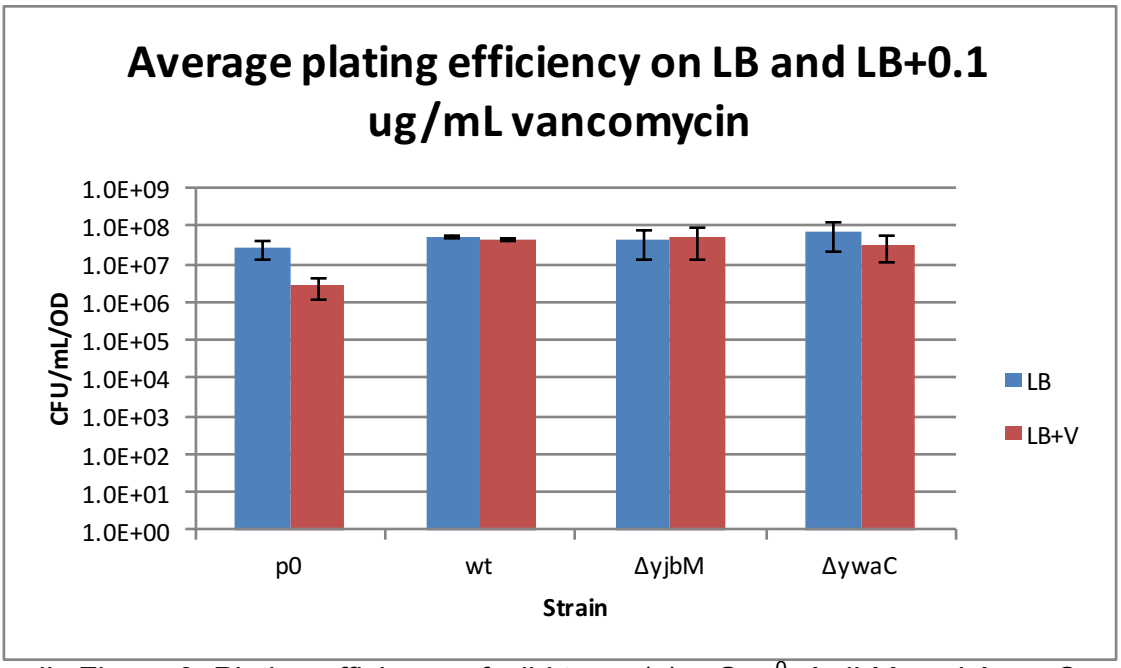

Appendix Figure 3. Plating efficiency of wild type, (p)ppGpp^0, Δ*yjbM*, and Δ*ywaC* on LB+vancomycin

Raw data

	LB Average	LB StDev	LB+V Average	LB+V StDev
(p)ppGpp^0	2.7E+07	14828163.19	2.6E+06	1391680.119
wt	5.4E+07	4903386.502	4.2E+07	4817142.728
Δ*yjbM*	4.6E+07	32090185.45	4.8E+07	34516564.12
Δ*ywaC*	6.8E+07	46093751.33	3.2E+07	20234456.3

Purpose: To determine if (p)ppGpp protects cells against vancomycin in plates at ~0.5X MIC.

Conditions:

Growth Media	LB
Strain Background	SMY
O/N Method	Single colony
Kill Curve end point	Not kill curve, plating directly onto plates containing drug
Treatment OD	0.2-0.5
N	3 (averaged data shown)

Conclusions: (p)ppGpp^0 protects 10-fold on plates, YwaC protects by 2-fold.

File Name: 2013-01-11-Vancomycin treatments of smy p0 and mutants (subMIC), Van averages tab

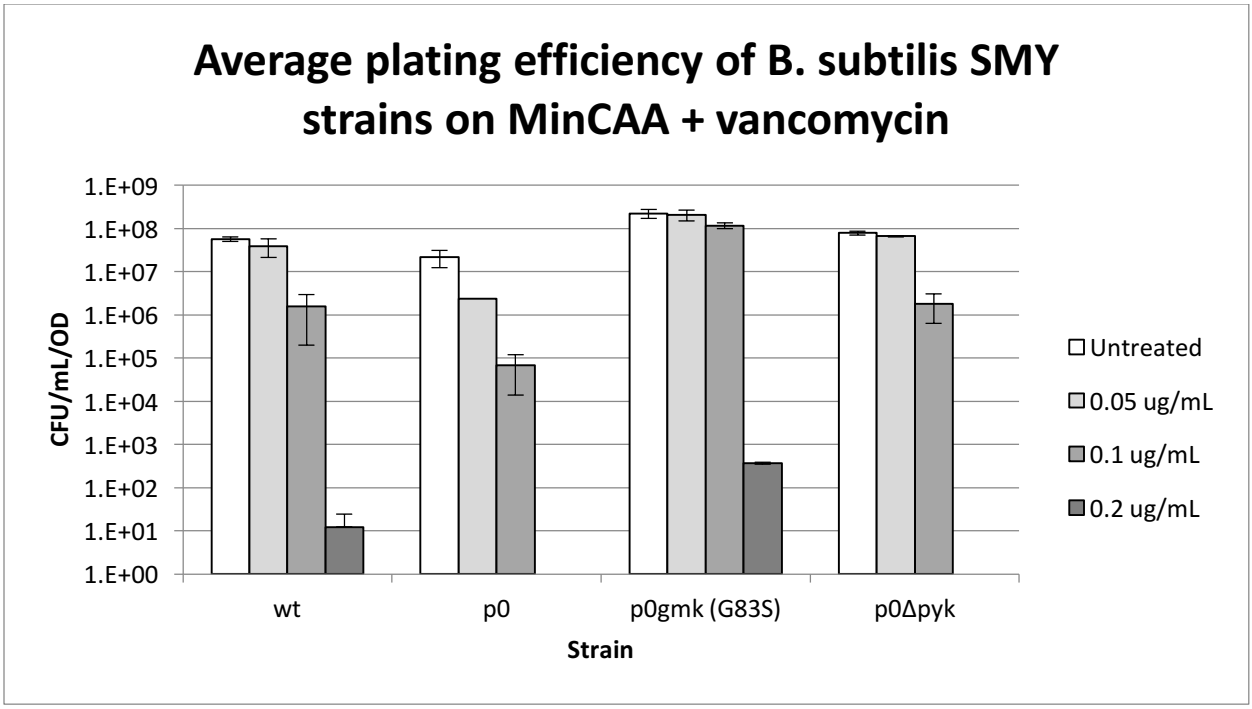

Appendix Figure 4. Plating efficiency of wild type, (p)ppGpp^0, and GTP biosynthesis mutants on S750+CAS+vancomycin.

Purpose: To determine if (p)ppGpp, decrease in GTP, or Δ*pyk* in (p)ppGpp^0 cells will survive vancomycin on plates.

Conditions:

Growth Media	S750+CAS
Strain Background	SMY
O/N Method	Single colony
Kill Curve end point	Not kill curve, plating directly onto plates containing drug
Treatment OD	0.2-0.5
N	At least 2

Conclusions: (p)ppGpp protects on 0.05-0.2 µg/mL vancomycin on plates. Lowering GTP in (p)ppGpp^0 *gmk*^{G83S} or deleting *pyk* also rescues cells in 0.1 µg/mL vancomycin.

File Name: 2013-06-10-Antibiotic plating efficiency

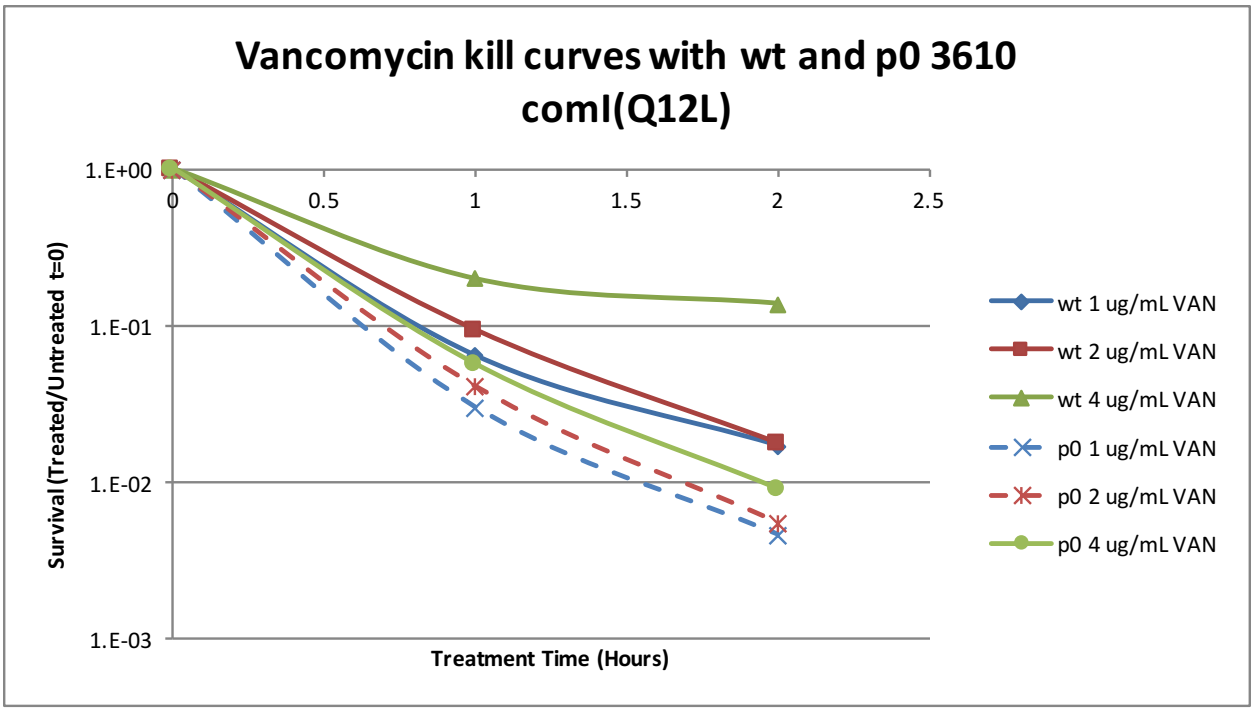

Appendix Figure 5. Kill curves of wild type and (p)ppGpp^0 cells using 1-4 µg/mL vancomycin

Purpose: To determine if (p)ppGpp protects cells against vancomycin killing at different concentrations.

Conditions:

Growth Media	S750+CAS
Strain Background	3610 *comI*^{Q12L} (JDW2144)
O/N Method	Likely single colony
Kill Curve end point	2 hr
Treatment OD	0.3-0.4
N	1

Conclusions: There appears to be a difference in killing at 4 µg/mL VAN, which is 16X MIC.

File Name: 2014-01-19-Vancomycin kill curves, 2014-01-19 tab

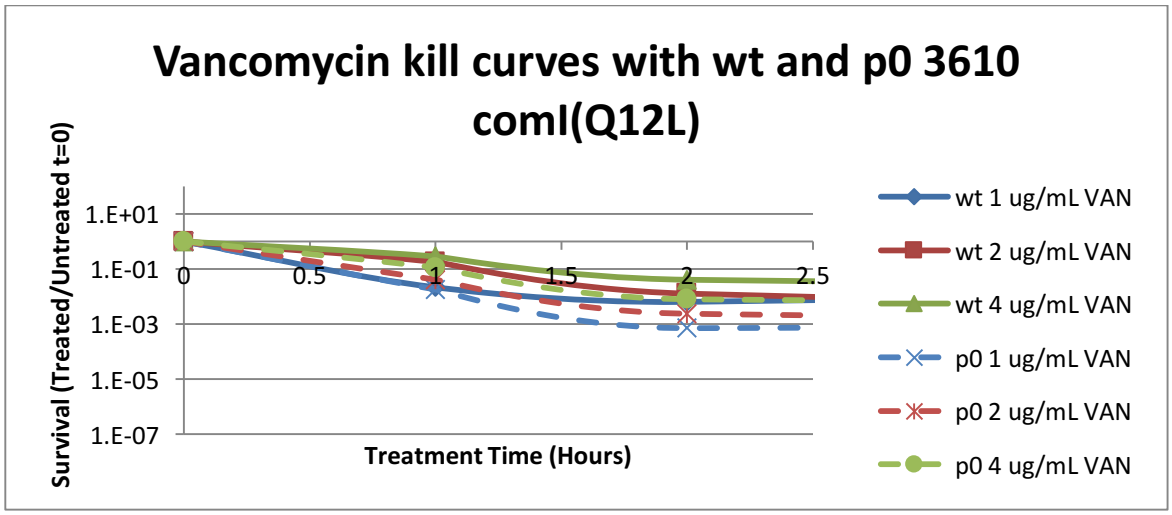

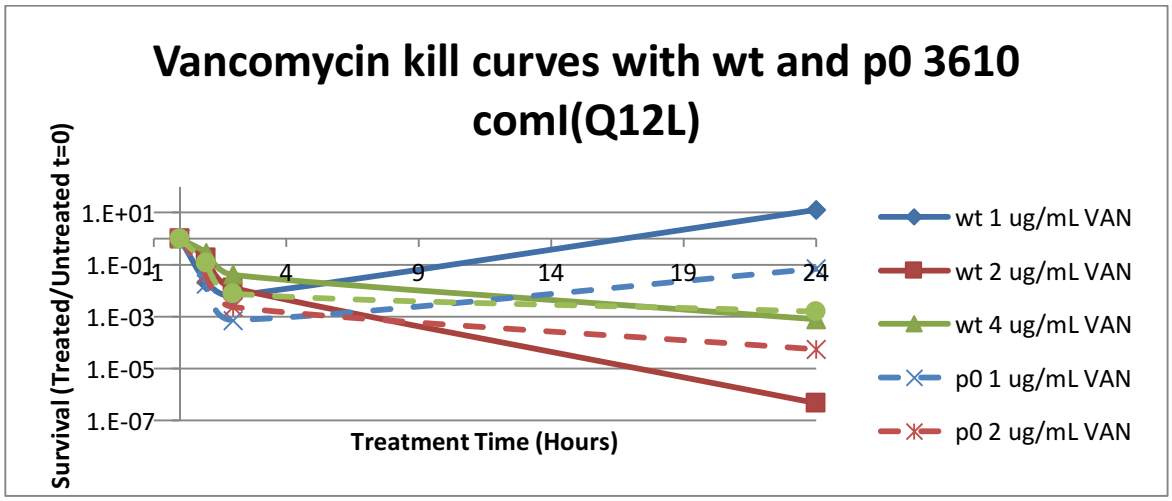

Appendix Figure 6. Extended kill curves of wild type and (p)ppGpp^0 cells treated with 1-4 µg/mL vancomycin.

Purpose: To determine if (p)ppGpp protects cells against vancomycin killing at different concentrations, repeat. The culture was treated for 24 hours and plated again.

Conditions:

Growth Media	S750+CAS
Strain Background	3610 *comI*^{Q12L} (JDW2144)
O/N Method	Likely single colony
Kill Curve end point	2 hr – 24hr
Treatment OD	0.3
N	1

Conclusions: Killing appears to be less clear here.

File Name: 2014-01-19-Vancomycin kill curves, 2014-01-21 tab

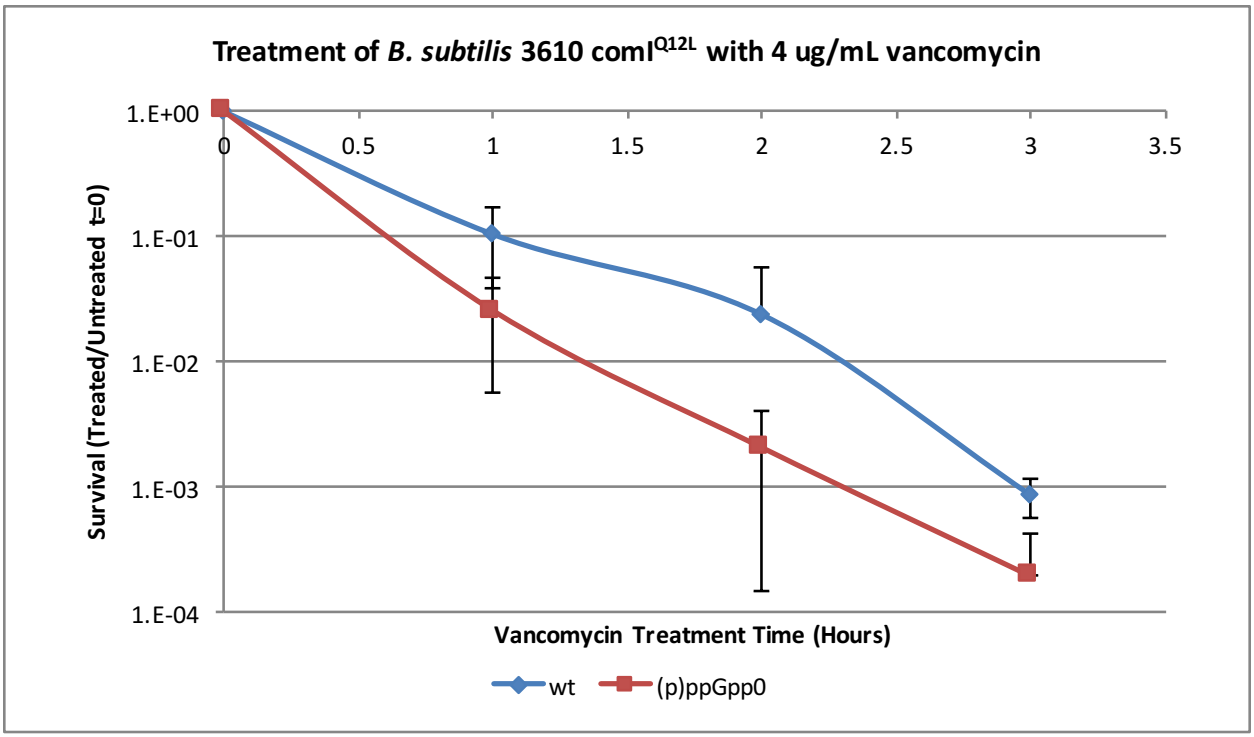

Appendix Figure 7. Kill curve of 3610 *comI*^{Q12L} wild type and (p)ppGpp^{0} treated with 4 µg/mL vancomycin.

Purpose: To determine if (p)ppGpp protects cells against vancomycin at 4 µg/mL.

Conditions:

Growth Media	S750+CAS
Strain Background	3610 *comI*^{Q12L} (JDW2144)
O/N Method	Likely single colony
Kill Curve end point	3hr
Treatment OD	0.25-0.4
N	4, from 6Feb14, 17Feb14, 21Feb14

Conclusions: Wild type survives VAN better than (p)ppGpp^{0} in kill surve.

File Name: 2014-01-19-Vancomycin kill curves, 2014-02-06-Triplicate tab

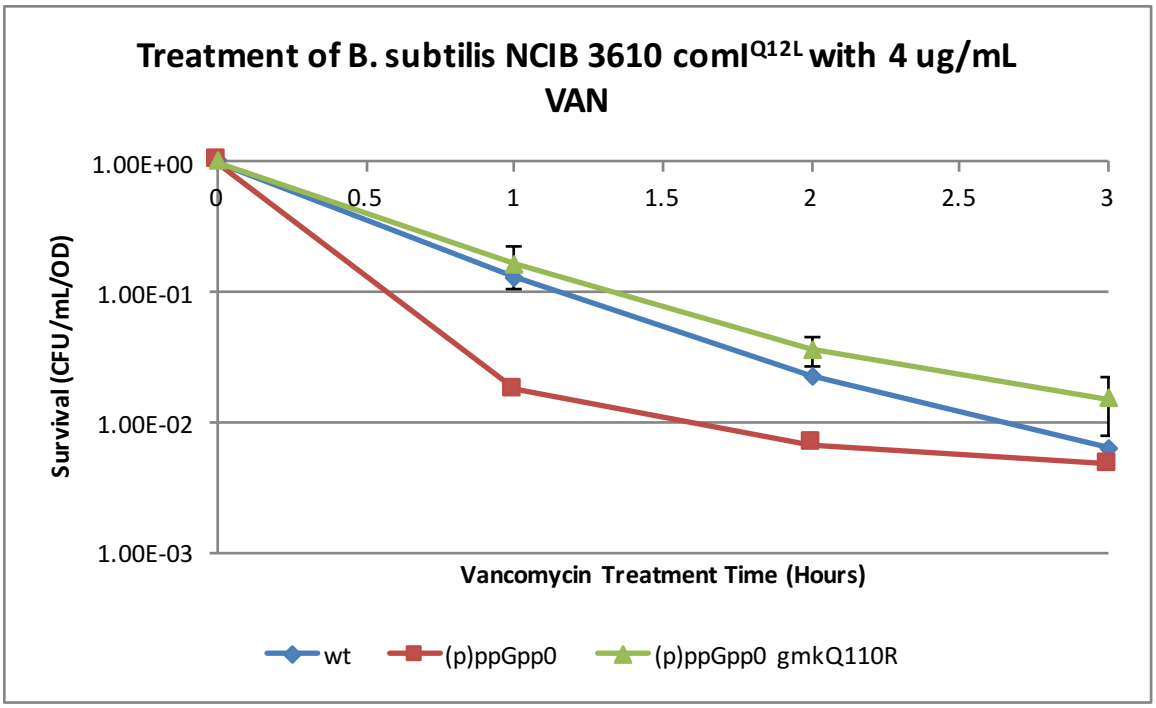

Appendix Figure 8. Kill curve of 3610 *comI*^{Q12L} wild type, (p)ppGpp^{0}, and (p)ppGpp^{0} *gmk*^{Q110R} treated with 4 µg/mL vancomycin.

Purpose: To determine if (p)ppGpp or decreasing GTP (using (p)ppGpp^{0} *gmk*^{Q110R}) in (p)ppGpp^{0} cells protects against vancomycin at 4 µg/mL.

Conditions:

Growth Media	LB
Strain Background	3610 *comI*^{Q12L} (JDW2144)
O/N Method	Likely single colony
Kill Curve end point	3hr
Treatment OD	0.2-0.3
N	3 for (p)ppGpp^{0} *gmk*^{Q110R}, N=1 for wt, (p)ppGpp^{0}

Conclusions: Wild type and (p)ppGpp^{0} *gmk*^{Q110R} survive similarly.

File Name: 2014-01-19-Vancomycin kill curves, 2015-09-13-gmk tab

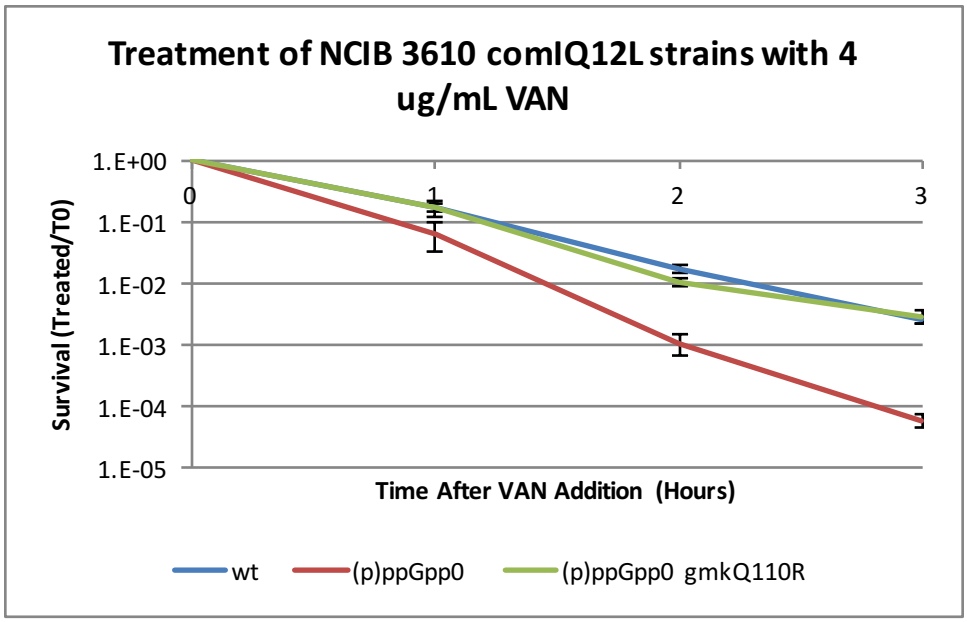

Appendix Figure 9. Kill curve of 3610 *coml*^{Q12L} wild type, (p)ppGpp^{0}, and (p)ppGpp^{0} *gmk*^{Q110R} treated with 4 µg/mL vancomycin.

Purpose: To determine if (p)ppGpp or decreasing GTP (using (p)ppGpp^{0} *gmk*^{Q110R}) in (p)ppGpp^{0} cells protects against vancomycin at 4 µg/mL.

Conditions:

Growth Media	S750+CAS
Strain Background	3610 *coml*^{Q12L} (JDW2144)
O/N Method	O/N plate, back-dilute to 0.005. O/N OD ranged from 0.144-0.56
Kill Curve end point	3hr
Treatment OD	0.2-0.27
N	3 for all

Conclusions: Wild type and (p)ppGpp^{0} *gmk*^{Q110R} survive similarly, but not (p)ppGpp^{0}.

File Name: 2015-11-05-VAN3610Repeat, Sheet1 tab

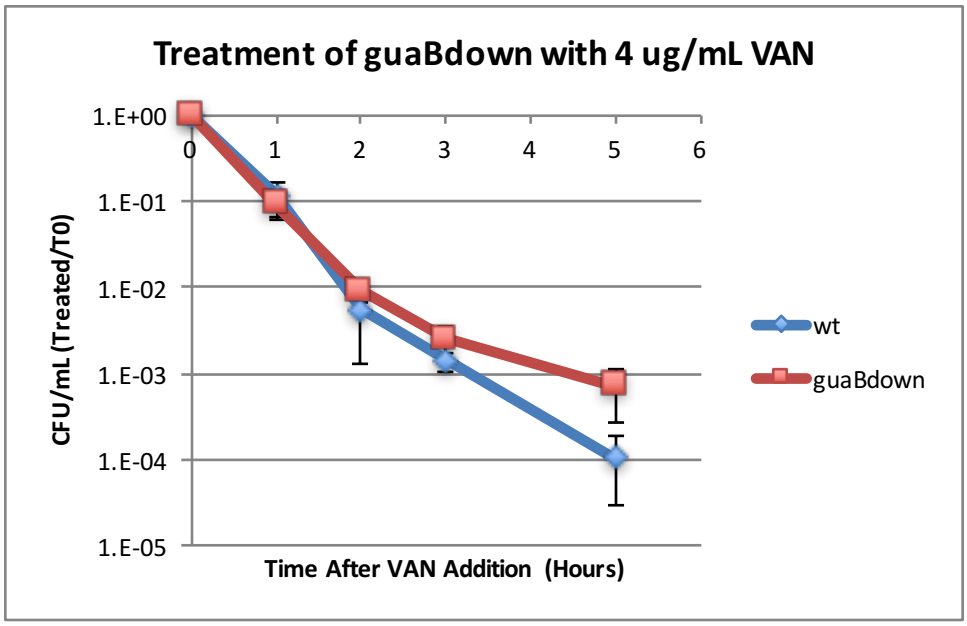

Appendix Figure 10. Kill curve of wild type and *guaB*^{down} treated with 4 µg/mL vancomycin.

Purpose: To determine whether decreasing GTP levels by depleting *guaB* will result in hypertolerance to 4 µg/mL vancomycin. *guaB* was depleted by growing the strain without IPTG for the duration of the experiment.

Conditions:

Growth Media	S750+CAS+WM
Strain Background	YB886
O/N Method	Single colony
Kill Curve end point	5hr
Treatment OD	0.2-0.4
N	2

Conclusions: Depleting GTP levels improves survival to vancomycin by about 10-fold.

File Name: 2016-07-05-guaBdownVAN, Average tab

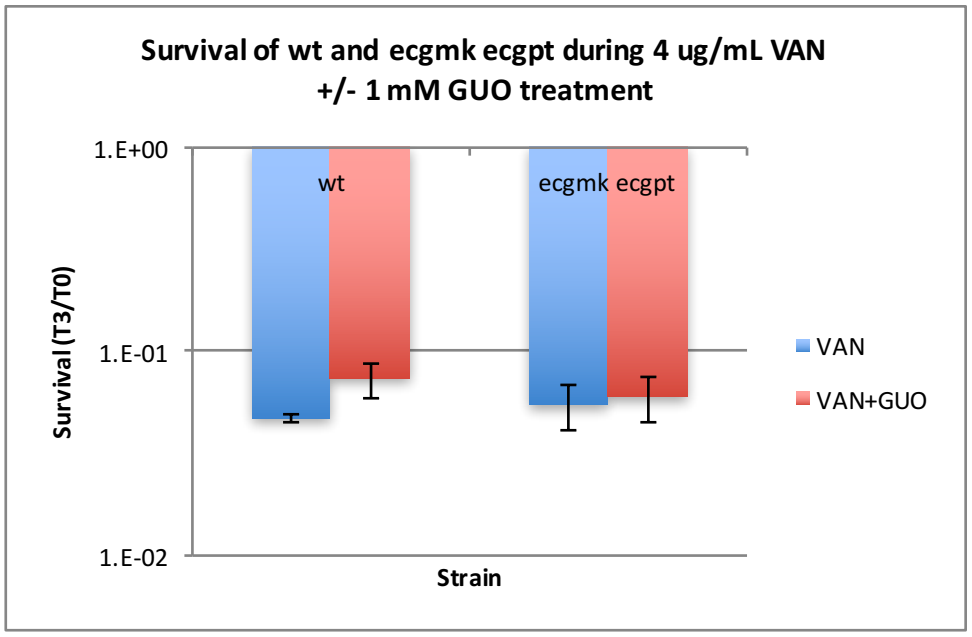

Appendix Figure 11. Kill curve of wild type and *ecgmk* treated with 4 µg/mL vancomycin and 1 mM guanosine.

Purpose: To determine whether increasing GTP levels in wild type cells (using Kuanqing Liu's *ecgmk ecgpt* strain [JDW2121]) will potentiate killing by 4 µg/mL vancomycin. Guanosine is added to increase GTP levels through the salvage pathway, since *E. coli* Gpt is not inhibited as much as *B. subtilis* HprT (see data in Chapter 4).

Conditions:

Growth Media	S750+CAS
Strain Background	SMY
O/N Method	O/N, start flasks at 0.001, reach 0.2, back-dilute to 0.04, then treat at OD = 0.2-0.4 (Type I persisters should be diluted out) O/N ODs range from 0.27-0.52
Kill Curve end point	End point at 3hr
Treatment OD	0.178-0.25
N	2

Conclusions: Increasing GTP in (p)ppGpp-containing cells does not seem to decrease survival to VAN. The values are very spread out within each strain.

File Name: 2015-10-09-ecgmkecgptGUOCIPVAN, 11-12-15-VANTreat tab

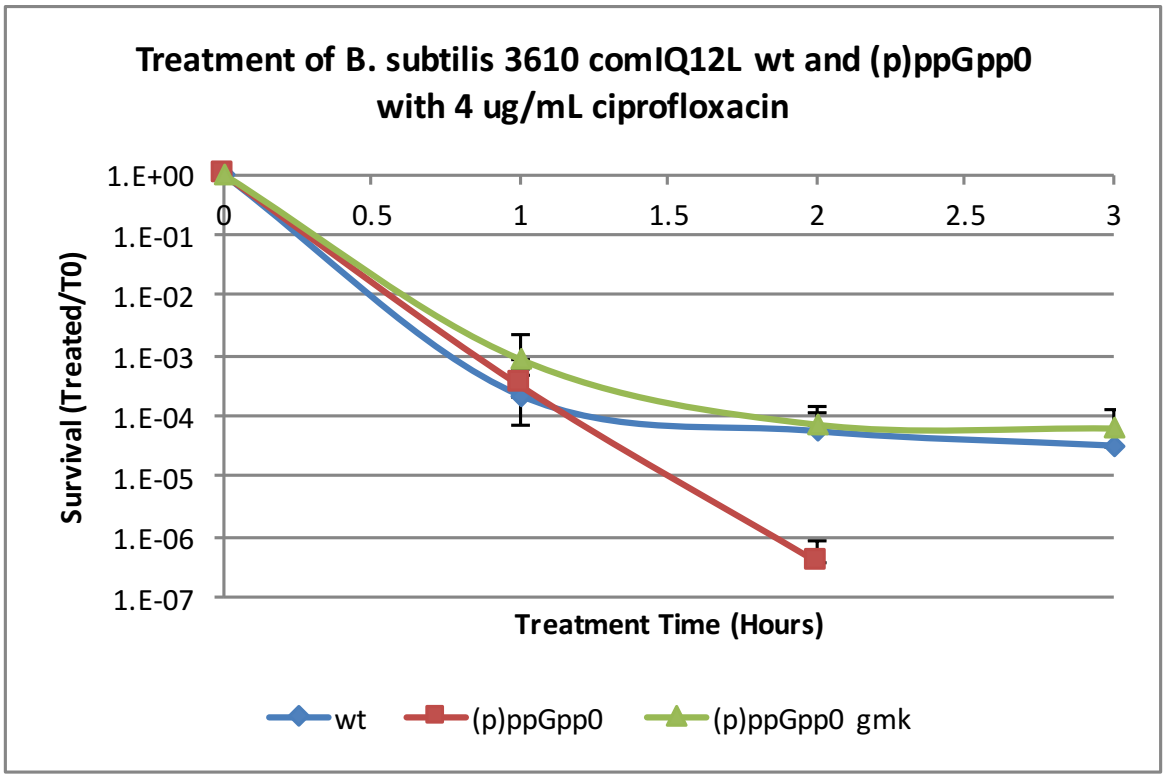

Appendix Figure 12. Kill curve of wild type, (p)ppGpp^0, and (p)ppGpp^0 *gmk*^{Q110R} treated with 4 µg/mL ciprofloxacin.

Purpose: To determine if (p)ppGpp or decreasing GTP in (p)ppGpp^0 cells protects against ciprofloxacin at 4 µg/mL. (p)ppGpp^0 at T=3 hours was not graphed because there were no colonies.

Conditions:

Growth Media	S750+CAS
Strain Background	3610 *coml*^{Q12L} (JDW2144)
O/N Method	Likely single colony
Kill Curve end point	3hr
Treatment OD	0.2-0.4
N	3

Conclusions: Wild type and (p)ppGpp^0 *gmk*^{Q110R} survive similarly and better than (p)ppGpp^0.

File Name: 2014-03-27-Ciprofloxacin kill curves, Summary tab

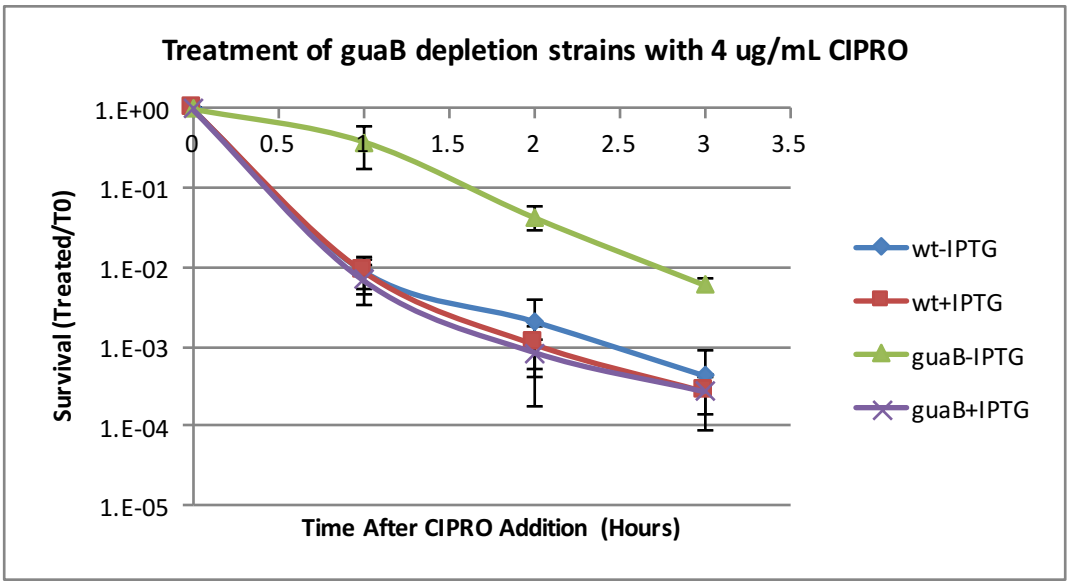

Appendix Figure 13. Kill curve of wild type and *guaB*^{down} treated with 4 µg/mL ciprofloxacin.

Purpose: To determine whether decreasing GTP levels by depleting *guaB* will result in hypertolerance to 4 µg/mL ciprofloxacin. *guaB* was depleted by growing the strain without IPTG for the duration of the experiment.

Conditions:

Growth Media	S750+CAS+WM
Strain Background	YB886
O/N Method	Single colony
Kill Curve end point	3hr
Treatment OD	0.2-0.26
N	3

Conclusions: Depleting GTP levels improves survival to ciprofloxacin. Further, comparing the wild type YB886 and 3610 *comI*^{Q12L}, there is a 10-fold increase in survival for YB886, suggesting that the SPβ phage plays a role in killing 3610.

File Name: 2014-10-22-GuaBDepletionVanCipro, CIPRO summary tab

Vancomycin treatment is also in this file, but I did not deplete *guaB* for the duration of this experiment.

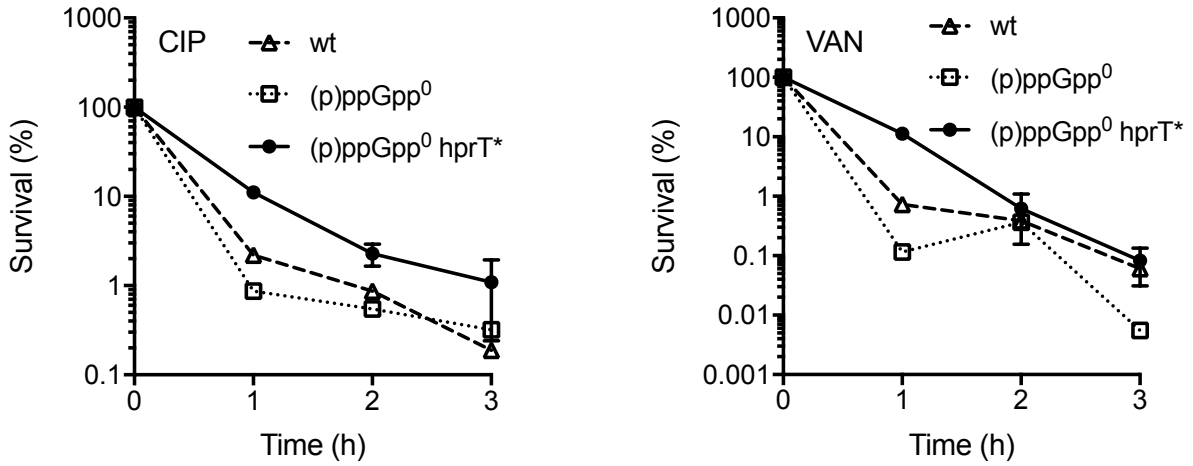

YB886 data
wt and (p)ppGpp0 are N=1
(p)ppGpp0 hprT* are N=3

Appendix Figure 14. Kill curve of wild type, (p)ppGpp^0, and (p)ppGpp^0 *hprT** treated with vancomycin and ciprofloxacin.

Purpose: To determine whether decreasing GTP levels in (p)ppGpp^0 (from an *hprT* suppressor (JDW1850, A insertion at position 14)) will improve survival to ciprofloxacin and vancomycin. (p)ppGpp^0 hprT is also a slow grower.

Conditions:

Growth Media	S750+CAS+WM
Strain Background	YB886
O/N Method	O/N on plates, O/N OD ranged from 0.3-0.8 for (p)ppGpp^0 *hprT**, 2.5 for wild type and (p)ppGpp^0. All back-diluted to 0.005. Did not record how old the overnight was.
Kill Curve end point	3hr
Treatment OD	0.2-0.33, 0.46 for (p)ppGpp^0 in CIP treatment
N	3 for (p)ppGpp^0 *hprT** only, N=1 for wild type and (p)ppGpp^0

Conclusions: Decreasing GTP and/or decrease in growth rate improves survival to ciprofloxacin and vancomycin. This is only N=1 for wild type and (p)ppGpp^0 though.

File Name: 2015-08-20-slowgrowthhprt, hprtVAN and hprtCIPRO tab

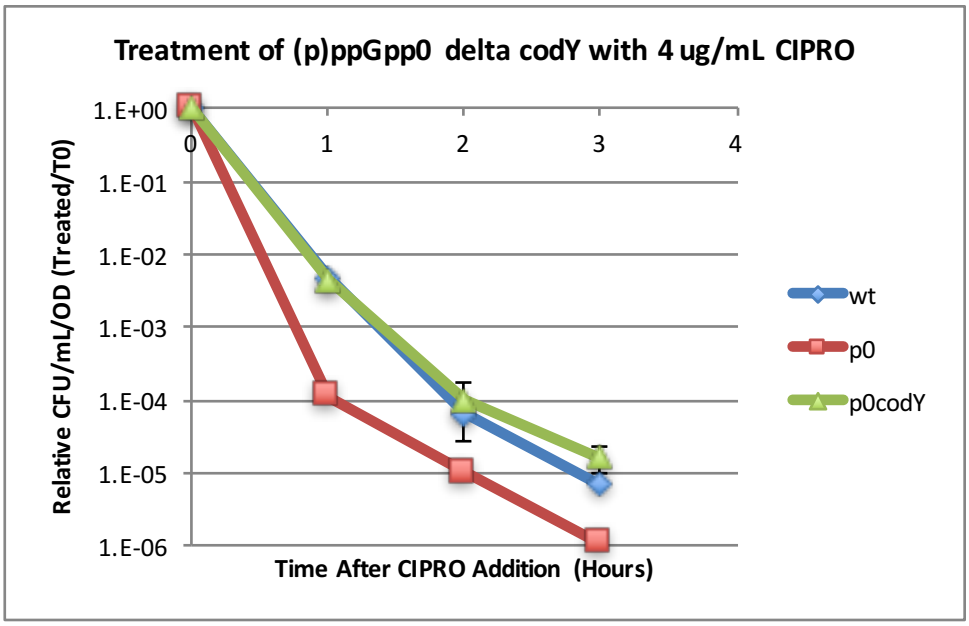

Appendix Figure 15. Kill curve of wild type, (p)ppGpp^0, and (p)ppGpp^0 Δ*codY* treated with ciprofloxacin.

Purpose: To determine whether CodY plays a role in ciprofloxacin survival.

Conditions:

Growth Media	S750+CAS
Strain Background	SMY
O/N Method	Grow to 0.13-0.18, back-dilute 100-fold, then treat
Kill Curve end point	3hr
Treatment OD	0.2-0.3
N	3 for (p)ppGpp^0 Δ*codY* only, N=1 for wt and (p)ppGpp^0

Conclusions: (p)ppGpp^0 Δ*codY* survives ciprofloxacin as well as wild type, likely because CodY controls transcription of *guaB* and decreases GTP in that manner, as explained in Kriel *et al*., 2012. A separate experiment comparing wt and Δ*codY* indicated no differences (see Chapter 3).

File Name: 2016-02-08-CodYCipro, Sheet1 tab

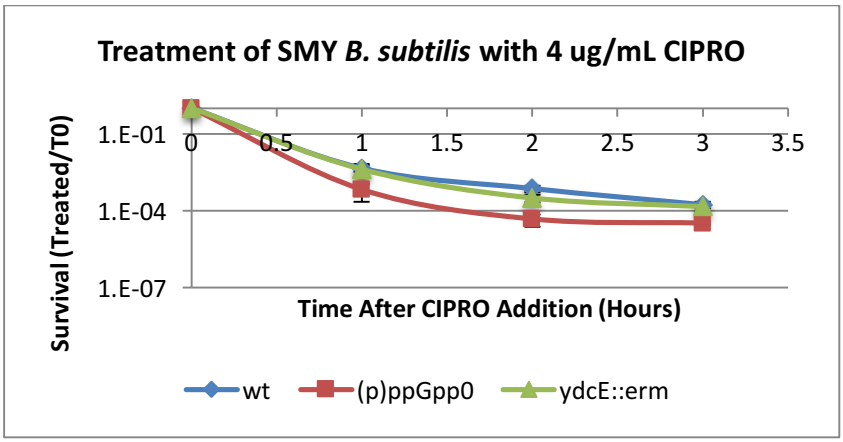

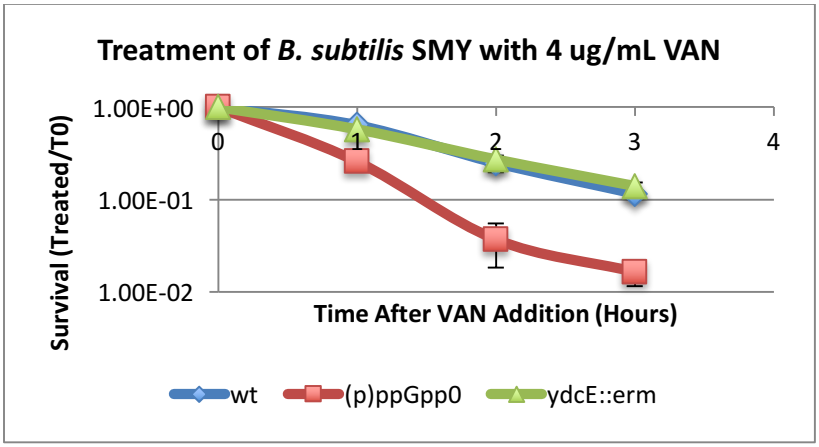

Appendix Figure 16. Kill curve of wild type, (p)ppGpp^0, and Δ*ydcE*::*erm* treated with vancomycin and ciprofloxacin.

Purpose: Determine whether Δ*ydcE*, a homolog of *E. coli* toxin MazF will affect survival during vancomycin and ciprofloxacin treatment.

Conditions:

Growth Media	S750+CAS
Strain Background	SMY
O/N Method	Likely single colony
Kill Curve end point	3hr
Treatment OD	0.2-0.4 for VAN, 0.2 for CIP
N	3

Conclusions: Δ*ydcE* does not affect survival to vancomycin or ciprofloxacin. Although deleting just one toxin is not sufficient to determine the effects of toxin-antitoxin modules, this conclusion is not changed after deletion of three known toxins, as demonstrated in Chapter 3.

File Name: 2015-02-17-ydcE Study, CIPSum and VANSum tabs.

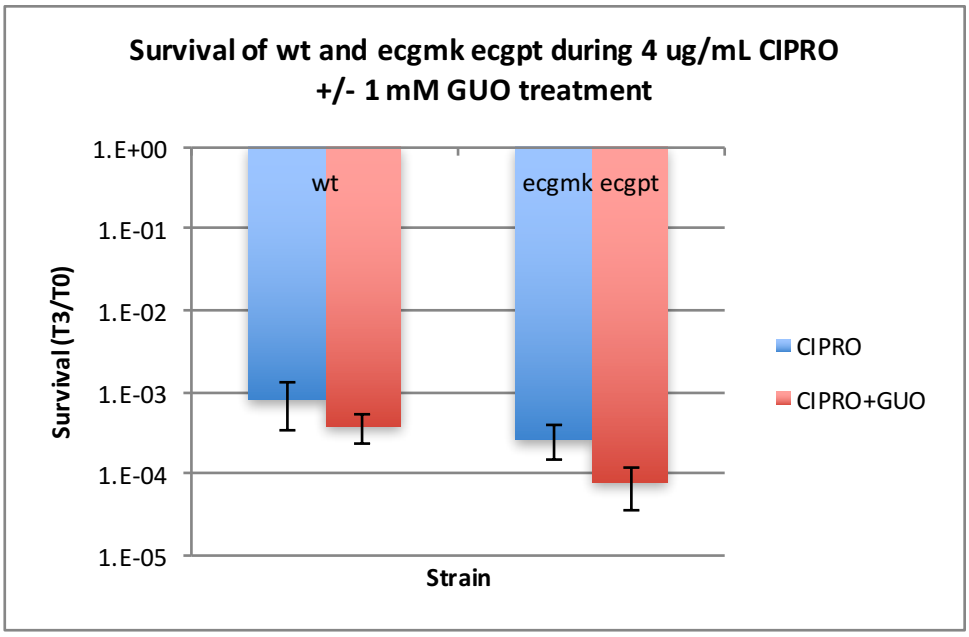

Appendix Figure 17. Kill curve of wild type and *ecgmk ecgpt* treated with 4 µg/mL ciprofloxacin and 1 mM guanosine.

Purpose: To determine whether increasing GTP levels in wt cells (using KQ's *ecgmk ecgpt* strain) will potentiate killing by 4 µg/mL ciprofloxacin. Guanosine is added to increase GTP levels through the salvage pathway, since *E. coli* Gpt is not inhibited as much as *B. subtilis* HprT.

Conditions:

Growth Media	S750+CAS
Strain Background	SMY
O/N Method	O/N, start flasks at 0.001, reach 0.2, back-dilute to 0.04, then treat at OD = 0.2-0.4 (Type I persisters should be diluted out) O/N ODs range from 0.27-0.52
Kill Curve end point	End point at 3hr
Treatment OD	0.178-0.25
N	2

Conclusions: Increasing GTP in (p)ppGpp-containing cells does not seem to decrease survival to CIPRO. The values are very spread out within each strain.

File Name: 2015-10-09-ecgmkecgptGUOCIPVAN, 11-12-15-CIPTreat tab

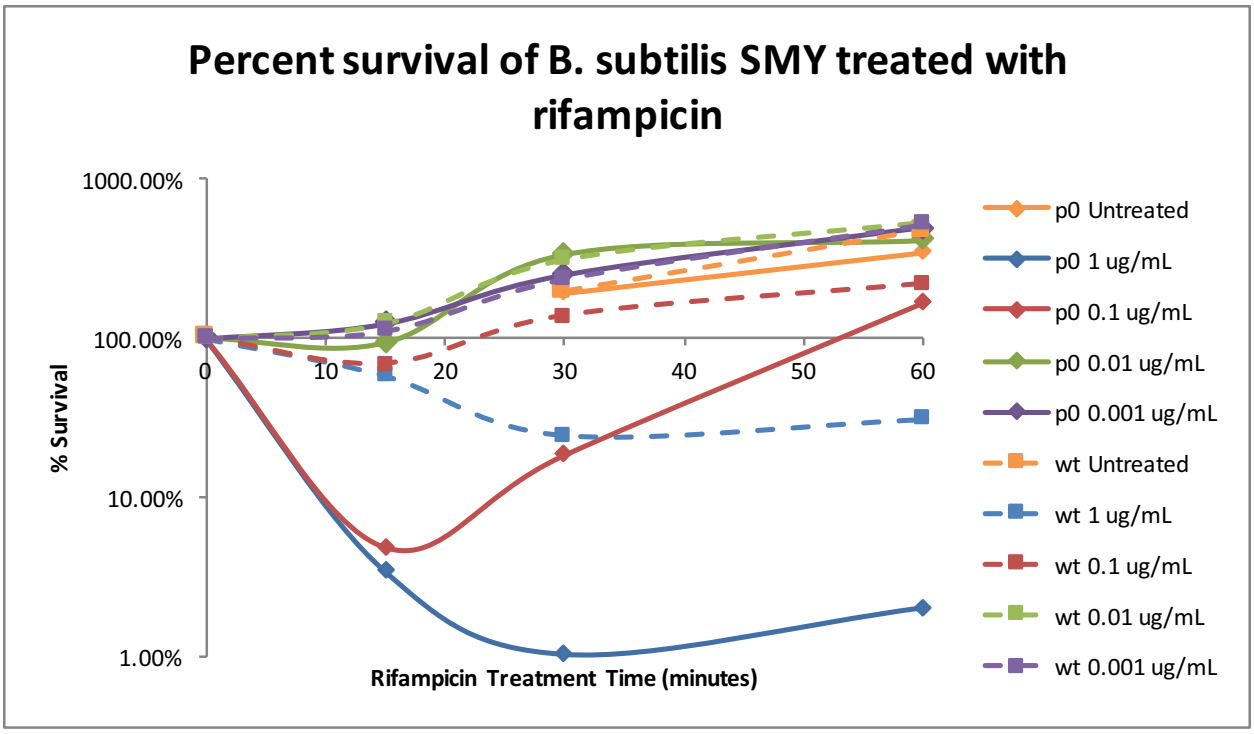

Appendix Figure 18. Kill curve of wild type and (p)ppGpp^0 cells treated with 0.001-1 µg/mL rifampicin.

Purpose: To determine if (p)ppGpp protects cells against rifampicin killing at different concentrations

Conditions:

Growth Media	LB
Strain Background	SMY
O/N Method	Single colony
Kill Curve end point	1 hr
Treatment OD	0.3
N	1

Conclusions: 10-20 fold difference between wild type and (p)ppGpp^0 at 1 µg/mL rifampicin, which is 0.5X MIC.

File Name: 2013-05-17-Rifampicin treatments of smy p0 and mutants, 17May13-CompareUntreated tab

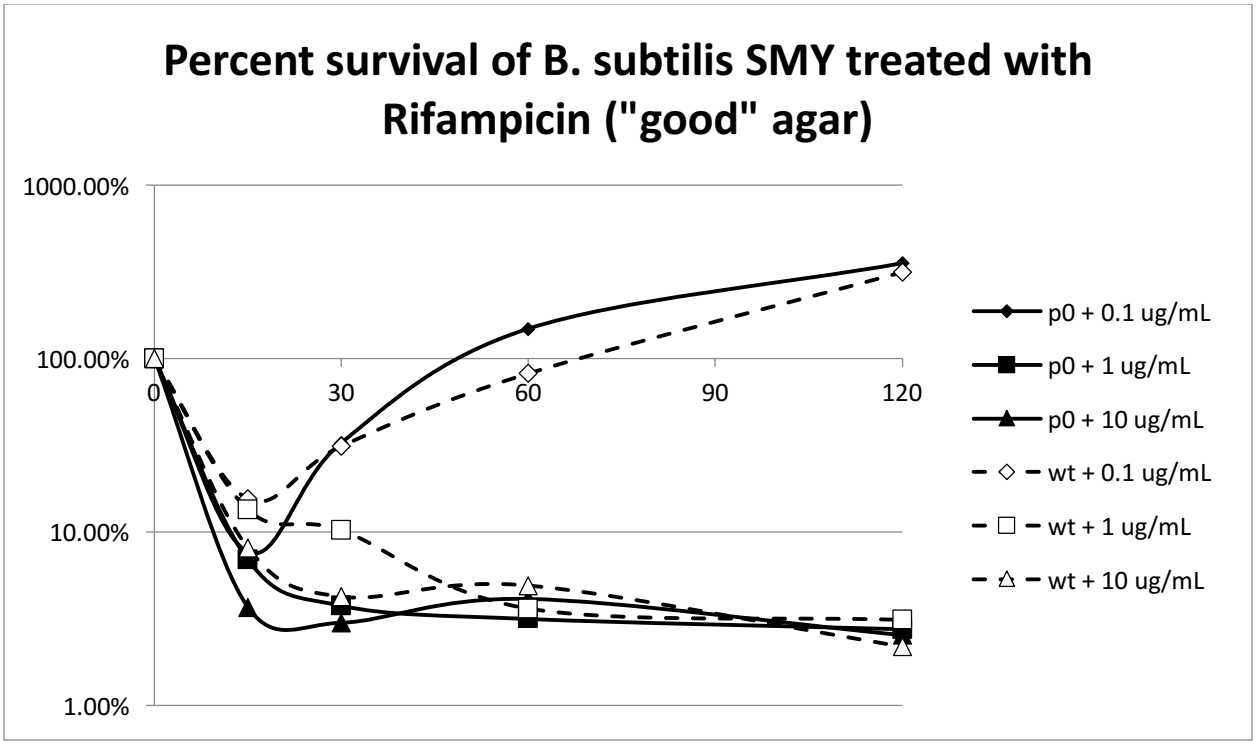

Appendix Figure 19. Kill curve of wild type and (p)ppGpp^0 cells treated with 0.1-10 µg/mL rifampicin

Purpose: To determine if (p)ppGpp protects cells against rifampicin killing at different concentrations. This experiment was performed in “good” agar, because a previous batch of agar was made using tryptone that smelled heavily of ammonia.

Conditions:

Growth Media	LB
Strain Background	SMY
O/N Method	Single colony
Kill Curve end point	2 hr
Treatment OD	0.25-0.3
N	1

Conclusions: Verification of 17May13 data – No differences detected at 1 µg/mL or 10 µg/mL rifampicin.

File Name: 2013-05-17-Rifampicin treatments of smy p0 and mutants, 23May13-RifTimeConc tab

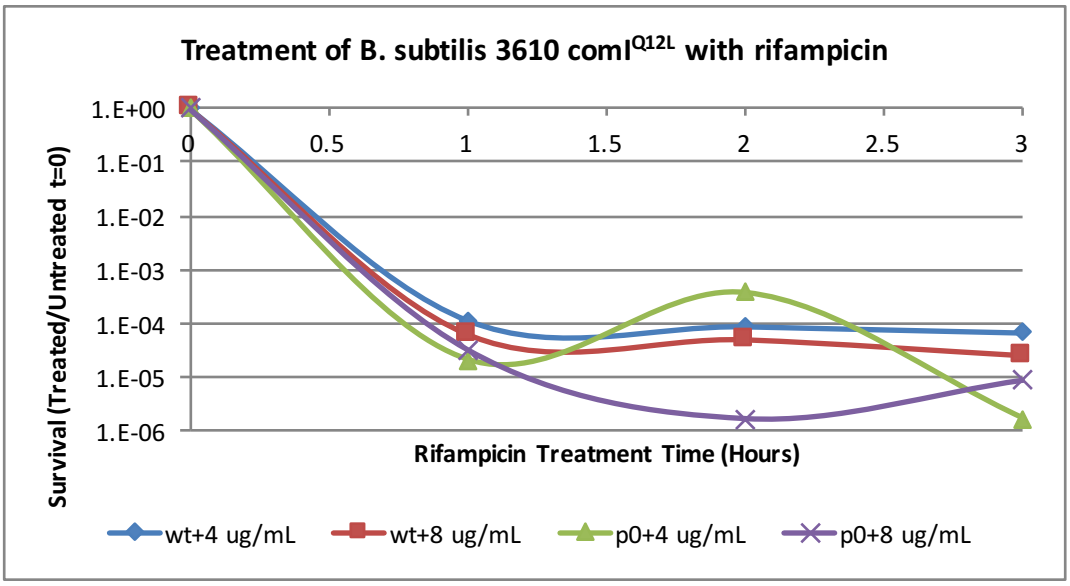

Appendix Figure 20. Kill curve of wild type and (p)ppGpp^0 cells treated with 4-8 µg/mL rifampicin.

Purpose: To determine if (p)ppGpp protects cells against rifampicin killing at 2X and 4X MIC (4 µg/mL and 8 µg/mL, respectively).

Conditions:

Growth Media	S750+CAS
Strain Background	3610 comIQ12L (JDW2144)
O/N Method	Likely single colony
Kill Curve end point	3hr
Treatment OD	0.2-0.3
N	1

Conclusions: Too much kill or no immediate differences between wild type and (p)ppGpp^0

File Name: 2014-03-07-Rifampicin kill curves, 2014-03-05 4-8ugml tab

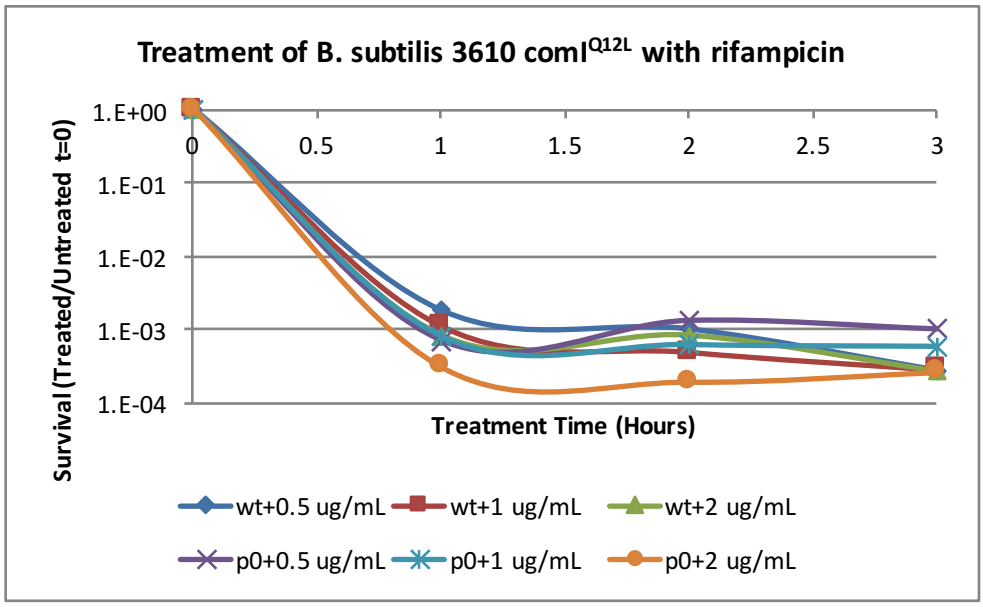

Appendix Figure 21. Kill curve of wild type and (p)ppGpp^0 cells treated with 0.5-2 µg/mL rifampicin.

Purpose: To determine if (p)ppGpp protects cells against rifampicin killing at 0.25X, 0.5X and 1X MIC (0.5 µg/mL, 1 µg/mL, 2 µg/mL respectively). These concentrations were chosen because the previous experiment at 2X and 4X MIC looked like it had too much kill.

Conditions:

Growth Media	S750+CAS
Strain Background	3610 comIQ12L (JDW2144)
O/N Method	Likely single colony
Kill Curve end point	3hr
Treatment OD	0.25
N	1

Conclusions: No immediate differences between wild type and (p)ppGpp^0

File Name: 2014-03-07-Rifampicin kill curves, 2014-03-07 0.5-2ugml tab

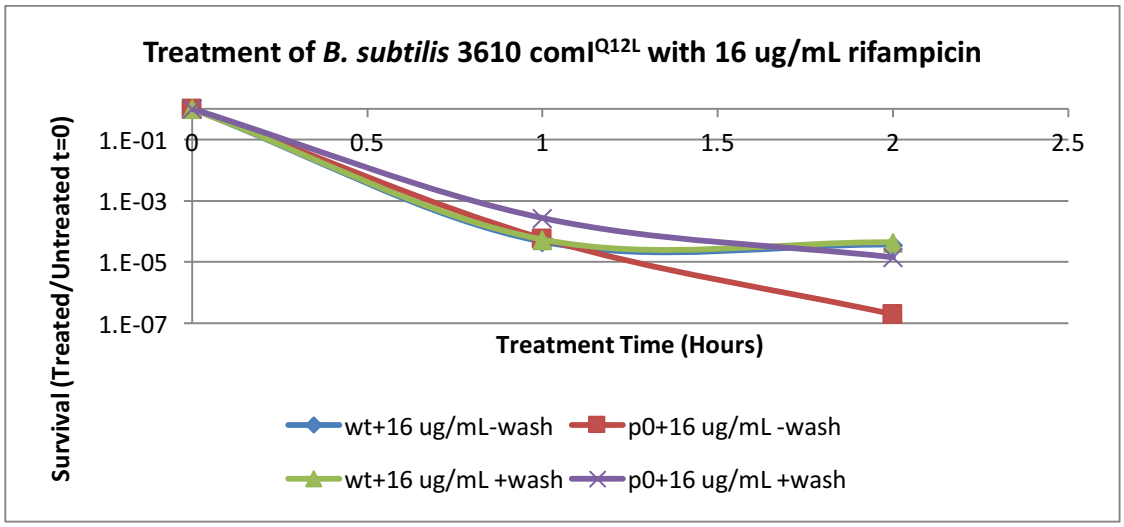

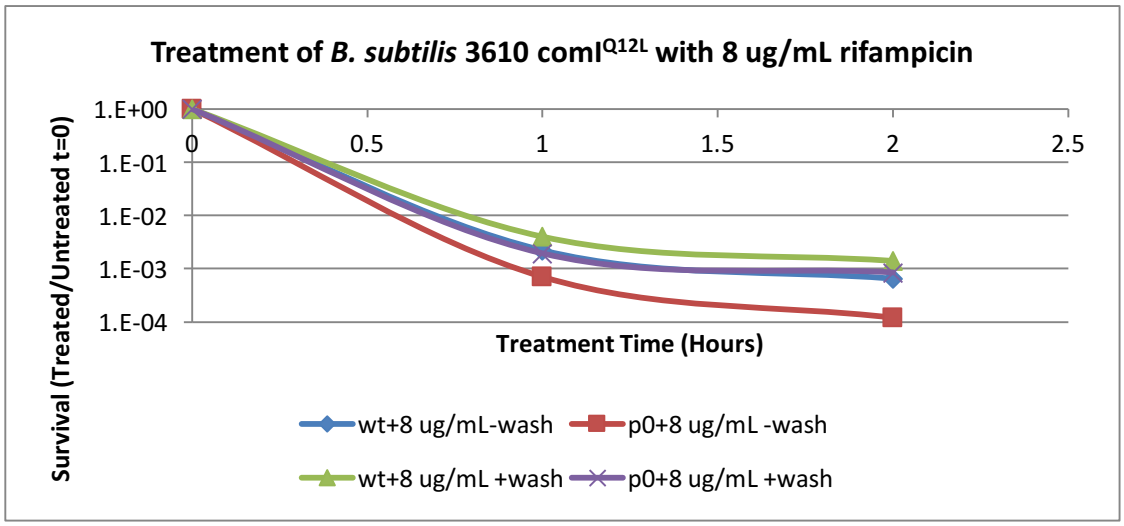

Appendix Figure 22. Kill curve of wild type and (p)ppGpp^0 cells treated with 8-16 µg/mL rifampicin with and without washing out the antibiotic.

Purpose: To determine if washing off rifampicin will reveal (p)ppGpp protection against rifampicin killing at 4X and 8X MIC (8 µg/mL and 16 µg/mL respectively).

Conditions:

Growth Media	S750+CAS
Strain Background	3610 *comI*^{Q12L} (JDW2144)
O/N Method	Likely single colony
Kill Curve end point	2hr
Treatment OD	0.2-0.3
N	2

Conclusions: Washing seems to make a difference for (p)ppGpp^0 cells. After washing, there is no immediate differences between wild type and (p)ppGpp^0 cells.

File Name: 2014-03-07-Rifampicin kill curves, 2014-04-02 WashingExp tab

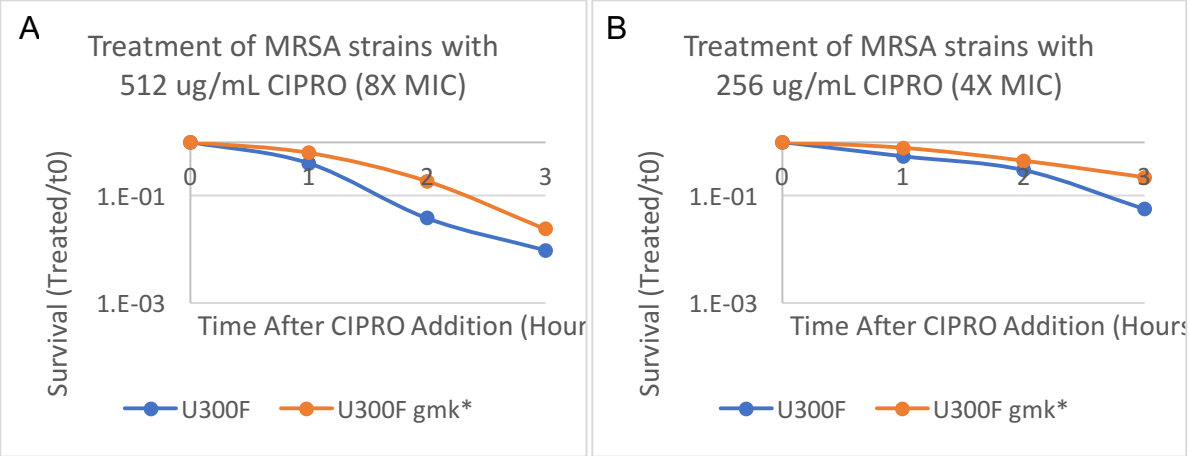

Appendix Figure 23. Kill curve of MRSA USA300 wild type and *gmk** (Mwangi MRSA collection) cells treated with A. 512 µg/mL and B. 256 µg/mL ciprofloxacin.

Purpose: To determine if decreasing GTP in MRSA strains will increase ciprofloxacin survival.

Conditions:

Growth Media	TSB
Strain Background	MRSA USA300
O/N Method	Single colony then overnight
Kill Curve end point	3hr
Treatment OD	0.2-0.4
N	1

Conclusions: The ciprofloxacin treatment concentration is very high and it turns out that USA300 is actually resistant to ciprofloxacin (Diep et al., 2006). It is still possible that the *gmk** mutant will show increased survival to antibiotics, but might require longer treatment times for the effects to be seen.

Diep, B.A., Gill, S.R., Chang, R.F., Phan, T.H., Chen, J.H., Davidson, M.G., Lin, F., Lin, J., Carleton, H. a., Mongodin, E.F., et al. (2006). Complete genome sequence of USA300, an epidemic clone of community-acquired meticillin-resistant Staphylococcus aureus. Lancet *367*, 731–739.

File Name: 2015-01-28-MRSACipro

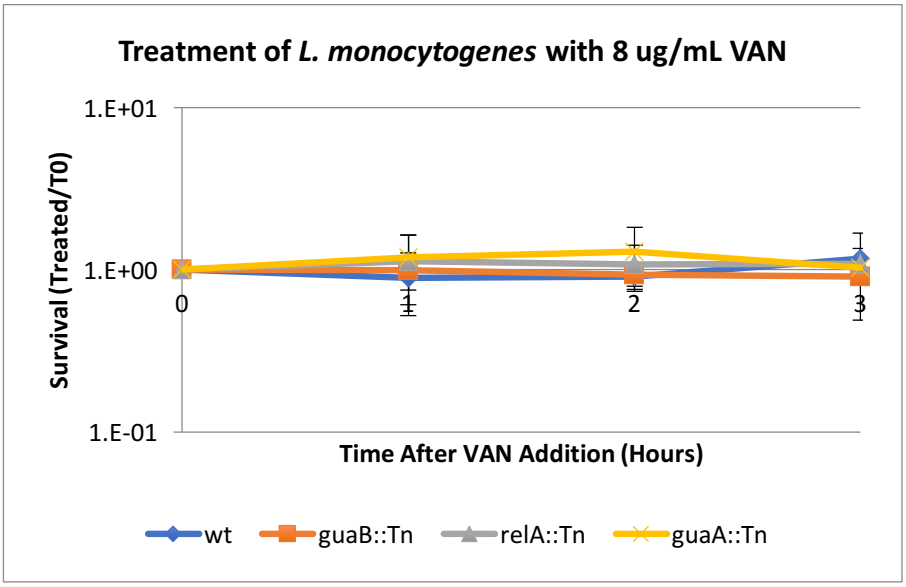

Appendix Figure 24. Kill curve of *Listeria monocytogenes* 10403s wild type, *guaB*::*Tn*, *relA*::*Tn*, and *guaA*::*Tn* treated with 8 µg/mL vancomycin (8X MIC).

Purpose: To determine if decreasing GTP in *Listeria monocytogenes* will increase ciprofloxacin survival. GTP mutants were obtained from a transposon screen conducted by Daniel Pensinger (Sauer Lab).

Conditions:

Growth Media	BHI
Strain Background	*L. monocytogenes* 10403s
O/N Method	Single colony then overnight
Kill Curve end point	3hr
Treatment OD	0.4-0.6 (normal treatment OD)
N	3

Conclusions: Treatment of *L. monocytogenes* strains with decreased GTP levels (due to transposon insertion), resulted in very similar kill curves, where 100% survival is shown. It is possible that if the kill curve time was extended, then differences can be seen.

File Name: Fung Tse - Low GTP induces persistence paper/Unpublished pathogen data/Listeria Experiments/Listeria kill curves